DEGRADATION OF POLYCARBONATE, BENTONITE, BARITE, CARBON FIBER AND GLASS FIBER FILLED POLYCARBONATE VIA GAMMA IRRADIATION AND POSSIBLE USE OF POLYCARBONATE IN RADIOACTIVE WASTE MANAGEMENT

A THESIS SUBMITTED TO
THE GRADUATE SCHOOL OF NATURAL AND APPLIED SCIENCES
OF
MIDDLE EAST TECHNICAL UNIVERSITY

BY

FIRAT HACIOĞLU

IN PARTIAL FULFILLMENT OF THE REQUIREMENTS
FOR
THE DEGREE OF DOCTOR OF PHILOSOPHY
IN
POLYMER SCIENCE AND TECHNOLOGY

FEBRUARY 2017

Approval of the thesis:

DEGRADATION OF POLYCARBONATE, BENTONITE, BARITE, CARBON FIBER AND GLASS FIBER FILLED POLYCARBONATE VIA GAMMA IRRADIATION AND POSSIBLE USE OF POLYCARBONATE IN RADIOACTIVE WASTE MANAGEMENT

submitted by **FIRAT HACIOĞLU** in partial fulfillment of the requirements for the degree of **Doctor of Philosophy in Polymer Science and Technology Department**, **Middle East Technical University** by,

Prof. Dr. Gülbin Dural Ünver
Dean, Graduate School of **Natural and Applied Sciences** ____________

Prof. Dr. Necati Özkan
Head of Department, **Polymer Science and Technology** ____________

Prof. Dr. İsmail Teoman Tinçer
Supervisor, **Polymer Science and Technology Dept., METU** ____________

Prof. Dr. Tonguç Özdemir
Co-Supervisor, **Chemical Engineering Dept.**, **Mersin University** ____________

Examining Committee Members:

Prof. Dr. Ahmet Muhtar Önal
Polymer Science and Tehcnology Dept., METU ____________

Prof. Dr. İsmail Teoman Tinçer
Polymer Science and Technology Dept., METU ____________

Assist. Prof. Dr. Elif Vargün
Chemistry Dept., Muğla Sıtkı Koçman Univ. ____________

Assoc. Prof. Dr. Ali Çırpan
Polymer Science and Technology Dept., METU ____________

Assoc. Prof. Dr. Mehmet Doğan
Textile Engineering Dept., Erciyes Univ. ____________

Date: ____________

I hereby declare that all information in this document has been obtained and presented in accordance with academic rules and ethical conduct. I also declare that, as required by these rules and conduct, I have fully cited and referenced all material and results that are not original to this work.

Name, Last name: Fırat Hacıoğlu

Signature :

ABSTRACT

DEGRADATION OF POLYCARBONATE, BENTONITE, BARITE, CARBON FIBER AND GLASS FIBER FILLED POLYCARBONATE VIA GAMMA IRRADIATION AND POSSIBLE USE OF POLYCARBONATE IN RADIOACTIVE WASTE MANAGEMENT

Hacıoğlu, Fırat
Ph.D., Department of Polymer Science and Technology
Supervisor: Prof. Dr. İsmail Teoman Tinçer
Co-Supervisor: Prof. Dr. Tonguç Özdemir

February 2017, 253 pages

Frequent use of bisphenol-a polycarbonate in daily life results with a huge amount of polycarbonate waste. The proper utilization of this waste would be an environmental friendly solution. As polymeric materials are used materials for radioactive waste embedding, having an aromatic structure within the main chain, the bisphenol-a polycarbonate is a candidate material to be used as an embedding matrix for the confinement of radioactive waste. This possibility would also solve the problem of huge amount of waste generated due to the use of polycarbonate. Bentonite and barite minerals have been used extensively in the radioactive waste management. On the other hand, glass and carbon fiber have been used as reinforcing agent for polymers. Incorporation of bentonite, barite, carbon fiber and glass fiber would enhance the resistance to radiation and load bearing property of polycarbonate. They would also enable to increase the initial dose rate of radioactive wastes which are intended to be embedded in to polycarbonate.

In this study, changes in the properties of neat, bentonite, barite, carbon fiber and glass fiber filled polycarbonate (Lexan® LS2) samples via high dose rate gamma irradiation and possible use of them in radioactive waste management were investigated. High dose rate irradiations were carried out in the irradiation facility (^{60}Co source) of Turkish Atomic Energy Authority located in Sarayköy. There were two dose options selected for neat and filled polycarbonates. Neat polycarbonate samples were irradiated with 10, 25, 50, 75, 684, 1291, 3280 and 4341 kGy. On the other hand, filled polycarbonate samples were irradiated up to four different doses which were 10, 25, 50, 75 kGy. To estimate the radiation stability of irradiated polymers, total irradiation doses, additives types (bentonite, barite, carbon fiber and glass fiber), and additives' content (%1, %2, %5, %10) used in formulation were parameters which were analyzed. Characterization of irradiated polycarbonate (neat and filled) samples were performed by tensile, Dynamic Mechanical Analysis (DMA), Thermogravimetric analysis (TGA), Attenuated Total Reflectance-Fourier Transform Infrared Spectroscopy (ATR-FTIR), spectrophotometric (for yellowness index) and Scanning Electron Microscopy (SEM) tests.

The dominant reaction mechanism generated via irradiation was the chain scission resulting with deterioration in tensile, thermal and morphological properties of polycarbonates at the doses of starting with 684 kGy. High doses with 684, 1291, 3280 and 4341 kGy diminished both tensile strength and elongations at break of polycarbonates significantly that end point criteria were exceeded at each doses. Carbon and glass fiber inclusion enhanced the mechanical properties of composites significantly. 10 wt. % carbon and glass fiber reinforced composites exhibited highest load-bearing property. Barite and carbon fiber reinforced polycarbonate gave more stable results upon irradiation and this was attributed to radiation attenuation property of barite and carbon fiber. 10 wt. % carbon fiber based composite had superior mechanical and thermal properties upon irradiation. 75 kGy did not compromise the mechanical, thermal and morphological properties of composites. 10 wt. % carbon fiber reinforced composite was found as the most radiation stable material among all irradiated samples in terms of mechanical and thermal properties. End point criterion were not reached at the dose of 75 kGy. End-point criteria and radiation index for neat and filled polycarbonate samples could be achieved in between 75 and 684 kGy doses. 75 kGy could be easily stated as the eventual dose that radioactive waste could be sustained for 300 years in polycarbonate. Therefore, it could be inferred that radioactive waste having initial contact dose rate of 1.126 Gy/h with the half-life of 5.27 years could be theoretically embedded into neat and filled (bentonite, barite, carbon fiber and glass fiber) polycarbonate with remote handling procedures for 300 years.

Keywords: Polycarbonate degradation via gamma irradiation, radioactive waste management, bentonite filled polycarbonate, barite filled polycarbonate, carbon fiber reinforced polycarbonate, glass fiber reinforced polycarbonate.

ÖZ

BENTONİT, BARİT, KARBON FİBER VE CAM ELYAF TAKVİYELİ VE TAKVİYESİZ POLİKARBONAT POLİMERLERİNİN GAMA RADYASYONU İLE BOZUNMASI VE POLİKARBONAT POLİMERİNİN RADYOAKTİF ATIK YÖNETİMİNDE OLASI KULLANIMI

Hacıoğlu, Fırat
Doktora, Polimer Bilim ve Teknolojisi Enstitü Anabilim Dalı
Tez Yöneticisi: Prof. Dr. İsmail Teoman Tinçer
Ortak Tez Yöneticisi: Prof. Dr. Tonguç Özdemir

Şubat 2017, 253 sayfa

Günlük yaşamda bisfenol a polikarbonatların yoğun kullanımı, yüksek miktarlarda polikarbonat atığı ortaya çıkarmaktadır. Bu atığın uygun bir şekilde kullanılmasıyla çevre dostu çözüm elde edilebilir. Polimerik malzemeler radyoaktıf atık yönetiminde kullanılmasından dolayı, ana zincirinde aromatik halka içeren polikarbonat, radyoaktif atıkların hapsedilmesinde kalıp olarak kullanılabilir. Bu olasılık, yüksek miktarlarda ortaya çıkan polikarbonat atığı için bir çözüm olabilir. Bentonit ve barit mineralleri radyoaktif atık yönetiminde yoğun olarak kullanılmaktadır. Öte yandan, cam elyaf ve karbon fiber polimerlerde güçlendirici katkı malzemesi olarak kullanılmaktadır. Bentonit, barit, karbon fiber ve cam elyaf takviyesi polikarbonatın radyasyon direncini ve yük mukavemeti özelliklerini artırabilir. Ayrıca, bu katkı malzemeleri, polikarbonatın içine gömülmesi planlanan radyoaktif atıkların ilk doz hızlarının artmasına da olanak sağlayabilir.

Bu çalışmada bentonit, barit, karbon fiber ve cam elyaf takviyeli polikarbonat ve takviyesiz polikarbonat örneklerinin yüksek doz hızında gama ışınımı ile bozunması ve bu polimerlerin radyoaktif atık yönetiminde olası kullanımı araştırılmıştır. Işınlamalar için iki farklı doz seçilmiştir. Bunlar yüksek doz (4341 kGy'ye kadar) ve düşük doz (75 kGy'ye kadar) olarak belirlenmiştir. Takviyesiz polikarbonatlar 10, 25, 50, 75, 684, 1291, 3280 ve 4341 kGy'e kadar ışınlanmıştır. Takviyeli polikarbonatlar ise 10, 25, 50 ve 75 kGy'ye kadar ışınlanmıştır. Işınlamalar, Türkiye Atom Enerjisi Kurumunun Sarayköy'deki tesisinde yüksek doz hızında ^{60}Co kaynağında gerçekleştirilmiştir. Işınlanan polimerlerin radyasyon kararlılığı değerlendirmesinde; toplam doz, katkı maddelerinin tipleri (bentonit, barit, karbon fiber ve cam elyaf) ve katkı maddelerinin miktarları (%1, %2, %5, %10) analiz edilen parametrelerdi. Işınlanan takviyeli ve takviyesiz polikarbonat örneklerinin karakterizasyonu mekanik (çekme ve sertlik), Dinamik Mekanik Analiz (DMA), Termal Gravimetrik Analiz (TGA), Zayıflatılmış Toplam Yansıma- Fourier Dönüşümlü Kızılötesi Spektroskopisi ATR-FTIR), Spektrofotometrik Analiz (sarılık indeksi için) ve Taramalı Elektron Mikroskobu (SEM) testleri ile gerçekleştirilmiştir.

Yüksek doz ışınlama (684 kGy ile başlayıp 4341 kGy'e kadar devam eden) ile ortaya çıkan baskın reaksiyon mekanizması, polikarbonatın mekanik, termal ve yapısal özelliklerinde bozulmaya yol açan zincir kırılmasıdır. 684, 1291, 3280 ve 4341 kGy'lik ışınlamalar, polikarbonatın çekme dayanımını ve uzamada kopma değerlerini önemli ölçüde düşürmüştür. 684 kGy ışınlama, polikarbonat polimerinin nihai kullanım dozunun ötesinde bulunmuştur. Karbon fiber ve cam elyaf takviyesi, kompozitlerin mekanik özelliklerini önemli derecede artırmıştır. % 10 karbon fiber ile güçlendirilmiş kompozit en iyi yük dayanım özelliğini göstermiştir. Barit ve karbon fiber katkılı polikarbonat örnekleri ışınlamayla birlikte daha kararlı sonuçlar göstermiştir. Bu durum karbon fiber ve barit mineralinin radyasyonu zayıflatma özelliğiyle ilişkilendirilmiştir. % 10 karbon fiber katkılı kompozit, ışınlamalarla birlikte üstün mekanik ve termal özellikler göstermiştir. 75 kGy ışınlama kompozitlerin mekanik, termal ve yapısal özelliklerini önemli ölçüde bozmamıştır. %10 karbon fiber ile güçlendirilmiş kompozit en fazla radyasyon kararlılığı gösteren malzeme olmuştur. 75 kGy ışınlama, polikarbonat polimerinin nihai kullanım dozuna ulaşamamıştır. Test sonuçlarına göre, polikarbonat polimeri için nihai kullanım ölçütlerine ve radyasyon indeksine 75 kGy ile 684 kGy arasında bir dozda erişilebilir. Radyoaktif atıkların polikarbonat içerisinde 300 yıl saklanabilmesi için 75 kGy rahatlıkla nihai doz olarak seçilebilir. Teorik olarak, ilk doz hızı ve yarılanma ömrü sırasıyla 1.126 Gy/saat ve 5.27 yıl olan radyoaktif atığın, takviyeli (bentonit, barit, karbon fiber ve cam elyaf) ve takviyesiz polikarbonat içerisinde 300 yıl gömülü olarak saklanabileceği çıkarımı yapılabilir.

Anahtar Kelimeler: Gama ışıması ile polikarbonatın bozunması, radyoaktif atık yönetimi, bentonit takviyeli polikarbonat, barit takviyeli polikarbonat, karbon fiber takviyeli polikarbonat, cam elyaf takviyeli polikarbonat.

To Şerife and Elif Duru

ACKNOWLEDGMENTS

I would like to express my deepest gratitude to my late supervisor Prof. Dr. Ali Usanmaz. Starting from the first day, he responded me very politely and always encouraged me with his positive attitude. I sincerely appreciate the time and efforts he had taken to train me and improve my thesis.

I would like to express my sincere thanks to my supervisor Prof. Dr. İsmail Teoman Tinçer for his invaluable guidance, support, suggestions and advice for the completion of my thesis and for everything.

I would like to thank to my co-supervisor Prof. Dr. Tonguç Özdemir for his guidance and support.

I would like to give special thanks to my dissertation committee. I owe a debt of gratitude to committee for their time and careful attention to detail my thesis which lead to improvement.

I sincerely acknowledge my friends Ümit Tayfun, Osman Yaslıtaş, Mevlüt Yücel Melih Aykan, and Abdullah Buruç for supporting and criticizing to help doing my best in almost every stage of this work.

I sincerely acknowledge my friends İhsan Sami Dedetaş, Mücahit Uğur, Mustafa Kıymet, Bahadır Kelez, Furkan Mustafa Çetin, Ahmet Furkan Saylık with whom I had spent most of time after working hours when preparing my thesis.

I am also thankful to my laboratory friends from 'Prof. Dr. Ali Usanmaz Research Group (Mert Akgün and Yurdaer Babuççuoğlu)' for their patience and politeness during my study.

I would like to thank to Mehtap Şahin for her help about characterization of the test specimens.

I would like to thank TSE (Turkish Standards Institution) for support during the doctoral qualifying exam and thesis defense stages by giving annual leave.

I would like to thank my parents and brothers for believing in me and giving me endless support.

I would like to thank my second family members Fatma Torun, Hüsniye Yücel and Ali Yücel Elbistan for believing in me and giving me endless support.

I would like to thank to my best friend Mücahit Duman for believing in me and giving me endless support.

Finally, my special thanks goes to my wife Şerife Özdemir Hacıoğlu and our baby Elif Duru Hacıoğlu. Words fail to express my gratitude to Şerife for her support, love and patience. Without her, none of this work could be accomplished. After our baby Elif Duru born, she became the meaning of our life.

TABLE OF CONTENTS

LIST OF TABLES

TABLES

LIST OF FIGURES

FIGURES

LIST OF EQUATIONS

EQUATIONS

LIST OF ABBREVIATIONS

ATR-FTIR	Attenuated Total Reflection Fourier Transform Infrared Spectroscopy
B	Bentonite
Ba	Barite
CF	Carbon Fiber
DMA	Dynamic Mechanical Analysis
DSC	Differential Scanning Calorimetry
DTG	Differential Thermogravimetric Analysis
DTG Curve	First Derivative of Thermogravimetric Curve
EDX	Energy-Dispersive X-ray Spectrometer
EPDM	Ethylene-Propylene Diene Monomer
ETFE	Ethylene-tetrafluoroethylene
EW	Exempt Waste
FTIR	Fourier Transform Infrared Spectroscopy
GF	Glass Fiber
HLW	High Level Waste
HVD	Half-Value-Dose
IAEA	International Atomic Energy Agency
ILW	Intermediate Level Waste
kGy	Kilogray (unit of absorbed dose)
LDPE	Low-Density Polyethylene
LLW	Low Level Waste
MFR	Melt Flow Rate
Non-Irra	Non Irradiated
PAN	Polyacrylonitrile

PC	Bisphenol A Polycarbonate
PC/1B	Polycarbonate containing 1 wt. % bentonite
PC/2B	Polycarbonate containing 2 wt. % bentonite
PC/5B	Polycarbonate containing 5 wt. % bentonite
PC/2Ba	Polycarbonate containing 2 wt. % barite
PC/5Ba	Polycarbonate containing 5 wt. % barite
PC/10Ba	Polycarbonate containing 10 wt. % barite
PC/2CF	Polycarbonate containing 2 wt. % carbon fiber
PC/5CF	Polycarbonate containing 5 wt. % carbon fiber
PC/10CF	Polycarbonate containing 10 wt. % carbon fiber
PC/2GF	Polycarbonate containing 2 wt. % glass fiber
PC/5GF	Polycarbonate containing 5 wt. % glass fiber
PC/10GF	Polycarbonate containing 10 wt. % glass fiber
PCU	Polycarbonate-Urethane
PEEK	Poly(ether ether ketone)
PMMA	Poly(methyl methacrylate)
PS	Poystyrene
PTFE	Polytetrafluoroethylene
SEM	Scanning Electron Microscopy
TGA	Thermogravimetric Analysis
TG Curve	Thermogravimetric Curve
T_5	Temperature at which 5 % weight loss occurs

T_{50}	Temperature at which 50 % weight loss occurs
T_g	Glass Transition Temperature
T_{max}	Temperature at which highest rate of weight loss occurs obtained from first derivative of thermogravimetric curve
T_{onset}	Onset Decomposition Temperature
UHMWPE	Ultra-Highmolecular Weight Polyethylene
XRD	X-Ray Diffraction
VSLW	Very Short Lived Waste
YI	Yellowness Index

CHAPTER 1

INTRODUCTION

1.1. Ionizing Radiation Effects on Polymers

Polymers and their composites are extensively used in areas where they are exposed to high-energy radiations. These areas involve nuclear power plants, sterilization systems, etc. Gamma (γ) rays, X-rays, and electron beams are the type of high-energy radiation to which polymers are exposed.

Irradiation of polymers generates chain scission, crosslinking, gas evaluation and unsaturation. Photons interact with polymer structure and produce fast electrons. The emerged electrons subsequently interact with the polymer chain to generate secondary electrons. As a result, ionizing radiation as gamma (γ) rays cause ion formation and electron ejection at the same time. Ejected electrons and generated ions recombined with each other to yield highly excited states. The excited states get rid of their excess energy by bond cleavages. Bond cleavages result in with free radical formation. The bond cleavages are based on C-C and C-H bond scission. The probability of C-H bond scission is higher than the C-C bond scission due to the fact that deposited energy in C-C migrate along the backbone of the polymer, whereas stored energy in C-H cannot transmitted along the polymer chain (Carlsson & Chmela, 1990). Moreover, the attribute of the C-C bond being more stable than the C-H bonds at the excited states is the other explanation for the higher probability of the C-H bonds scission over C-C scission. The cleavage of C-C bonds results with chain scission, whereas C-H bond scission causes hydrogen evolution, unsaturation and crosslinking reactions (Carlsson & Chmela, 1990). In addition, in the presence of the oxygen, peroxidic radical formation occurs. The peroxidic radicals initiate the polymer chain cleavage known as oxidative degradation. The effects of these reactions on polymer’s properties are given below (Carlsson & Chmela, 1990; Hill & Whittaker, 2004; International Atomic Energy Agency, 1999; Charlesby, 1960; Tamboli, et al., 2004; Carraher, 2014):

- **Crosslinking:** Increases tensile strength, molecular weight, glass transition temperature and decrease in ultimate elongation. It is expressed as constructive.

- **Chain Scission:** Decreases tensile strength, ultimate elongation, glass transition temperature and molecular weight. It is expressed as destructive.

- **Hydrogen gas evolution:** Lead to crosslinking or side-chain deterioration. It is expressed as both constructive and destructive.

- **Formation of peroxy radicals in the presence of oxygen:** Decreases tensile strength, ultimate elongation, glass transition temperature and molecular weight. It is expressed as destructive.

- **Unsaturation production or deterioration:** They are expressed as both constructive and destructive.

The effects of ionizing radiation on polymers depend on structure of polymer, dose rate and presence of oxygen in the medium. Having a quaternary carbons and functional groups of COOH, C-Halogen, SO_2, C=C and NH_2 make polymer be sensitive to the radiation induced degradation (Carraher, 2014; Reichmanis, et al., 1993). On the other hand, presence of aromatic groups in the main chain of the polymers (especially phenolic and biphenyl groups) enhances the radiation resistance of polymeric materials (Reichmanis, et al., 1993). On the other hand, low-dose-rate irradiation accelerates oxidative degradation by allowing increased time for oxygen penetration (International Atomic Energy Agency, 1999). Polymers with low oxygen permeability are more radiation resistant (Booth, 2001).

In most cases, crosslinking and chain scission reactions take place at the same time upon irradiation in a competing manner. However, one of these reactions dominates over the other. Therefore, polymers are mainly categorized into two groups which are crosslinking (or radiation resistant) polymer and degrading polymer upon irradiation. Examples for polymers categorized as radiation resistant and degrading are given below (Massey, 2004; Hill & Whittaker, 2004):

- **Radiation Resistant Polymers:** Polystyrene, Polyurethane, Polycarbonate, Polyacrylamide, Polyamides, Polyethylene, Main-chain aromatic polymers, Poly(vinyl alcohol), Poly(vinyl chloride), Polyamides, Polyesters.

- **Radiation Degrading Polymers:** Polyisobutylene, Polymethacrylates, Fully fluorinated thermoplastics, Poly(vinylidene chloride), Polychlorotrifluoroethylene, Cellulosics.

However, in atmospheric conditions, some of the above polymers may lose their properties faster than expected due to the oxidative degradation.

1.2. Radioactive Waste Management

Any materials containing or contaminated via radionuclides (nuclides that have properties of spontaneous disintegration) at concentrations greater than the clearance levels determined by regulatory authorities are classified as radioactive wastes (IAEA, 2010; Ojovan & Lee, 2005). Clearance levels (i.e. exemption) require both low amount (total activity in Bq) and low concentration (activity per unit mass or volume in Bq/g or Bq/m^3). **Table 1** and **Figure 1** show exemption levels according to IAEA (Ojovan & Lee, 2005). Many activities including the use of radionuclides and the production of nuclear energy results with the formation of radioactive wastes (IAEA, 2009). Radioactive wastes, for which no use is foreseen, are classified into six levels entitled as exempt wastes (EW), very short lived waste (VSLW), very low level waste (VLLW), low level waste (LLW), intermediate level waste (ILW), and high level waste (HLW) (IAEA, 2009). Spent fuels and wastes emerged from primarily chemical reprocessing of spent fuels are considered as HLW. Wastes emerged from nuclear operations, reprocessing, decontamination, decommissioning and further activities in the nuclear power plants are considered as VLLW, LLW and ILW (IAEA, 2009). Activity and the half-life of the radionuclide included in the materials are important criteria for the classification of radioactive wastes. In addition to classification depicted above, radioactive wastes are classified in to two parts with respect to radionuclides' half-live namely short-lived and long-lived wastes. Short-lived radioactive wastes include radionuclides of which half-lives are less than that of Cesium (^{137}Cs, 30.17 years) (Ojovan & Lee, 2005). Concentrations of the short-lived waste are generally limited to 4000 Bq/g in a singular waste bundle (Ojovan & Lee, 2005). Short-lived LLW and ILW require near-surface disposal. On the other hand, long-lived wastes include radionuclides with half-lives greater than that of Cesium (^{137}Cs, 30.2 years) and they require deep underground disposal (Ojovan & Lee, 2005). ^{3}H, ^{90}Sr, ^{60}Co, ^{106}Ru, ^{134}Cs, ^{137}Cs, ^{144}Ce, ^{147}Pm, ^{151}Sm and ^{154}Eu are short-lived radionuclides and ^{14}C, ^{99}Tc, ^{129}I, ^{238,239,240,242}Pu and ^{237}Np are long-lived radionuclides (Ojovan & Lee, 2005). **Figure 2** depicts scheme (Activity content vs Half Life) that matches types of radionuclides with types of wastes. **Table 2** shows the half-life and activity of radionuclides types for disused radioactive sources that are notated in **Figure 2**. **Figure 3** shows the radioactive waste classes and corresponding disposal sites (IAEA, 2009). According to the figure shown below, various types of wastes are disposed via using near and deep surface disposal.

Table 1 Exemption Levels Set by the IAEA

(Ojovan & Lee, 2005)

Nuclide	**Activity Concentrations** $(\frac{\mathbf{Bq}}{\mathbf{g}})$	**Activity (Bq)**
^{3}H	1.0×10^{6}	1.0×10^{9}
^{14}C	1.0×10^{4}	1.0×10^{7}
^{40}K	1.0×10^{2}	1.0×10^{6}
^{60}Co	1.0×10^{1}	1.0×10^{5}
^{90}Sr	1.0×10^{2}	1.0×10^{4}
^{99}Tc	1.0×10^{4}	1.0×10^{7}
^{106}Ru	1.0×10^{2}	1.0×10^{5}
^{125}I	1.0×10^{3}	1.0×10^{6}
^{129}I	1.0×10^{2}	1.0×10^{5}
^{134}Cs	1.0×10^{1}	1.0×10^{4}
^{135}Cs	1.0×10^{4}	1.0×10^{7}
^{137}Cs	1.0×10^{1}	1.0×10^{4}
^{144}Ce	1.0×10^{2}	1.0×10^{5}
^{147}Pm	1.0×10^{4}	1.0×10^{7}
^{151}Sm	1.0×10^{4}	1.0×10^{8}
^{154}Eu	1.0×10^{1}	1.0×10^{6}
^{222}Rn	1.0×10^{1}	1.0×10^{8}
^{226}Ra	1.0×10^{1}	1.0×10^{4}
^{232}Th	1.0×10^{0}	1.0×10^{3}
^{235}U	1.0×10^{1}	1.0×10^{4}
^{238}U	1.0×10^{1}	1.0×10^{4}
^{237}Np	1.0×10^{0}	1.0×10^{3}

Table 1 Exemption Levels Set by the IAEA

(Ojovan & Lee, 2005)

Nuclide	**Activity Concentrations** $(\frac{\mathbf{Bq}}{\mathbf{g}})$	**Activity (Bq)**
^{239}Np	1.0×10^{2}	1.0×10^{7}
^{238}Pu	1.0×10^{0}	1.0×10^{4}
^{239}Pu	1.0×10^{0}	1.0×10^{4}
^{240}Pu	1.0×10^{0}	1.0×10^{3}
^{241}Pu	1.0×10^{2}	1.0×10^{5}
^{242}Pu	1.0×10^{0}	1.0×10^{4}
^{241}Am	1.0×10^{0}	1.0×10^{4}
^{242}Am	1.0×10^{3}	1.0×10^{6}
^{243}Am	1.0×10^{0}	1.0×10^{3}
^{242}Cm	1.0×10^{2}	1.0×10^{5}
^{243}Cm	1.0×10^{0}	1.0×10^{4}
^{244}Cm	1.0×10^{1}	1.0×10^{4}
^{245}Cm	1.0×10^{0}	1.0×10^{3}
^{246}Cm	1.0×10^{0}	1.0×10^{3}

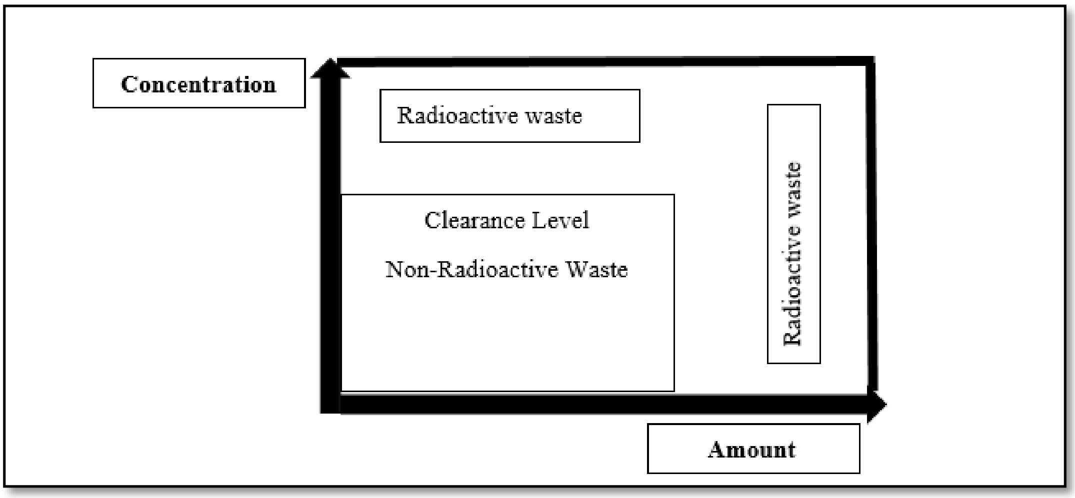

Figure 1 Acceptability criteria of wastes as radioactive in either concentrations or amounts of radionuclides beyond clearance levels IAEA (Ojovan & Lee, 2005).

Table 2 Disused Radioactive Sources with Corresponding Disposal Option Given in **Figure 2**
(IAEA, 2009)

Notations in Figure 2	**Half Life**	**Activity (Bq)**
i	<100 days	100 MBq
ii	<100 days	5 TBq
iii	<15 year	<10 MBq
iv	<15 year	<100 TBq
v	<30 year	<1 MBq
vi	<30 year	<1 PBq
vii	>30 year	<40 MBq
viii	>30 year	<10 GBq

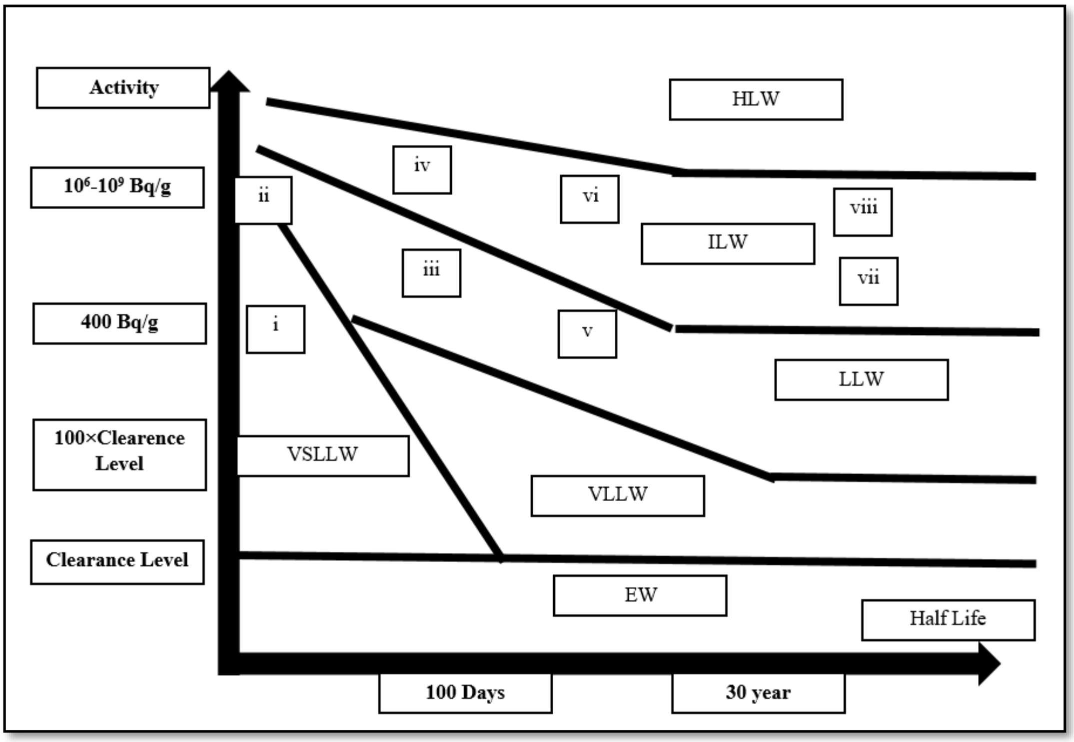

Figure 2 Application of the radioactive waste classification pattern (IAEA, 2009).

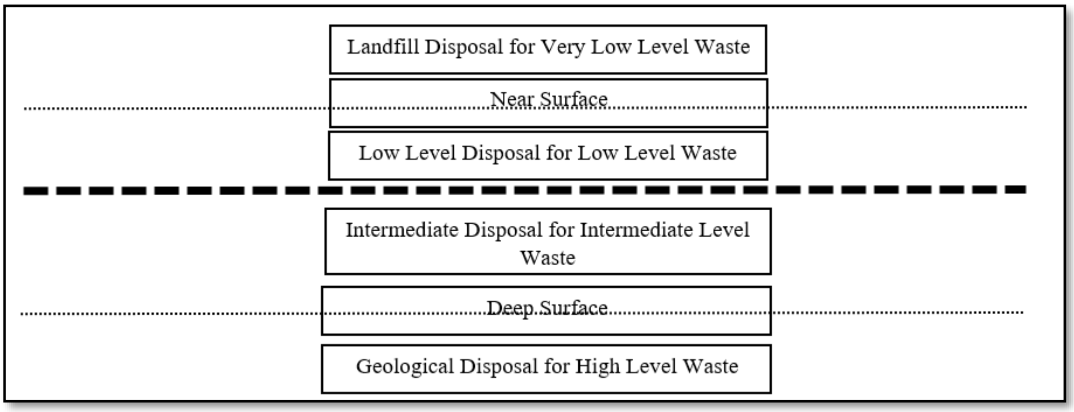

Figure 3 Diagram depicting disposal options corresponding to wastes' classes (IAEA, 2009).

Radioactive waste management is categorized in to two parts, which are (1) predisposal and (2) disposal. The minimization of the radioactive waste via reducing the amount and the activity is essential. On the other hand, minimization of waste volume is an essential requirement. It diminishes the potential for migration or dispersion of radionuclides including contaminants. This case is achieved during pre-disposal methods. For this reason, minimization process is applied to all types of wastes. Due to the fact that, the largest volume of radioactive wastes, which are generated in nuclear plants and in other activities, are VLLW and LLW, waste minimization processes are mainly applied to them (IAEA, 2010; IAEA, 2009; Ojovan & Lee, 2005). Pre-disposal waste management includes pre-treatment, treatment, conditioning, immobilization, transportation and storage. Pre-treatment comprise collection, segregation, chemical adjustment and decontamination. Treatment process is applied in order to improve safety and economy (volume reduction, radionuclide removal, change of chemical and physical composition) via changing wastes characteristics. Treatment processes comprise incineration of combustible waste, compaction of dry solid waste so as to achieve volume reduction, evaporation, filtration, ion exchange of liquid waste streams so as to accomplish radionuclide removal, neutralization and precipitation of chemical species in order to change the composition (IAEA, 2010; Ojovan & Lee, 2005). Conditioning converts the wastes into an appropriate form for handling, transportation, storage and disposal. It includes the immobilization of radionuclides, placing them in to canisters and supplying supplementary packaging. Immobilization eases handling, transportation, storage and disposal of radioactive waste via conversion of it by solidification (including fixation and encapsulation), embedding or encapsulation (IAEA, 2010; Ojovan & Lee, 2005). Radioactive wastes (generally low and intermediate level liquid radioactive waste) are chemically incorporated into the structure of a suitable matrix (generally glass or ceramic) in order to be captured and unable to migrate. Encapsulation, which is an immobilization technique of waste, is performed by physically surrounding of wastes in to bitumen, cement, glass or polymer to be isolated (Ojovan & Lee, 2005). After pre-treatment, treatment, immobilization and conditioning processes, activities including storage and transportation are applied prior to disposal (Ojovan & Lee, 2005).

Immobilization technique plays an important role in low and intermediate level radioactive waste. The main aim of the immobilization is to convert the waste in a monolithic block, which has reduced leaching potential (Cota, et al., 2009). In addition, it should have properties, which are (IAEA, 2004):

- A monolith, with no free standing water;
- Free standing without an outer container;
- Little degradation of the product with time;
- An acceptable degree of radiation damage over the design storage period;
- Matrix material and the solidified waste should be compatible;
- Mechanical properties should be sufficient to external effects (compression, shock, erosion);
- Mixed materials should have low leaching rate;
- When it is exposed to fire, it composition (waste and embedding material) should not be impressed detrimentally.
- Readily reproducible on an industrial scale;
- A low overall production cost.

Cements, bitumen, polymers and ceramics, which contain glasses and oxide ceramics, play an important role in the immobilization of radioactive waste. Among these methods, due to the low cost and simple processing, the most used technique is cementation (IAEA, 2004). Due to the fact that long term stability of organic matrix is doubtful, immobilization of wastes to polymers are not common with respect to cement and bitumen. Limited use of polymeric materials in radioactive waste are emerged due to the lack of extensive research. There have been various studies regarding polymeric materials degradation and stability via irradiation but topics related with usage of polymers in radioactive waste management is limited. Moreover, there have been various types of polymers that could be a candidate embedding materials for low and intermediate level radioactive waste management. As mentioned above, low production cost is an important factor for all applications including waste management. Polymers are used in everywhere extensively. After use, most of them become useless and their recycling to nature last very long. Recycling of used polymers in radioactive waste management will lead to both low cost for waste management and facilitating the conservation of the nature. Via lesser materials, higher output becomes possible.

1.3. Use of Polymers in Radioactive Waste Management

Polymers have been involved in radioactive waste management (Brownstein, 1991; Skidmore & Fondeur, 2013). Epoxy polymers have been used for the solidification of radioactive waste as solidification agent (Brownstein, 1991). Moreover, it was reported that polymers including EPDM (ethylene-propylene diene monomer), PEEK (polyetheretherketone), PTFE (polytetrafluoroethylene), ETFE (ethylene-tetrafluoroethylene) copolymer, PTFE (polytetrafluoroethylene) and UHMWPE (ultra-highmolecular weight polyethylene) have been used as sealing components in radioactive waste processing systems (Skidmore & Fondeur, 2013).

Several studies related with radiation stability and possible use of polymers in radioactive waste management were performed by various scientists (Rabinovich & Lemysh, 1997; Cota, et al., 2009; Onishi, et al., 2004; Sakr, et al., 2003). In order to provide radiation protection from radioactive waste containers and storehouses were used. The polymer-organic concrete and combination of metal, which were resistant to corrosion, with high strength fibers (glass and carbon) were the suggested materials for the wastes of which specific activity were greater than 10^{-3} Ci/kg (Rabinovich & Lemysh, 1997). Cota et al. studied the possible use of low-density polyethylene (LDPE) as an embedding matrix in radioactive waste management (Cota, et al., 2009). They reported that use of polymer for immobilization could successfully become an alternative to the other immobilization techniques regarding low-level radioactive wastes (Cota, et al., 2009). Another study was about the immobilization of radioactive waste into a mixture of cement, clay and polymer (Sakr, et al., 2003). It was intended to design a container by enhancing the strength and leachability characteristics of cement included waste, which were formed either by mixing epoxy polymer with cement clay at predetermined ratios or by coating cement-clay mixtures with an epoxy layer. (Sakr, et al., 2003). It was found that 7.5 wt.% clay and 6 wt.% epoxy inclusion to the cement improved the strength of cement (mixed with 40 wt.% water) and reduced the leachibility of ions from cement included mixture (Sakr, et al., 2003).

Another study that was carried out for developing a super radiation-resistant motor, of which the intended insulating materials were radiation resistant polymers (Poly(benz-imidazole), Poly(arylate), poly(phenyl-ether)) improved by aluminum micro-flakes, in order to be used in nuclear power plant (Onishi, et al., 2004).

Furthermore, in our previous studies, possible uses of polymers in radioactive waste management were investigated (Ozdemir & Usanmaz, 2007; Ozdemir & Usanmaz, 2008; Ozdemir & Usanmaz, 2009; Hacioglu, et al., 2013; Hacıoğlu, et al., 2016). Poly (carbonate urethane) (PCU), poly(biphenyl-a-epichlorohydrin), poly(methyl methacrylate) and EPDM polymers' degradation via gamma (γ) irradiation and possible use of them as a radioactive waste embedding matrix were investigated. The results indicated that Poly (carbonate urethane) (PCU), poly(biphenyl-a-epichlorohydrin), poly(methyl methacrylate) and EPDM polymers might be candidates as embedding matrix for long term low-level radioactive waste storage. In addition, Monte Carlo simulations for wastes encapsulated in these polymer matrices were studied. The activity of wastes that could be embedded into a drum and the dose rate distribution in the drum arising from the wastes were simulated for 15, 30 and 300 years after embedding (Ozdemir & Usanmaz, 2009; Ozdemir & Usanmaz, 2009; Ozdemir, 2014).

1.4. Polycarbonates (Bisphenol-A) and Their Radiation Stability

Polycarbonate, which is the type of polyesters, is the second largest used engineering thermoplastic next to polyamides (Ebewele, 2000). Polycarbonate includes aromatic rings in the main chain. It is amorphous (Ebewele, 2000). Polycarbonate has properties of extreme toughness, transparency, resistance to burning. These superior properties make the polycarbonates to become the second most used thermoplastics. Polycarbonates are used for variety of application. They are utilized extensively in medical, automotive, electrical, electronic, and technical applications (Mark & Kroschwitz, 2004). Furthermore, the superior properties make polycarbonates to be subject to conditions including gamma irradiations for several purposes. Polycarbonate can be used to detect ion beam as dosimeter or solid state nuclear track detector. Moreover, they can be used in the area of medical devices used in sterile conditions and synthesizing of metal/polycarbonate matrix (nanocomposite) are the purposes that utilize gamma irradiation (Massey, 2004; Hareesh, et al., 2015; Tayel, et al., 2015). Due to the extensive use in healthcare and medical applications at which materials should be put on the market as sterile (reported as the sixth commonly used polymer in medical device manufacturing), polycarbonate grades used in medical applications are subject to sterilization process (Massey, 2004). Commonly, they are sterilized via using gamma (γ) irradiation. Deterioration of polycarbonate upon gamma irradiation and formation of yellow color is one of the main disadvantages of using this polymer for medical purposes (Massey, 2004). On the other hand, degree of yellowing can be used for measuring high gamma (γ) doses as radiation dosimeters (Galante & Campos, 2012).

As mentioned, polycarbonate was reported as the fifth radiation resistant polymer used in medical device manufacturing (Massey, 2004). The dominant effect of gamma (γ) radiation on polycarbonate is crosslinking at lower doses (around 30 kGy) (Acierno, et al., 1980; Acierno, et al., 1981; Araujo, et al., 1998). On the other hand, chain scission takes place significantly at larger doses (around 200 kGy) (Acierno, et al., 1980; Acierno, et al., 1981; Araujo, et al., 1998; Massey, 2004). However, high chain stiffness makes many of the broken chains recombined (Massey, 2004). In addition, aromatic ring in the structure supplies polycarbonate to absorb more energy from gamma (γ) source than aliphatic structure (Massey, 2004). There have been various studies regarding behavior of polycarbonate under electron beam and gamma (γ) radiation (Weber, et al., 2010; Hareesh, et al., 2013; Araujo, et al., 1998; Chen, et al., 2005; Kinalir, 2011; Galante & Campos, 2012). According to the studies, polycarbonates were irradiated to various doses (up to maximum dose of 340 kGy). Up to 25 kGy, the loss of mechanical properties in the polycarbonate were not observed, however, optical properties showed sensitivity (Araujo, et al., 1998). The exposure of 340kGy gamma (γ) dose to polycarbonate did not alter the degree of crosslinking, but backbone scission of polymeric chain was reporteed (Weber, et al., 2010). Up to 225 kGy, mechanical properties and average molecular weight of polymer were decreased via electron beam irradiation such a way that chain scission was the dominant reactions rather than crosslinking (Hareesh, et al., 2013). Mechanical properties such as tensile strength decreased via irradiation up to 150 kGy (Chen, et al., 2005).

In addition, the study regarding polycarbonate stability under gamma (γ) irradiation were focused on measuring the color changes (spectrophotometrically at 412 nm) generated via irradiation between 9.73 and 69.7 kGy in order to assess whether the optical densities measured were proportional to the total dose or not (Galante & Campos, 2012). Proportionality between total dose with optical density indicated that polycarbonate could be used as inactive dosimeter (Galante & Campos, 2012). It was also concluded that optical densities were proportional to the corresponding total dose values, thus it could be candidate material used for characterizing dose distribution in irradiated products (Galante & Campos, 2012).

In another study, FTIR, DSC and XRD methods were used to investigate the effect of gamma irradiation on polycarbonate (Sinha, et al., 2004). Formation of phenolic groups due to the cleavage of the ester bonds were determined when the samples were irradiated up to 1000 kGy. It was also found that, chain scission caused an increase in the mobility of chains, therefore glass transition temperature of polycarbonate were decreased (Sinha, et al., 2004).

Furthermore, it was also reported that Lexan mark polycarbonate samples were deteriorated to a limited extent up to 500 kGy (5×10^4 krad) with respect to FTIR study (Singh & Prasher, 2005).

Due to the fact that extensive use of polycarbonate results in higher polycarbonate garbage, it becomes an increasing problem in waste management of polycarbonate with aromatic types that are considered as non-biodegradable (Artham & Doble, 2008). It was concluded that there was not an appropriate waste treatment method to landfill or incinerate the polycarbonate wastes (Antonakou & Achilias, 2013). To solve this problem various studies were conducted (Artham & Doble, 2008; Elmaghor, et al., 2004; Rosi, et al., 2015; Nikje & Askarzadeh, 2013). One of them was about to enhance biodegradability and recycling of polycarbonate upon pretreatment techniques including gamma (γ) irradiation (Artham & Doble, 2008). It was concluded that gamma (γ) irradiation made polycarbonate biologically degradable (Artham & Doble, 2008). To develop an alternative solution for polycarbonate garbage, it would be beneficial to determine whether the possible use of this garbage in radioactive waste management could be ancillary solutions for reuse of polymers or not.

1.5. Radiation Stability of Glass Fibers and Glass Fiber Reinforced Polycarbonates

Glass fibers, mainly composed of SiO_2 and Al_2O_3, are used as filler in polymer composites. Having both high modulus (depending on Al_2O_3 it varies from 69 to 430 GPa) and strength (depending on surface and fiber structure uniformity it varies from 0.37 to 5.67 GPa) make the glass fiber to become one of the most important reinforcement agents used in polymers (Brunelle & Korn, 2005; Wallenberger & Bingham, 2010; Carraher, 2014). These properties make the composites to have superior mechanical properties by increasing the tensile and flexural strength, modulus, and impact strength (Brunelle & Korn, 2005; Wallenberger & Bingham, 2010; Carraher, 2014).

Glass fibers have ability of absorbing gamma ray and this ability is proportional to the density of the fibers (Wallenberger & Bingham, 2010). Therefore, glass fibers with high densities (for example lead-, barium- and bismuth-containing) are considered as radiation resistant and used as radiation protective materials (Wallenberger & Bingham, 2010).

Glass fibers reinforced plastics have been used in irradiated areas. These plastics are present as the electrical insulators of superconducting magnet systems which are operated in high radiation fields such as Japan Proton Accelerator Research Complex (J-PARC) jointly operated by Japan Atomic Energy Agency (JAEA), High Energy Accelerator Research Organization (KEK) and the Large Hadron Collider (LHC) at the European Organization for Nuclear Research (CERN) (Idesaki, et al., 2016).

The effect of glass fibers on mechanical, thermal properties of the rubber/waste polyethylene upon irradiation were investigated (Hassan, et al., 2014). Rubbers from automobile tires, polyethylene samples and glass fibers were compounded using Brabender mixer to obtain the composites having 5, 10, 15, and 20 wt. % glass fiber reinforced composites. The composites were irradiated by gamma source up to 150 kGy and they were characterized via mechanical and thermal tests. Mechanical tests revealed that tensile strength were improved with increase in the glass fiber content.

The increase in the tensile strength values were clarified by enhanced interfacial adhesion between glass fibers and matrix. Tensile strength values first slightly increased up to 50 kGy for 5 and 10 % glass fiber loaded composites, and then decreased upon further irradiation dose. Elongations at break were proportional to the tensile strength values. Irradiations up to 150 kGy were resulted in significant decrease in elongation at break values. Thermogravimetric analysis including decomposition temperatures and thermograms showed that both glass fiber and irradiation increased the thermal stability of the composites and this might be attributed to the increase in magnitude of the interfacial linking and radiation induced crosslinks (Hassan, et al., 2014).

Effects of the gamma radiation on the glass fiber reinforced polypropylene were reported (Miranda, et al., 2010). Extrusion and injection molding techniques were applied for compounding to obtain the test specimens. Loading of 15 percent of continuous glass fiber and the irradiation doses, which were 30, 50 and 150 kGy, were the variables. Characterization of the specimens was carried out by tensile test. Tensile test showed that the introduction of the glass fibers into polypropylene matrix doubled the strength values whereas elongations at break were diminished by 83 times. Irradiation decreased the strength and ultimate elongations of both specimens (pure polypropylene and glass fiber reinforced composite). However, it was reported that the deterioration in the neat polymer was more prevalent (Miranda, et al., 2010).

In literature, there has not been any study regarding behavior of polycarbonate-glass fiber composite under gamma irradiation. On the other hand, various studies related with polycarbonate-glass fiber composites claiming positive effects on the properties of the composites were reported (Wee, et al., 2015; Jawali, et al., 2007; Alewelt, et al., 1979). Polycarbonate-glass fiber composites were compounded in order to investigate the mechanical properties (Jawali, et al., 2007). 10, 20 and 30 wt. % glass fiber included composites were prepared by applying extrusion and injection molding methods consecutively. Composites were analyzed by different tests. Hardness, tensile strength, Young’s modulus and impact strength values were compared. Results reported that, glass fiber improved the mechanical properties of the composites such a way that tensile strength (80 to 107.4 MPa), Young’s modulus (1600 to 2966 MPa) and hardness (87 to 93) values were increased, whereas decrease in the impact strength (66.5 to 31.5 J/m) values were reported (Jawali, et al., 2007). It was clearly seen from the literature regarding glass fibers and glass fiber reinforced polymers that glass fibers enhance the mechanical and thermal properties of the composites (Wee, et al., 2015; Jawali, et al., 2007; Alewelt, et al., 1979).

1.6. Radiation Stability of Carbon Fibers and Carbon Fiber Reinforced Polycarbonates

Carbon fiber is the one of the prominent reinforcement material in polymeric composites. The ability of the carbon fibers to manipulate the physical, chemical, electrical and thermal properties of the composites makes it appropriate across a wide range of commercial applications (Mark & Kroschwitz, 2004). Carbon fibers could be produced from polyacrylonitrile (PAN) fibers, mesophase pitch (MPP) and cellulose fibers (rayon). The majority of the carbon fibers are made from polyacrylonitrile (PAN) fibers, whereas carbon fibers based on cellulose fibers (rayon) and mesophase pitch (MPP) are produced in limited quantities (Ruland, 1990). Production of carbon fibers based on polyacryolonitrile (PAN) fibers consists of several steps. These steps are sequenced as (Mark & Kroschwitz, 2004; Zhao, et al., 2016):

- Revolving of precursor fiber,
- Stabilization involving dehydrogenation and cyclization procedures at the temperature of 200-300 ℃ in air,
- Carbonization at the temperatures laid down between 1000 to 3000 ℃ in an inert atmosphere,
- Sizing and surface treatments (called as post carbonization) sequentially

Carbon fibers are used as the reinforcement agent for improving the mechanical and thermal properties of the composites intended to be designed as shielding materials in the radiation protection field (Wang, et al., 2015)

Studies regarding behavior of carbon fibers and its base material which is polyacrylonitrile fibers upon irradiation are available in the scientific literature (Zhao, et al., 2016; Xu, et al., 2010; Sui, et al., 2016; Hao, et al., 2013).

It was reported that, polyacrylonitrile fibers were stabilized under controlled temperature areas and stabilized fibers were irradiated with 100 and 400 kGy doses via Co-60 source emitting gamma radiation (Zhao, et al., 2016). Structure changes and tensile strengths of carbon fibers that were derived from the stabilized samples were compared. According to the results given, carbon fibers derived from irradiated samples had higher tensile strength values compared to the non-irradiated samples. This situation had been explained that cross-linked structures were generated upon irradiation (Zhao, et al., 2016). This situation inhibited the pyrolysis throughout carbonization process and improved the carbon yield of resulting carbon fiber.

In another study, Effects of gamma radiation on carbon fibers were reported (Xu, et al., 2010). Polyacrylonitrile based carbon fibers were irradiated by using ^{60}Co source with five different doses. The doses of irradiation were 200, 500, 1000, 1500 and 2000 kGy. Changes in microstructural and mechanical properties were reported. It was stated that up to 200 kGy, tensile strength of the carbon fibers was increased by 10 percent. Above 1000 kGy, the tensile strength values were diminished significantly that they were below the values of non-irradiated samples. Formation of free radicals on the carbon-carbon double and triple bonds upon irradiation were found to be responsible from these changes in the tensile strengths. Moreover, it was stated that generated radicals produced new ring structure and thereby decreasing the flaws in carbon fibers. Decreasing the number of flaws resulted in improvement of strength of the carbon fibers. Further irradiation might enhance the graphitization, which was supported by X-ray diffraction characterization, and it might grow the crystal size. Due to the inverse relationship between graphitization and grow of the crystal size with tensile strength, mechanical properties of the samples were diminished after 200 kGy. It was easily understood from the article that carbon fibers do not adversely affected from gamma irradiation until reaching the total dose of 200 kGy (Xu, et al., 2010).

The articles in the literature supported the improvement in the properties of carbon fibers upon gamma irradiation (Sui, et al., 2016; Hao, et al., 2013). Carbon fibers had excellent tensile strength, but the experimentally obtained tensile strength values for carbon fiber were lower than theoretical values (Xu, et al., 2010; Hao, et al., 2013). Moreover, surface modification methods enhances the surface activity of carbon fiber but decrease the mechanical strength due to the occurrence of grooves and flaws in the surface (Sui, et al., 2016). In order to improve the mechanical properties and the surface activity of carbon fibers, gamma-irradiation was reported as an effective method ensuring progress in surface activities and mechanical properties simultaneously (Sui, et al., 2016). Increase in the tensile strength in 100 kGy irradiation were reported such a way that that tensile strength were proceeded from 5.97 GPa to 6.83 GPa corresponding 14.4 % improvement (Sui, et al., 2016). Another improvement via radiation was stated that tensile strength was become superior reaching a value 5.4 GPa from 4.6 GPa corresponding %17.4 enhancement (Hao, et al., 2013). According to the scanning electron microscope images, surface defects increased due to etching gamma photons upon irradiation (Hao, et al., 2013).

Radiation effects on carbon fiber loaded composites were also studied (Hoffman & Skidmore, 2009). Epoxy (bisphenol-A based)-carbon fiber composite were irradiated up to 2000 kGy and change in mechanical properties were assessed (Hoffman & Skidmore, 2009). Test results revealed that half value dose (i.e. radiation index which is logarithmic of dose at which properties were reached to end-point criteria specified in TS EN 60544-4) in fracture stress were not achieved in composites (Turkish Standards Institution, 2004; Hoffman & Skidmore, 2009). 2000 kGy did not compromise the strength of the composites significantly (Hoffman & Skidmore, 2009; Turkish Standards Institution, 2004; Wilski, 1987).

Although, there have been various studies regarding polycarbonate and carbon fiber composites (Uawongsuwan & Ichikawa, 2014; Phua & Ishak, 2010; Caldeira, et al., 1998), no reports exist on the degradation of carbon fiber reinforced polycarbonate in the literature.

Carbon fiber reinforced polycarbonate composites with different fiber loading were fabricated using a new fabrication method called direct fiber feeding injection molding (Uawongsuwan & Ichikawa, 2014). The new technique was compared with the conventional method including extrusion and injection molding consecutively. In the new technique, extrusion and injection molding of the polycarbonate-carbon fiber were processed at the same time. The aim of introducing the new technique is to select appropriate conditions as to minimize the excessive fiber attrition. In that study, carbon fiber contents were selected as 10, 20 and 30% by weight. Tensile properties (including tensile strength values, izod impact strength) and SEM analysis were reported. The conclusions for that study stated that tensile strength values were significantly increased from around 60 to 80, 120 and 130 MPa via changing fiber contents to 10, 20, 30% by weight, respectively. Izod Impact strength values via carbon fiber addition were changed from 15 kJ/m^2 to 7 and 8 kJ/m^2 at the contents of 20 and 30%. Two techniques were compared and shown that, tensile strengths of samples prepared by conventional method were slightly higher than the new technique reported. On the other hand, the case for izod impact strengths were vice versa. Samples fabricated by new technique had higher values. Therefore, it was concluded that the new integrated injection molding technology without an extrusion step could be easily adapted and replaced with the existing one (Uawongsuwan & Ichikawa, 2014).

Polycarbonates with hybrid composites including carbon fibers and glass fibers were also studied (Phua & Ishak, 2010). Composites were prepared in different ratios of glass fiber with length of 4.5 mm and carbon fiber with length of 6 mm via keeping the fiber content at 40 % by weight. Preparation of specimens was conducted by using extrusion and injection molding techniques at which compounding and injection temperatures were set to 280 and 275℃, respectively. Mechanical, thermal and morphological properties of all composites and neat polycarbonates were compared with each other. It was shown that tensile strength of polycarbonate filled with glass fiber (40 wt. %) was found to be slightly higher than that of composite containing carbon fiber (40 wt. %). Tensile strength increase in glass fiber loaded composites is more pronounced than composites with carbon fiber. In fact, tensile strength values were expected to be higher at the polymers reinforced with carbon fiber. This was explained by relatively poor fiber-matrix interfacial adhesion between carbon fiber and polycarbonate (Phua & Ishak, 2010). SEM micrographs carried out (Phua & Ishak, 2010) supported the poor adhesion as well. By the addition of carbon fiber and glass fiber, the impact strength of materials resulted in a dramatic reduction. Glass fiber and carbon fiber, considered as stiff materials, increased the stiffness and decreased the toughness of the composites simultaneously. Impact strength values were higher at the higher glass fiber contents, which were explained by the fact that glass fiber was relatively more ductile than the carbon fiber (Phua & Ishak, 2010). It was reported that storage modulus values below the glass transition temperature of the hybrid composites increased with carbon fiber and glass fiber addition (Phua & Ishak, 2010).

On the other hand, storage modulus values were higher in composites rich with carbon fiber (Phua & Ishak, 2010).

Another study including polycarbonate and carbon fiber composites was published in 1998 (Caldeira, et al., 1998). Carbon fibers with length of 50 to 100 µm and average diameter of 0.2 µm were incorporated into the injection molding grade polycarbonate having number average molecular weight of 16000 and weight average molecular weight of 32000. Test specimens were prepared by using the extrusion and the compression molding techniques consecutively. The mechanical properties of the composites having 5, 10, and 20 wt. % carbon fibers were compared. As a result of the study, yield strength of composites linearly improved by gradual addition of carbon fiber such that polycarbonate with 20 wt. % carbon fiber reached the yield stress value 1.5 times higher than value of the pristine polycarbonate. On the other hand, the addition of carbon fiber to the polymer matrix significantly changed the impact strength values negatively (Caldeira, et al., 1998).

1.7. Use of Bentonite in Radiated Areas and Polycarbonate-Bentonite Composites

Bentonites are classified as inorganic polymers and used extensively in the industry (Carraher, 2014). They have been produced by mining. Mixing the bentonite with sodium carbonate during crushing results with divalent metals in bentonite to be changed with Na^+ resulting with improved swelling property (Turkish Standards Institution, 2010). Most of the industrial applications of bentonite are because of the fact that swelling property allows forming viscous water suspensions (Clem & Doehler, 1963). Bentonites have been used in detergents, ceramics, rubber industry (as thickener), drilling fluids. Moreover, treatment of water intended for human consumption and radioactive waste disposal activities are the areas that bentonites have been extensively consumed (Turkish Standards Institution, 1996; Turkish Standards Institution, 1992; Turkish Standards Institution, 1993; Turkish Standards Institution, 1994; Turkish Standards Institution, 1994; Turkish Standards Institution, 1994; Turkish Standards Institution, 2010; Turkish Standards Institution, 2010; Ojovan & Lee, 2005). Bentonites have been used extensively in the radiation areas and they are considered as the key material in the geological disposal of the high-level radioactive wastes. Geological disposal of the high level radioactive waste includes two objectives: (1) the constructed system will isolate the wastes from the biosphere for extremely long periods of time (i.e. at least 300 years), and (2) maintain residual radioactive wastes reaching the biosphere with insignificant reactivity. The isolation of the waste from biosphere includes multi barrier system having natural geological barrier (called as host rock) and engineered barrier system (canister). Multi-barrier system improves the safety via comprising the waste in different materials with different desired properties. These properties are sequenced as having corrosion-resistance and low-permeability to groundwater movement (Sellin & Leupin, 2013). Bentonites are used as buffer material between the canister holding waste and the host rock or as seals in mined disposal galleries. The low hydraulic permeability, plasticity, self-sealing ability, capability to hold radionuclides by physico-chemical adsorption on it and durability of properties over long time make the bentonite to be used extensively in geological disposal of waste as buffer material (Sellin & Leupin, 2013; Delage, et al., 2010; Holmboe, et al., 2009). Use of bentonite in radioactive waste management mainly aims to maintain the overall safety of waste, which corresponds confinement and retardation (Sellin & Leupin, 2013). Schematic representation on use of bentonite in radioactive waste management is shown in **Figure 4**.

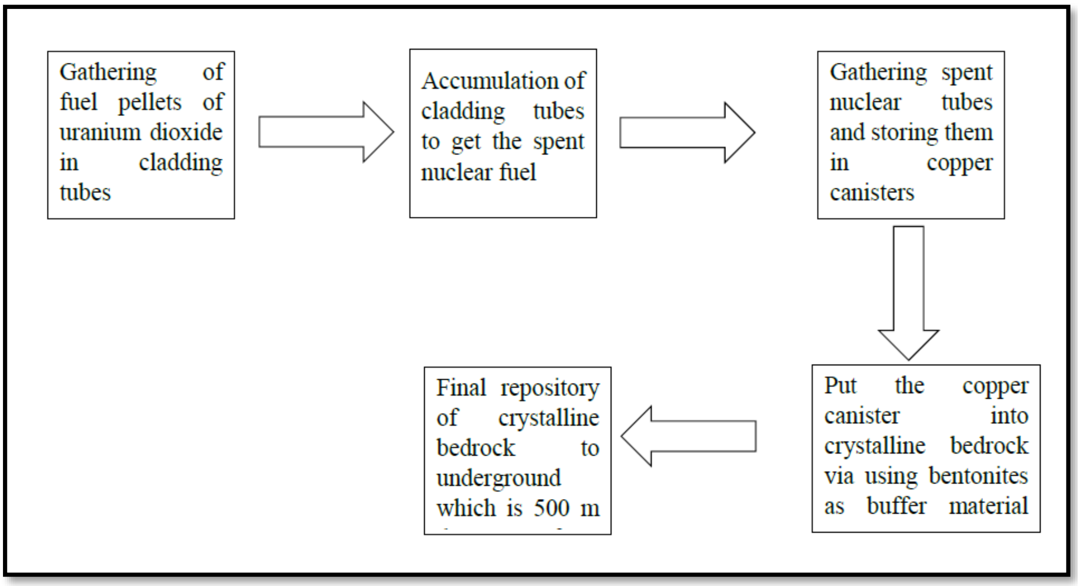

Figure 4 The radioactive waste management method applied in Sweden (Sellin & Leupin, 2013)

The flowsheet shown above includes several steps. Spent fuels are put into the canisters made of copper. The canister is restrained into bedrock and surrounded by bentonite. Similarly, **Figure 5** illustrates the application in Canada (Sellin & Leupin, 2013). The concept includes involvement of bentonites as buffer material between the rock and waste involved in canister.

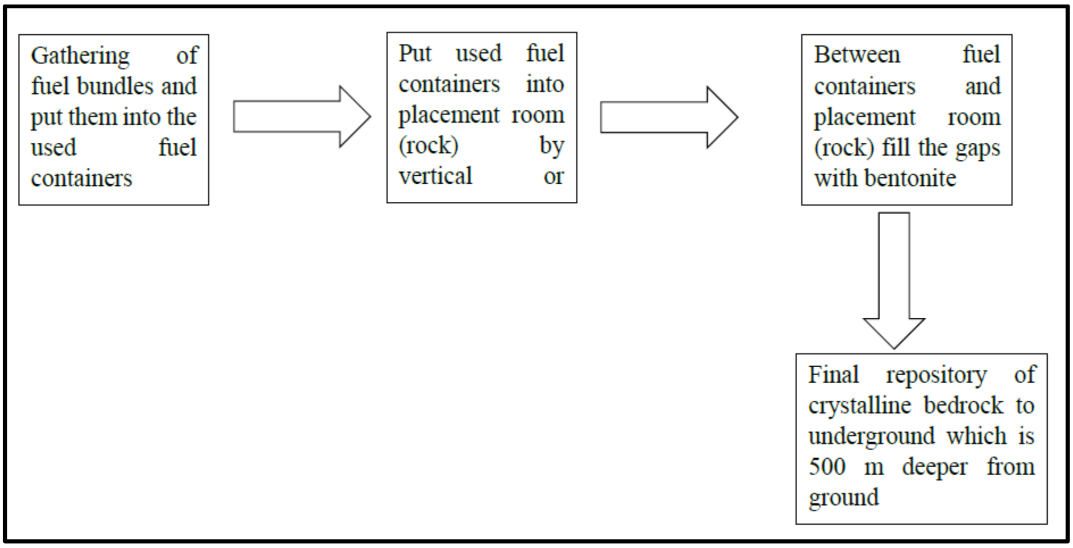

Figure 5 The radioactive waste management method applied in Canada (Sellin & Leupin, 2013)

The most of the concepts present in radioactive waste quarry comprises the use of bentonite as buffer material. Low and intermediate level of radioactive wastes are encapsulated into cement, bitumen or polymers to achieve leaching resistance and mechanical, physical and chemical stability in handling, transporting and disposal (Mahmoud & Geleel, 2012). One of the most prominent technique for handling of low and intermediate level wastes is the immobilization of radioactive waste into cement. To eliminate the unfavorable property of cement, which has relatively high leachibility, improvement techniques on the solidification matrix were studied. Bentonites-cement mixtures were studied to achieve a candidate matrix for immobilization of waste (Mahmoud & Geleel, 2012).

There have been various studies based on polycarbonate/organoclay composites (Orden, et al., 2013; Yoon, et al., 2003; Yoon, et al., 2003; Xiao, et al., 2013).

One of them was related with the degradation of the polycarbonate-clay nanocomposites during the melt processing (Orden, et al., 2013). Three organically modified montmorillonites were used as dispersed phase. Polycarbonate composites having 2 percent of clay were compounded by using twin-screw micro extruder. To investigate the possible degradation of composites; TGA, UV and FTIR techniques were applied during the study reported (Orden, et al., 2013). Results revealed that, clay addition to polymer resulted with thermal degradation. TGA and DTG implied the degradation at around 400 ℃ given a small peak on DTG curves of the composites corresponding at least 5 percent of total mass concentration, which was not present in the curve of the pure polycarbonate. This was associated with (1) the thermal elimination of the organic modification applied to clay and (2) the loss of polymer fraction with low thermal stability, which were generated during melt processing of the composites. On the other hand, T_{max} (temperature at which maximum weight loss rate occur) were higher in composites implying that addition of clays resulted with improved thermal stability. Thermal decomposition of polycarbonate was based on two-step. First step was weight loss due to the thermal decomposition of the polymer and the second was decomposition of char, which were formed in the first step. Char formation was based on crosslinking reactions by heating. Formation of char reduced permeability and restrained the volatile decomposition products. Therefore, increase in the T_{max} was observed. The reason behind the thermal improvement was explained by the formation of large amounts of char caused by clay. New band appearing around 287 nm (applying normalized absorbance method $R=A_{287}/A_{265}$) in the UV spectra were linked with phenolic unit formation and thereby degradation of polycarbonate. In addition, FTIR spectra were found to differ from each other due to appearance of a weak shoulder at around 1730 cm^{-1}, indicating formation of carbonyl groups due to degradation of polymer during processing (Orden, et al., 2013).

The other study was divided into two parts (Yoon, et al., 2003; Yoon, et al., 2003). The polymer-organoclay composites including various percent of dispersed phase (up to 4.7 % by weight) were prepared by using twin-screw extruder at 260 ℃ of barrel temperature and 280 rpm of screw speed (Yoon, et al., 2003; Yoon, et al., 2003). Polycarbonates were selected according to the molecular weights, one was medium and the other was high molecular weight polymer samples. The mechanical properties were taken into account in the first part, while the color formation and thermal degradation during melt processing were considered in the second part. In both cases, mechanical properties of composites were changed with organoclay content. Elastic modulus (2.15 GPa to 3.63 GPa) and yield strength (58.2 MPa to 70.2) values were increased, whereas elongation at break values (144 % to 4.7 %) and thereby impact strength values were decreased significantly (Yoon, et al., 2003). Additionally, the tensile tests of the samples showed that high molecular weight polycarbonates gave better results in terms of stiffness and ductility than medium molecular weight samples. This was clarified by the fact that the higher melt viscosity resulted in higher shear stress, which was considered as major provider for higher modulus (Yoon, et al., 2003). In the second part, the degradation and color formation of polycarbonate-montmorillonite (modified by surfactant) composites were investigated (Yoon, et al., 2003). Discoloration of the polycarbonate indicated the degradative process including chain scission. Surfactants, which were based on ammonium alkyl in the organoclay, started to degrade at 180 °C so that it initiated the color formation resulting with the degradation of polycarbonate. To determine the extent of degradation yellowness index, UV-Vis Spectroscopy and molecular weight determination techniques were applied (Yoon, et al., 2003). The results showed that the clay content was proportional to yellowness index. The R-value, which was ratio of absorbance at 265 nm (referring to ester moiety) to 287 nm (referring to phenolic groups), were selected to determine the degree of degradation. R-values were diminished via increasing the clay content, which corresponded to degradation. This situation was supported by molecular weight determination. Eventually, it was concluded from the study that longer residence time, which resulted in greater dispersion with increased surface area of dispersed phase, and higher clay content produced phenolic end group and brought about molecular weight reduction (Yoon, et al., 2003).

The last study of polycarbonate-clay composites was related with the degradation of composites during the melt processing (Xiao, et al., 2013). Polycarbonate samples were first mixed with hexadecyl trimethyl ammonium chloride modified montmorillonite (OMT). Thermal degradative behaviors of 5 wt. % clay containing composites and pure polycarbonates were compared (Xiao, et al., 2013). Thermogravimetric curves of the samples revealed that onset decomposition temperature corresponding to 5 wt. % weight loss was 65 °C higher in the pure polycarbonate. During the thermal decomposition, clay layers were well dispersed and this hinders the small pyrolysis products such as phenols. Due to evolving of the pyrolysis products slowly, the accumulating phenol behaved as Bronsted acid. Therefore, it initiated the thermal degradation of polycarbonate chains or bisphenol A. Surfactant (alkyl ammonium cations) in clay undergone the Hoffman elimination reaction at around 200 ℃. At the end of reaction, aggregation of the bronsted acid between the aluminosilicate galleries in OMT was occurred. This situation also accelerated the degradation of composite (Xiao, et al., 2013).

The bentonite-polycarbonates studies were focused on the thermal degradation. Due to the presence of surfactants (mostly alkyl ammonium salts) used in surface modifications of bentonite to achieve better exfoliation, polymer matrix undergone degradation at elevated temperatures (at around 180 ℃) (Yoon, et al., 2003). Therefore, it initiated and accelerated the degradation of polycarbonate in melt mixing process. The color formation was detected via yellowness index and UV Vis spectroscopy (Yoon, et al., 2003). Molecular weight reduction and increase in the yellowness index were two important indicators for determining the extent of degradation (Yoon, et al., 2003).

Although there have been various studies on polycarbonate-clay composites, behaviors of these composites under gamma irradiation have not been studied.

1.8. Use of Barite and Its Composites in Radiation Areas

Barite is a natural mineral and is produced by applying mining, crushing, washing, sieving and drying steps (Turkish Standards Institution, 2013). Types of barite are differentiated with each other by barium sulphate ($BaSO_4$) content such that they are classified as either Class A ($BaSO_4$ content at least 90 % percent by weight) or Class B ($BaSO_4$ content at least 80 % percent by weight) (Turkish Standards Institution, 2001). Barites have been used in paints (as an extender), glass making (as an oxidizer and decolorizer), rubber industry (as extender), drilling fluids and medical purposes (as an indicator in medical X-ray photography). Moreover, treatment of water intended for human consumption, design of concrete for the construction facilities handling nuclear materials and radioactive waste disposal activities are the areas that barites have been extensively consumed (Turkish Standards Institution, 2001; Turkish Standards Institution, 2013; Turkish Standards Institution, 2013; Turkish Standards Institution, 2010; Council of Europe, 2005; Ciullo, 1996; Shaaban & Assi, 2011). Barites have been used extensively in the radiation areas due to its ability to shield gamma radiation (Ciullo, 1996).

There have been various studies in literature on the use of barite in radiation areas (Akkurt, et al., 2010; Akkurt, et al., 2014; Shaaban & Assi, 2011; Oto, et al., 2013). The studies have mainly focused on the use of barite in construction materials to improve the radiation attenuation. Lead and tungsten are the suitable materials to be used in radiation shielding but these heavy metals cannot be incorporated into concrete (Akkurt, et al., 2010). For this reason, alternative materials such as barite play an important role for radiation attenuation (Akkurt, et al., 2010).

As mentioned, a study based on radiation attenuation of barite were available in literature (Akkurt, et al., 2010). Barite containing cement were produced and linear attenuation coefficients of the composite material, barite and lead were compared. Linear attenuation tests showed that the best material was lead. Barite could be an alternative shielding material to be incorporated in concrete (Akkurt, et al., 2010). Barite containing concrete was also compared with ordinary concrete. It was reported that concrete with barite indicated better radiation attenuation property (Oto, et al., 2013).

Possible use of barites in radioactive waste management was also reported (Shaaban & Assi, 2011). For low-level radioactive waste management, incorporation of waste into a matrix was the one of the most applied method. Solidification by cementation included encapsulation of radioactive waste. To eliminate the undesired property of cement like high leachability of radionuclides, barite was used as additive (Shaaban & Assi, 2011). Radioactive wastes (including ^{134}Cs) first were embedded into cement and barite containing cement. Then, leaching rates of the radioactive material (in this study ^{134}Cs were used) on solidified wastes were compared. Results revealed that leaching rates were improved by using barite such that barite significantly reduced the leaching rate. It was concluded that cement mixed with barite could be a candidate matrix to be used for incorporation of radioactive waste (Shaaban & Assi, 2011).

Barite was used in coating of cotton-polyester type of fabric designed for radiation workers in nuclear facilities in order to improve the radiation shielding property of the fabric (Akkurt, et al., 2014). The cotton-polyester fabrics were coated via 40, 50, 60 wt% of barite and the produced fabrics' linear attenuation coefficients were determined. Test implied that linear attenuation coefficients were enhanced and they were proportional to the barite contents (Akkurt, et al., 2014).

In the literature, there has not been any study encountered regarding barite containing polycarbonate or radiation degradation of barite containing polymer.

1.9. Aim of the Study

In the application areas where exposure to radiation is inevitable, there have been several materials used as the radiation shielding purposes. These are aligned as polyethylene, glasses, epoxy resin, lead, colemanite, boron steel, boron-containing fabric, boron included paraffin, concrete and Pb-B polyethylene (Duan, et al., 2011; Erdem, et al., 2010). Nevertheless, the mechanical properties and heat resistance of the lead-boron (Pb-B) containing polyethylene was found deficient such a way that it has a tensile strength of 10 MPa polyethylene (Duan, et al., 2011). Furthermore, possible use of polymers including EPDM, PTFE, ETFE, PTFE, PMMA, PCU, LDPE, PS and UHMWPE in the radioactive waste management were studied (Skidmore & Fondeur, 2013; Brownstein, 1991; Cota, et al., 2009; Ozdemir, 2014; Ozdemir & Usanmaz, 2007; Ozdemir, 2006; Hacıoğlu, 2010; Bonin, et al., n.d.). It was concluded from the literature review that it would be beneficial to conduct a study for exploring a candidate polymeric material (with its' composites) to be used in radioactive waste management. For this reason, it was decided to select a polymer with radiation resistance and high tensile strength. On the other hand, radiation shielding and reinforcement properties were the parameters used in selection of additives.

Due to its' considerable radiation resistance and being one of the most widely used plastics, polycarbonates were selected to be studied for assessment of the possible use of it in radioactive waste management (Ebnesajjad & Modjarrad, 2014; Massey, 2004; Legrand & Bendler, 2000; Brunelle & Korn, 2005). Bentonite and barite were selected as the filler due to the reason that they are widely used in the radiated areas (Sellin & Leupin, 2013; Delage, et al., 2010; Akkurt, et al., 2010; Akkurt, et al., 2014; Shaaban & Assi, 2011; Oto, et al., 2013). Carbon fiber and glass fiber were selected because they were widely used additives and give mechanical improvement to the composites (Zhao, et al., 2016; Xu, et al., 2010; Sui, et al., 2016; Hao, et al., 2013; Brunelle & Korn, 2005; Wallenberger & Bingham, 2010; Carraher, 2014).

In this study, degradation of polycarbonate and its composites were investigated. The study was divided mainly into two parts.

In the first part, both degradation stability of polycarbonate under high dose rate (737 Gy/h) irradiation by gamma (γ) source and possible use of polycarbonate in the radioactive waste management were investigated. Polycarbonate samples were irradiated up to four different doses (684, 1291, 3280, 4341 kGy). The high dose rate irradiations were performed and relatively high doses were achieved in order to analyze behavior of material under irradiation. Furthermore, determination of the total dose at which polycarbonate could resist was another goal. Irradiated samples were characterized by applying tensile testing, DMA, TGA, ATR-FTIR, and SEM techniques.

In the second part, polycarbonate composites were compounded by melt mixing process. Two type of particle-reinforced composites and two type of fiber-reinforced composites were compounded. The dispersed phases of composites were chosen according to their availability in the market and functionality upon radiation. Three of the selected additives were inorganic fillers, whereas one of the additive was organic filler. Carbon fiber and glass fiber were obtained from a company producing in Turkey. Barite and bentonite minerals have been present and mined in Turkey as well. Carbon fiber and glass fiber have been widely known as reinforcing agents for polymer composites due to having high mechanical strength and modulus. Barite and bentonites have been extensively used minerals in radioactive waste management due to their specific and unique properties such as the adsorption of radionuclide, swelling property and ability of radiation shielding. In this thesis, the properties of the polycarbonate composites compounded with bentonite, barite, carbon fiber and glass fiber were investigated. Moreover, changes in the properties of the composites under gamma irradiation (up to dose of 75 kGy) were studied. Possible use of different composites in the radioactive waste management were assessed. The composites were compounded via applying extrusion and injection molding steps sequentially. Then composites were irradiated with gamma source (^{60}Co) up to 4 different doses which were 10, 25, 50 and 75 kGy. Samples were characterized by applying tensile testing, hardness (Shore D), DMA, TGA, ATR-FTIR, Spectrophotometry (for yellowness index) and SEM techniques.

CHAPTER 2

MATERIALS AND METHODS

2.1. Materials

In this study, the bisphenol-A-polycarbonate used was Lexan LS2™, which was a commercial product produced by Sabic Innovative Plastics (Saudi Arabia). The used polymer was supplied as UV stabilized. The characteristics of the used polycarbonate met the specifications stated in TS EN ISO 11963 and ASTM D3935 standards (Turkish Standards Institution, 2013; ASTM International, 2009). ASTM D3935 classifies industrial polycarbonates into groups, classes, and grades. They are divided into five groups, which are differentiated from each other by their structures (i.e. homopolymer or copolymer). Then the groups are split in to five classes in terms of used fillers, which give specific property to polymer (general purpose, flame retarded, UV Stabilized, Impact Modified, FDA Compliant formulations-medical grade). Eventually, the classes were grouped into seven grades, which are associated with the polymers melt flow rate (ASTM International, 2009). The selected polycarbonate was medium viscosity grade. It is especially designed for the applications with high optical requirements with respect to clarity and light transmission (SABIC Chemical Manufacturing Company, 2016). According to the ASTM classification, the Lexan LS2™ is classified as Group 1, Class 3 (UV Stabilized) and Grade 3 (ASTM International, 2009). The characteristics of the polycarbonate with respect to TS EN ISO 11963 and ASTM D3935 are given in the **Table 3**.

Table 3 Characteristics of the Polycarbonate Used According to the TS EN ISO 11963 and ASTM D3935 Standards

Property	**Test Method**	**Required Value**
Tensile Stress at Yield, σ_y	EN ISO 527-2	≥ 55 MPa
Nominal Tensile Strain at Break, ε_{TB}	EN ISO 527-2	≥ 60 %
Specific Gravity	ASTM D792	1.19-1.22
Vicat Softening Temperature	EN ISO 306	≥ 145 ℃

Four different additives (bentonite, barite, carbon fiber and glass fiber) were used for compounding of the polymer samples. Two of the additives were in the class of fiber and the remaining two fillers were in the form of powder. Bentonite and barite are inorganic materials in the form of powder. Glass fiber is also inorganic but available in the fiber form. Carbon fiber is the organic material and it is in the fiber form. Bentonite and barite are minerals mined in Turkey. Carbon fiber and glass fiber are synthetic materials and produced in Turkey.

The whole fillers were supplied from Turkey. Bentonite and barite were procured from Karakaya Bentonite Incorporation. They were met the specification according to TS EN ISO 13500 standard. The characteristics of the bentonite and barite are shown in **Table 4** and **Table 5**, respectively.

Carbon fiber, which was in the chopped form, was purchased from DowAksa İleri Kompozit Malzemeler Sanayi LTD. ŞTİ. The general properties of the chopped carbon fiber are shown in **Table 6**.

Glass fibers were procured from Şişecam Cam Elyaf Sanayii A.Ş. and the product specifications are shown in **Table 7**.

Table 4 Characteristics of the Bentonite According to the TS EN 13754 Standard (Turkish Standards Institution, 2010)

Property	**Test Method**	**Typical Values**
Composition of the Bentonite	EN 12902 EN 12485 EN 12485 EN 12485 EN 12485	$50 \leq SiO_2 \leq 70$, %wt $10 \leq Al_2O_3 \leq 20$, %wt $1 \leq MgO \leq 4.5$, %wt $0.5 \leq CaO \leq 4$, %wt $0.5 \leq Na_2O \leq 3$, %wt
Mass Loss at 105 °C	EN 12902	0 ≤ Mass Loss ≤ 15, %wt
Specific Gravity	-	2 g/cm^3 ≤ Absolute Density ≤ 2.4 g/cm^3
Bulk Density Packed	EN 12902	800 kg/m^3 ≤ Bulk Density ≤ 1000 kg/m^3
Particle Size Distribution	EN 12902	At least 95 wt% t of the bentonite have a particle size ≤ 500 µm
Particle Size Analysis	ISO 13320	Volume Mean Diameter: 20.6 µm
Particle Size Analysis	ISO 13320	Volume Median Diameter: 7.45 µm

Table 5 Characteristics of the Barite According to the TS EN 12912 Standard (Turkish Standards Institution, 2013)

Property	**Test Method**	**Typical Values**
Composition of the Barite	EN 12912 EN 12902	92 ≤ $BaSO_4$, %wt Acid Soluble Material ≤ 3, %wt
Specific Gravity	-	4.2 g/cm^3 ≤ Absolute Density ≤ 4.5 g/cm^3
Bulk Density Loose	EN 12902	2200 kg/m^3 ≤ Bulk Density ≤ 2400 kg/m^3
Bulk Density Packed	EN 12902	2500 kg/m^3 ≤ Bulk Density ≤ 2600 kg/m^3
Particle Size Analysis	ISO 13320	Volume Mean Diameter: 9.4 µm
Particle Size Analysis	ISO 13320	Volume Median Diameter: 4.95 µm

Table 6 Characteristics of the Carbon Fiber According to the Producer Specification (Product Code: AC 1101)
(DowAksa İleri Kompozit Malzemeler Sanayi LTD. ŞTİ., 2014)

Property	**Test Method**	**Typical Values**
Tensile Strength	ISO 10618	4200 MPa
Tensile Modulus	ISO 10618	240 GPa
Elongation	ISO 10618	1.8 %
Density	EN 10119	1.76 g/cm^3
Fiber Length	-	3 mm
Sizing Emulsion	-	Epoxy and Phenoxy Based
Sizing Contents	-	1.5 – 3.0 wt. %
Applications	-	Thermosets- Epoxy, Vinylester, Polyester, PC, PPS, Amide, SAN, ABS

Table 7 Characteristics of the Glass Fiber According to the Producer Specification (Şişecam Cam Elyaf Sanayii A.Ş., 2016)

Property	**Typical Values**
Product Code	PH2
Glass Type	E
Sizing Content	0.90 ± 0.15
Sizing Type	Silane
Filament Diameter	13 µm
Chopped Length	4.5 mm
Moisture Content	≤ 0.07 wt. %
Resin Compatibility	Phenolic

2.2. First Part of the Study

In the first part of the study, the dog bone and the bar shaped polycarbonate samples were procured (Kinalir, 2011). The bar shaped and dog bone shaped materials' cross sections sizes were 5 mm in width and 4 mm in thickness. Supplied polycarbonate samples were produced by using a small-scale industrial type injection-molding machine (with trademark of Permak Baby Plast) (Kinalir, 2011). The process parameters for the samples used in the first part were as follow: The injection pressure was 80 bars, the barrel temperature was around 280 ℃ and the mold temperature varied between 25-45 ℃.

Irradiations were carried out in self-contained dry-storage gamma irradiator named Tenex Issledovatel model ^{60}Co γ-source with a dose rate of 737 Gy/h in the presence of oxygen (IAEA, n.d.; IAEA, 2010). The irradiator was designed for research and small-scale irradiation based sterilization (IAEA, n.d.; IAEA, 2010). Irradiations were conducted in Sarayköy Nuclear Research and Training Center of the Turkish Atomic Energy Authority (TAEK). Four different dose values were selected for irradiations and these were 684, 1291, 3280, 4341 kGy. The last sample were irradiated approximately 8 months and such a dose were not available in literature regarding polycarbonate degradation under gamma irradiations. Due to the long irradiation period, decay in the activity of the irradiation source was the key factor in determining and calculating the total dose of irradiation. Total dose of irradiation was calculated using **Equation 1** (Hacioglu, et al., 2013; Zumdahl & Zumdahl, 2010). Where, "TD" was the total irradiation dose, "DR_i" was the initial dose rate, "k" was the constant calculated via dividing the half-life of radionuclide into $\ln 2$, "t" was the irradiation time. Irradiation periods and doses delivered to the test specimens were depicted in **Table 8**.

$$\mathrm{TD} = \int_{0}^{t} \mathrm{DR_i} \times e^{-kt} dt \rightarrow \mathrm{TD} = \frac{\mathrm{DR_i}}{k}(1 - e^{-kt})$$

Equation 1 Total dose calculation

Table 8 Total Doses and Their Corresponding Irradiation Periods

Initial Dose Rate (Gy/h)	**Total Dose (kGy)**	**Period (day)**
737 Gy/h	684 kGy	39 day
737 Gy/h	1291 kGy	74 day
737 Gy/h	3280 kGy	192 day
737 Gy/h	4341 kGy	257 day

2.3. Second Part of the Study

The second part of the study includes the preparation of the samples of neat polycarbonate and polycarbonate with bentonite, barite, carbon fiber and glass fiber. In this part, preparation of the samples was accomplished in three steps. In the first step, polymer granules and fillers (bentonite, barite, carbon fiber and glass fiber) were mixed by using a twin-screw micro extruder (DSM Xplore$^{®}$) (Xplore Instruments, n.d.). In the second step, the materials were cut into small parts (to obtain granule to feed the micro injector) via using pruning shears. Lastly, obtained granules were injected molded by using a micro-injector with 4 ml of barrel and 3.5 ml of molds (DACA Instruments, Santa Barbara, California, USA) to get the dog-bone and the rectangular-bar shaped samples (Daca Instruments, 1999). Extrusion and the injection molding conditions are shown in **Table 9** and **Table 10**, respectively.

Table 9 Conditions for Extrusion of Polycarbonate
(Suin & Khatua, 2012; Dhibar, et al., 2012; Xplore Instruments, n.d.; SABIC Chemical Manufacturing Company, 2016)

Melt Temperature	Screw Speed	Mixing Time	Extrusion Volume	Number of Cycles for Each Compounding for Each Composite
285 ℃	100 rpm	6 min	15 ml (~18.0 gr of PC)	6 cycle

Table 10 Conditions for Injection Molding of Test Specimens
(ASTM International, 2009; Daca Instruments, 1999; European Committee for Standardization, 2006; SABIC Chemical Manufacturing Company, 2016; European Committee for Standardization, 1998)

Injection Parameters	**Values of Injection Parameters**
Melt Temperature	290 ℃
Mold Temperature	90 ℃
Injection Pressure	980 bar (98 MPa)
Residence Time (Melting)	5 min
Injection Time	1-2 sec
Holding Time	5-7 sec
Cooling Time	60 sec
Cycle Time	75-80 sec
Mold Volume	3.5 ml

Prior to compounding, all materials including polycarbonate, barite, bentonite, carbon fiber and glass fiber were dried in oven at 120 ℃ for 5 hour to avoid moisture induced thermal degradation of the components (Suin & Khatua, 2012; ASTM International, 2009; SABIC Chemical Manufacturing Company, 2016; European Committee for Standardization, 2006). The injection molding conditions fulfilled the requirements set out in EN ISO 7391 and ASTM D3935 standards. The extruder and the injection-molding machine used in this study are shown in **Figure 6** and **Figure 7**, respectively.

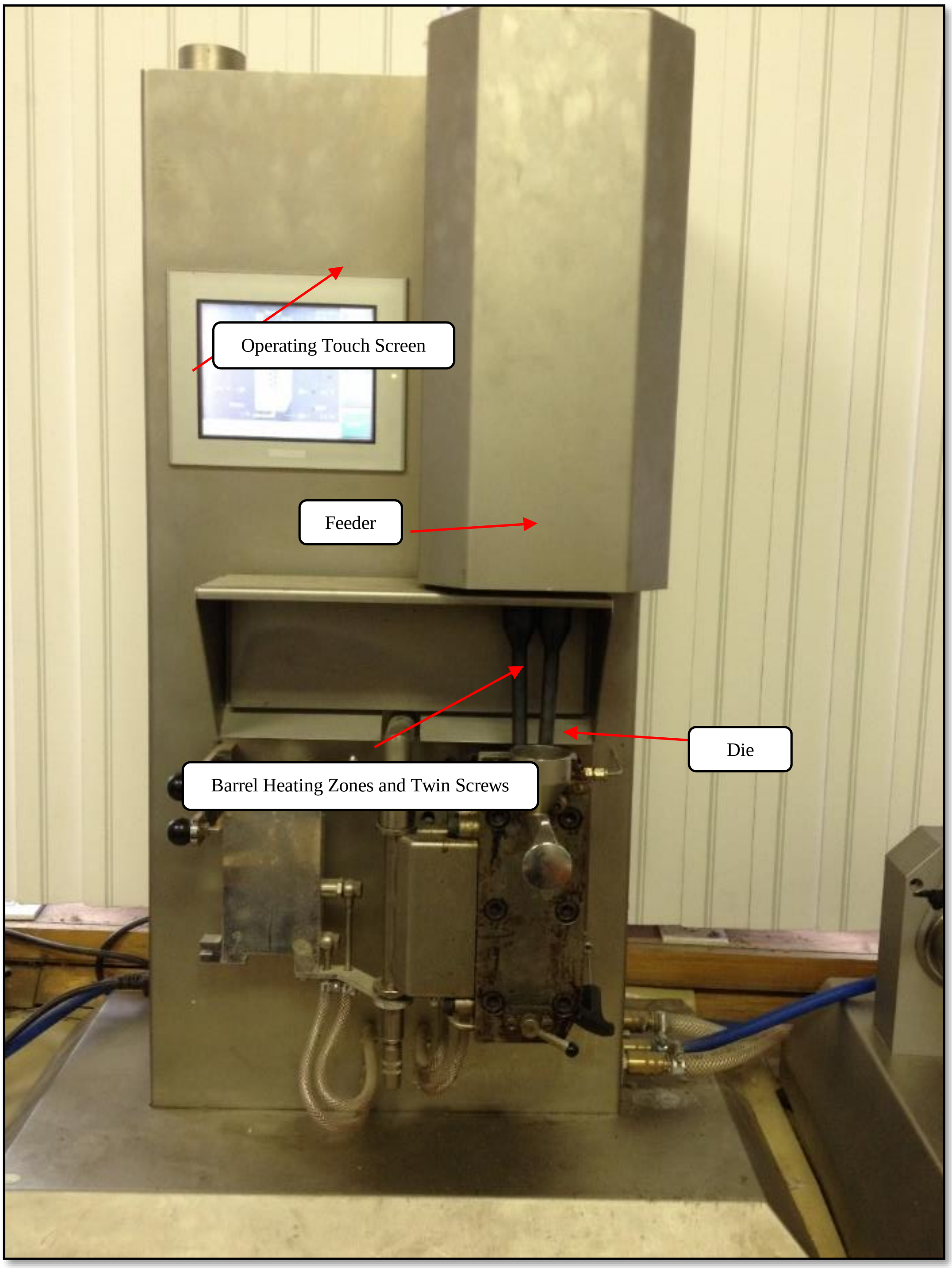

Figure 6 Photograph of the Extruder (15 ml Micro Compounder, DSM Xplore$^{®}$)

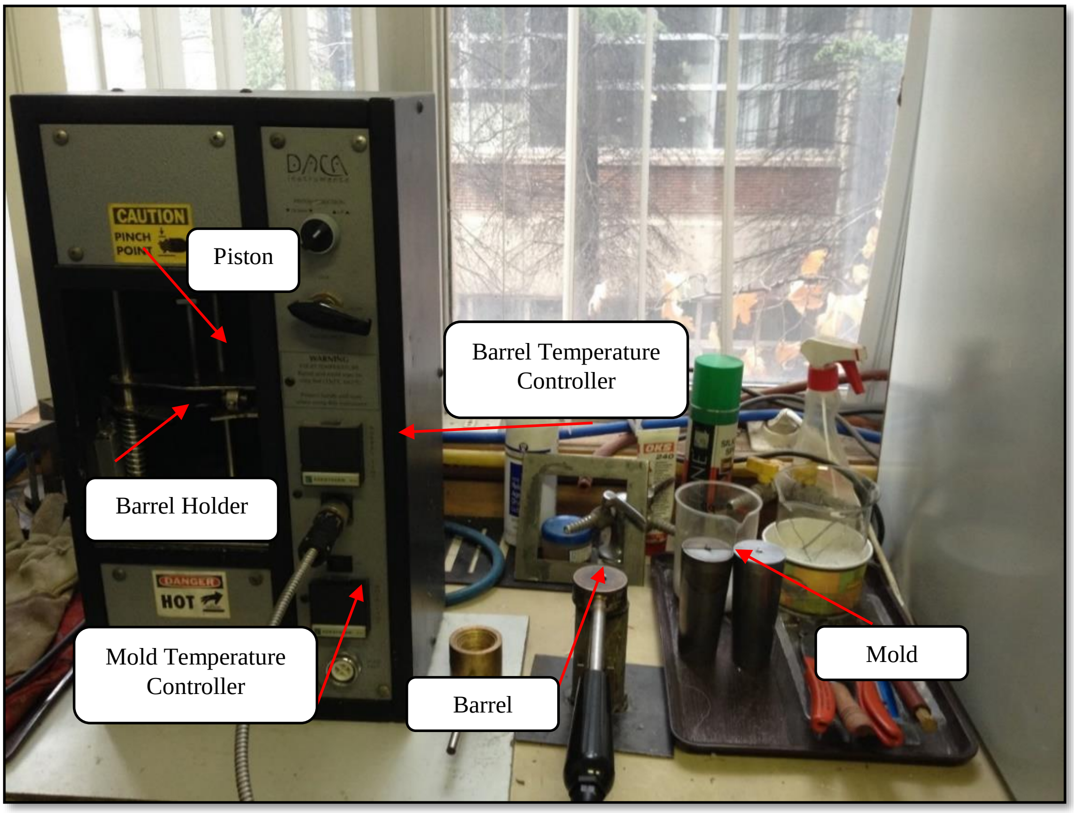

Figure 7 Photograph of the Injection Molding Device(Daca Micro-Injector)

Each type of composites and neat polycarbonate were extruded via 6 consecutive cycles in order to supply enough amount of material for injection molding. Injection molding device were run for consecutive 25 cycles for each type of composites and neat polycarbonate. The dog bone shaped materials were obtained from molds. Their dimensions are tabulated in **Figure 8**.and **Table 11**.

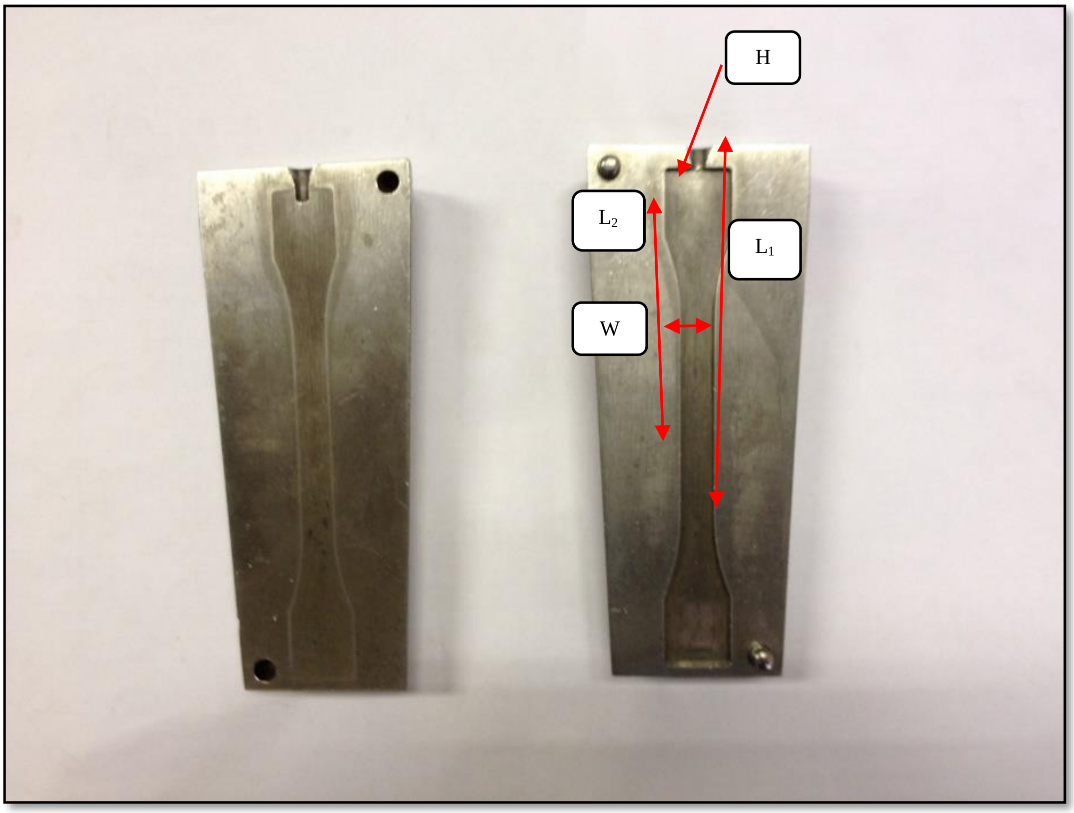

Figure 8 Photograph of the Mold Used to Obtain Dog-Bone and Bar Shaped Materials.

Table 11 Dimensions of Dog Bone Test Specimens Produced (Daca Instruments, 1999; European Committee for Standardization, 2014)

Designation	**Description**	**Dimensions**
L_1	Overall length	110 mm
L_2	Distance between broad parallel-sided portions	60 mm
W	Width at narrow portion	7.5 mm
H	Thickness	2 mm

Rectangular bar-shaped specimens used in DMA analysis were composed from dog-bone shaped materials by cutting them from both ends to obtain eventually narrow parallel-sided portions. Rectangular bar-shaped materials dimensions are shown in **Table 12** and **Figure 9**.

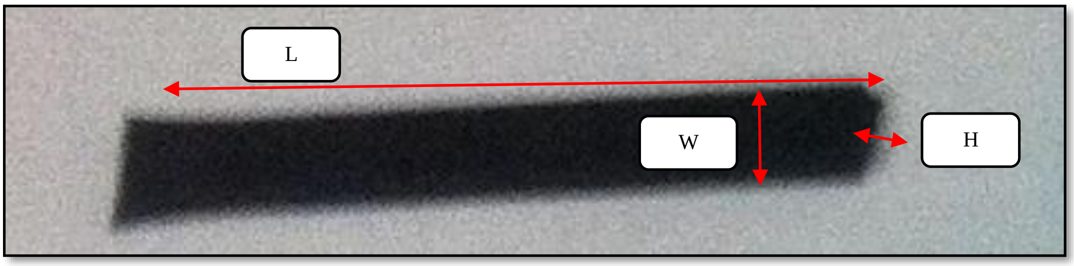

Figure 9 Photograph of the Rectangular Bar Shaped Test Specimen

Table 12 Dimensions of Rectangular Bar-Shaped Test Specimens Produced (Daca Instruments, 1999; European Committee for Standardization, 2014)

Designation	**Description**	**Dimensions**
L	Length	45 mm
W	Width at narrow portion	7.5 mm
H	Thickness	2 mm

For each filler type, three different filler percentages were prepared. The contents of the additives in the composites are given in the **Table 13**.

Table 13 Compositions of Compounded Materials with Different Filler

Composite	**1st Quantity of Additive**	**2nd Quantity of Additive**	**3rd Quantity of Additive**
Polycarbonate + Bentonite	1 % wt	2 % wt	5 % wt
Polycarbonate + Barite	2 % wt	5 % wt	10 % wt
Polycarbonate + Carbon Fiber	2 % wt	5 % wt	10 % wt
Polycarbonate + Glass Fiber	2 % wt	5 % wt	10 % wt

10 percent bentonite incorporation to the polycarbonate caused difficulties in the compounding stage such that the injection molding of the dog-bone shaped specimens were not obtained properly. Therefore, the content of the bentonite incorporation was set different than the content of the other fillers.

To enhance the compatibility between the bentonite and the polymer matrix, bentonite is chemically modified by replacing the interlayer cations with organic ammonium cations (Orden, et al., 2013; Xie, et al., 2001). Alkyl ammonium salts have been used for the modification of bentonite (Orden, et al., 2013; Xie, et al., 2001). However, alkyl ammonium salts undergo chemical degradation at around 180 ℃ (Xie, et al., 2001; Yoon, et al., 2003). This situation triggers the thermal degradation of the polymer chain during melt processing occurring at higher temperatures (Orden, et al., 2013; Xie, et al., 2001; Xiao, et al., 2013; Yoon, et al., 2003). Process temperature of the polycarbonate is around 285 ℃ (SABIC Chemical Manufacturing Company, 2016). Therefore, bentonite and barite minerals were not chemically modified with alkyl ammonium salts.

After neat polycarbonate and composites were compounded and injection molded, the preparations of the test specimens were carried out. Four dog-bone shaped and one rectangular bar shaped specimens for each type of composite and neat polycarbonate were packaged by aluminum folio for each dose of exposure planned.

Irradiations were carried out in Category IV type of irradiator, which was called panoramic wet source storage irradiator. The irradiator had ^{60}Co γ-sources in the form of pencils and they were used for industrial irradiations including food irradiations and medical devices sterilization (IAEA, n.d.; IAEA, 2010). Irradiations were carried out in Sarayköy Nuclear Research and Training Center of the Turkish Atomic Energy Authority (TAEK). Four different dose were selected for irradiations. Doses delivered to the neat and filled polycarbonates are given in **Table 14**.

Table 14 Doses Delivered to the Composites and Neat Polycarbonate

Composites	**1st Total Dose**	**2nd Total Dose**	**3rd Total Dose**	**4th Total Dose**
Neat Polycarbonate	10 kGy	25 kGy	50 kGy	75 kGy
Polycarbonate + Bentonite	10 kGy	25 kGy	50 kGy	75 kGy
Polycarbonate + Barite	10 kGy	25 kGy	50 kGy	75 kGy
Polycarbonate + Carbon Fiber	10 kGy	25 kGy	50 kGy	75 kGy
Polycarbonate + Glass Fiber	10 kGy	25 kGy	50 kGy	75 kGy

2.4. Characterization of Samples

2.4.1 Tensile Test

Mechanical properties of the composites were determined via tensile test. Universal Testing Machine (Zwick Roell Z005 Testing Device having ability to load up to 5 kN was used in order to perform tensile tests. The test specimens called as dog bone shaped conformed the specifications set out in EN ISO 527-2 and EN ISO 20753. Test samples were extended along longitudinal axis at a specific speed, which were predetermined with respect to EN 7391-2 standard. The test was continued until the specimen fractures. During the test, load endured by specimen and elongation were measured and recorded via automatic recording system. To initiate the test, test specimen was placed into grips ensuring the alignment of longitudinal axis of the specimen to the axis of machine. Test speed of polycarbonate and composite samples were fixed at a rate of 50 mm/min, which were specified in EN ISO 7391-2 standard. Stress vs Strain curve were drawn. The stress and the strain were recorded with respect to formulas given in **Equation 2** and **Equation 3** (European Committee For Standardization, 2012).

$$\sigma = \frac{F}{A}$$

Equation 2 Engineering Stress

where “σ” is stress value expressed in MPa, “F” is the force in N, “A” is the cross-sectional area of the test specimen.

$$\varepsilon = \frac{\Delta L_0}{L_0} \times 100,$$

Equation 3 Engineering Strain

where “ε” is strain value expressed in percentage, “L_0” is the gauge length of the test specimen in mm, “ΔL_0” is the increase in the length of sample expressed in mm.

To get an accurate stress-strain diagram, the most important parameters that should be given to the software was gauge length, specimen thickness and width. Testing device records the load in Newton that specimen bear and the increment of crosshead displacement. The load and displacement values were manipulated via several calculations, which is based on equations given above in order to get the stress (MPa) and strain (%) values. Initial cross section area of specimen, which was calculated by multiplying thickness and width of the specimen, was the conversion factor for stress value (in MPa). In other respects, gauge length was the factor for percentage strain.

The example of a Stress-Strain curve from polycarbonate composites is shown in **Figure 10**. Tensile properties, which were obtained from Stress-Strain curve and used for characterization and comparison, were depicted on that curve. Tensile strength and elongation at break values were the properties evaluated for the determination and the assessment of the test specimens’ radiation stability in terms of mechanical aspect. Designation and description of the symbols on the stress-strain curve are given in **Table 15**.

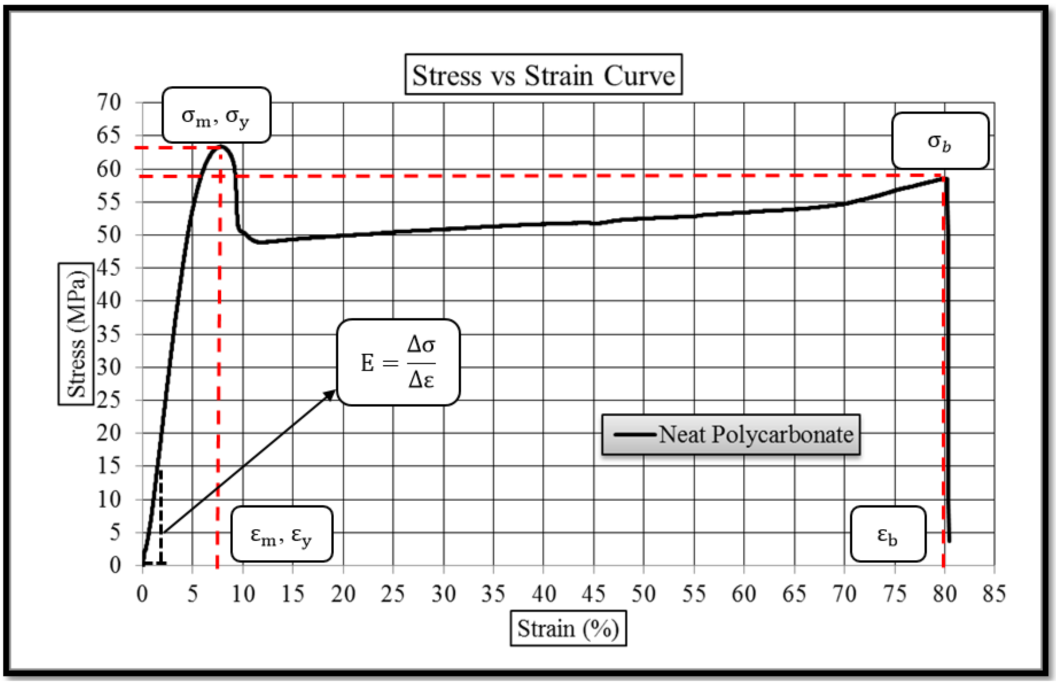

Figure 10 Stress-Strain Curve of Neat Polycarbonate (experimentally obtained)

Table 15 Designation and Description of the Symbols on the Stress-Strain Curve (European Committee For Standardization, 2012)

Symbols	**Description**
ε_y	Strain at yield: The first occurrence in the strain increment without stress increase. It is expressed as percentage.
ε_m	Strain at tensile strength: Strain at which tensile strength is reached. It is expressed as percentage.
ε_b	Strain at break: Strain at the point that stress disappears (i.e. Fracture in the specimen occur). It is expressed as percentage.
σ_y	Yield Strength: Stress at yield strain. It is expressed in MPa.
σ_m	Tensile Strength: Stress at the first local maximum observed in the stress-strain curve. It is expressed in MPa.
σ_b	Stress at break: Stress at test sample breaks. It is expressed in MPa.
E	Elastic Modulus: Slope of the stress-strain curve in the elastic region. It is expressed in MPa.

For each type of composites and their corresponding doses, the average values of each tensile property were taken and recorded from the dog-bone specimens tested. Tensile test machine used in characterization of the specimens is shown in **Figure 11**.

Figure 11 Tensile Test Device (Zwick Roell Z005 Testing Device)

2.4.2 Hardness

Hardness is the mechanical property that determines the resistance of specimens to localized plastic deformation (Callister, Jr., 2007). Hardness tests were carried out by using Zwick 3130 Digital Hardness Tester. The used device was a classified as type D Durameter designed for harder materials. The unit of the hardness was “Shore Hardness D”. Hardness tests were carried out according to the TS EN ISO 868 standard (Turkish Standards Institution, 2006).The thickness of the specimens should be at least 4 mm. 3 dog-bone specimens were added up to reach 6 mm thickness. Then, indenter in the durameter was forced into the specimens and after 15 seconds, the depth of penetration was recorded. For each test, five consecutive measurements at different positions on the test sample were carried out and average of them were recorded. The test device used in hardness measurement is shown in **Figure 12**.

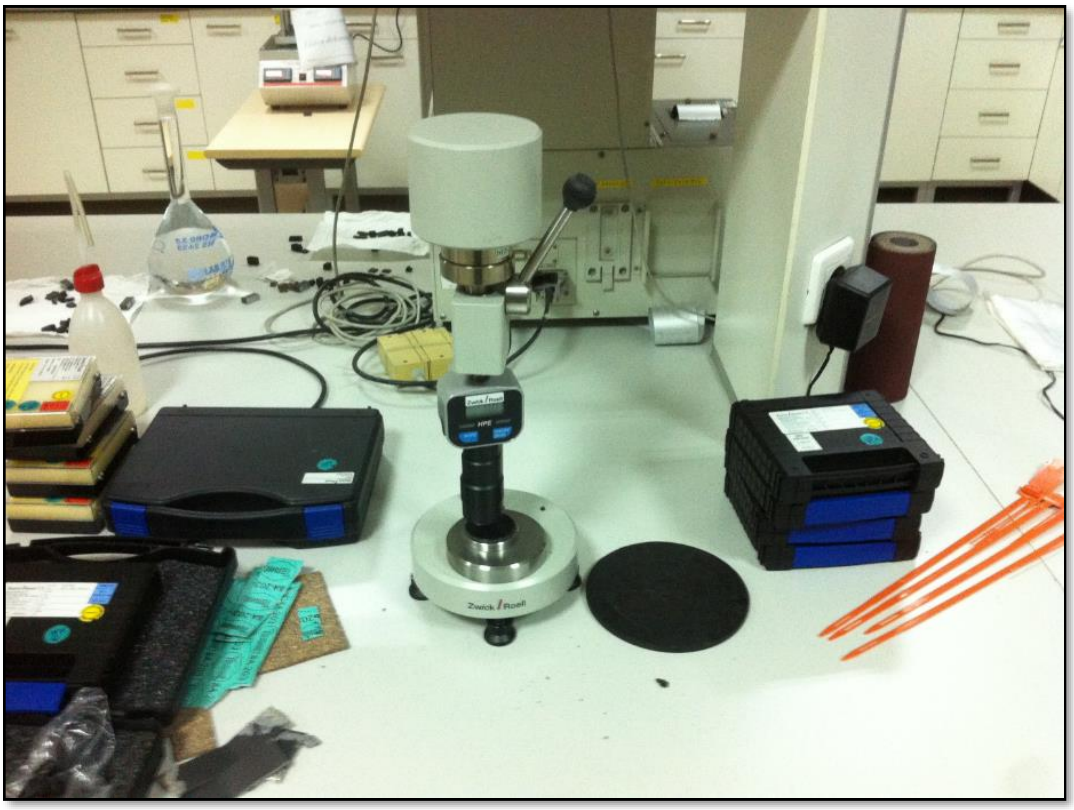

Figure 12 Hardness Test Device (Zwick 3130 Digital Hardness Tester.)

2.4.3 Yellowness Index (YI) and CIELAB Color Scales

Yellowness is a property of color perception such a way that a material color is changing from colorless or white toward yellow (ASTM International, 2010). Yellowness index is a number obtained from spectrophotometric data via several calculations. It reveals the degree of changing an object’s color from white or colorless toward yellow (ASTM International, 2010).

The spectrophotometric results are converted into color scales. CIELAB is the one of the color scales. Data acquired from spectrophotometric results are manipulated to obtain color scales. CIELAB color scales are defined as opponent color scales and these are represented by letters “L^*”, “a^*” and “b^*”. “a^*” get positive values in the red direction and negative values in the green direction. On the other hand, “b*” takes positive values in the yellow direction and negative values in the blue direction (ASTM International, 2013). Yellowness index and CIELAB color scales are calculated from CIE Tristimulus values, which are defined as X, Y and Z.

Yellowness index and CIELAB color scales values of glass fiber reinforced composite and neat polycarbonate were measured by using XRITE ColorEye® Spectrophotometer. Yellowness index test were carried out with respect to ASTM E313. On the other hand, CIELAB color scales were measured according to the ASTM E308 standards. The test device used in measurements is shown in **Figure 13**.

Figure 13 XRITE ColorEye® Spectrophotometer.

2.4.4 Attenuated Total Reflection Fourier Transform Infrared Spectroscopy (ATR-FTIR)

Infrared Spectroscopy is one of the most common spectroscopic method in identification of polymer structure (Carraher, 2014). Infrared region is in the range from 0.78 to 1000 μm in wavelength and 12,800 to 10 cm^{-1} in wavenumber (ASTM International, 2015). Infrared radiation stimulates molecular vibrations. Test samples absorb some frequencies of the Infrared Radiation and transmit the remainder light. Transmitted light is collected by detector as interferogram, (record of signal measured). By using Fourier Transform, which is a mathematical process, interferogram is converted to amplitude-wavelength spectrum (ASTM International, 2015).

Attenuated Total Reflection Fourier Transform Infrared (ATR-FTIR) spectra of irradiated composites and neat polycarbonate samples were noted at 25 ℃ on a Perkin Elmer Spectrum BX Fourier Transform Infrared Spectrophotometer with Attenuated Total Reflection (ATR) accessory. Samples were scanned from 4000 cm^{-1} to 600 cm^{-1} with a resolution of 16 cm^{-1}. The ATR-FTIR test device is shown in **Figure 14**.

.

Figure 14 Perkin Elmer Spectrum BX Fourier Transform Infrared Spectrophotometer with Attenuated Total Reflection (ATR) Accessory

2.4.5 Thermogravimetric Analysis (TGA)

Thermogravimetry determines the decomposition rates of polymers and their corresponding temperatures (Turkish Standards Institution, 2014). Moreover, it helps to determine the amount of highly volatile matter, medium volatile matter, combustible material and ash content (ASTM International, 2014).

Decomposition, oxidation and volatilization bring about mass loss in the polymer. The change of sample's weight with respect to temperature and instantaneous rate of this change (i.e. derivative of the curve) give valuable information about the thermal stability of the polymer. For this reason, TG curves are used to compare the thermal stabilities of polymers and their composites, which are grouped in same generic family (Turkish Standards Institution, 2014). Some specific temperatures obtained from TGA are used for evaluation of thermal stability polymers and their composites. These temperatures are classified as T_{onset} (onset decomposition temperature), T_{max} (temperature at which highest rate of weight loss occurs obtained from first derivative of TG curve) and T_{50} (temperature at which 50 % weight loss occur) (Pashaei, et al., 2011).

Termogravimetric measurements were done in dynamic mode, which included weight change versus temperature (Turkish Standards Institution, 2014). Test specimens were heated with a specified heating rate and the change in weight were obtained with respect to temperature. Then the changes in the weight with respect to temperature were plotted as a thermogravimetric curve (TG) by software (Turkish Standards Institution, 2014).

Thermogravimetric analysis (TGA) was carried out on Perkin Elmer Pyris 1 Thermogiravimetric Analyzer. TGA studies were carried out according to the specifications drawn up in ASTM E1131 and TS EN ISO 11358-1 standards. Test parameters are shown in **Table 16**.

Table 16 Thermogravimetric Analysis Parameters
(ASTM International, 2014; Turkish Standards Institution, 2014).

Heating Rate	**Atmosphere**	**Temperature**	
		Initial	**Final**
$10\ \frac{^{\circ}\mathrm{C}}{\mathrm{min}}$	N_2	25 ℃	800 ℃

The example of TG curve and first derivative of the TG Curve are shown in **Figure 15** and **Figure 16**, respectively (ASTM International, 2014; Turkish Standards Institution, 2014; Perkin Elmer Corporation, 2015).

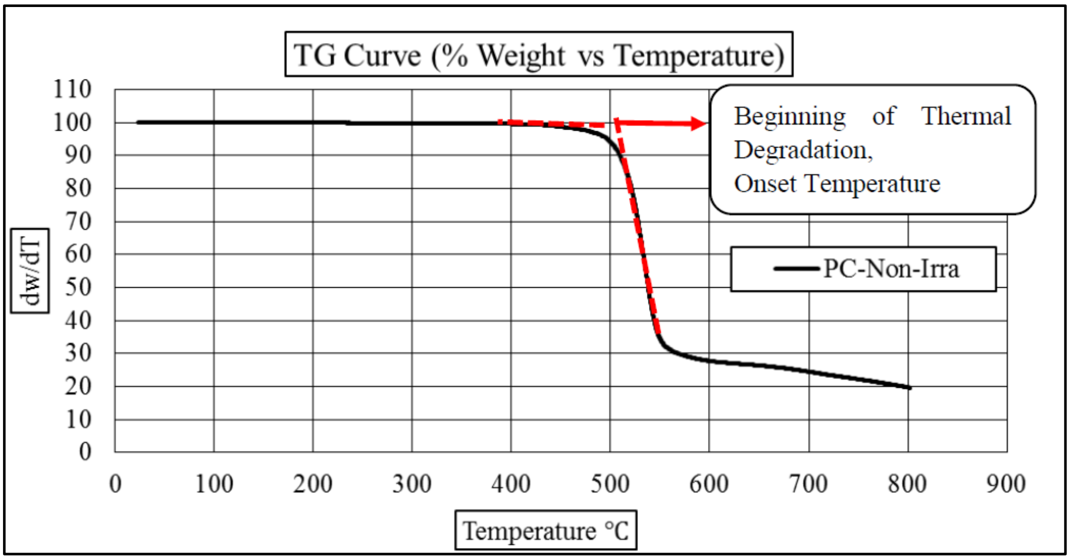

Figure 15 Thermogravimetric (TG) Curve of Neat Polycarbonate (experimentally obtained)

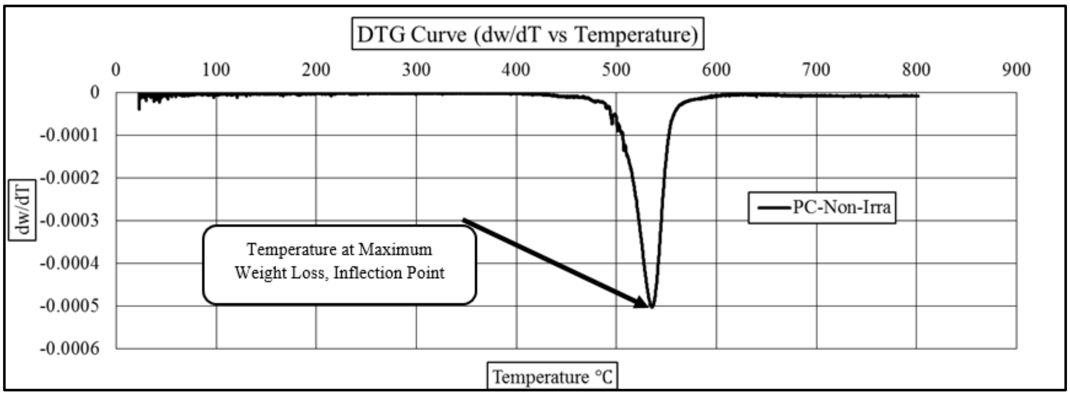

Figure 16 First Derivative of Thermogravimetric (DTG) Curve for Neat Polycarbonate (experimentally obtained)

2.4.6 Dynamic Mechanical Analysis (DMA)

Dynamic Mechanical Analysis (DMA) characterizes a polymer's properties as a function of temperature. Test specimen is forced to an oscillating force and its' response to that force are analyzed (Turkish Standards Institution, 2011; Menard, 2008; TA Instruments Corporation, 2016; Perkin Elmer Corporation, 2013). The test specimen with rectangular shaped geometry is subjected to mechanical oscillation, which is identified by two characteristics called as mode of deformation and mode of vibration (Turkish Standards Institution, 2011). DMA determines the storage and loss modulus of polymers over specified temperature range by changing the temperature with respect to predetermined heating rate. Storage modulus (maximum energy stored during a loading cycle and it is elastic component) and loss modulus (energy dissipated during one loading cycle through molecular motion and it is viscous component) curves infer viscoelastic properties of polymer (Turkish Standards Institution, 2011; Menard, 2008; TA Instruments Corporation, 2016; Perkin Elmer Corporation, 2013). Prompt changes in storage modulus and loss modulus curves at distinct temperatures are indicative of transition regions. These transitions occurred in storage modulus are called as gamma (γ), beta (β) and alpha (α) transitions. Storage modulus (measure of stiffness) is dependent on temperature and applied stress (Menard, 2008). Via increasing the temperature, stiffness of polymers is reduced and thereby decreasing the modulus. This decrease becomes significant when the polymer passes through its glass transition (i.e. transformation from glassy state to rubbery state). The significant decrease in storage modulus is explained by alpha (α) transition, which is associated with gradual chain movement (Menard, 2008). Therefore, the alpha transition temperature (T_α) is considered as glass transition temperature (T_g) at the same time (Menard, 2008; International Organization for Standardization, 2012; Perkin Elmer Corporation, 2013; TA Instruments Corporation, 2016; ASTM International, 2015).

When polymer loses elasticity via heating, it becomes more viscous. This trigger situation that loss modulus enhanced. At the peak point of the loss modulus vs temperature curve, the glass transition of polymer begins. Therefore, the temperature at peak point of loss modulus is considered as T_g (Menard, 2008; International

Organization for Standardization, 2012; Perkin Elmer Corporation, 2013; TA Instruments Corporation, 2016; ASTM International, 2015).

Beside the storage modulus and loss modulus, there is one more important parameter in DMA, which is phase angle (δ). It is a phase difference between sinusoidal stress and sinusoidal strain. It varies from 0 to 90 degrees. As polymers become elastic, the phase angle approaches to zero. On the other hand, the angle approaches to 90, when the material loses elasticity and viscous part is enhanced. The tangent of the phase angle (damping: tan δ) is defined as ratio of loss modulus to storage modulus. It supplies information about efficiency that how polymer drops energy to molecular rearrangements and internal friction (Menard, 2008; International Organization for Standardization, 2012; Perkin Elmer Corporation, 2013; TA Instruments Corporation, 2016; ASTM International, 2015). It is also indicative of glass transition temperature. Peak point of tan δ is considered as T_g (Menard, 2008; International Organization for Standardization, 2012; Perkin Elmer Corporation, 2013; TA Instruments Corporation, 2016; ASTM International, 2015).

DMA curves of irradiated samples were taken by using the Perkin Elmer Diamond Dynamic Mechanical Analyzer. DMA studies were carried out with a heating rate of 5 ℃/min and at 1 Hz frequency. The temperature range for the DMA analysis was between 25 and 300℃. Mode of vibration was selected as constant frequency (1 Hz) and the mode of deformation was chosen as flexural vibration. The glass transition temperatures were determined according to the ISO 6721-11 and ASTM D 7028 standards. Glass Transition temperatures could be determined via Storage Modulus, Loss Modulus and Tan δ Curves. In this study, the “Tan δ & Temperature Curves” (peak points) and “Loss Modulus & Temperature Curves” (peak point) were used for determination of glass transition temperatures.

The example of DMA curves are shown in **Figure 17**, **Figure 18** and **Figure 19**. The description of symbols and showings on the DMA curves are given in **Table 17**.

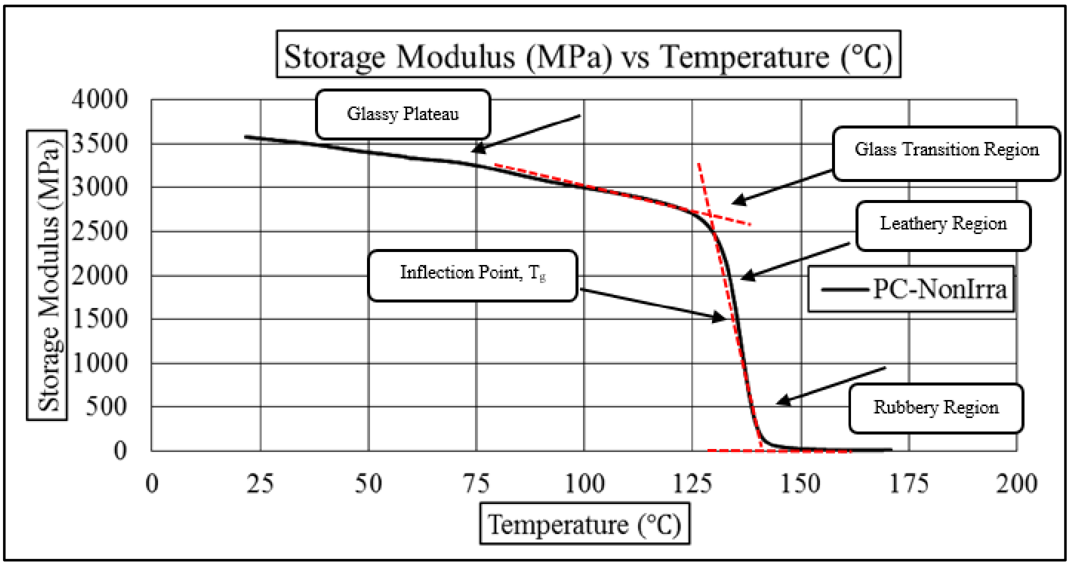

Figure 17 Storage Modulus (MPa) vs Temperature (°C) Curve for Neat Polycarbonate (experimentally obtained)

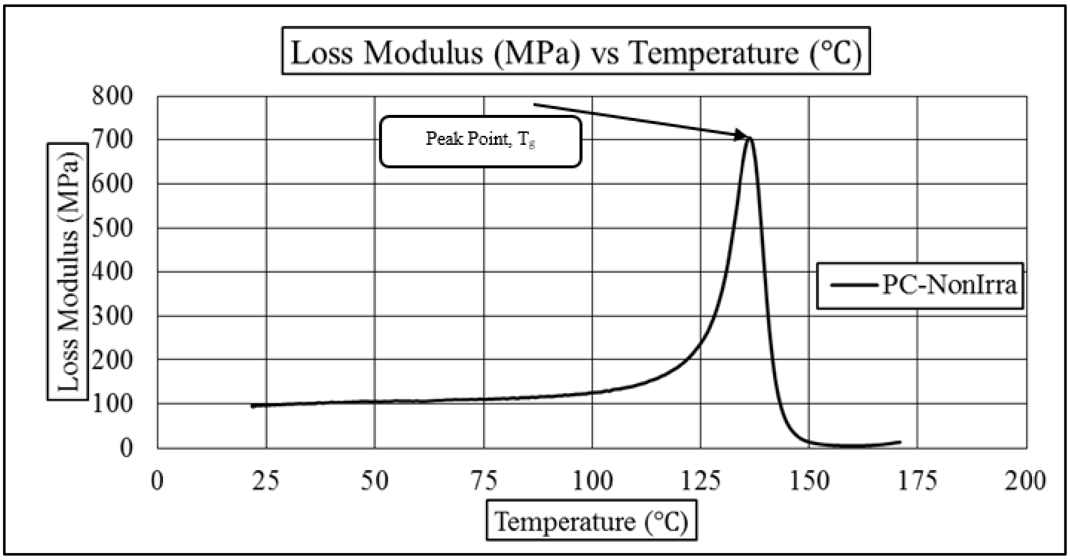

Figure 18 Loss Modulus (MPa) vs Temperature (°C) Curve for Neat Polycarbonate (experimentally obtained)

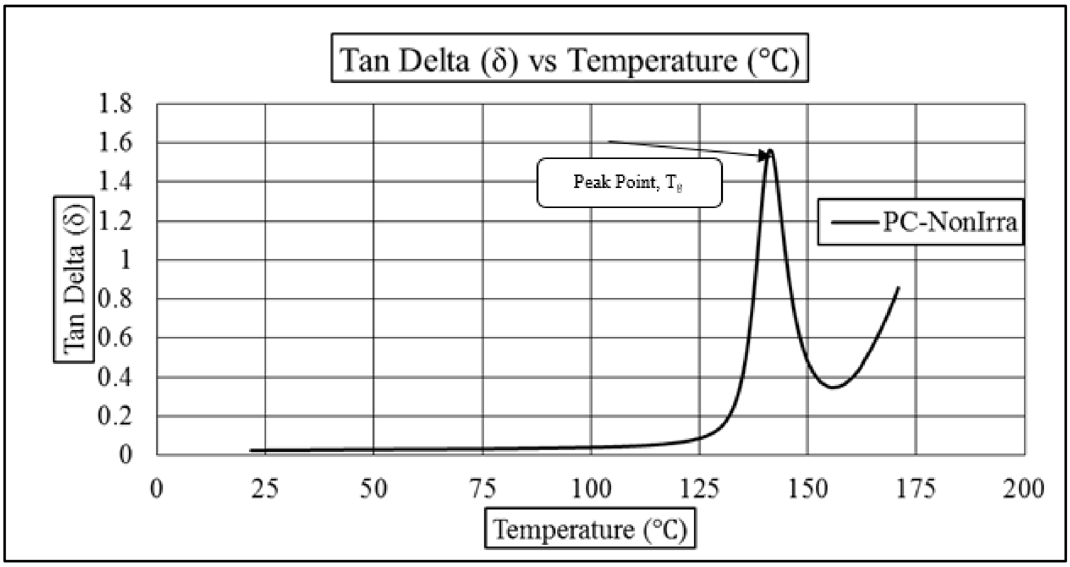

Figure 19 Tan δ vs Temperature (℃) Curve for Neat Polycarbonate (experimentally obtained)

Table 17 Symbols and Showings in DMA Curves
(Perkin Elmer Corporation, 2013; Menard, 2008; Carraher, 2014)

Symbols	**Definitions**
Glassy Plateau	Specimen is hard. Ability of chains movement is limited. Little molecular motion present below T_g. Stress response is strain independent (Elastic behavior). Free volume increases and thereby occurring localized bond movements and side chain movements by increasing the temperature below T_g.
Glass Transition Region	Free volumes significantly increase such that chains initiate large-scale motions. Specimen loses hardness. Storage modulus decreases and tan delta increases.

Table 17 Symbols and Showings in DMA Curves
(Perkin Elmer Corporation, 2013; Menard, 2008; Carraher, 2014)

Symbols	**Definitions**
Leathery Plateau	Movement of chains enhanced. Specimen softens. Therefore, it becomes tough and flexible.
Rubbery Plateau	Specimen chains gain sufficient mobility to slide by each other.
Glass Transition Temperature	The temperature at which sufficient free volume and energy is achieved to initiate the main chain gradual movement. Polymer changes from hard glassy state to more flexible rubbery state.

2.4.7 Melt Flow Rate (MFR)

Melt Flow Rate (MFR) test is used to determine the rate of extrusion of molten polymers by extrusion plastometer. Barrel of plastometer are fed by polymer granules and after a preheating time, one of the standard load is applied to the piston. Piston descends under gravity and extrudates of polymer were collected between specified time intervals (cut-off time interval) by using timer. Cut-off extrudates are then collected and weighted. Average weight in gram per specified time is converted into g/10 min.

Melt Flow Rate determination was based on mass-measurement method (Procedure A, TS EN ISO 1133-1) and results were given as melt mass-flow rate, which was expressed as g/10 min. Test were conducted with respect to TS EN ISO 1133-1 standard by using Coesfield Material Test- Meltflixer LT extrusion plastometer.

The test parameters including temperature, load weight, preheating time, charging time of polymer into barrel, extrudate cut-off time and the weight of the test sample are given in **Table 18**. The photograph of the test device is given in **Figure 20**.

Table 18 Melt Flow Rate Parameters
(Turkish Standards Institution, 2012)

Temperature	**Load Weight**	**Charging Time of Polymer into Polymer**	**Preheating time**	**Cut Off Time Interval**	**Weight of Sample**
280 ℃	2.16 kg	≤ 1 min	5 min	12 seconds	4-8 gr

Figure 20 Coesfield Material Test- Meltflixer LT Extrusion Plastometer

2.4.8 Scanning Electron Microscopy (SEM)

Scanning Electron Microscopy (SEM) allows the observation and characterization of polymers and their composites on nanometer (nm) to micrometer (μm) scale. Scanning Electron Microscopy is mainly used for retrieval of topographic images in the magnification range 10-10000 X (Goldstein, et al., 2003).

In the SEM, polymer surface is irradiated via finely focused electron beam to form images. Each point on the surface of sample, which is bombarded with electron beams, emits signals in the form of electromagnetic radiation (Goldstein, et al., 2003). These signals are in the type of secondary electrons, backscattered electrons, characteristic x-rays, and other photons of having different energies. The emitted signals are obtained by detector. Collected signals are amplified and showed on computer monitor in order to interpret the surface topography of samples. For surface topography, most important signals are considered as secondary electrons, backscattered electrons that vary with respect to differences in topography (Goldstein, et al., 2003).

Characteristic x-rays are emitted after electron bombardment. These emitted x-ray signals provide both qualitative and quantitative elemental information of specimen (in the region of 1 μm of diameter and in depth) (Goldstein, et al., 2003). The accessory addition of Scanning Electron Microscope allows measuring the emitted X-rays. This accessory is called Energy-Dispersive X-ray Spectrometer (EDX). Scanning Electron Microscope incorporated with EDX supplies qualitative and quantitative analysis such a way that it collects characteristic x-rays from major elements (all elements having atomic number larger than 4), which have weight proportion larger than 10 % (Goldstein, et al., 2003).

For analysis of polymers, due to having low atomic numbers elements, the yield resulting from secondary electron signals is low. These low yielding results in poor signal to noise ratio and thereby observing deficiencies in high-resolution imaging. To enhance the signal to noise ratio, metal coating (mostly gold) is applied to the polymer (Goldstein, et al., 2003). The other reason for metal coating is to prevent the contamination occurred by charging of nonconductive polymers. Charging of nonconductive specimen causes the domination of contamination in image and thereby causing misinterpretation (Goldstein, et al., 2003).

Scanning electron microscope (SEM) images were taken by using a FEI Quanta 400F Scanning Electron Microscope with a thin layer of golden coating. Original and fracture surfaces of the samples were used in the SEM studies.

2.4.9 Test Matrices of the Polycarbonate Specimens

Applied tests used for characterization of each neat polycarbonate and composite specimens for each irradiation dose were given in **Table 19**.

Table 19 Test Matrices of Specimens

Test Sample	Dose kGy	Tensile Test	Hardness	ATR-FTIR	TGA	DMA	SEM	MFR	YI
PC	0	✓	✓	✓	✓	✓	✓	✓	✓
PC	10	✓	✓	✓	✓	✓	-	✓	✓
PC	25	✓	✓	✓	-	-	✓	✓	✓
PC	50	✓	✓	✓	✓	✓	✓	✓	✓
PC	75	✓	✓	✓	✓	✓	✓	✓	✓
PC	684	✓	-	✓	✓	✓	✓	-	-
PC	1291	✓	-	✓	✓	✓	✓	-	-
PC	3280	✓	-	✓	✓	✓	✓	-	-
PC	4341	-	-	✓	✓	-	✓	-	-
PC/1B	0	✓	✓	-	-	-	-	✓	-
PC/1B	10	✓	✓	-	-	-	-	-	-
PC/1B	25	✓	✓	-	-	-	-	-	-
PC/1B	50	✓	✓	-	-	-	-	-	-
PC/1B	75	✓	✓	-	-	-	-	-	-
PC/2B	0	✓	✓	-	-	-	-	-	-
PC/2B	10	✓	✓	-	-	-	-	-	-
PC/2B	25	✓	✓	-	-	-	-	-	-
PC/2B	50	✓	✓	-	-	-	-	-	-
PC/2B	75	✓	✓	-	-	-	-	-	-
PC/5B	0	✓	✓	✓	✓	✓	✓	✓	-
PC/5B	10	✓	✓	✓	✓	✓	-	-	-
PC/5B	25	✓	✓	✓	✓	✓	✓	-	-

Table 19 Test Matrices of Specimens

Test Sample	Dose kGy	Tensile Test	Hardness	ATR-FTIR	TGA	DMA	SEM	MFR	YI
PC/5B	50	✓	✓	✓	✓	✓	✓	-	-
PC/5B	75	✓	✓	✓	✓	✓	✓	-	-
PC/2Ba	0	✓	✓	-	-	-	-	✓	-
PC/2Ba	10	✓	✓	-	-	-	-	-	-
PC/2Ba	25	✓	✓	-	-	-	-	-	-
PC/2Ba	50	✓	✓	-	-	-	-	-	-
PC/2Ba	75	✓	✓	-	-	-	-	-	-
PC/5Ba	0	✓	✓	-	-	-	-	✓	-
PC/5Ba	10	✓	✓	-	-	-	-	-	-
PC/5Ba	25	✓	✓	-	-	-	-	-	-
PC/5Ba	50	✓	✓	-	-	-	-	-	-
PC/5Ba	75	✓	✓	-	-	-	-	-	-
PC/10Ba	0	✓	✓	✓	✓	✓	✓	✓	-
PC/10Ba	10	✓	✓	✓	✓	✓	-	-	-
PC/10Ba	25	✓	✓	✓	✓	✓	✓	-	-
PC/10Ba	50	✓	✓	✓	✓	✓	✓	-	-
PC/10Ba	75	✓	✓	✓	✓	✓	✓	-	-
PC/2CF	0	✓	✓	-	-	-	-	✓	-
PC/2CF	10	✓	✓	-	-	-	-	-	-
PC/2CF	25	✓	✓	-	-	-	-	-	-
PC/2CF	50	✓	✓	-	-	-	-	-	-
PC/2CF	75	✓	✓	-	-	-	-	-	-
PC/5CF	0	✓	✓	-	-	-	-	✓	-
PC/5CF	10	✓	✓	-	-	-	-	-	-
PC/5CF	25	✓	✓	-	-	-	-	-	-
PC/5CF	50	✓	✓	-	-	-	-	-	-
PC/5CF	75	✓	✓	-	-	-	-	-	-
PC/10CF	0	✓	✓	✓	✓	✓	✓	✓	-
PC/10CF	10	✓	✓	✓	✓	✓	-	-	-

Table 19 Test Matrices of Specimens

Test Sample	Dose kGy	Tensile Test	Hardness	ATR-FTIR	TGA	DMA	SEM	MFR	YI
PC/10CF	25	✓	✓	✓	✓	✓	✓	-	-
PC/10CF	50	✓	✓	✓	✓	✓	✓	-	-
PC/10CF	75	✓	✓	✓	✓	✓	✓	-	-
PC/2GF	0	✓	✓	-	-	-	-	✓	✓
PC/2GF	10	✓	✓	-	-	-	-	-	✓
PC/2GF	25	✓	✓	-	-	-	-	-	✓
PC/2GF	50	✓	✓	-	-	-	-	-	✓
PC/2GF	75	✓	✓	-	-	-	-	-	✓
PC/5GF	0	✓	✓	-	-	-	-	✓	✓
PC/5GF	10	✓	✓	-	-	-	-	-	✓
PC/5GF	25	✓	✓	-	-	-	-	-	✓
PC/5GF	50	✓	✓	-	-	-	-	-	✓
PC/5GF	75	✓	✓	-	-	-	-	-	✓
PC/10GF	0	✓	✓	✓	✓	✓	✓	✓	✓
PC/10GF	10	✓	✓	✓	✓	✓	-	-	-
PC/10GF	25	✓	✓	✓	✓	✓	✓	-	✓
PC/10GF	50	✓	✓	✓	✓	✓	✓	-	✓
PC/10GF	75	✓	✓	✓	✓	✓	✓	-	✓

The abbreviations of PC, B, Ba, CF, GF were used for polycarbonate, bentonite, carbon fiber and glass fiber, respectively. The sample coded as PC/1B represents the sample containing 1 wt.% bentonite.

2.5.Flow Chart of the Study

From first stage to final stage of the study including preparation of materials prior to compounding, extrusion, cutting, injection molding, irradiation and characterization processes were illustrated as a flow chart in **Figure 21** and **Figure 22**.

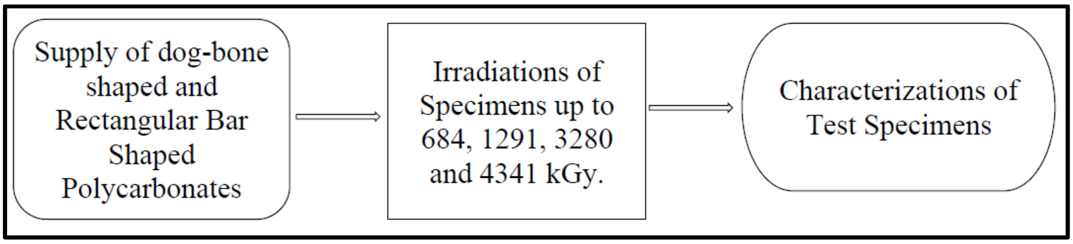

Figure 21 Flow Chart for the First Part of the Study

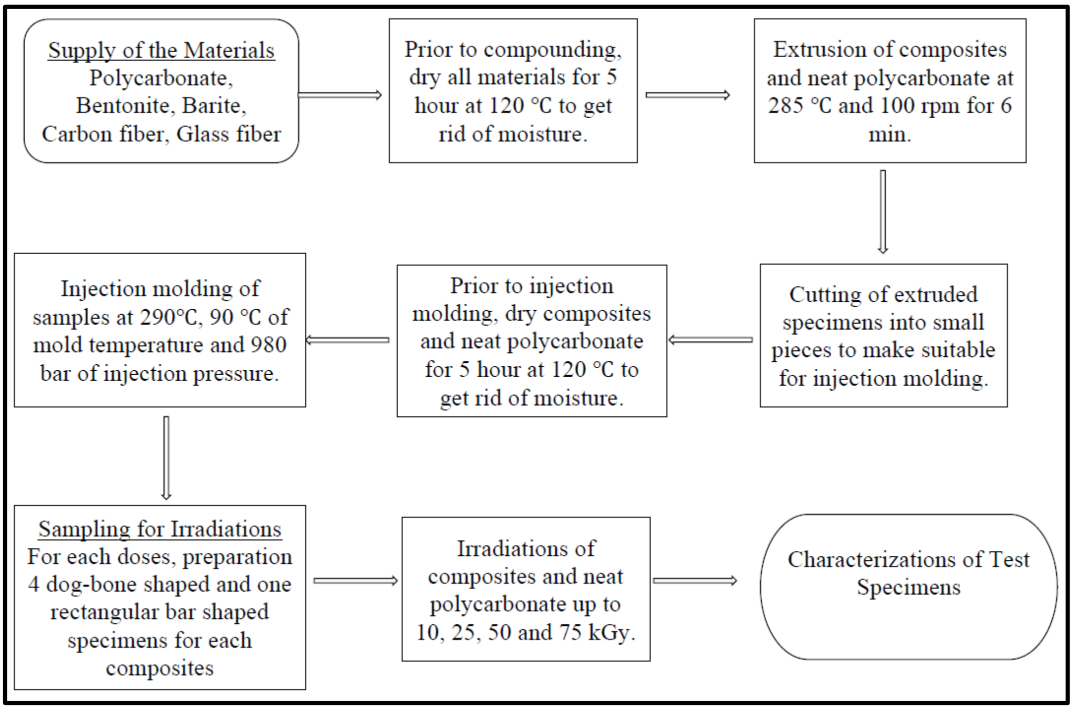

Figure 22 Flow Chart for the Second Part of the Study

CHAPTER 3

RESULTS AND DISCUSSIONS

3.1. Polycarbonates Samples Irradiated with 684, 1291, 3280 and 4341 kGy

Results and their interpretation of neat polycarbonate samples, which were irradiated to the dose of 684, 1291, 3280 and 4341 kGy, were given below. Characterization of specimens included analysis methods, which were given as follow:

- Tensile Test,
- DMA,
- TGA
- ATR-FTIR
- SEM-EDX

3.1.1 Tensile Test Results

Change in elongation at break, tensile strength and stress at break values upon irradiation were given in **Table 20**. Moreover, **Figure 23**, **Figure 24** and **Figure 25** illustrated change in the tensile strength, elastic modulus and elongation at break values via increasing the irradiation doses, respectively. **Figure 26** depicted the relative changes in elongation at break, tensile strength and stress at break values corresponding the total doses.

Inspection of **Figure 24** revealed a gradual increase in elastic modulus with increasing the total dose. This increase in the elastic modulus might be due to the radiation induced restructuring and recombination reactions occurring after scission reactions. Due to chain scission reactions, both number of short chain molecules and the number of secondary bonds increased which made the polymer more stiff (Callister, Jr., 2007). Tensile strength values decreased significantly via irradiation. Tensile strength values were proportional with molecular weight and it was a function of the number-average molecular weight (Callister, Jr., 2007). Half-value-dose (HVD) was defined as the dose value that diminished a mechanical property of the material to 50 % of its initial value under fixed environmental conditions (Seguchi & Morita, 1999). HVD was considered as characteristic property of radiation resistance for polymers. It was easily observed that elongation at break values were reduced via increasing the total dose. In the first dose, which was 684 kGy, both tensile strength and elongation at break values for polycarbonates were diminished more than 50 % of its initial value. At 4341 kGy, the test specimens' tensile test could not be accomplished due to the being fragile at hand. The total dose, which polycarbonate could bear regarding radioactive waste management, was determined as around 3280 kGy from the mechanical test results.

Inspection of **Figure 26**, clearly showed that gamma irradiation caused drastic changes in the mechanical properties of the polycarbonate. Although non-irradiated polycarbonate had ductile property, a ductile to brittle transition at room temperature was observed upon irradiation. Decrease in tensile strength, elongation at break values and behaving as brittle with increasing doses revealed the fact that dominant mechanism upon irradiation up to 684, 1291, 3280 and 4341 kGy was chain scission.

Table 20 Tensile Properties of Neat Polycarbonate Samples Irradiated up to 3280 kGy

Total Dose (kGy)	**Elastic Modulus**	**Elongation at Break**	**Tensile Strength**
Non-Irra.	2285 ± 219 MPa	78.8 ± 10.4 %	59.7 ± 1.1 MPa
684 kGy	2533 ± 163 MPa	1.2 ± 0.2 %	28.1 ± 3.5 MPa
1291 kGy	2545 ±389 MPa	0.55 ± 0.09 %	13.8 ± 1.6 MPa
3280 kGy	2990 ± 127 MPa	0.066 ± 0.002 %	1.9 ± 0.1 MPa

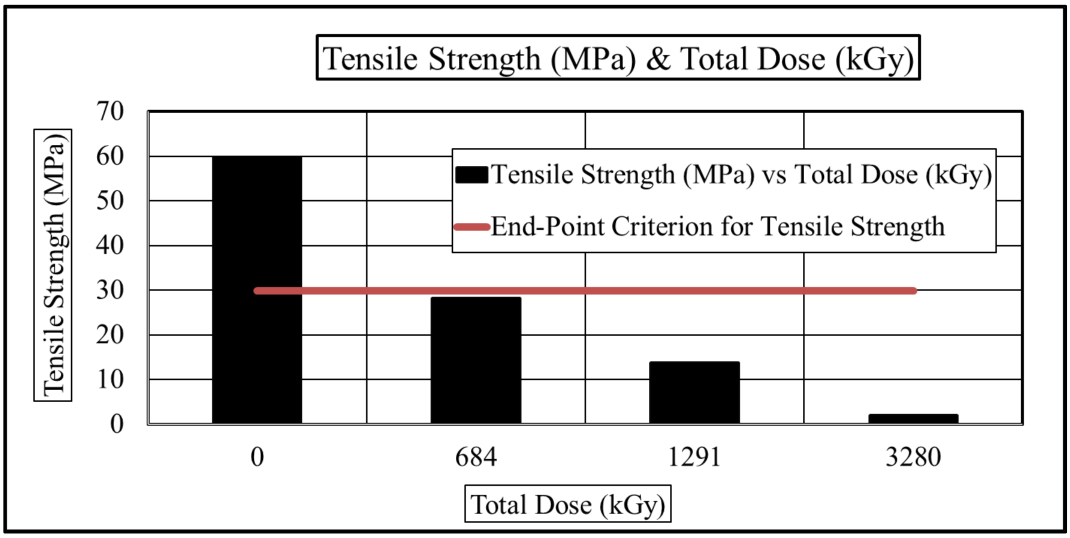

Figure 23 Tensile Strength (MPa) vs Total Dose (kGy) Graph for Neat Polycarbonate Irradiated up to 3280 kGy

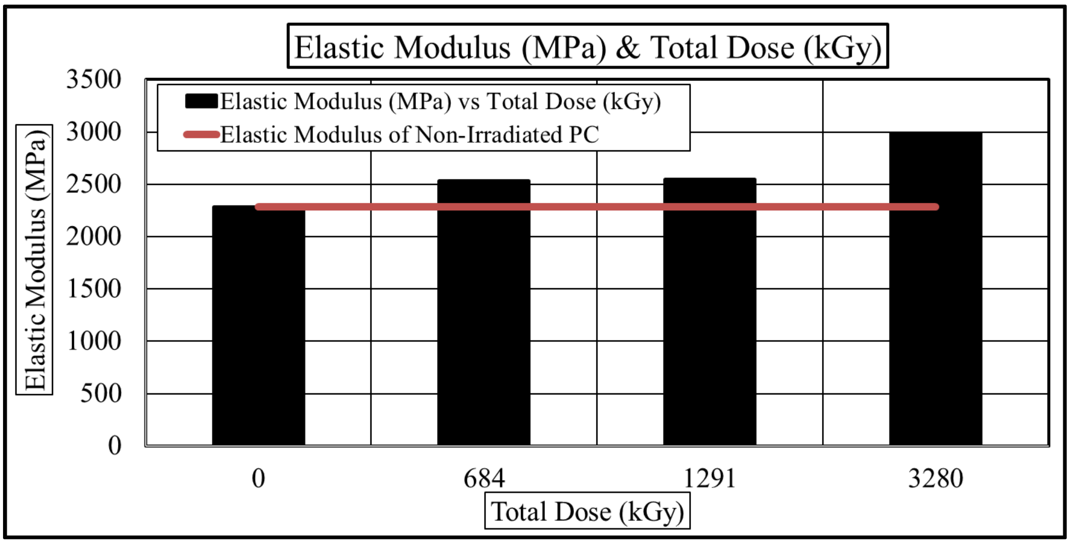

Figure 24 Elastic Modulus (MPa) vs Total Dose (kGy) Graph for Neat Polycarbonate Irradiated up to 3280 kGy

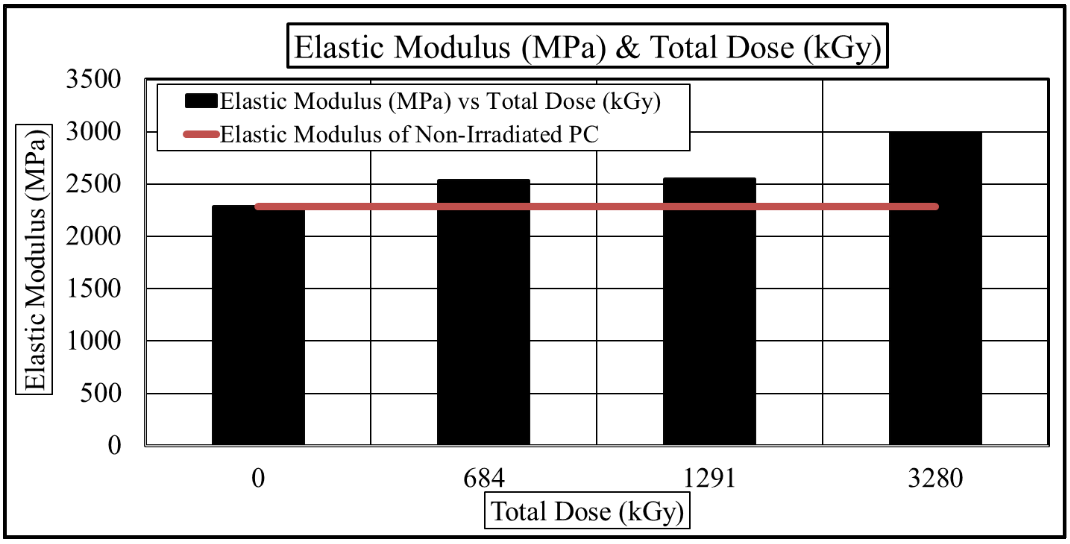

Figure 25 Elongation at Break (%) vs Total Dose (kGy) Graph for Neat Polycarbonate Irradiated up to 3280 kGy

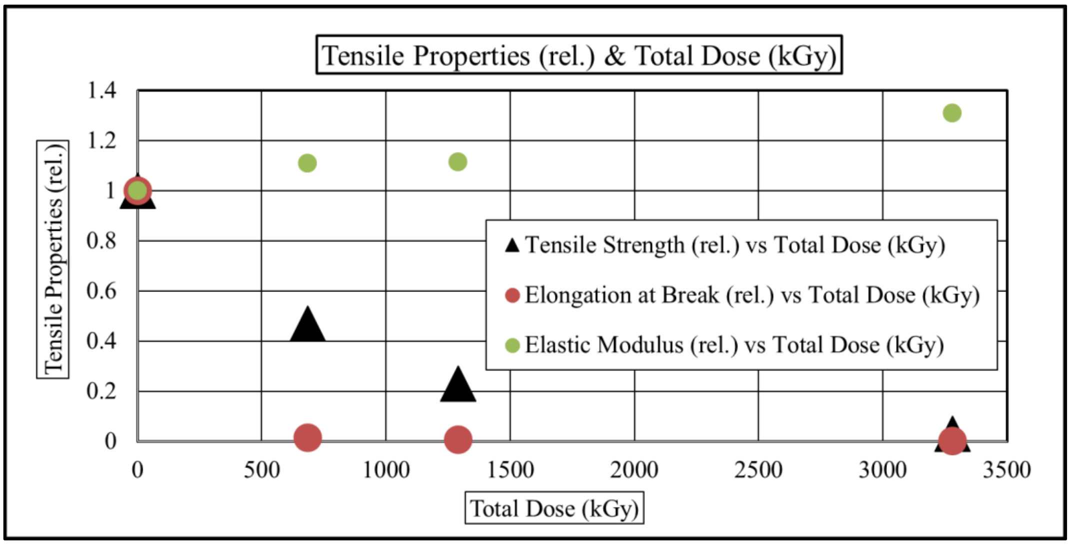

Figure 26 Relative Changes in Elongation at Break, Tensile Strength and Stress at Break Values with respect to Total Doses

3.1.2 Dynamic Mechanical Analysis (DMA)

Dynamic Mechanical analysis results were given in **Figure 27**, **Figure 28** and **Figure 29**. The glass transition temperatures for samples were given in **Table 21**.

It was clear that the glass transition temperature decreased with irradiation. Gamma irradiation caused scissions of molecular chains and this proceeded to increase of the molecular mobility. Molecular mobility change was inversely proportional to glass transition temperature. Therefore, reduction in the glass transition temperature was an explicit indication of radiation-induced degradation (Sinha, et al., 2004). Moreover, the decrease in the glass transition temperature upon irradiation could be associated with the increase in the number of the end groups due to the chain scission. This led to increase in the free volume and therefore reduction in the glass transition temperature. Storage modulus values were increased up to 1291 kGy values. Storage modulus gathered from DMA analysis was related with stiffness of the polymer (Kwan, 1998; ASTM International, 2013; ASTM International, 2012; Turkish Standards Institution, 2011). It could be seen easily that storage modulus values at room temperature and elastic modulus values were in accordance with each other. Storage modulus values showed increasing pattern via irradiation, this increase could be explained by occurrence of recombination reactions after scission reactions, and increase in the intermolecular forces due to the smaller species resulted with chain scission reactions. Further irradiation to 3280 kGy decreased the storage modulus showing the effect of radiation induced chain scission. On the other hand, storage modulus values at elevated temperature (i.e. at around 140 ℃) were decreased upon irradiation, indicating deterioration in the load-bearing property of polycarbonate at elevated temperature. The lowest stiffness at room and elevated temperature were observed in 3280 kGy irradiated specimen:

It was important to observe that the storage modulus for non-irradiated and 3280 kGy irradiated samples showed similar patterns. Storage modulus of 684 and 1291 kGy irradiated samples showed consistent patterns. For the case of non-irradiated and 3280 kGy irradiated samples, storage modulus did not vary very much with temperature before gradual decrease of the storage modulus, whereas, temperature dependence was more obvious in the 684 and 1291 kGy irradiated specimens. In other words, storage modulus decreased with temperature before the gradual decrease in the storage modulus in the 684 and 1291 kGy irradiated specimens. This temperature dependent behavior was due to the secondary forces. Further irradiation probably caused small mobile molecules to leave the polymeric matrix and lead to disappearance of the effect of secondary bonding with a decrease in storage modulus as shown in **Figure 27** for the 3280 kGy irradiated sample case.

Table 21 Glass Transition Temperatures for Neat Polycarbonates Samples Irradiated up to 3280 kGy.

Total Dose	**T_g (°C) from Tan δ vs Temperature (°C) Curve**	**T_g (°C) from Loss Modulus (MPa) vs Temperature (°C) Curve**
Non-Irra.	153.1 ℃	146.1 ℃
684 kGy	148.8 ℃	140.6 ℃
1291 kGy	144.6 ℃	135.6 ℃
3280 kGy	139.5 ℃	130.9 ℃

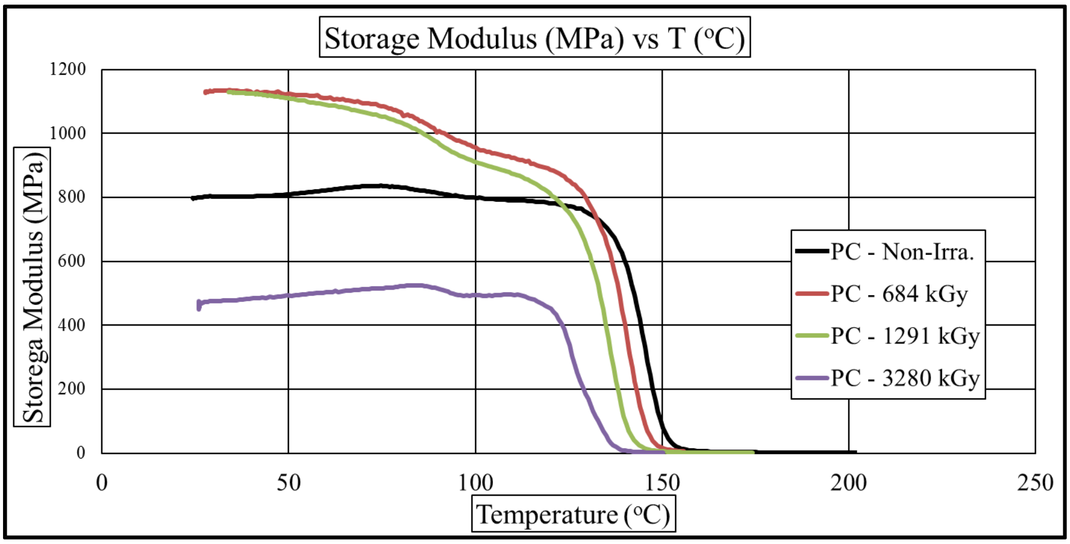

Figure 27 Storage Modulus (MPa) vs Temperature (°C) curve for neat polycarbonate irradiated up to 3280 kGy

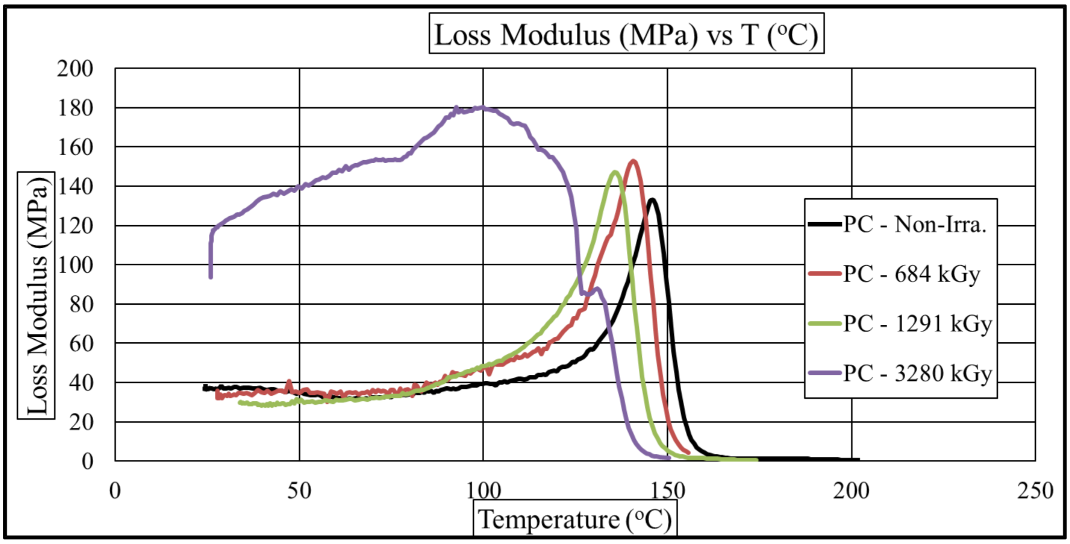

Figure 28 Loss Modulus (MPa) vs Temperature (°C) curve for neat polycarbonate irradiated up to 3280 kGy

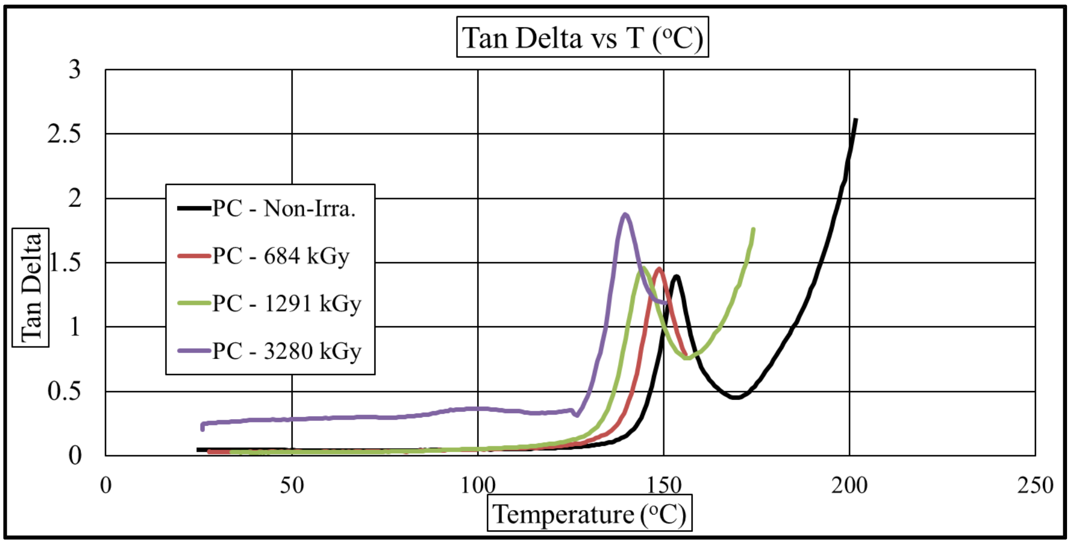

Figure 29 Tan Delta (δ) vs Temperature (°C) curve for neat polycarbonate irradiated up to 3280 kGy

3.1.3 Thermogravimetric Analysis (TGA)

TGA results were shown in **Figure 30** and **Figure 31**. T_5 (temperature at which 5 % weight loss occur), T_{50} (temperature at which 50 % weight loss occur) and T_{max} (temperature at which highest rate of weight loss occurs obtained from first derivative of TG curve) and temperatures were given in **Table 22**.

According to the TGA results, all polycarbonate samples were stable up to 350 ℃ until which any significant weight loss was not detected. Between the temperatures of 400 to 800℃, significant weight losses were observed for the whole test samples. TG and DTG curves (with two distinct plateau and peaks, respectively) indicated multistep degradation on polycarbonate specimens (Ma, et al., 1997; Sharma, et al., 2016). In multistep degradation, firstly, carbonate and isopropyl groups in the polycarbonate chain were degraded, and then decomposition of aromatic rings was occurred as second step (Ma, et al., 1997; Sharma, et al., 2016). Onset temperatures and T_5 values were lower for the irradiated samples when compared with non-irradiated test sample. The difference between the T_5 values of non-irradiated and 4341 kGy irradiated specimens was measured as 62 ℃. The onset temperature for weight loss was considered as beginning of thermal decomposition (Perkin Elmer Corporation, 2015; Turkish Standards Institution, 2014). It was clear that decomposition of polymer samples started at lower temperatures upon irradiation. This could be associated with chain scission reactions generation via irradiation such that occurrence of small fragments with smaller bond dissociation energies (i.e. resulting with lower activating energies for decomposition). This led to T_5 and onset temperature occurring at lower temperatures upon irradiation. T_{max} was observed at about 520 ℃ and T_{max} was slightly increased with irradiation due to removal of chain scission products from the polymer matrix and increase of aromatic content within the polymeric material.

Table 22 T_5, T_{max} and T_{50} Temperatures for Neat Polycarbonates Samples Irradiated up to 4341 kGy.			
Total Dose (kGy)	**T_5 (°C)**	**T_{max} (°C)**	**T_{50} (°C)**
Non-Irra. kGy	464 °C	517 °C	514 °C
684 kGy	450 °C	520 °C	512 °C
1291 kGy	422 °C	507 °C	502 °C
3280 kGy	439 °C	525 °C	518 °C
4341 kGy	402 °C	522 °C	510 °C

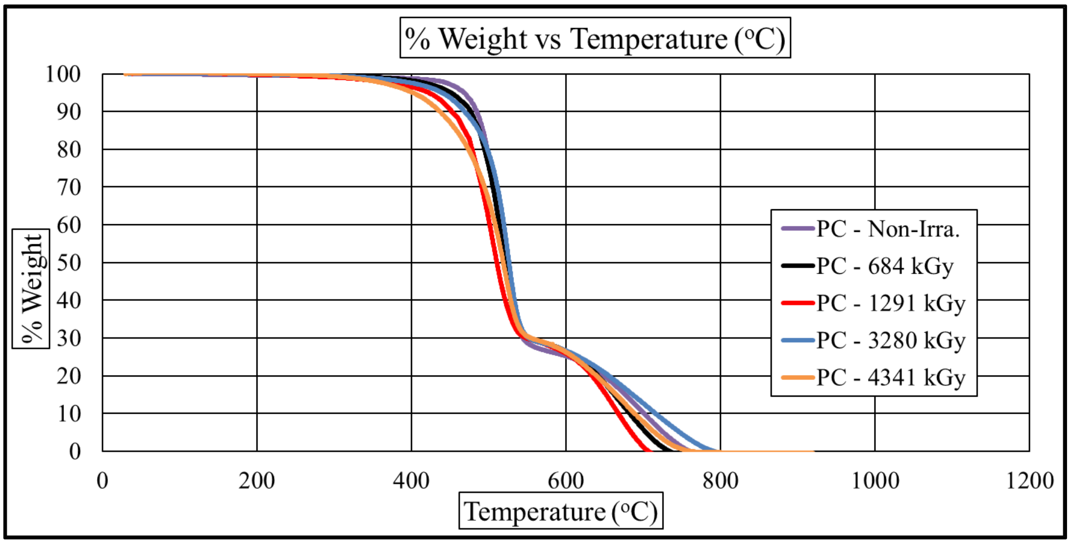

Figure 30 TGA curve (% Weight vs Temperature) for Neat Polycarbonate Irradiated up to 4341 kGy

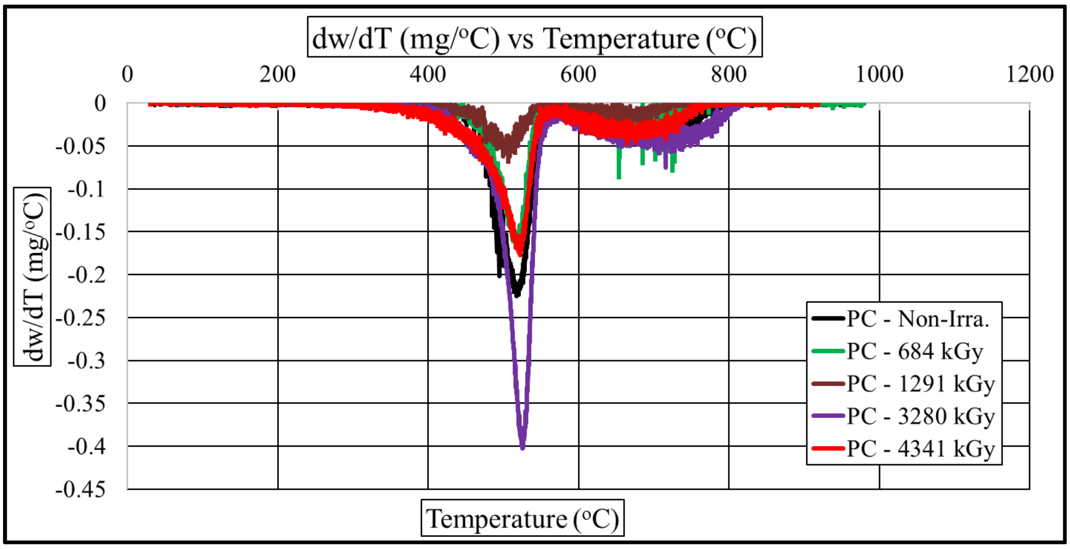

Figure 31 DTG Curve (dw/dt vs Temperature) for Neat Polycarbonate Irradiated up to 4341 kGy

3.1.4 Scanning Electron Microscopy (SEM) with Energy Dispersive X-Ray Spectroscopy (EDX)

SEM images of irradiated polycarbonate taken at magnitude of 25000X were shown in **Figure 32**. The surface of the non-irradiated polycarbonate sample was rough with surface cracks. When the sample irradiated with 684 kGy, propagation in the surface cracks was observed. For the further irradiation to total doses of 1291, 3280 and 4341 kGy, the fractures and surface roughness became more distinct.

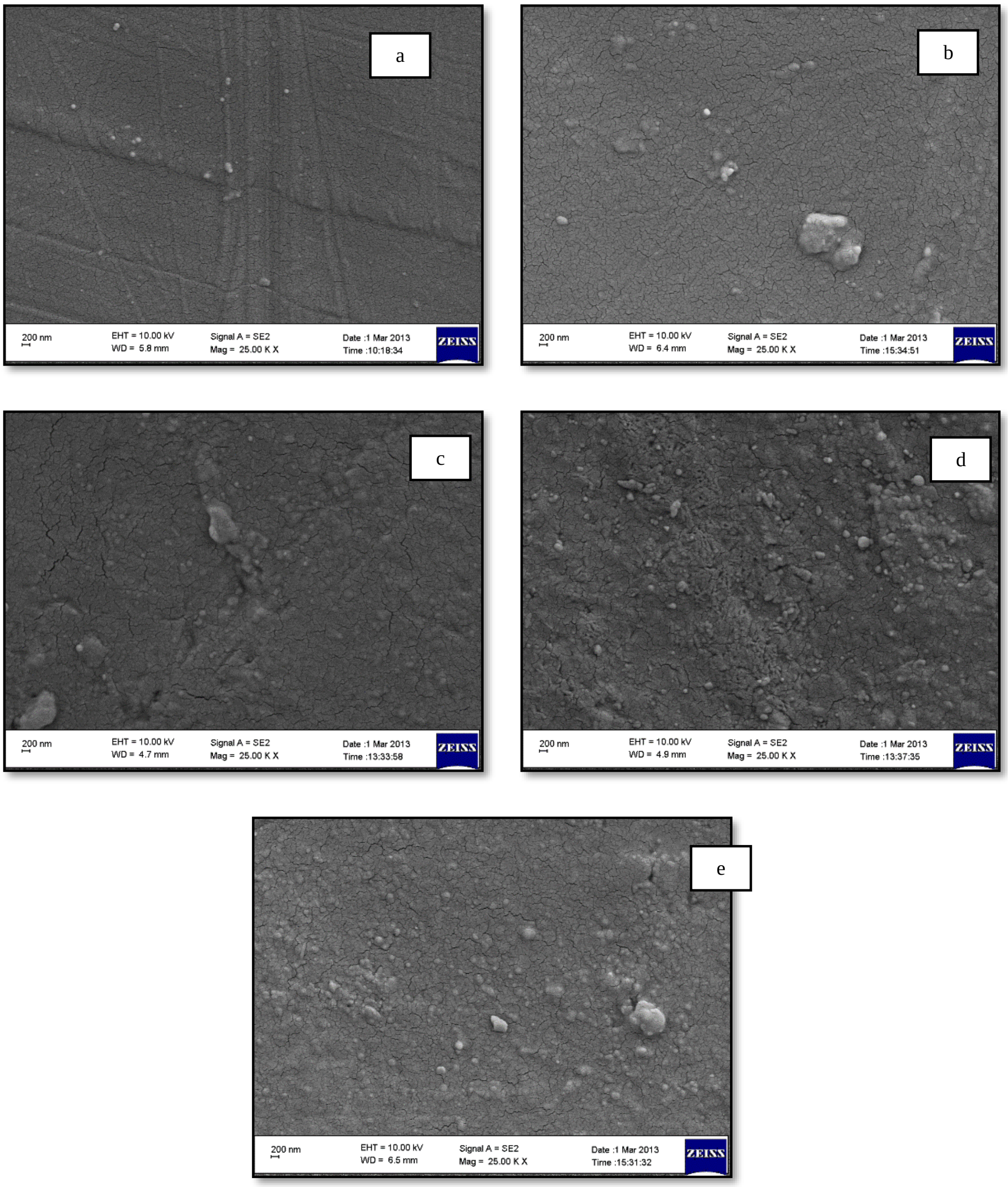

Figure 32 SEM Images of Irradiated Polycarbonate Specimens Monitored at Magnitude of 25k a)Non-Irradiated, b) 684 kGy Irradiated, c) 1291 kGy Irradiated, d) 3280 kGy Irradiated, e) 4341 kGy Irradiated

EDX study results were given in **Figure 33**. The EDX results showed that carbon to oxygen rate (C/O) rate changed. The EDX result gave C/O rate as 3.8, which were very close to the chemical formula ratio of 4 theoretical value. The C/O ratio was increased with irradiation dose. The increase in the ratio was probably due to the degradation occurred in the oxygen containing part (carbonate chain) of the bisphenol-a polycarbonate. This yielded with smaller and mobile molecules. Then, they were removed from the polymer matrix during and after the irradiation process. The decrease of C/O ratio for the case of 3820 kGy was a clear representation of the radiooxidation showing the oxygen attack to the polymer matrix. Diffusion of oxygen increased with time and it resulted with the decrease of the C/O ratio.

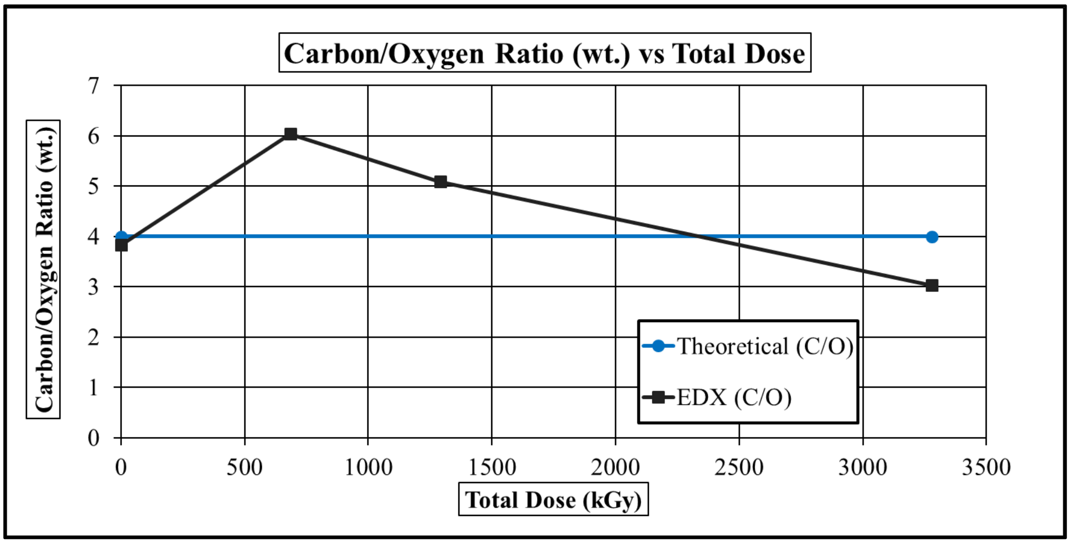

Figure 33 C/O Ratio (wt) from EDX Test Results for Neat Polycarbonates Irradiated up to 3280 kGy.

3.1.5 Attenuated Total Reflection Fourier Transform Infrared Spectroscopy (ATR-FTIR)

The ATR-FTIR spectrums of pristine polycarbonate irradiated to the total doses of 684, 1291, 3280 and 4341 kGy were shown in **Figure 34**. **Table 23** gave the frequencies of the main absorption bands of bisphenol-a polycarbonate (Delpech, et al., 2002; Silverstein, et al., 2005; Sinha, et al., 2004). According to the **Figure 34**, neither total destruction nor formation of new peaks and no appreciable changes were observed at the dose of 684 kGy (Singh & Prasher, 2005). On the other side, increase in the irradiation dose resulted in significant intensity decreases of peaks corresponding to C-H bond of methyl group (2969 cm^{-1}), C=O bond (1771 cm^{-1}), C-H bond of aromatic ring (1506 and 1015 cm^{-1}), C-O-C bonds (1190 cm^{-1}). This implied that scissioning of these bonds were started at first irradiation (684 kGy) and proceeded dramatically upon further irradiation (Sinha, et al., 2004). At the dose of 4341 kGy, the majority of characteristic peaks were decreased significantly. There was no appearance of peak near 3500 cm^{-1}, which depicted presence of O-H bands via irradiation. The intensity decreased around peak located 1773 cm^{-1} corresponding carbonyl bond indicated that chain scission occurred at the carbonate site (Kumar, et al., 2006). It was revealed from ATR-FTIR curves that chain scission mechanism were dominant upon irradiation.

Table 23 Characteristic Absorption Peaks of Bisphenol-A Based Polycarbonate (Delpech, et al., 2002; Silverstein, et al., 2005; Sinha, et al., 2004)**.**

Frequency (cm^{-1})	**Bonds**	**Vibrational Mode**
3529	OH (phenolic hydroxyl)	Stretching
3039	C-H (aromatic ring)	Stretching
2969	C-H (methyl group)	Symmetrical stretching
2500-1800	Aromatic ring	Combination bands
1773	O-(C=O)-O (carbonyl)	Stretching
1602 and 1465	C=C (aromatic ring)	Stretching
1506	C-H (aromatic ring)	In-plane bending
1387	C-H (methyl group)	Symmetrical bending
1232	C-O-(C=O)-O-C	Asymmetrical stretching
1206	C-O-C	Asymmetrical stretching
999	C-H (aromatic ring)	Out-of-plane bending
757	C-H (aromatic ring)	Out-of-plane bending
667	C=C (aromatic ring)	Out-of-plane bending

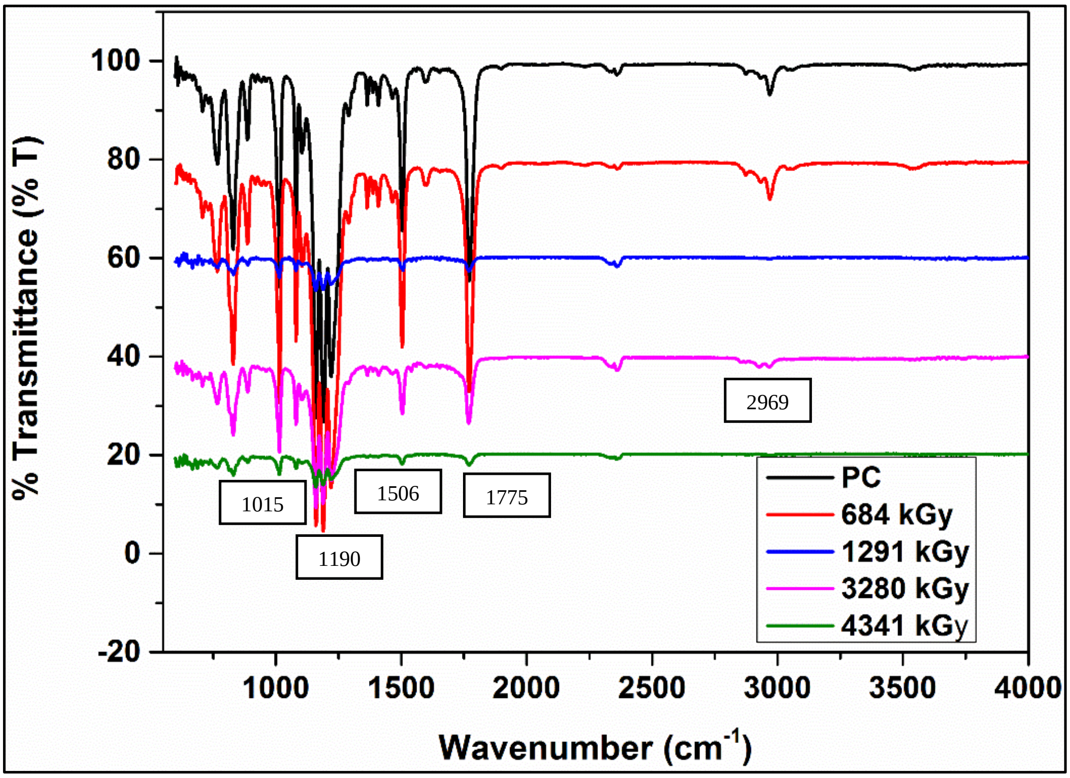

Figure 34 ATR-FTIR Spectrums of Irradiated Polycarbonate Samples Exposed to Total Dose of 684, 1291, 3280 and 4341 kGy

3.2. Polycarbonate Composites Irradiated up to 10, 25, 50 and 75 kGy

Results and their interpretation of neat polycarbonate and its' composites with bentonite, barite, carbon fiber and glass fiber, which were irradiated with 10, 25, 50, 75 kGy, were given below. Characterization of specimens included analysis methods, which were given as follow:

- Tensile Test,
- Hardness,
- YI and CIELAB Color Scales Measurement
- ATR-FTIR,
- MFR,
- DMA,
- TGA,
- SEM.

3.2.1 Tensile Test Results

3.2.1.1. Tensile Strength and Elongation at Break Values for Neat Polycarbonate and Composites

Tensile strength and elongation at break values of the composites were given in **Table 24**. **Figure 35** and **Figure 36** illustrated corresponding values graphically.

Table 24 Tensile Strength and Elongation at Break Values for Neat Polycarbonate and Composites

Test Sample	**Tensile Strength**	**Elongation at Break**
PC	62.6 ± 1.0 MPa	71.6 ± 12.5 %
PC /1B	66.5 ± 1.7 MPa	23.4 ± 12.0 %
PC /2B	65.9 ± 2.9 MPa	8.4 ± 1.7 %
PC /5B	65.2 ± 3.1 MPa	10.0 ± 2.4 %
PC/2Ba	64.2 ± 1.0 MPa	22.5 ± 5.0 %
PC/5Ba	63.2 ± 0.5 MPa	44.0 ± 17.0 %
PC/10Ba	62.5 ± 1.0 MPa	18.0 ± 4.4 %
PC/2CF	68.6 ± 1.2 MPa	37.0 ± 23.0 %
PC/5CF	74.4 ± 0.7 MPa	12.0 ± 0.1 %
PC/10CF	87.7 ± 1.4 MPa	9.1 ± 0.2 %
PC/2GF	66.4 ± 0.9 MPa	25.0 ± 8.5 %
PC/5GF	70.2 ± 0.6 MPa	11.0 ± 0.4 %
PC/10GF	75.1 ± 1.4 MPa	9.6 ± 0.5 %

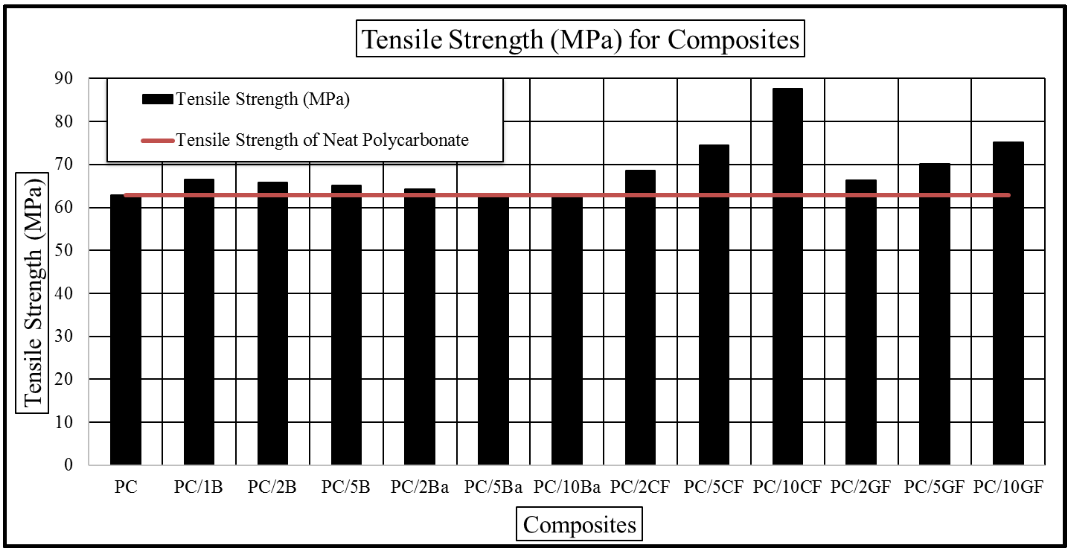

Figure 35 Column Chart for Tensile Strength Values of Polycarbonate Composites

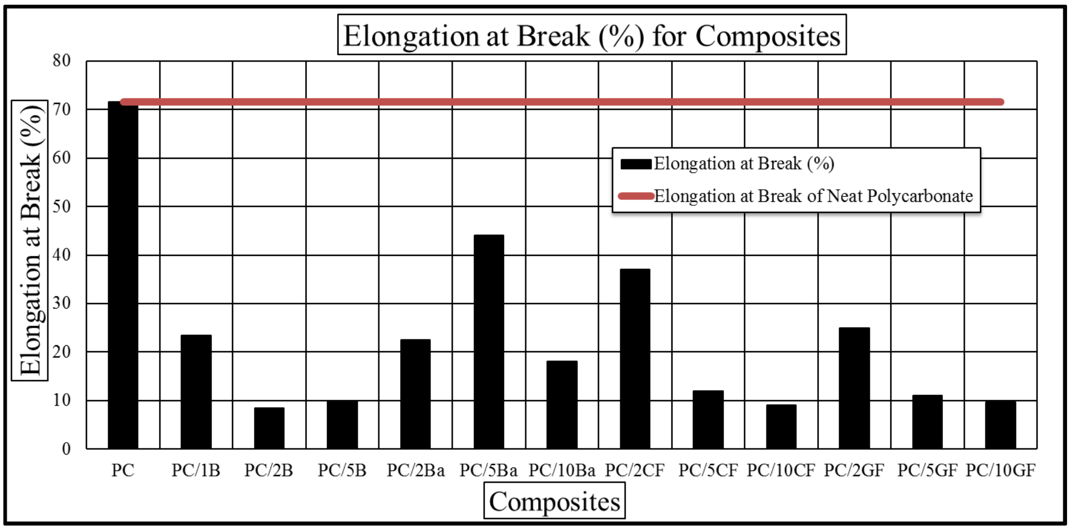

Figure 36 Column Chart for Elongation at Break Values of Polycarbonate Composites

According to the test results, it was clear that carbon fiber and glass fiber increased the tensile strength values significantly. On the other hand, the change recorded for the tensile strength values in cases of bentonite and barite filled composites were not significant.

Higher content for bentonite and barite resulted with lower tensile strength. This situation was vice versa for carbon fiber and glass fiber composites such that gradual addition of the fibers (from 2 wt.% to 10 wt.%) increased the tensile strength. Glass fiber reinforced composites had lower tensile strength values compared to the carbon fiber reinforced composites. On the other hand, bentonite filled composites had higher tensile strength values than barite filled ones.

Elongations at break values were significantly reduced with addition of filler. Particulate composites including bentonite and barite showed variations in terms of elongation at break when loading of fillers was increased. 1 wt.% bentonite and 5 wt.% barite filled composites had highest elongation at break values in their groups. Increase in the glass fiber and carbon fiber contents (from 2 wt.% to 10 wt.%) in composites brought about decreased pattern in ultimate elongation.

Polycarbonate is amorphous and it is classified as hard and tough material according to the stress-strain behavior. It’s stress strain curve includes high yield and tensile strength with higher elongation. However, glass fiber and carbon fiber addition (10 percent by weight) to the polycarbonate samples ended with brittleness. 10 wt. % fiber addition made the polymer composite hard and brittle indicating that stress-strain curve involved high tensile strength with lower elongation. Neck formation of polymer samples during tensile test was dissipated in 10 % fibers loaded specimens. 10 wt.% carbon and glass fiber containing composites showed brittle fractures and non-linear deformation at high loading. This could be associated with the reduction of the load bearing property of the carbon and glass fibers emerged from the interfacial microfailure around fibers. Presence of lots of carbon and glass fibers, causing the restriction of plastic deformation of the matrix, could be the reason for the brittle fracture of the composites 10 wt.% carbon and glass fibers (Savas, et al., 2016; Sato, et al., 1991).

The reasons behind the findings mentioned above were sequenced as:

- Mechanical properties of the composites were affected by volume fraction of the constituent materials (Callister, Jr., 2007). Dispersed phase (fillers) and continuous phase (polycarbonate) had great influence on the tensile strength values of the composites. “Rule of Mixtures” explained the situation that the content and the mechanical strength of the additives determined the mechanical property of the composite (Callister, Jr., 2007). Higher content of additives with higher tensile strength increased the mechanical property. The specific tensile strength values were reported for chopped carbon fiber as 4200 MPa, for E-glass type glass fiber as 3100-3800 MPa, whereas 30 MPa and 5.8 MPa were stated as strength values for bentonite and barite, respectively (DowAksa İleri Kompozit Malzemeler Sanayi LTD. ŞTİ., 2014; Wallenberger, et al., 2001; Dowdy & Larson, 1971; Jatuwan, 2004). Therefore, it was expected that the tensile strength values of carbon fiber reinforced composites showed the greatest tensile strength. Glass fiber, bentonite and barite filled polycarbonate followed the order in terms of tensile strength. Moreover, carbon fiber and glass fiber included epoxy and silane based sizing to give better polymer compatibility, which eventually improved the mechanical property of composite that they formed with polycarbonate (Carraher, 2014). Meanwhile, composites with inorganic minerals (bentonite and barite) did not include any organically modification, which was the one reason for lower tensile strength of particulate filled composite than that of fiber reinforced ones (Yoon, et al., 2003).

- The mechanical strength of the carbon fibers and glass fibers were significantly larger than the polycarbonates indicating that increase the content of filler resulted with improved tensile strength (Uawongsuwan & Ichikawa, 2014; Phua & Ishak, 2010). On the other side, bentonite and barite strength values (stated in literature as around 30 MPa and 5.8 MPa) were lower with respect to values of neat polycarbonate samples (62.6 MPa) representing that increase in the filler content brought about decrease in the tensile strength. The situation based on “Rules of Mixtures” was experimentally achieved. In the literature, there were articles representing similar behaviors for tensile strength while addition of carbon fiber, glass fiber and bentonite to the polymers (Uawongsuwan & Ichikawa, 2014; Phua & Ishak, 2010; Alsagayar, et al., 2015; Shokrieh, et al., 2012).

- The decrease of tensile strength and elongation at break of particulate composites by the addition of more filler could be explained by incomplete dispersion, possibility of air-traps and intensifying of micro void creation. These outcomes increased the stress concentration in the composites thereby causing early failure during tensile test (Alsagayar, et al., 2015; Shokrieh, et al., 2012). The possible reason of incomplete dispersion was eliminated by applying melt-mixing method. Compounding process included 6-minutes mixing time by twin-screw extruder and it was considered as enough for homogenous dispersion. SEM pictures of the fracture surfaces of the particulate composites proved the sufficient dispersion.

- Bentonite and barite with mean diameters of 20 and 9.4 μm made them medium and coarse particles influencing mechanical properties negatively (Otterstedt & Brandreth, 1998). Although the mean diameters of the bentonites and barites were 20 and 9.4 μm, SEM pictures of particulate composites at the fracture surfaces revealed the fact that the diameters of the particles in the composites were larger than their mean diameters. Therefore, it could be stated that these fillers behaved as agglomerate. This situation was also associated with lower elongation at break, deficient strength and early failure of the particulate composites during mechanical test (Otterstedt & Brandreth, 1998; Alsagayar, et al., 2015; Shokrieh, et al., 2012) .

3.2.1.2. Tensile Strength and Elongation at Break Values for Neat Polycarbonate Samples Exposed to 10, 25, 50 and 75 kGy Irradiation

Tensile strength and elongation at break values for neat polycarbonate samples upon irradiation were given in **Table 25**, **Table 26** and illustrated in **Figure 37**, **Figure 38**, respectively.

Table 25 Tensile Strength Values for Neat Polycarbonate Samples (Irradiated up to 75 kGy)

Test Sample	**Tensile Strength (MPa) Values with respect to Total Doses (kGy)**				
	NON-IRRA	**10 kGy**	**25 kGy**	**50 kGy**	**75 kGy**
PC	62.9 ± 1.0	63.5 ± 0.9	65.3 ± 1.7	65.5 ± 2.2	62.7 ± 1.3

Table 26 Elongation at Break Values for Neat Polycarbonate Samples (Irradiated up to 75 kGy)

Test Sample	**Elongation at Break (%) Values with Respect to Total Doses (kGy)**				
	NON-IRRA	**10 kGy**	**25 kGy**	**50 kGy**	**75 kGy**
PC	71.6 ± 12.5	50.0 ± 9.9	110.5 ± 2.1	109.5 ± 5.0	70.0 ± 31.0

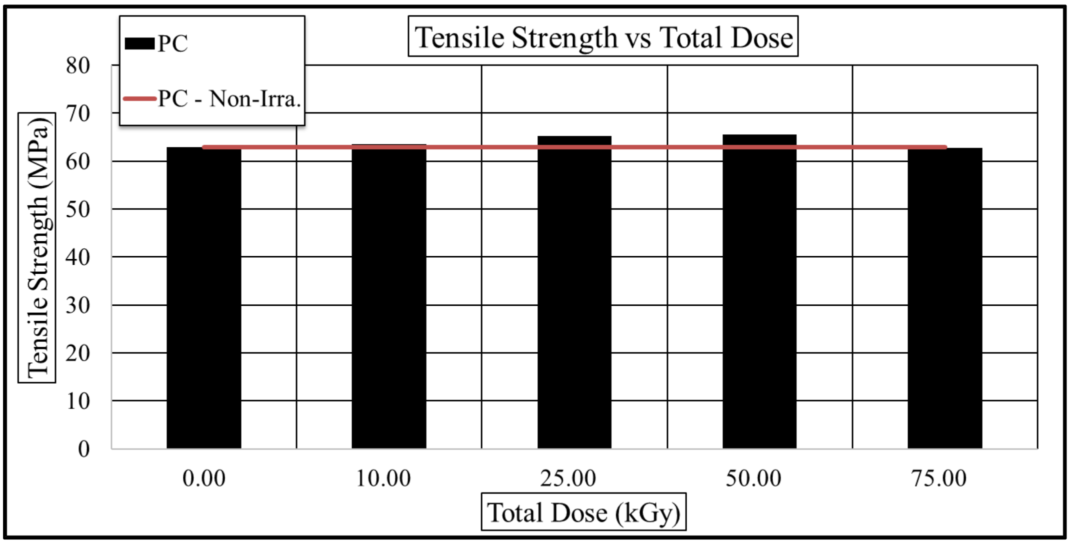

Figure 37 Change of Tensile Strength with Total Dose for Neat Polycarbonate

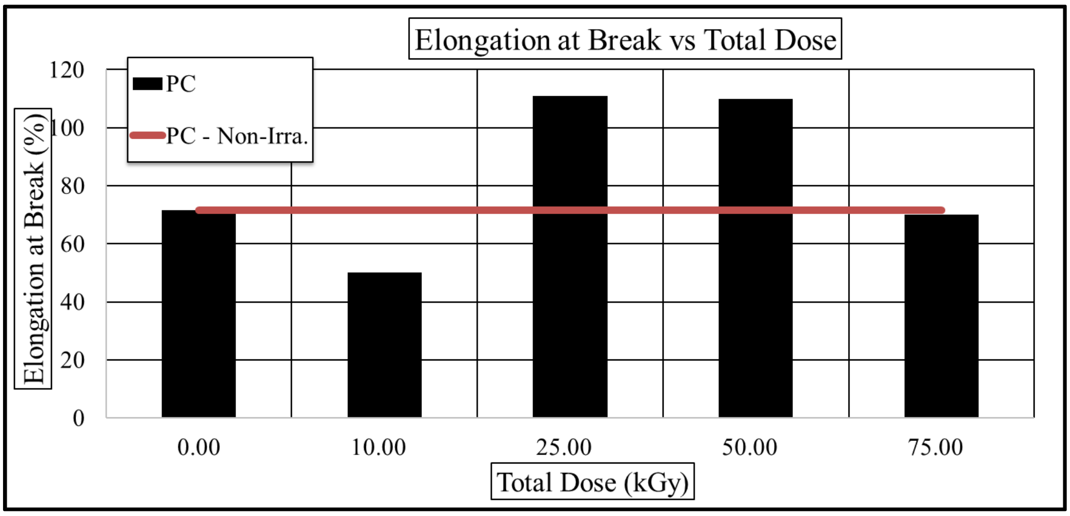

Figure 38 Change of Elongation at Break with Total Dose for Neat Polycarbonate

According to the test results, tensile strengths of the polycarbonate samples were increased up to 50 kGy. After 50 kGy, tensile strength values showed decreasing trend. For all doses, the strength values of specimens were higher than the values of neat polycarbonate. Elongation at break values was also enhanced via irradiation at the 25 and 50 kGy doses. The irradiation up to 75 kGy did not compromise the mechanical properties. Up to 50 kGy, mechanical properties enhanced. Although decrease in strength and elongation at break values were observed after 50 kGy, mechanical properties at 75 kGy were similar to the neat polycarbonate's values.

It could be inferred from the tensile test results that enhancement in the mechanical properties up to 50 kGy were associated with the radiation induced crosslinking. Further irradiation triggered the chain scission reactions taking place in higher amounts (Acierno, et al., 1981; Acierno, et al., 1980; Araujo, et al., 1998). Loss in mechanical properties were not observed during the irradiation period and this could be attributed to specimens being UV stabilized grade, implying retardation of the undesired effects of the irradiation. The trend in the mechanical properties complied with previous studies (Acierno, et al., 1981; Araujo, et al., 1998; Chen, et al., 2005; Golden, et al., 1964). It was revealed that the optimum dose range for neat polycarbonate in terms of mechanical aspect was between 25 and 50 kGy such that improvement in both the tensile strength and elongation at break was observed.

The results of the mechanical tests clearly showed that neat polycarbonate samples did not show any significant change in the mechanical properties up to 75 kGy dose. Thus, radioactive waste having initial contact dose rate of 1.126 Gy/h with the half-life of 5.27 years could be theoretically embedded into neat polycarbonate with remote handling procedures for 300 years (IAEA, 2009; IAEA, 1998).

3.2.1.3. Tensile Strength and Elongation at Break Values for Polycarbonate-Bentonite Composites Exposed to 10, 25, 50 and 75 kGy Irradiation

Tensile strength and elongation at break values for bentonite filled polycarbonate specimens were given in **Table 27**, **Table 28** and illustrated in **Figure 39**, **Figure 40**, respectively.

Table 27 Tensile Strength Values for Bentonite Filled Polycarbonate Samples (Irradiated up to 75 kGy)

Test Sample	**Tensile Strength (MPa) Values with respect to Total Doses (kGy)**				
	NON-IRRA	**10 kGy**	**25 kGy**	**50 kGy**	**75 kGy**
PC	62.9 ± 1.0	63.5 ± 0.9	65.3 ± 1.7	65.5 ± 2.2	62.7 ± 1.3
PC/1B	66.5 ± 1.7	64.6 ± 0.9	64.0 ± 0.7	63.6 ± 0.3	63.0 ± 0.2
PC/2B	65.9 ± 2.9	63.4 ± 0.6	63.6 ± 0.4	63.9 ± 0.2	62.5 ± 0.5
PC/5B	65.2 ± 3.1	63.4 ± 0.6	57.3 ± 7.8	63.1± 0.8	61.9 ± 0.3

Table 28 Elongation at Break Values for Bentonite Filled Polycarbonate Samples (Irradiated up to 75 kGy)

Test Sample	**Elongation at Break (%) Values with Respect to Total Doses (kGy)**				
	NON-IRRA	**10 kGy**	**25 kGy**	**50 kGy**	**75 kGy**
PC	71.6 ± 12.5	50.0 ± 9.9	110.5 ± 2.1	109.5 ± 5.0	70.0 ± 31.0
PC/1B	23.4 ± 12.0	40.0 ± 23.0	54.0 ± 35.0	44.0 ± 8.5	46.0 ± 20.0
PC/2B	8.4 ± 1.7	21.0 ± 7.8	81.0 ± 4.6	19.0 ± 4.2	24.0 ± 4.2
PC/5B	10.0 ± 2.4	15.7 ± 10.3	16.0 ± 3.3	22.0 ± 7.1	19.0 ± 10.0

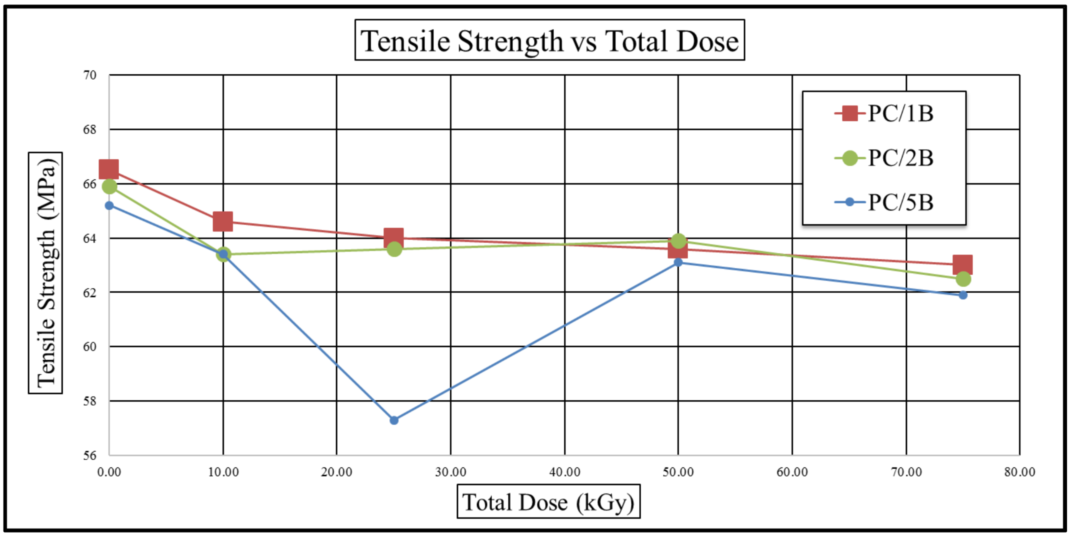

Figure 39 Change of Tensile Strength with Total Dose for Bentonite Filled Polycarbonate

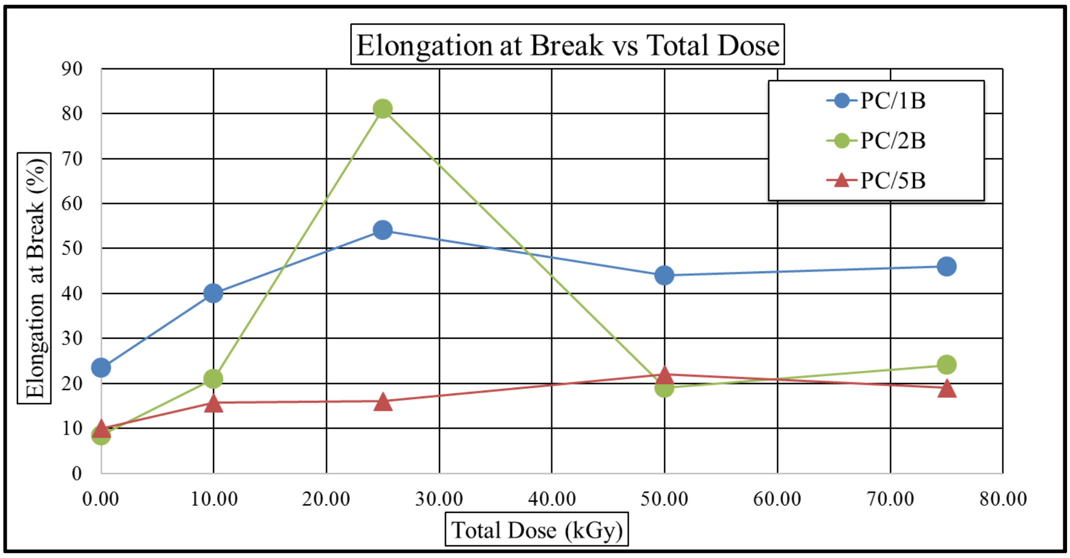

Figure 40 Change of Elongation at Break with Total Dose for Bentonite Filled Polycarbonate

According to the test results, tensile strength values for all compositions of bentonite-loaded polycarbonates were decreased via irradiation. On the other hand, elongations at break values were improved. The integration of bentonite with irradiation had an effect analogous to plasticizer. The trend in mechanical properties for bentonite-filled specimens was totally opposite than the trend observed in neat polycarbonate. 1 and 2 wt.% bentonite filled composites with 25 kGy had better mechanical stability. However, they could not reach the strength and elongation values of 75 kGy irradiated neat polycarbonate. It was hard to state the dominant reaction type, which were crosslinking affecting the strength values positively and chain scission affecting elongation negatively. The behavior of the composites did not conform those situations one-to-one. On the other hand, it was clear that neat specimens surpassed the bentonite-filled composites in terms of mechanical properties upon irradiation.

The results of the mechanical tests clearly showed that bentonite filled polycarbonate samples did not show any significant change in the mechanical properties up to 75 kGy dose. Thus, radioactive waste having initial contact dose rate of 1.126 Gy/h with the half-life of 5.27 years could be theoretically embedded into bentonite incorporated polycarbonate with remote handling procedures for 300 years (IAEA, 2009; IAEA, 1998).

3.2.1.4. Tensile Strength and Elongation at Break Values for Polycarbonate-Barite Composites Exposed to 10, 25, 50 and 75 kGy Irradiation

Tensile strength and elongation at break values for barite filled polycarbonate specimens were given in **Table 29**, **Table 30** and illustrated in **Figure 41**, **Figure 42**, respectively.

Table 29 Tensile Strength Values for Barite Filled Polycarbonate Samples (Irradiated up to 75 kGy)

Test Sample	**Tensile Strength (MPa) Values with Respect to Total Doses (kGy)**				
	NON-IRRA	**10 kGy**	**25 kGy**	**50 kGy**	**75 kGy**
PC	62.9 ± 1.0	63.5 ± 0.9	65.3 ± 1.7	65.5 ± 2.2	62.7 ± 1.3
PC/2Ba	64.2 ± 1.0	65.0 ± 0.4	63.5 ± 0.2	63.0 ± 0.4	62.5 ± 0.4
PC/5Ba	63.2 ± 0.5	65.2 ± 0.6	63.7 ± 1.5	63.8 ± 1.1	63.5 ± 0.5
PC/10Ba	62.5 ± 1.0	62.6 ± 0.3	62.2 ± 0.7	62.5 ± 0.7	61.0 ± 0.7

Table 30 Elongation at Break Values for Barite Filled Polycarbonate Samples (Irradiated up to 75 kGy)

Test Sample	**Elongation at Break (%) Values with Respect to Total Doses (kGy)**				
	NON-IRRA	**10 kGy**	**25 kGy**	**50 kGy**	**75 kGy**
PC	71.6 ± 12.5	50.0 ± 9.9	110.5 ± 2.1	109.5 ± 5.0	70.0 ± 31.0
PC/2Ba	22.5 ± 5.0	53.0 ± 34.0	47.0 ± 14.0	26.0 ± 12.0	34.0 ± 8.8
PC/5Ba	44.0 ± 17.0	20.0 ± 0.6	34.0 ± 15.0	44.0 ± 28.0	30.0 ± 24.0
PC/10Ba	18.0 ± 4.4	46.0 ± 2.2	29.0 ± 14.0	26.0 ± 17.0	27.0 ± 13.0

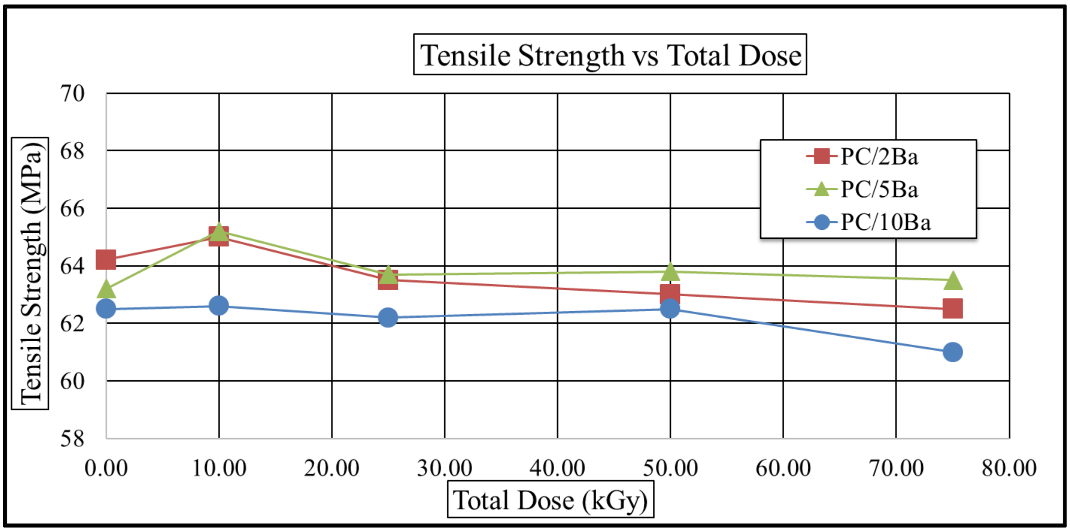

Figure 41 Change of Tensile Strength with Total Dose for Barite Filled Polycarbonate

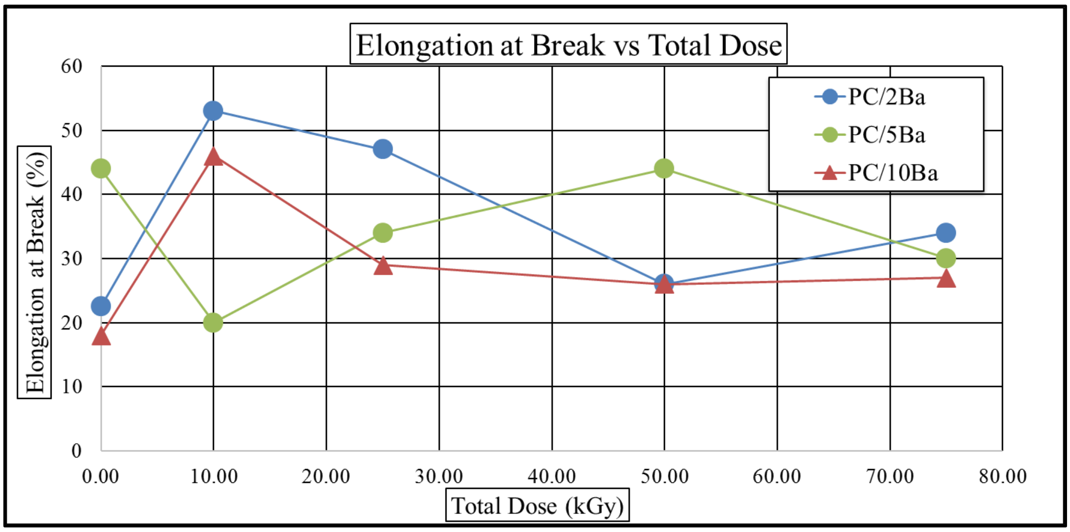

Figure 42 Change of Elongation at Break with Total Dose for Barite Filled Polycarbonate

Tensile strength values of 2 and 5 wt. % barite filled specimens first increased via irradiation up to 10 kGy. Further irradiation decreased the strength values to some extent. The decreasing trend in the specimens with 2 wt. % barite was higher when compared the other barite-based specimens. 5 and 10 wt. % barite filled samples showed better stability in tensile strength values. Tensile strength values of 10 wt. % barite loaded samples with 0, 10, 25, 50 kGy irradiation doses were closer to each other revealing the fact that radiation shielding property of barite could retard the radiation induced reactions. This tendency was similar in 5 % barite loaded specimens exposed to 25, 50, 75 kGy irradiation doses. It might be stated that increase in the content of barite diminished the variation in the strength values upon irradiation. The variation in the strength values via irradiation was higher in the specimens of which bentonite was used as filler, when it was compared to the barite filled specimens.

Elongation at break values of the specimens with 2 and 10 wt. % barite showed maximum at 10 kGy. The further irradiation decreased the elongation to some extent but the values were higher than the values of non-irradiated samples. It was clear that

% 2 barite loaded polycarbonate with 10 kGy irradiation dose had the optimum values mechanically among the all barite loaded compositions.

The results of the mechanical tests clearly showed that barite filled polycarbonate samples did not show any significant change in the mechanical properties up to 75 kGy dose. Thus, radioactive waste having initial contact dose rate of 1.126 Gy/h with the half-life of 5.27 years could be theoretically embedded into barite incorporated polycarbonate with remote handling procedures for 300 years (IAEA, 2009; IAEA, 1998).

3.2.1.5. Tensile Strength and Elongation at Break Values for Polycarbonate-Glass Fiber Composites Exposed to 10, 25, 50 and 75 kGy Irradiation

Tensile strength and elongation at break values for glass fiber reinforced polycarbonate specimens were given in **Table 31**, **Table 32** and illustrated in **Figure 43**, **Figure 44**, respectively.

Table 31 Tensile Strength Values for Glass Fiber Filled Polycarbonate Samples (Irradiated up to 75 kGy)

Test Sample	**Tensile Strength (MPa) Values with Respect to Total Doses (kGy)**				
	NON-IRRA	**10 kGy**	**25 kGy**	**50 kGy**	**75 kGy**
PC	62.9 ± 1.0	63.5 ± 0.9	65.3 ± 1.7	65.5 ± 2.2	62.7 ± 1.3
PC/2GF	66.4 ± 0.9	66.1 ± 1.0	65.5 ± 0.4	66.0 ± 0.5	65.3 ± 0.3
PC/5GF	70.2 ± 0.6	69.4 ± 0.9	69.4 ± 0.5	69.3 ± 0.7	68.3 ± 0.5
PC/10GF	75.1 ± 1.4	78.5 ± 7.0	72.4 ± 0.6	73.2 ± 1.3	73.0 ± 1.6

Table 32 Elongation at Break Values for Glass Fiber Filled Polycarbonate (Irradiated up to 75 kGy)

Test Sample	**Elongation at Break (%) Values with Respect to Total Doses (kGy)**				
	NON-IRRA	**10 kGy**	**25 kGy**	**50 kGy**	**75 kGy**
PC	71.6 ± 12.5	50.0 ± 9.9	110.5 ± 2.1	109.5 ± 5.0	70.0 ± 31.0
PC/2GF	25.0 ± 8.5	15.0 ± 1.6	31.0 ± 4.5	16.0 ± 1.6	15.0 ± 1.0
PC/5GF	11.0 ± 0.4	10.0 ± 0.2	12.0 ± 0.8	14.0 ± 0.7	11.0 ± 0.1
PC/10GF	9.6 ± 0.5	8.8 ± 0.5	8.3 ± 0.1	9.2 ± 0.7	8.2 ± 0.2

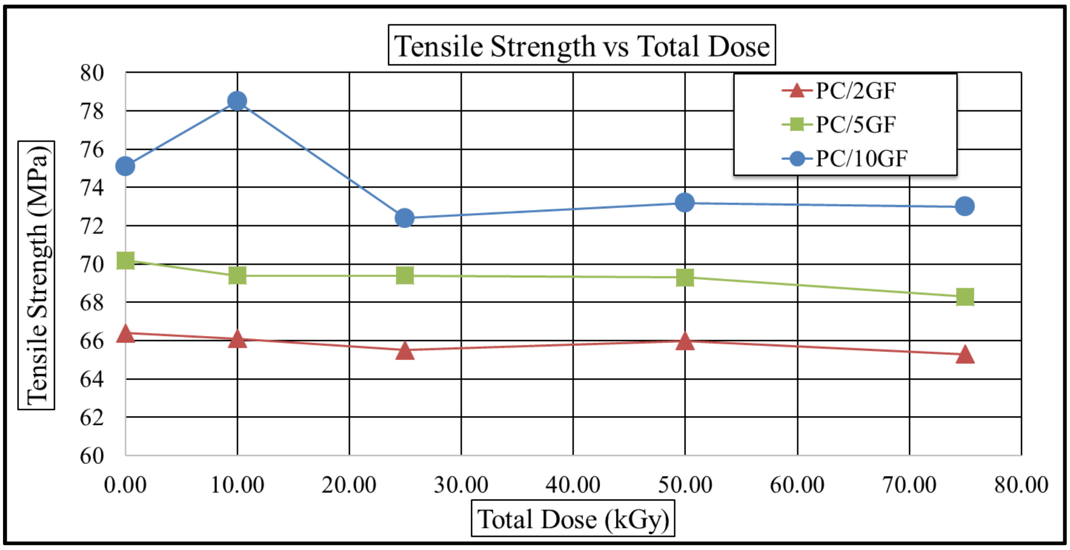

Figure 43 Change of Tensile Strength with Total Dose for Glass Fiber Filled Polycarbonate

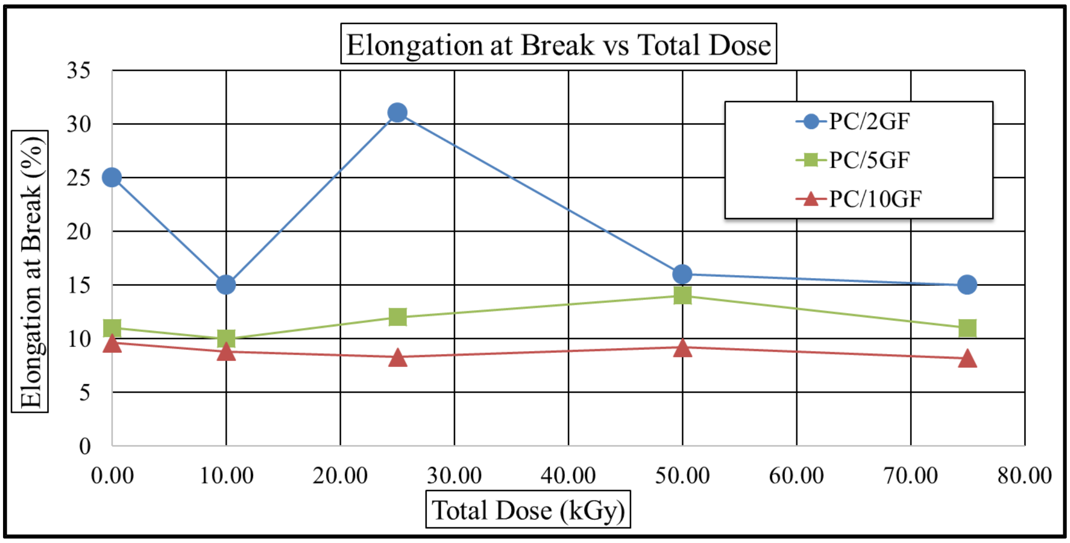

Figure 44 Change of Elongation at Break with Total Dose for Glass Fiber Filled Polycarbonate

Tensile strength values of glass fiber reinforced composites were slightly decreased via irradiation. The relative reduction (comparing the data of non-irradiated and 75 kGy irradiated) in the strength values were 1.66, 2.71 and 2.80 % corresponding 2, 5 and 10 wt. % glass fiber filled specimens, respectively. 10 wt. % glass fiber loaded polycarbonates had highest tensile strength values at all doses when compared with 2 and 5 wt. % glass fiber reinforced composites. Elongations at break values for polycarbonate were also diminished via irradiation. In glass fiber reinforced composites, relative change of the elongation at break values were narrower than neat and particle filled samples. Relative decreases in ultimate elongation of 2, 5 and 10 wt. % glass fiber incorporated polycarbonate (comparing the data of non-irradiated and 75 kGy irradiated) were 40, 0 and 14.6 % percent, respectively. Uniformity in the initial fiber length and the homogeneous dispersion of the glass fibers within polymer matrix, which were demonstrated on SEM analysis, gave consistency in the ultimate elongations of the composites upon irradiation. Homogeneous dispersion of the fibers also avoided early failure of the composites containing 5 and 10 wt. % glass fibers during tensile test. Polycarbonate with 10 percent glass fiber composites showed the highest mechanical strength at 10 kGy and composite with 2 percent glass fiber showed maximum elongation at the irradiation dose of 25 kGy.

The results of the mechanical tests clearly showed that glass fiber reinforced polycarbonate samples did not show any significant change in the mechanical properties up to 75 kGy dose. Thus, radioactive waste having initial contact dose rate of 1.126 Gy/h with the half-life of 5.27 years could be theoretically embedded into glass fiber reinforced polycarbonate with remote handling procedures for 300 years (IAEA, 2009; IAEA, 1998). From the perspective of half value dose, 5 and 10 percent glass fiber loaded polycarbonate, which exhibited more stability in terms of strength and elongation, was more suitable in radioactive waste treatment than 2 percent loaded one.

3.2.1.6. Tensile Strength and Elongation at Break Values for Polycarbonate-Carbon Fiber Composites Exposed to 10, 25, 50 and 75 kGy Irradiation

Tensile strength and elongation at break values for carbon fiber reinforced polycarbonate specimens were given in **Table 33**, **Table 34** and illustrated in **Figure 45**, **Figure 46**, respectively.

Table 33 Tensile Strength Values for Carbon Fiber Filled Polycarbonate Samples (Irradiated up to 75 kGy)

Test Sample	**Tensile Strength (MPa) Values with Respect to Total Doses (kGy)**				
	NON-IRRA	**10 kGy**	**25 kGy**	**50 kGy**	**75 kGy**
PC	62.9 ± 1.0	63.5 ± 0.9	65.3 ± 1.7	65.5 ± 2.2	62.7 ± 1.3
PC/2CF	68.6 ± 1.2	68.6 ± 0.4	68.4 ± 1.1	68.9 ± 0.1	67.6 ± 0.9
PC/5CF	74.4 ± 0.7	75.5 ± 0.6	74.0 ± 1.1	73.5 ± 2.3	73.8 ± 0.7
PC/10CF	87.7 ± 1.4	87.7 ± 0.2	87.3 ± 1.1	89.6 ± 0.1	87.5 ± 0.1

Table 34 Elongation at Break Values for Carbon Fiber Filled Polycarbonate Samples (Irradiated up to 75 kGy)

Test Sample	**Elongation at Break (%) Values with Respect to Total Doses (kGy)**				
	NON-IRRA	**10 kGy**	**25 kGy**	**50 kGy**	**75 kGy**
PC	71.6 ± 12.5	50.0 ± 9.9	110.5 ± 2.1	109.5 ± 5.0	70.0 ± 31.0
PC/2CF	37.0 ± 23.0	14.0 ± 2.8	19.0 ± 1.7	21.0 ± 7.0	22.0 ± 7.6
PC/5CF	12.0 ± 0.1	13.0 ± 2.5	12.0 ± 1.7	11.0± 0.7	10.5 ± 0.7
PC/10CF	9.1 ± 0.2	8.9 ± 1.2	8.4 ± 0.2	8.4 ± 0.9	8.5 ± 1.2

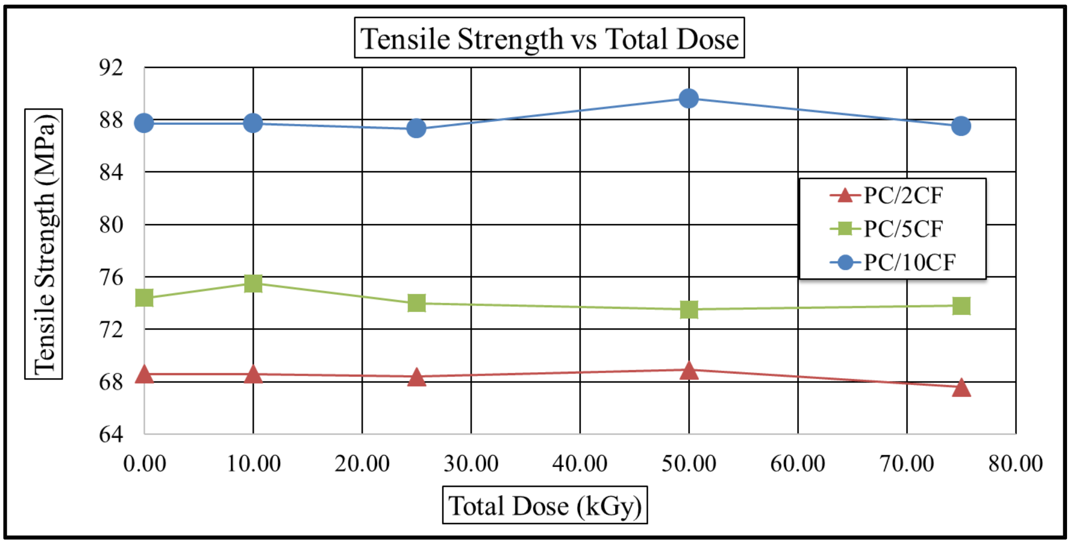

Figure 45 Change of Tensile Strength with Total Dose for Carbon Fiber Filled Polycarbonate

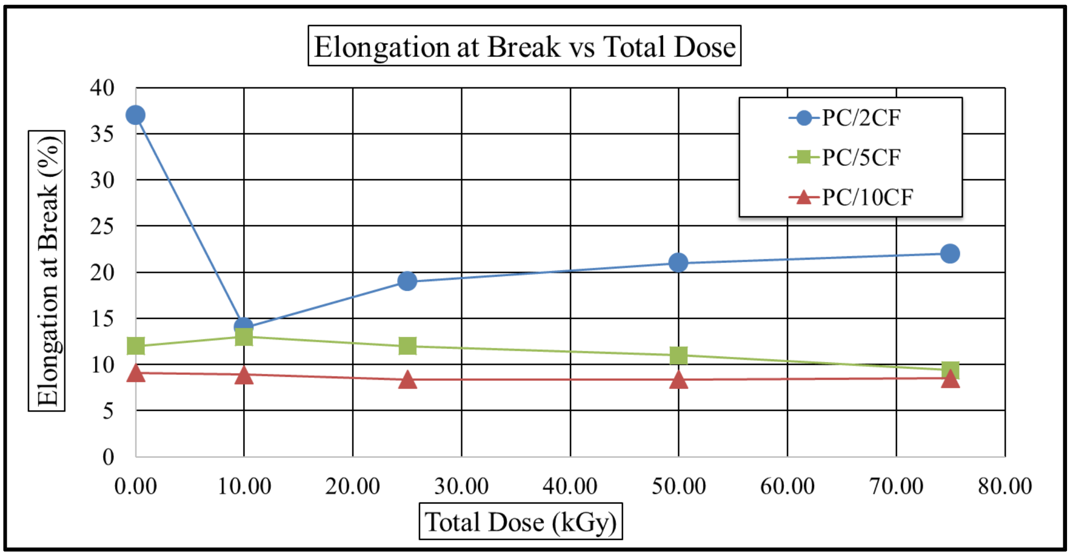

Figure 46 Change of Elongation at Break with Total Dose for Carbon Fiber Filled Polycarbonate

Tensile strength values of carbon fiber loaded composites did not change significantly via irradiation that strength values for each dose were close to each other. The relative reduction (comparing the values of non-irradiated and 75 kGy irradiated samples) in strength values were 1.46, 0.81 and 0.23 % for 2, 5 and 10% carbon fiber filled specimens, respectively. On the other hand, relative reduction in the ultimate elongation (comparing the values in non-irradiated and the total dose of 75 kGy) was 40.54, 21.67 and 6.59 % for 2, 5 and 10% carbon fiber filled specimens, respectively. Carbon fiber included composites showed best stability among all composites under irradiation in terms of strength. Increasing the content of carbon fiber enhanced the radiation shielding of composites, which were proved by strength values. The attenuation of carbon fiber was demonstrated on past studies that carbon fiber used as couch inserts in radiotherapy had ability to attenuate the penetrating radiation by 3.4-10.8 percent (Seppälä & Kulmala, 2011). Moreover, the enhancement in the mechanical properties (10 to 14.7 percent) of carbon fibers up to 100 kGy was reported by various scientists (Xu, et al., 2010; Sui, et al., 2016). The information obtained past studies explained the reason for the stabilities in the test results upon irradiation. Polycarbonate with 10 wt. % carbon fiber composites showed the highest mechanical strength at 50 kGy and composite with 2 wt. % carbon fiber showed maximum elongation at 75 kGy among all irradiated composites based on carbon fiber.

The results of the mechanical tests clearly showed that carbon fiber reinforced polycarbonate samples did not show any significant change in the mechanical properties up to 75 kGy dose. Thus, radioactive waste having initial contact dose rate of 1.126 Gy/h with the half-life of 5.27 years could be theoretically embedded into carbon fiber reinforced polycarbonate with remote handling procedures for 300 years (IAEA, 2009; IAEA, 1998). From the perspective of half value dose, 5 and 10 percent carbon fiber loaded polycarbonates, which exhibited more stability in terms of strength and elongation, were more suitable in radioactive waste treatment than 2 percent carbon fiber loaded one.

3.2.1.7. Discussion about Possible Use of Neat, Bentonite, Barite, Glass Fiber and Carbon Fiber Loaded Composites in Radioactive Waste Management in terms of Tensile Properties

Tensile test results showed that 75-kGy irradiation did not diminished the mechanical properties significantly. Radiation induced degradation were not considerably observed. Radiation resistance of polymer used extensively in radiated areas has been determined according to the procedure given in TS EN ISO 60544-2 and TS EN ISO 60544-4 standards. These standards have specified the end-point criteria for critical properties. Tensile strength, elongation at break and hardness have been classified as critical properties (Turkish Standards Institution, 2004; Turkish Standards Institution, 2013). The specified end-point criterion for tensile strength and elongation at break values is 50 % of the initial values. End-point criterions have been indicator of end use requirement. Relative values (expressed as percentages) of the tensile strength and ultimate elongation upon irradiation were given in **Table 35** and **Table 36**.

Table 35 Relative Elongation at break (expressed as percentage) Values of Polycarbonate Specimens

$(\frac{\text{Ultimate Elongation at Irradiation Dose}}{\text{Ultimate Elongation at Non−Irradiated}})$

Composites	**Relative values (expressed as Percentage)**				
	NON-IRRA	**10 kGy**	**25 kGy**	**50 kGy**	**75 kGy**
PC	100	69.8	154.3	152.9	97.8
PC/1B	100	170.9	230.8	188.0	196.0
PC/2B	100	250.0	964.3	226.2	285.7
PC/5B	100	157.0	160.0	220.0	190.0
PC/2Ba	100	235.6	208.9	115.6	151.1
PC/5Ba	100	45.5 [*]	77.3	100.0	68.2
PC/10Ba	100	225.6	161.1	144.4	150.0
PC/2CF	100	37.8	51.4 [*]	56.8	59.5
PC/5CF [**]	100	108.3	100.0	91.7	87.5
PC/10CF [**]	100	97.8	92.3	92.3	93.4
PC/2GF	100	60.0	124.0	64.0	60.0
PC/5GF [**]	100	90.9	109.1	127.3	100.0
PC/10GF [**]	100	91.7	86.5	95.8	85.4

[*] Lowest radiation resistance material in terms of ultimate elongation

[**] Highest radiation resistance materials in terms of ultimate elongation

Table 36 Relative Tensile Strength (expressed as percentage) Values of Specimens $\left(\frac{\text{Ultimate Elongation at Irradiation Dose}}{\text{Ultimate Elongation at Non−Irradiated}}\right)$

Composites	**Relative values (expressed as Percentage)**				
	NON-IRRA	**10 kGy**	**25 kGy**	**50 kGy**	**75 kGy**
PC	100.0	101.0	103.8	104.1 *	99.7
PC/1B	100.0	97.1	96.2	95.6	94.7
PC/2B	100.0	96.2	96.5	97.0	94.8
PC/5B	100.0	97.2	87.9 **	96.8	94.9
PC/2Ba	100.0	101.2	98.9	98.1	97.4
PC/5Ba	100.0	103.2	100.8	100.9	100.5
PC/10Ba	100.0	100.2	99.5	100.0	97.6
PC/2CF	100.0	100.0	99.7	100.4	98.5
PC/5CF ***	100.0	101.5	99.5	98.8	99.2
PC/10CF ***	100.0	100.0	99.5	102.2	99.8
PC/2GF	100.0	99.5	98.6	99.4	98.3
PC/5GF ***	100.0	98.9	98.9	98.7	97.3
PC/10GF ***	100.0	104.5	96.4	97.5	97.2

* Highest relative tensile strength

** Lowest relative tensile strength

*** Highest radiation resistance materials in terms of load bearing capacity

The highest and the lowest relative strength values were highlighted by red in the **Table 36**. The relative strength values of specimens were laid down between the 87.9 % (correspond to 5 wt. % bentonite filled specimen at 25 kGy) to 104.6 % (correspond to neat polycarbonate at 50 kGy). According to the relative values, neither composites nor neat polycarbonate converged to the value set by the standard (which was 50 % of initial value) in all doses indicating that they had superior stabilities in terms of tensile strength.

On the other hand, the relative elongation values of specimens showed deviations with respect to the irradiation. The particulate-based composites had higher deviations than fiber reinforced composites. 2 wt. % carbon fiber and 5 wt. % barite filled specimens were the least radiation resistant material in terms of ultimate elongation among all composites such that the threshold value (50 % of initial value) were exceeded at 10 kGy.

When the relative values of strength and ultimate elongation were taken in to account together, it was clear that fiber reinforced composites (especially for specimens containing 5, 10 wt. % carbon and glass fiber) showed highest resistance to ionizing radiation in terms of both load bearing capacity and ultimate elongation. This was attributed to the following findings:

- The deviations for both parameters (tensile strength and elongation at break) were smallest among all specimens.
- The closeness of the relative values at different doses was indicator of radiation attenuation
- The strength values of the carbon and glass fiber (5 and 10 wt.%) containing composites were comparatively higher than the strength value of 75 kGy irradiated polycarbonate. Tensile strength values of 5 wt.% glass fiber, 10 wt.% glass fiber, 5 wt.% carbon fiber and 10 wt.% carbon fiber reinforced composites improved by 8.9, 16.4, 17.7 and 39.6 %, respectively.

Polymers including polycarbonate urethane and polybisphenol-a-epichlorohydrin were found as radiation stable polymers and they were proposed as embedding matrix for low-level radioactive waste (Ozdemir, 2006). The strength values at 71 kGy were determined as 50.3, 52.1 and 30.3 MPa for polycarbonate urethane, polybisphenol-a-epichlorohydrin and polymethyl methacrylate. The relative elongation at break values were found as 1.01, 0.15, 0.57 for polymers mentioned above, respectively.

Boron fiber reinforced polystyrene (PS), polymethyl methacrylate (PMMA), Devcon 10210 epoxy, and polyetheretherketone (PEEK) were investigated in order to determine the possible use of them as an alternative to metals in design of radioactive waste container (Bonin, et al., n.d.). The tensile strength values were found as 41.9, 49.1, 51.5, 57.0, 52.0, 57.6, 88.1 and 82.6 for PS (with 50 % boron), PS (with (70 % boron), PMMA (with 50 % boron), PMMA (with 70 % boron), epoxy (with 50 % boron), epoxy (with 70% boron), PEEK (with 50% boron), PEEK (with 70 % boron), respectively (Bonin, et al., n.d.).

It was clear that the strength and relative elongation at break values of the polycarbonate specimens including composites were comparatively higher than polymers including polycarbonate urethane, polybisphenol-a-epichlorohydrin and polymethyl methacrylate at equivalent doses (i.e. around 70-75 kGy). The mechanical properties were also superior for polycarbonate specimens with respect to polymers including boron fiber reinforced polystyrene (PS), polymethyl methacrylate (PMMA) and Devcon 10210 epoxy.

It could be stated that polycarbonate and its composites surpassed the polymers (except for PEEK) studied in previous studies in terms of tensile properties regarding possible use in radioactive waste management around 75 kGy.

All specimens met the requirements set out in TS EN ISO 60544-2 and TS EN ISO 60544-4 standards. The half value dose and radiation index (logarithm of the absorbed dose in grays at which end-point criteria were achieved) were not observed (Turkish Standards Institution, 2004). Radioactive waste with initial contact dose rate of 1.126 Gy/h and half-life of 5.27 year could be theoretically immobilized into neat, bentonite, barite, glass fiber and carbon fiber filled polycarbonate. Polycarbonate specimens under study could be resisted more than 75 kGy without reaching end-point criteria. Therefore, initial contact dose rate of waste, which would be intended to be encapsulated into polycarbonate specimens, could be theoretically larger than 1.126 Gy/h. For this reason, it could be beneficial to conduct further irradiations to obtain the dose at which radiation index would be reached.

3.2.2 Hardness Results

Hardness values of neat, bentonite, barite, glass fiber and carbon fiber filled polycarbonate samples were shown in **Table 37**. Column Chart for hardness values for non-irradiated specimens was illustrated on **Error! Reference source not found.**.

Table 37 Hardness Values of Neat, Bentonite, Barite, Glass Fiber and Carbon Fiber Reinforced Polycarbonates

Composite	**Hardness (Shore D) Values**				
	NON-IRRA	**10 kGy**	**25 kGy**	**50 kGy**	**75 kGy**
PC	77.0	78.4	78.6	78.8	79.6
PC/1B	76.1	78.0	78.6	79.5	78.5
PC/2B	77.8	79.0	79.3	78.8	78.9
PC/5B	77.4	78.9	79.2	79.0	79.3
PC/2Ba	78.2	78.2	78.2	78.8	79.1
PC/5Ba	77.2	78.9	79.9	78.9	79.5
PC/10Ba	77.7	79.7	79.7	79.6	79.4
PC/2CF	77.7	79.6	79.4	78.5	78.8
PC/5CF	80.0	80.2	79.8	80.5	79.7
PC/10CF	80.3	80.9	80.9	81.1	79.8
PC/2GF	79.3	79.3	79.2	78.7	78.6
PC/5GF	79.6	80.1	79.3	79.4	79.7
PC/10GF	80.1	-	79.4	79.7	79.8

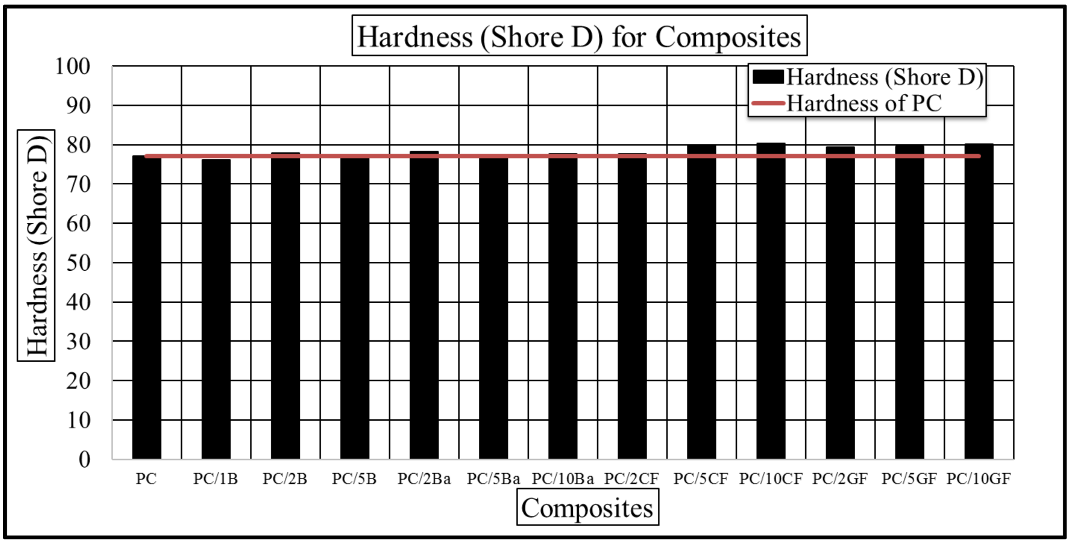

Figure 47 Column Chart of Hardness Values for Non-Irradiated Specimens (Neat Polycarbonate, Bentonite, Barite, Glass Fiber and Carbon Fiber loaded Polycarbonate Composites)

Error! Reference source not found. showed that hardness values of glass and carbon fiber reinforced composites were greater than the neat, bentonite and barite filled polycarbonates in non-irradiated case. Tensile strength and hardness values were proportional to each other (Callister, Jr., 2007). Therefore, loading of reinforcing agents of glass fiber and carbon fiber to the polycarbonates increased the hardness of specimens.

Hardness was identified as critical property for determining radiation resistance of polymers used extensively in radiation environments. End-point criterion for the hardness was determined as 10-unit change in Hardness value (Turkish Standards Institution, 2013; Turkish Standards Institution, 2004). **Table 37** revealed the fact that 10-unit change were not reached by 75 kGy irradiation for all types of specimens. This indicated that radiation index number ($\log_{10} 75{,}000 = 4.87$) and dose for end-point criteria were above the 4.87 and 75 kGy, respectively. Tensile test results also supported the results obtained from hardness. In addition, 75 kGy could be possibly selected for the calculation for initial dose rate of radioactive waste, which was intended to be immobilized into the polymers in question.

The previous study focusing on possible use of ethylene propylene diene terpolymer (EPDM) in radioactive waste management stated that 386 kGy was the dose at which 10-unit change was observed in hardness value (Hacıoğlu, 2010). Radiation index value for EPDM was calculated as 5.59, which corresponded $\log_{10} 386{,}000$. To compare the radiation resistance EPDM elastomer with the polycarbonate composites in terms of hardness values, it would be beneficial to conduct a study at which total dose was set to 386 kGy.

Moreover, report on effects of radiation-induced aging on polymer-based cables used as insulators at CERN were published (Ilie & Setnescu , 2009). Radiation index of polymers used in CERN were stated in the report. The minimum radiation index numbers for selected polymers were found as (Ilie & Setnescu , 2009):

- Ethylene propylene rubber (EPR): 5.9
- Ethylene-vinyl acetate copolymer (EVA): 5.8
- Low density polyethylene (LDPE): 4.2
- High density polyethylene (HDPE): 5.4

These results showed that radiation index numbers for neat, bentonite, barite, glass fiber and carbon fiber loaded polycarbonates were higher than LDPE that used in CERN. To compare the maximum supportable dose of polycarbonates with rest of the polymers stated above, further irradiation beyond 75 kGy would be required. Apart from the possible use in radioactive waste management, polycarbonates and its composites with bentonite, barite, glass fiber and carbon fiber could be used as insulating materials in radiation environments such as facilities at which radiation sterilization have been conducted. Nuclear power plants and reactor fuel-processing sites could be the other facilities that polycarbonates could be involved. To conduct accurate interpretation for the possible use of polymer in highly radiated areas such as CERN, it could be recommended to determine the mechanical properties at 500 kGy to assess whether end-point criteria would be reached or not (European Organization for Nuclear Research, 2005).

3.2.3 Yellowness Index (YI) and CIELAB Color Scales

Yellowness Index (YI) and CIELAB Color Scales (b*) values of neat and glass fiber reinforced polycarbonate samples upon irradiation were given in **Table 38**, **Table 39** and shown in **Figure 48**, **Figure 49**, **Figure 50**, **Figure 51**. Composites with carbon fiber, bentonite and barite had intense colors and therefore the yellowness index measurements of these composites were not carried out.

Table 38 Yellowness Index (YI) Values of Neat Polycarbonate and Glass Fiber Reinforced Composites

Composite	**Yellowness Index (YI)**				
	NON-IRRA	**10 kGy**	**25 kGy**	**50 kGy**	**75 kGy**
PC	4.15	8.18	15.37	30.01	36.63
PC/2GF	1.24	7.51	17.31	28.22	31.99
PC/5GF	3.71	10.02	19.73	31,93	31.92
PC/10GF	3.58	-	13.95	31.26	32.97

Table 39 CIELAB Color Scales (b) Values of Neat Polycarbonate and Glass Fiber Reinforced Composites

Composite	**CIELAB Color Scales (b*) Values**				
	NON-IRRA	**10 kGy**	**25 kGy**	**50 kGy**	**75 kGy**
PC	1.09	2.11	3.88	7.07	9.44
PC/2GF	1.11	2.66	4.21	8.52	8.01
PC/5GF	1.13	2.88	5.51	8.68	8.30
PC/10GF	1.23		5.58	8.79	8.64

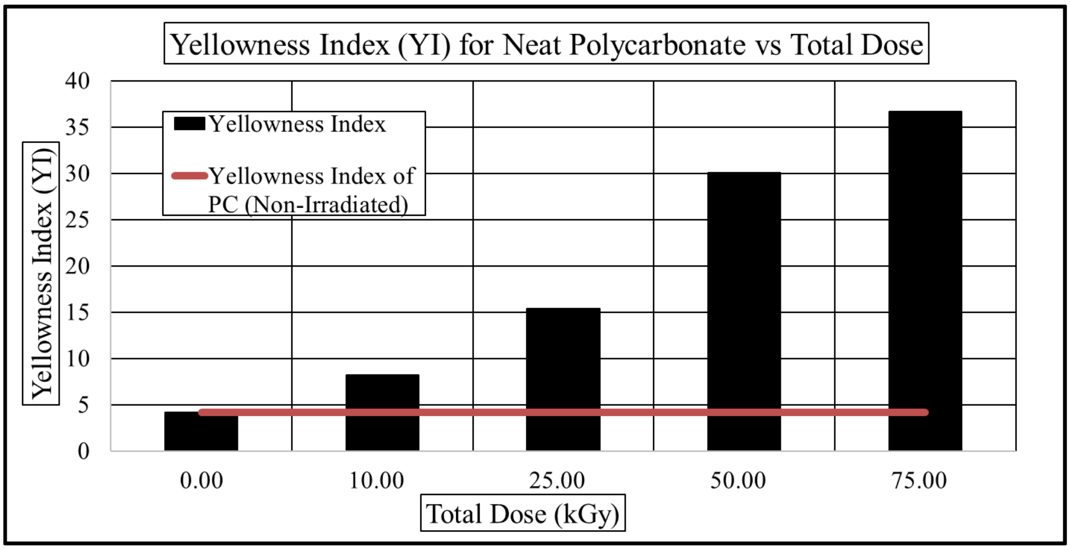

Figure 48 Column Chart of Yellowness Index (YI) for Neat Polycarbonate upon Irradiation

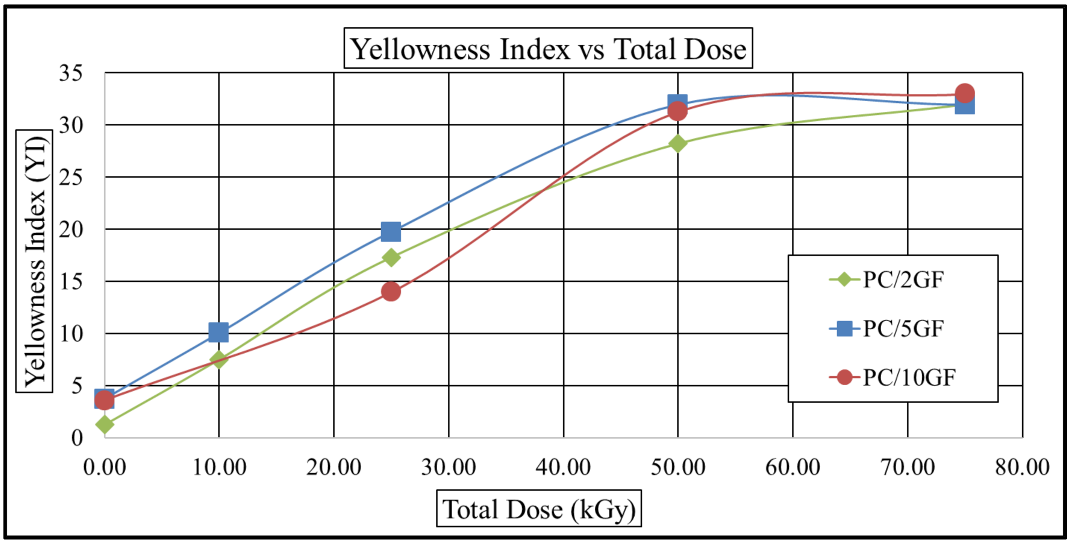

Figure 49 Graph for Yellowness Index (YI) for Glass Fiber Reinforced Polycarbonate upon Irradiation

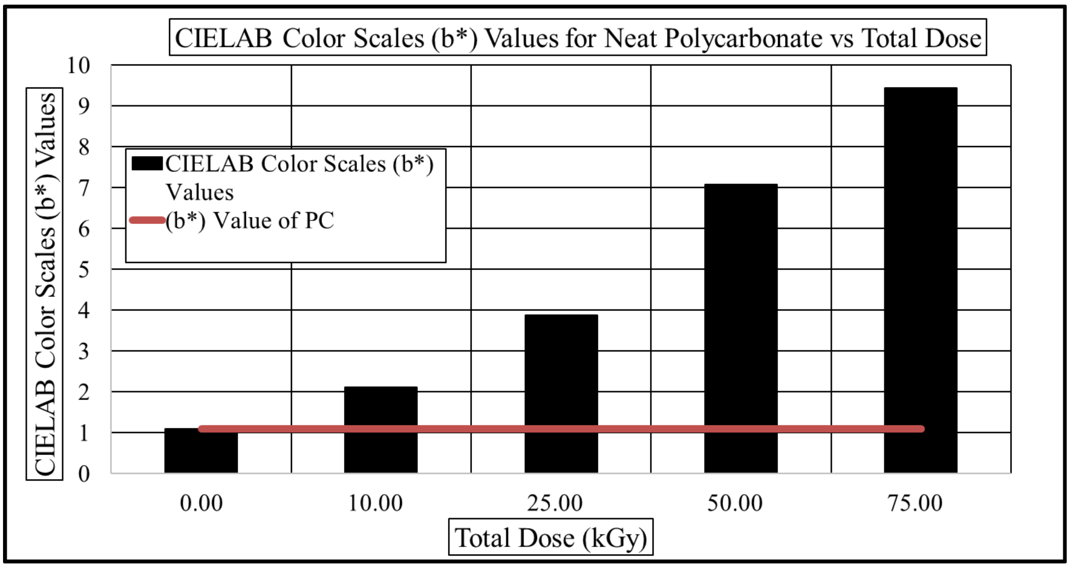

Figure 50 Column Chart of CIELAB Color Scales (b*) Values for Neat Polycarbonate upon Irradiation

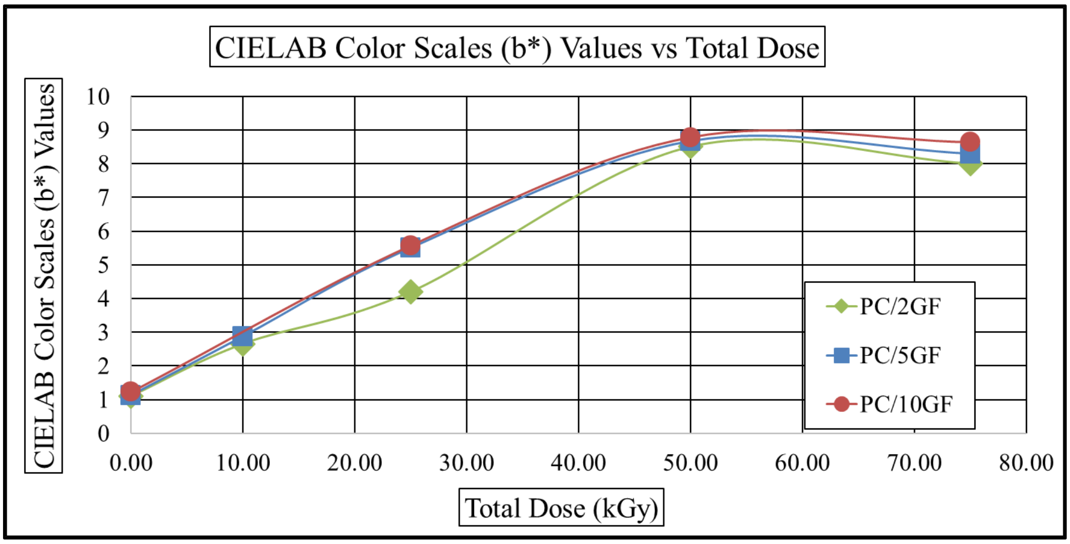

Figure 51 Graph of CIELAB Color Scales (b*) Values for Glass Fiber Reinforced Polycarbonate upon Irradiation

Yellowness index is an indicator for the presence of radiation induced chain scission reactions. For comparisons within the polymer upon irradiation, higher yellowness index indicates higher radiation induced chain scission (Massey, 2004). Moreover, CIELAB Color Scales value designated as “b” supports information that yellowness index gives in the same manner (Ferreira, et al., 2011; ASTM International, 2013).

Previous studies revealed that, irradiation of polycarbonate produced phenyl and phenoxy radicals (Araujo, et al., 1998; Ferreira, et al., 2011). The formations of phenyl and phenoxy radicals triggered the increase in the yellowness index and “b” values (Araujo, et al., 1998; Ferreira, et al., 2011; Massey, 2004).

According to the test results, yellowness index and the “b” values of neat and glass fiber reinforced polycarbonates were significantly increased upon irradiation. The increase in the “b” value and yellowness index were associated with the presence of radiation induce chain scission. The higher doses were resulted with higher yellowness index and “b” values such a way that extent of radiation induced chain scission was increased via irradiation. The C-O bond, which was adjacent to the carbonyl group, is the weakest bond in the main chain of the polymer due to the lack of resonance stabilization (Araujo, et al., 1998; Ferreira, et al., 2011; Zimmerman, et al., 1993; Rabek, 1995). Irradiation of this bond caused the chain scission yielding with phenyl and phenoxy radicals (Araujo, et al., 1998; Ferreira, et al., 2011; Zimmerman, et al., 1993; Rabek, 1995).

At 75 kGy, “b” and yellowness index values of the glass fiber reinforced polycarbonate were lower than the values of neat polycarbonates. It could be inferred from the results that glass fiber acted as scavenger of phenoxy and phenyl radicals upon irradiation and reduced the amount of chain scission reactions relatively.

The phenoxy and phenyl radicals produced via gamma irradiation and vulnerable bonds in the main chain of the polycarbonate were shown in **Figure 52** and **Figure 53**, respectively.

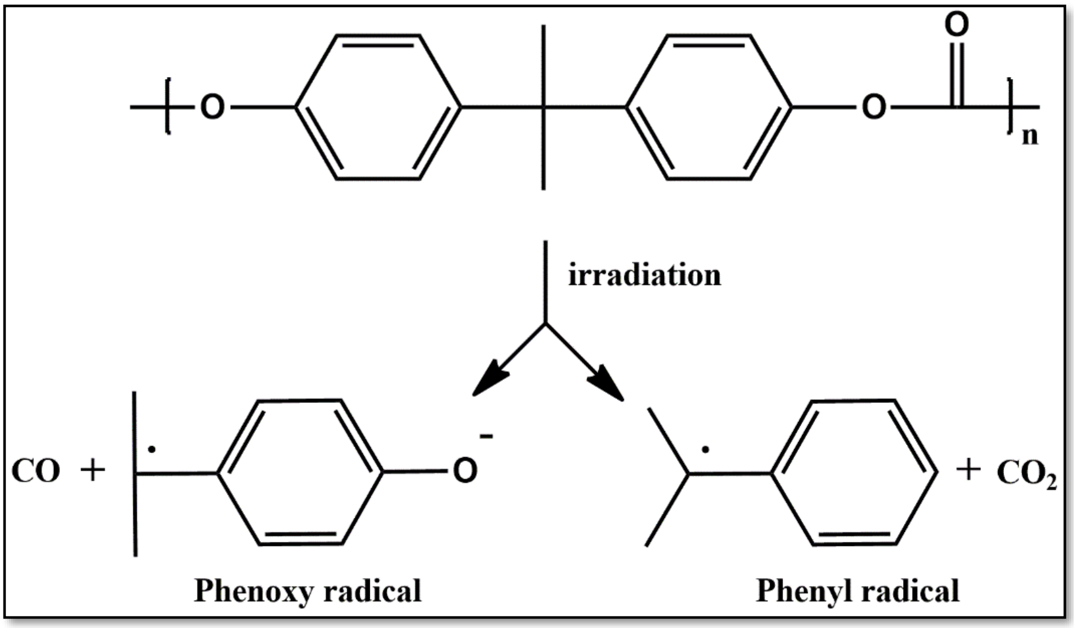

Figure 52 Schematic representation of phenyl and phenoxy radicals formation upon irradiation in polycarbonate specimens (Hareesh, et al., 2013).

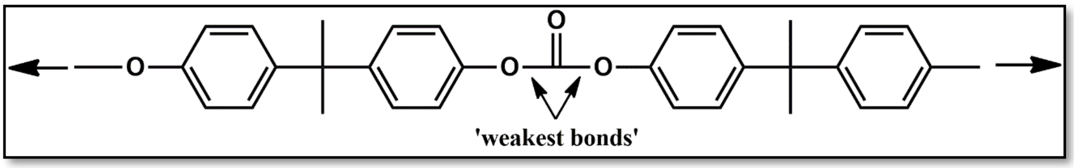

Figure 53 Weakest bond in the main chain of polycarbonate (Zimmerman, et al., 1993).

3.2.4 Attenuated Total Reflection Fourier Transform Infrared Spectroscopy (ATR-FTIR)

The main absorption peaks of polycarbonate were given in **Table 40**. ATR-FTIR spectrums of the neat, bentonite, barite, glass fiber and carbon fiber loaded polycarbonate samples were illustrated on **Figure 54**, **Figure 55**, **Figure 56**, **Figure 57** and **Figure 58**.

Table 40 Characteristic Absorption Peaks of Bisphenol-A Based Polycarbonate (Delpech, et al., 2002; Silverstein, et al., 2005; Sinha, et al., 2004)**.**

Frequency (cm^{-1})	**Bonds**	**Vibrational Mode**
3529	OH (phenolic hydroxyl)	Stretching
3039	C-H (aromatic ring)	Stretching
2969	C-H (methyl group)	Symmetrical stretching
2500-1800	Aromatic ring	Combination bands
1773	O-(C=O)-O (carbonyl)	Stretching
1602 and 1465	C=C (aromatic ring)	Stretching
1506	C-H (aromatic ring)	In-plane bending
1387	C-H (methyl group)	Symmetrical bending
1232	C-O-(C=O)-O-C	Asymmetrical stretching
1206	C-O-C	Asymmetrical stretching
999	C-H (aromatic ring)	Out-of-plane bending
757	C-H (aromatic ring)	Out-of-plane bending
667	C=C (aromatic ring)	Out-of-plane bending

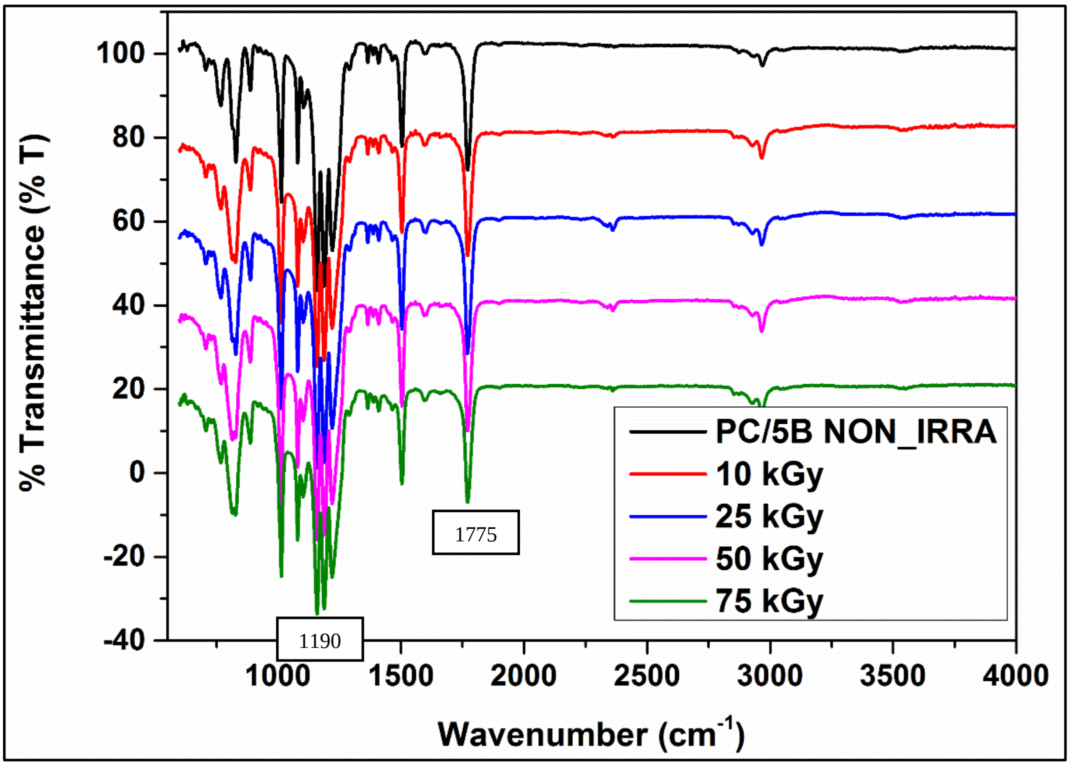

Figure 54 ATR-FTIR Spectrum of 5 % wt. Bentonite Loaded Polycarbonate

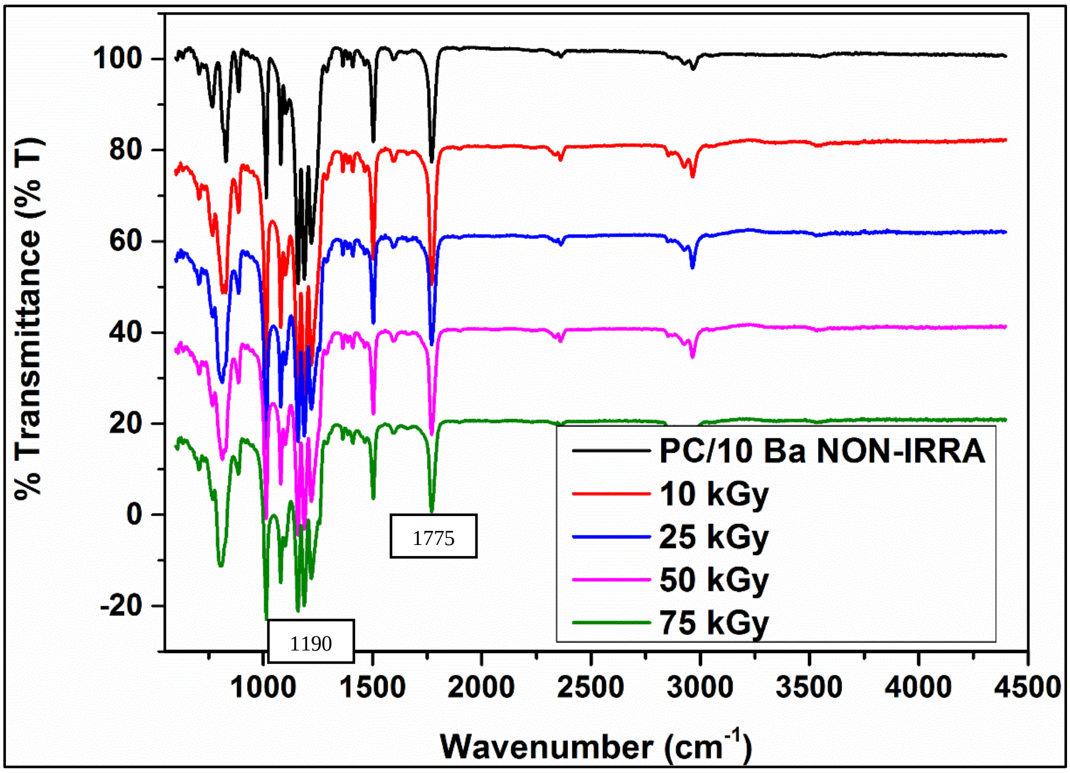

Figure 55 ATR-FTIR Spectrum of 10 % wt. Barite Loaded Polycarbonate

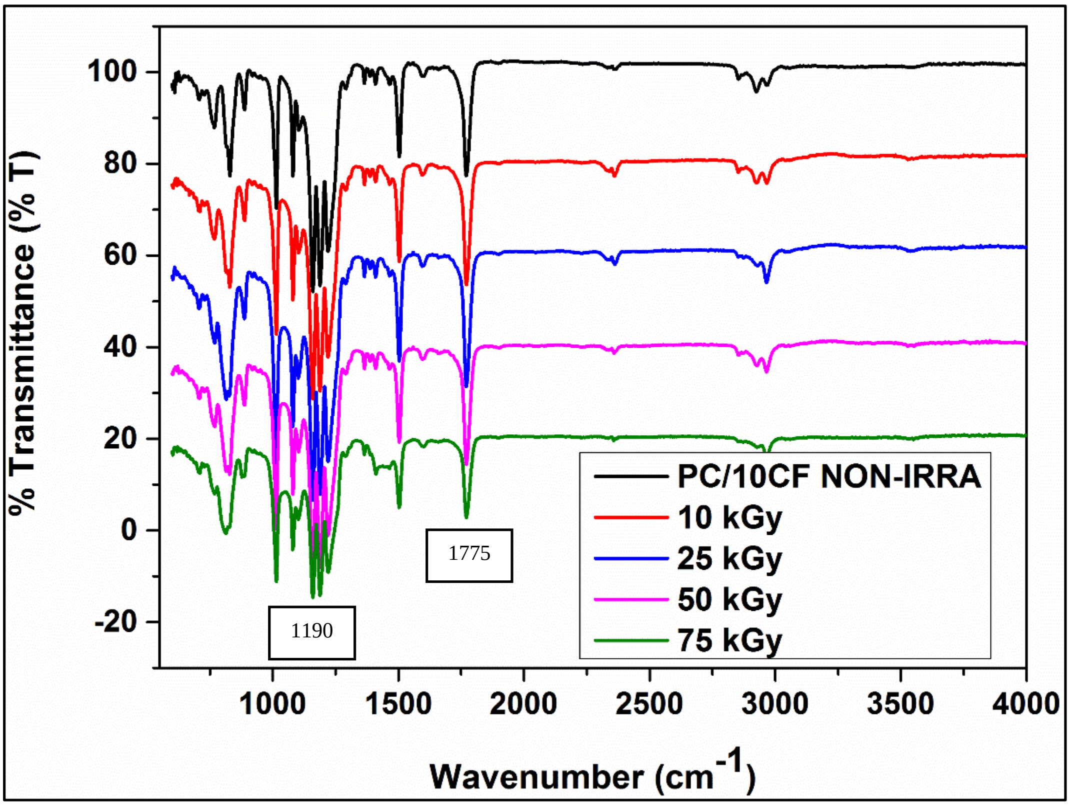

Figure 56 ATR-FTIR Spectrum of 10 % wt. Carbon Fiber Loaded Polycarbonate

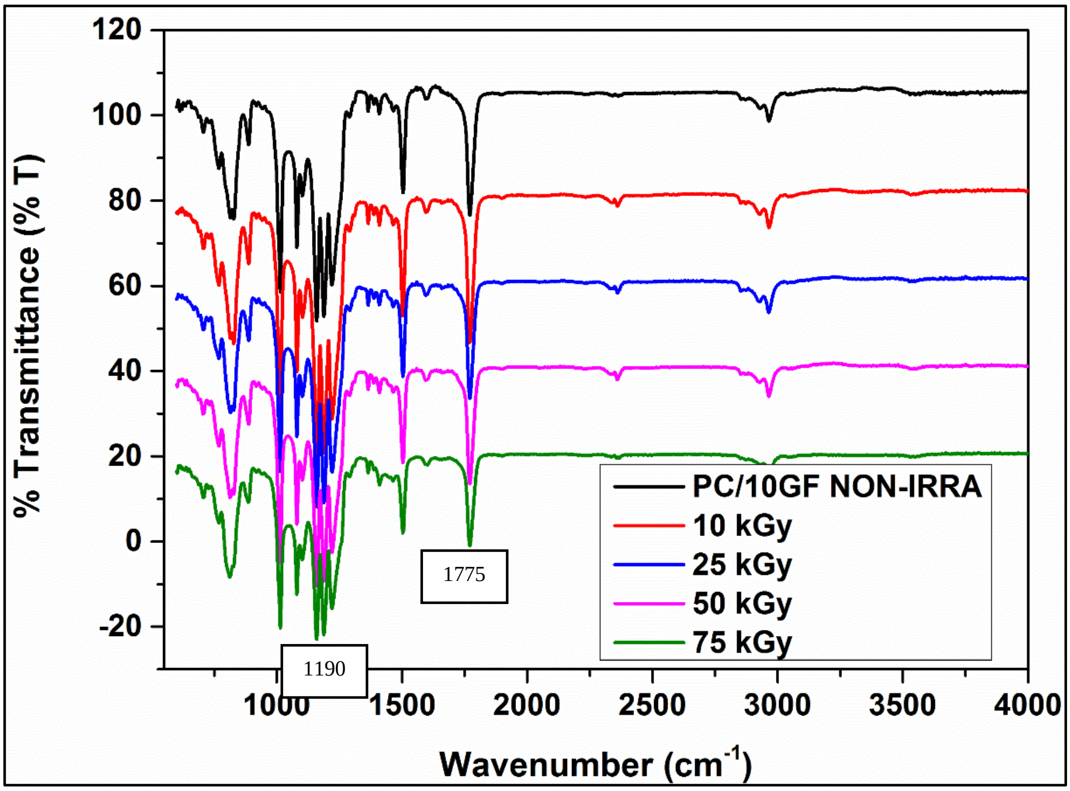

Figure 57 ATR-FTIR Spectrum of 10 % wt. Glass Fiber Loaded Polycarbonate

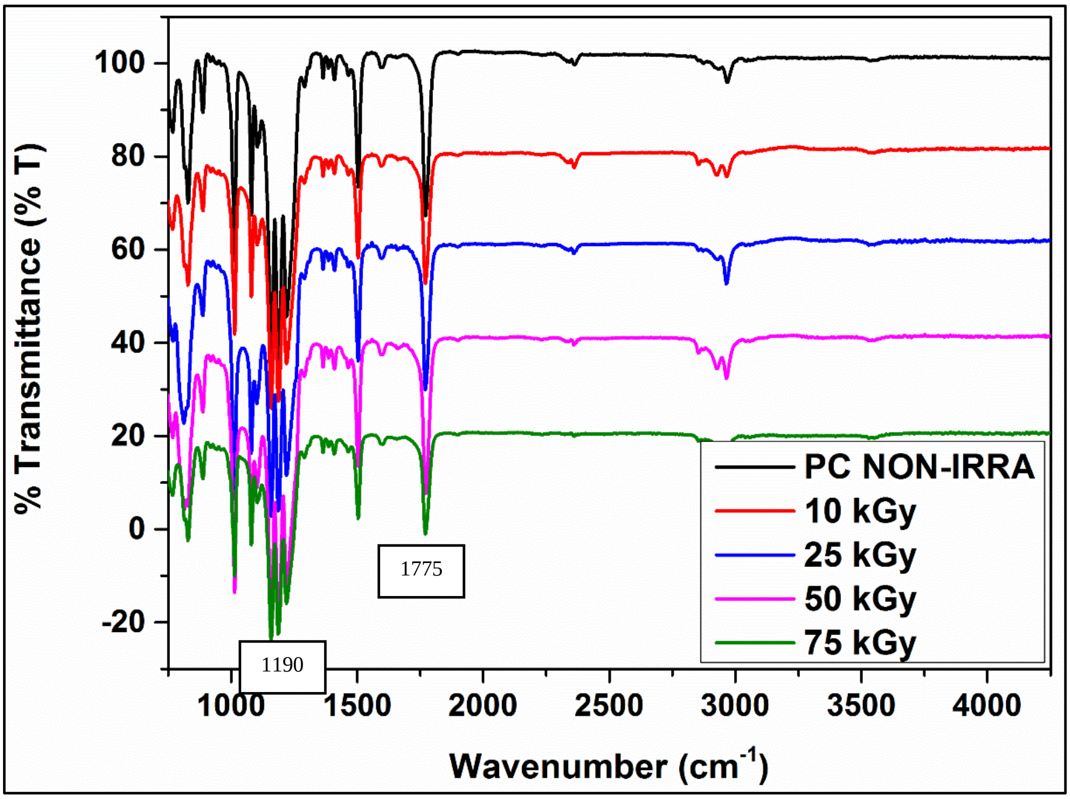

Figure 58 ATR-FTIR Spectrum of Neat Polycarbonate

Table 40 gave the frequencies of the main absorption bands of bisphenol-a polycarbonate (Delpech, et al., 2002; Silverstein, et al., 2005; Sinha, et al., 2004). ATR-FTIR test results of the neat, particle and fiber reinforced polycarbonates revealed that neither total destruction nor formation of new peaks were observed. No appreciable changes were present for all specimens up to 75 kGy as well. On the other hand, intensity decrease around 1775 and 1190 cm^{-1} was significant at 75 kGy-irradiated specimens. Intensities around 1775 and 1190 cm^{-1} correspond to the C=O bond and C-O-C bond vibrations, respectively. The decrease in the intensities of carbonyl and ether bonds could be associated with the presence of radiation-induced chain-scissions resulting with phenyl and phenoxy radicals formation (Sinha, et al., 2004; Hareesh, et al., 2013; Rabek, 1995). The vulnerable bonds present in the main chain of polycarbonates were C-O-C bonds. The high-energy radiation deteriorated the main chain at the weakest sites. The phenoxy and phenyl radicals produced via gamma irradiation and vulnerable bonds in the main chain of the polycarbonate were shown in **Figure 52** and **Figure 53**, respectively. The results obtained from yellowness index and ATR-FTIR analysis supported with each other (Sinha, et al., 2004; Hareesh, et al., 2013).

3.2.5 Melt Flow Rate (MFR)

MFR results of neat, particle and fiber filled composites were given in **Table 41** and **Figure 59**.

Table 41 Melt Flow Rate (MFR)Values of Neat, Particle and Fiber Filled Polycarbonate Samples

Composite	**Melt Flow Rate** $(\frac{\mathbf{g}}{\mathbf{10\ min}})$
PC	14.79
PC/1B	20.69
PC/5B	19.92
PC/2Ba	16.15
PC/5Ba	15.43
PC/10Ba	16.50
PC/2GF	12.75
PC/5GF	12.39
PC/10GF	13.21
PC/2CF	14.04
PC/5CF	12.61
PC/10CF	14.58

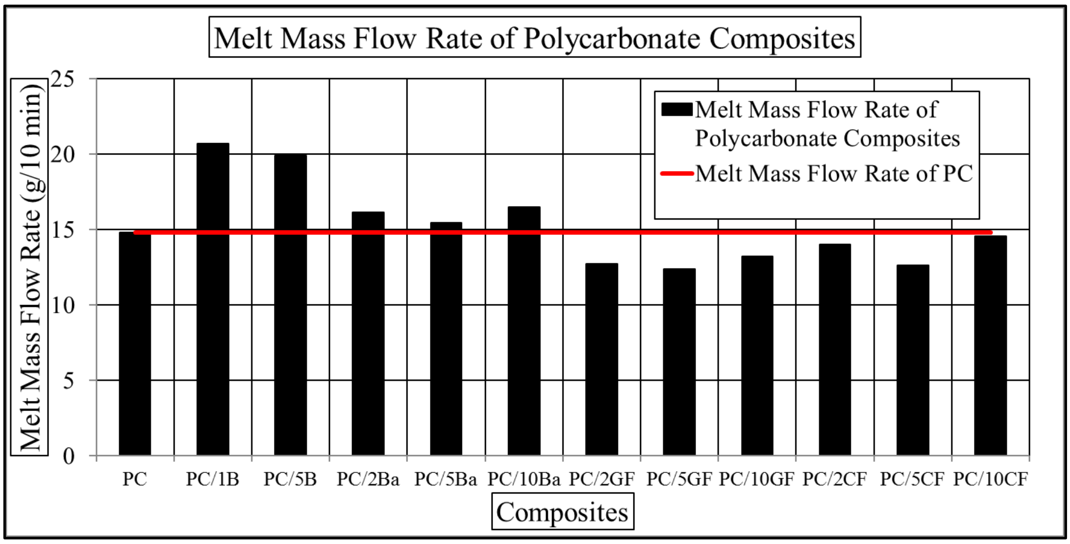

Figure 59 Colum Chart for Melt Flow Rate of Neat, Particle and Fiber Filled Polycarbonate Samples

MFR results revealed that particle filled composites had higher MFR than that in neat polycarbonate. On the other hand, MFR values of fiber-reinforced polycarbonate were comparatively lower than that of neat polycarbonate. High additive-matrix interfacial interaction resulted with decreases in the MFR values (George, et al., 1996).

Carbon fiber and glass fiber, exposed to surface modification by silane and epoxy, respectively, thereby decreasing the MFR values due to high fiber-polymer interfacial interaction (George, et al., 1996). On the other hand, bentonite and barite, to which no surface modification was applied, increased the MFR values by means of poor particle-polymer interfacial interaction.

In comparison of MFR values within the particle filled composites, bentonite based composites had higher MFR values. It could be associated with the higher mean particle size of bentonite such a way that it brought about poorer interfacial interaction. Plate like structure of the bentonite could be also associated with the poorer interfacial interaction between the matrix and filler, indicating higher MFR.

3.2.6 Thermogravimetric Analysis (TGA)

3.2.6.1. Thermogravimetric Analysis (TGA) for Neat Polycarbonate and Composites

Thermogravimetric (TG) curves and First Derivative of the Thermogravimetric (DTG) Curves of neat polycarbonate and composites were shown in **Figure 60**, **Figure 61**. T_{max} (temperature, at which highest rate of weight loss occurs, was obtained from first derivative of TG curve) and T_{50} (temperature, at which 50 % weight loss occur, was obtained from TG curve) values of neat, particulate and fiber filled polycarbonate samples were given in **Table 52** and **Table 52**.

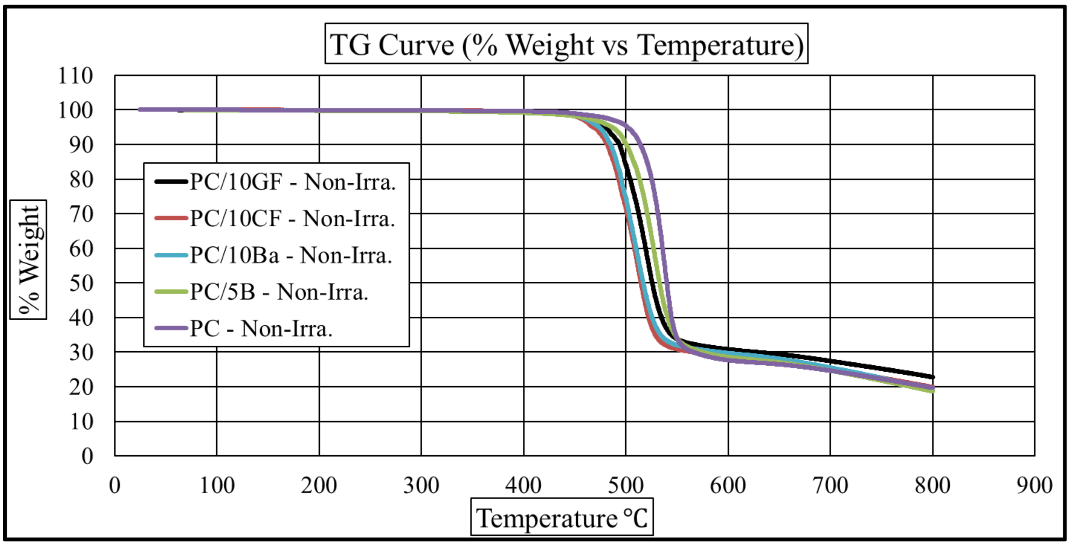

Figure 60 TG Curves of Neat, Particle and Fiber Filled Polycarbonate Samples

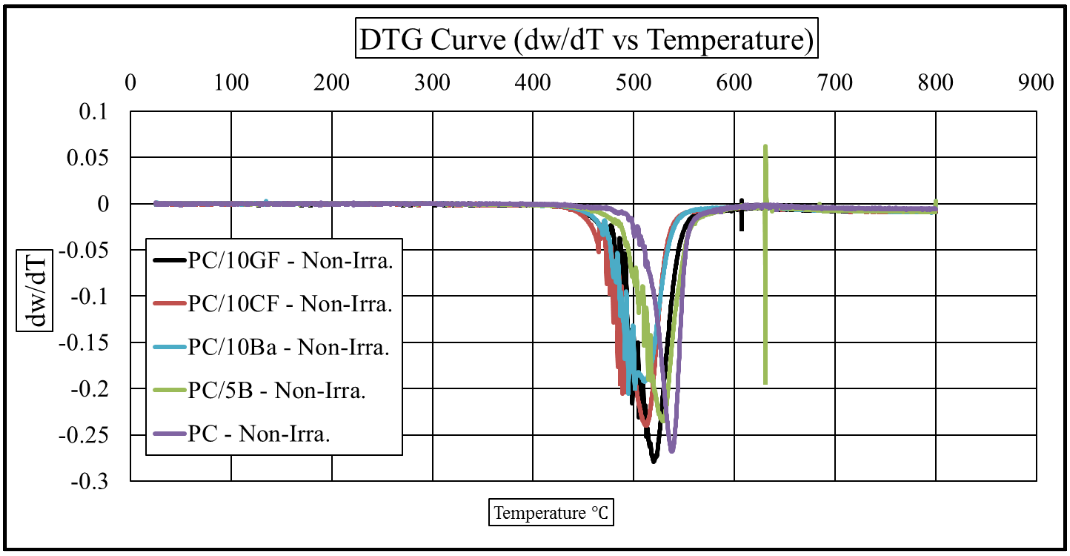

Figure 61 DTG Curves of Neat, Particle and Fiber Filled Polycarbonate Samples

Table 42 T_{max} Values for Neat, Particle and Fiber Filled Polycarbonate Samples

Test Sample	**T_{max} (°C) Values**
PC	537.7 °C
PC/5B	528.2 °C
PC/10Ba	510.6 °C
PC/10CF	512.6 °C
PC/10GF	519.7 °C

Table 43 T_{50} Values for Neat, Particle and Fiber Filled Polycarbonate Samples

Test Sample	**T_{50} (℃) Values**
PC	539.8 ℃
PC/5B	532.7 ℃
PC/10Ba	516.8 ℃
PC/10CF	514.7 ℃
PC/10GF	525.7 ℃

According to the TGA results, specimens were stable up to 400 ℃ until which any significant weight loss was not detected. Between the temperatures of 400 to 800℃, significant weight losses were observed for the whole test samples.

TGA and DTG curves showed that neat polycarbonate had highest thermal stability among all composites. In addition, highest T_{max}, T_{50} and T_{onset} values were observed in neat polycarbonate.

Thermal stability of the composites containing 10 wt. % carbon and glass fiber were lower than the thermal stability of neat polycarbonate. 25.1 and 18℃ drop were observed in the T_{max} of the carbon and glass fiber (10 wt. %) containing composites, respectively. Higher thermal conductivity of the carbon and glass fibers could favor the decomposition of the composites, and so decreasing the thermal stability of the composites (Dao, et al., 2016). Thermal stability was comparatively higher in the composites containing 10 wt. % glass fiber with respect to composites including 10 wt. % carbon fiber. Carbon fibers had higher thermal conductivity than glass fibers and this could induce the thermal degradation of the carbon fiber reinforced composite occurred at lower temperature with respect to glass fiber reinforced composite (Kalogiannakis, et al., 2004).

Thermal stability of 5 wt. % bentonite incorporated polycarbonate were lower than that in the neat polycarbonate. The previous studies on clay-included polycarbonate supported the reduced thermal stability (Xiao, et al., 2013; Severe, et al., 2000; Feng, et al., 2012). Bentonite could catalyze the thermal degradation of polycarbonate chains and decrease the thermal stability of composite (Xiao, et al., 2013). On the other hand, the 5 wt. % bentonite loaded composites had higher T_{max}, T_{50} values than that of barite, glass fiber and carbon fiber loaded composites. Plate like structure of the bentonite could retard the diffusion of the volatile products and so making the composite showing higher thermal stability than barite, carbon fiber and glass fiber filled composite.

Thermal stability of 10 wt. % barite incorporated polycarbonate were lower than that in the neat polycarbonate. Barite did not include any surface modification resulting with poorer intercalation between matrix and filler. This could be the reason of lower thermal stability with reduced T_{max}, T_{50}.

3.2.6.2. Thermogravimetric Analysis (TGA) for Neat Polycarbonate Exposed to 10, 25, 50 and 75 kGy Irradiation

Thermogravimetric (TG) curves and First Derivative of the Thermogravimetric (DTG) Curves of neat polycarbonate samples (irradiated up to 75 kGy) were shown in **Figure 62** and **Figure 63**. T_{max} (temperature, at which highest rate of weight loss occurs, was obtained from first derivative of TG curve) and T_{50} (temperature, at which 50 % weight loss occur, was obtained from TG curve) values of neat polycarbonate samples (irradiated up to 75 kGy) were given in **Table 44** and **Table 45**.

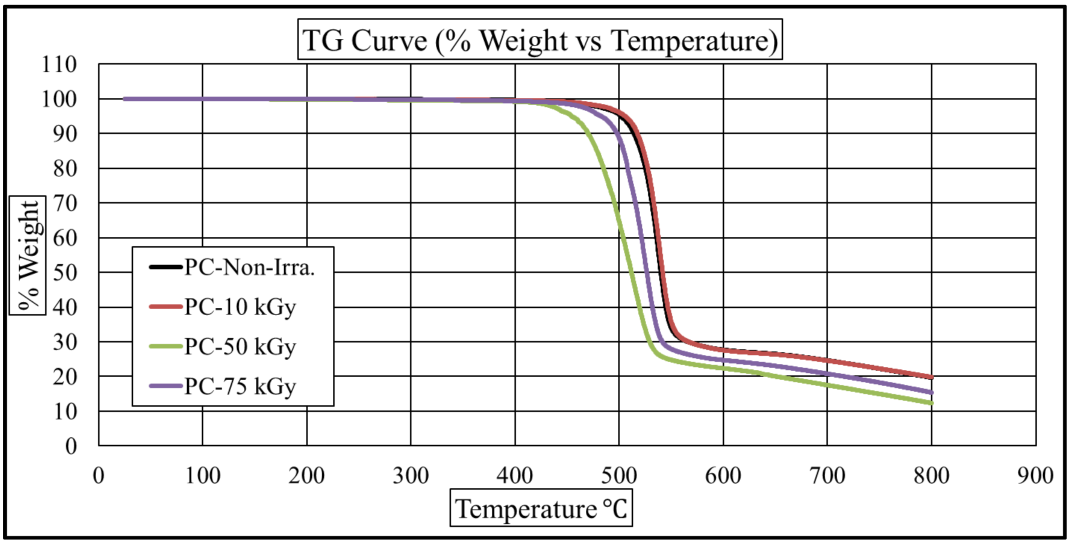

Figure 62 TG Curves of Neat Polycarbonate Samples Irradiated with 10, 50 and 75 kGy

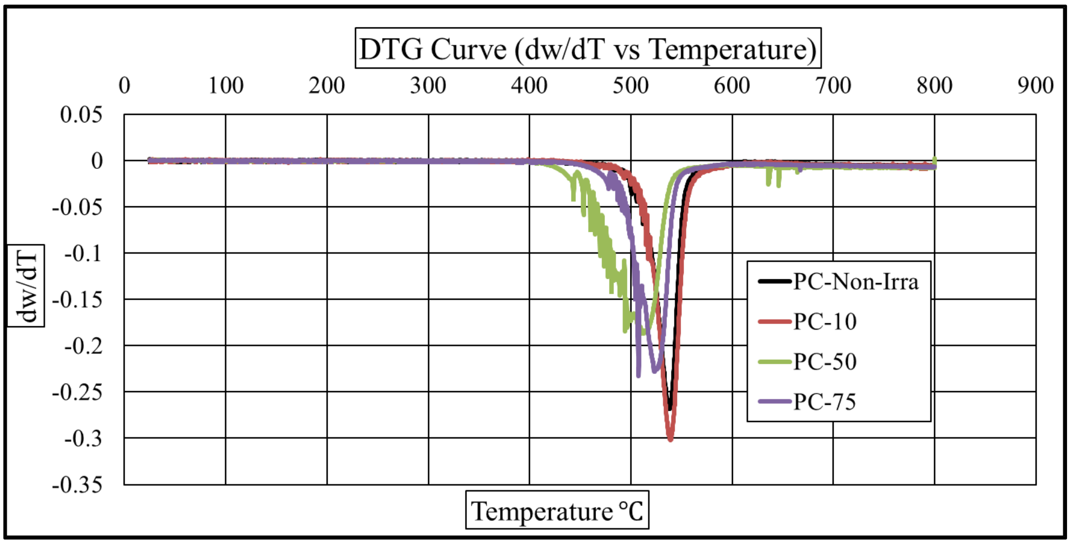

Figure 63 DTG Curves of Neat Polycarbonate Samples Irradiated with 10, 50 and 75 kGy

Table 44 T_{max} Values for Neat Polycarbonate Samples Irradiated up to 75 kGy

Test Sample	**T_{max} (°C) Values with Respect to Total Doses (kGy)**				
	NON-IRRA	**10 kGy**	**25 kGy**	**50 kGy**	**75 kGy**
PC	537.7 °C	539.2 °C	-	512.7 °C	523.2 °C

Table 45 T_{50} Values for Neat Polycarbonate Samples Irradiated up to 75 kGy

Test Sample	**T_{50} (°C) Values with Respect to Total Doses (kGy)**				
	NON-IRRA	**10 kGy**	**25 kGy**	**50 kGy**	**75 kGy**
PC	539.8 °C	541.7 °C	-	511.7 °C	526.3 °C

Irradiation of neat polycarbonate first improved the thermal stability of polycarbonate such that 10-kGy irradiation increased the T_{max}, T_{50} values by 1.5 and 1.9℃. Further irradiation diminished the thermal stability of neat polycarbonate with reduced T_{max} and T_{50}. 50-kGy irradiation decreased the T_{max} and T_{50} values by 25 and 28.1℃. On the other hand, 75-kGy irradiation resulted with 14.5 and 13.5℃ diminishment in T_{max} and T_{50} values. The similar study was also present in literature supporting that compromising in thermal stability of polycarbonate upon irradiation (Kinalir, 2011). The lower thermal stability could be explained by increase in the extent of radiation induced chain scission reactions. Between 50 kGy and 75 kGy, T_{max} and T_{50} were slightly increased with irradiation due to removal of chain scission products from the polymer matrix and increase of aromatic content within the polymeric material.

3.2.6.3. Thermogravimetric Analysis (TGA) for 5 wt. % Bentonite Loaded Polycarbonate Exposed to 10, 25, 50 and 75 kGy Irradiation

Thermogravimetric (TG) curves and First Derivative of the Thermogravimetric (DTG) Curves of 5 wt. % bentonite loaded polycarbonate samples (irradiated up to 75 kGy) were shown in **Figure 64** and **Figure 65**. T_{max} (temperature, at which highest rate of weight loss occurs, was obtained from first derivative of TG curve) and T_{50} (temperature, at which 50 % weight loss occur, was obtained from TG curve) values of 5 wt. % bentonite loaded polycarbonate samples (irradiated up to 75 kGy) were given in **Table 46** and **Table 47**.

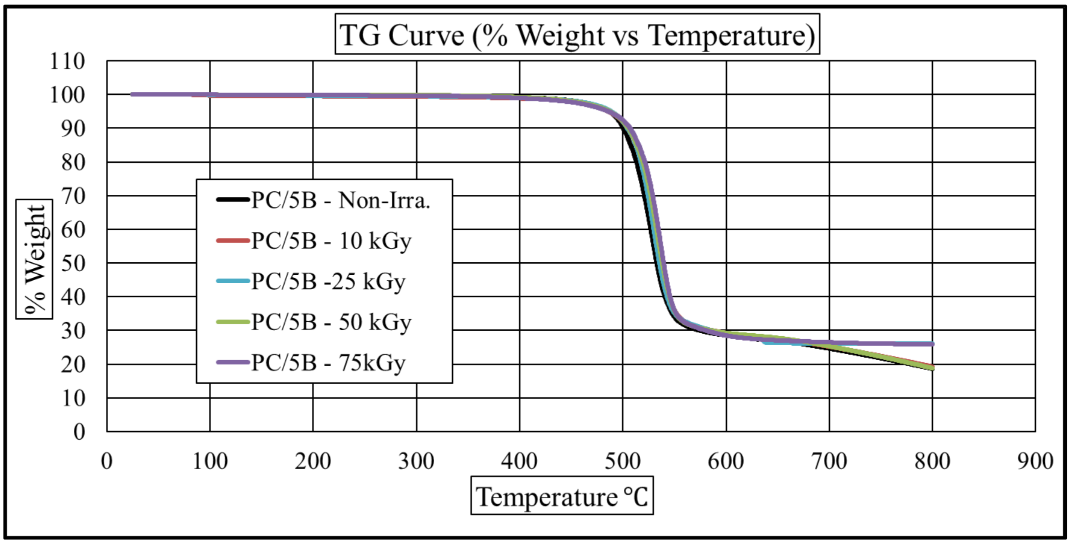

Figure 64 TG Curves of 5 wt. % Bentonite Loaded Polycarbonate Samples Irradiated with 10, 25, 50 and 75 kGy

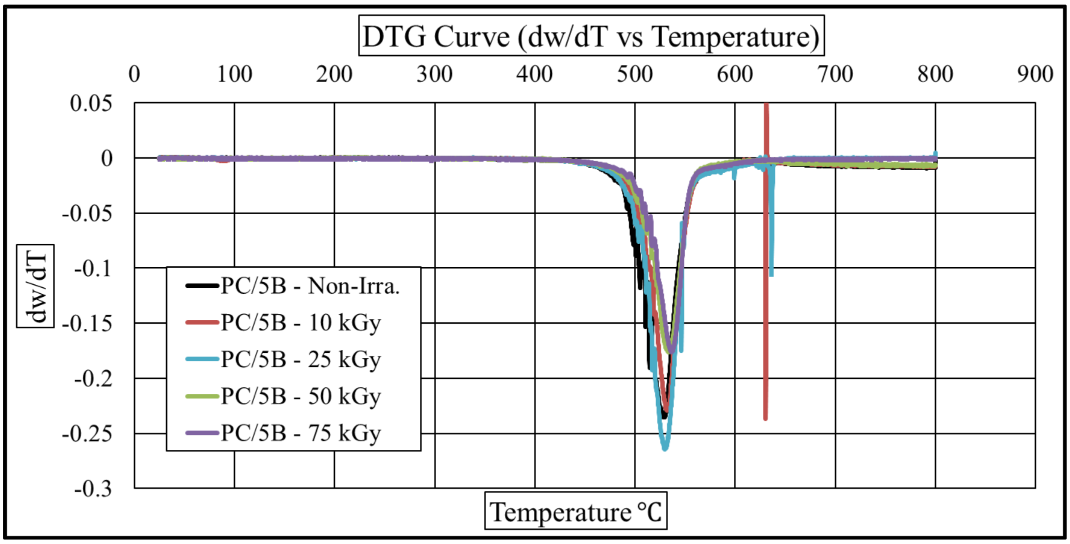

Figure 65 DTG Curves of 5 wt. % Bentonite Loaded Polycarbonate Samples Irradiated with 10, 25, 50 and 75 kGy

Table 46 T_{max} Values for 5 wt. % Bentonite Loaded Polycarbonate Samples Irradiated up to 75 kGy

Test Sample	**T_{max} (°C) Values with Respect to Total Doses (kGy)**				
	NON-IRRA	**10 kGy**	**25 kGy**	**50 kGy**	**75 kGy**
PC/5B	528.2 °C	531.8 °C	529.7 °C	533.2 °C	536.2 °C
PC	537.7 °C	539.2 °C	-	512.7 °C	523.2 °C

Table 47 T_{50} Values for 5 wt. % Bentonite Loaded Polycarbonate Samples Irradiated up to 75 kGy

Test Sample	**T_{50} (℃) Values with Respect to Total Doses (kGy)**				
	NON-IRRA	**10 kGy**	**25 kGy**	**50 kGy**	**75 kGy**
PC/5B	532.7 ℃	536.7 ℃	535.4 ℃	538.0 ℃	539.5 ℃
PC	539.8 ℃	541.7 ℃	-	511.7 ℃	526.3 ℃

Decomposition temperatures of the bentonite-filled composites were increased upon irradiation. T_{max} was improved by 3.6, 1.5, 5.0 and 8.0℃, which were correspond to 10, 25, 50 and 75 kGy irradiation, respectively. T_{50} was improved by 4.0, 2.7, 5.3 and 6.8℃, which were correspond to 10, 25, 50 and 75 kGy irradiation, respectively. Incorporation of bentonite into polycarbonate enhanced the thermal stability of the composites upon irradiation. Bentonite could retard the degradation of the composites. Therefore, deterioration in the thermal stability of the composites containing (5 wt.% bentonite) was not observed up to 75 kGy irradiation. In the DTG curve of the bentonite-filled polycarbonate, an additional intense peak was observed. This was associated with the presence of the bentonite. DTG curve of the bentonite, which was given in Appendix, had an intense peak in between 600-700℃.

3.2.6.4. Thermogravimetric Analysis (TGA) for 10 wt. % Barite Loaded Polycarbonate Exposed to 10, 25, 50 and 75 kGy Irradiation

Thermogravimetric (TG) curves and First Derivative of the Thermogravimetric (DTG) Curves of 10 wt. % barite loaded polycarbonate samples (irradiated up to 75 kGy) were shown in **Figure 66** and **Figure 67**. T_{max} (temperature, at which highest rate of weight loss occurs, was obtained from first derivative of TG curve) and T_{50} (temperature, at which 50 % weight loss occur, was obtained from TG curve) values of 10 wt. % barite loaded polycarbonate samples (irradiated up to 75 kGy) were given in **Table 48** and **Table 49**.

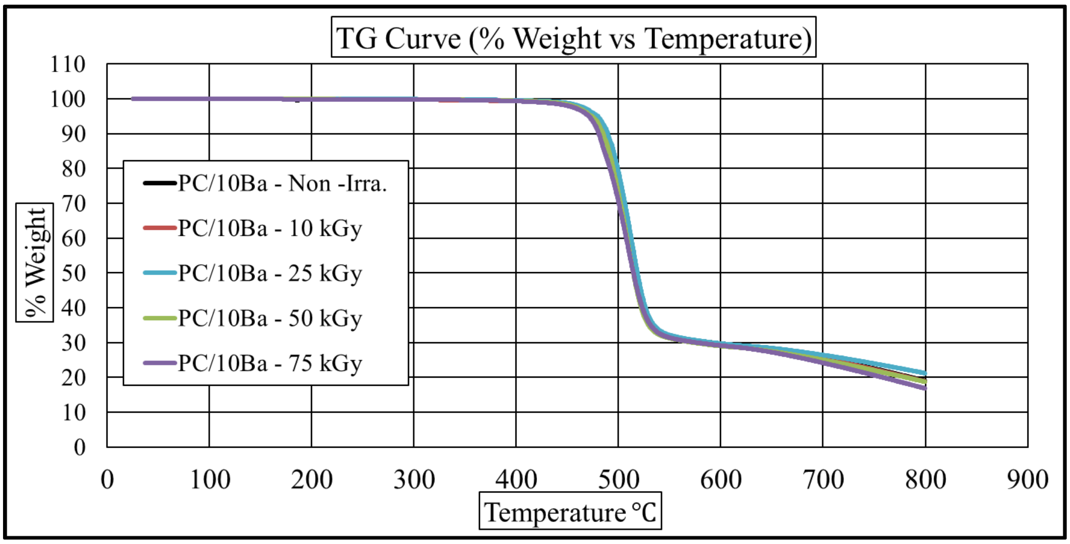

Figure 66 TG Curves of 10 wt. % Barite Loaded Polycarbonate Samples Irradiated with 10, 25, 50 and 75 kGy

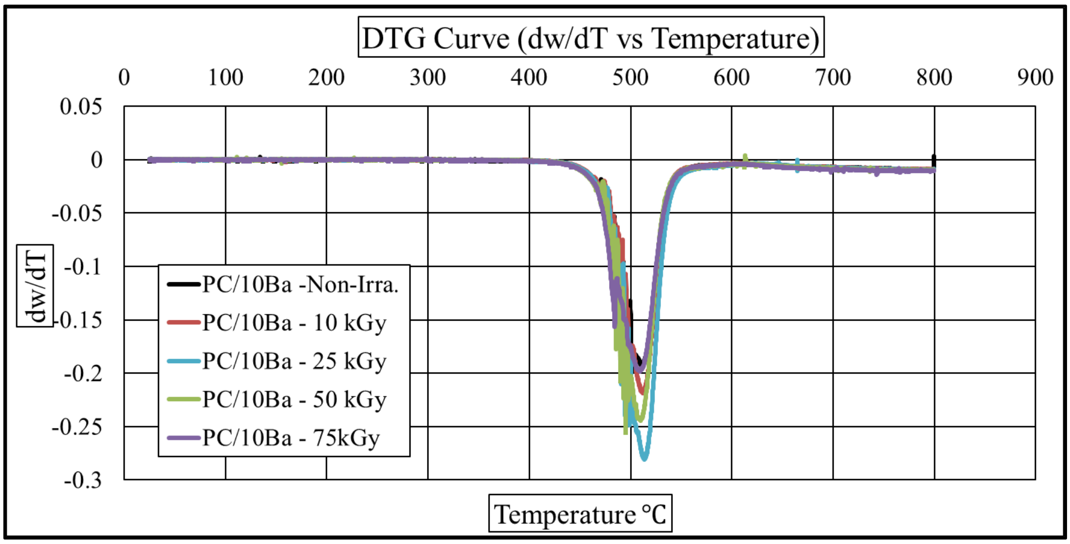

Figure 67 DTG Curves of 10 wt. % Barite Loaded Polycarbonate Samples Irradiated with 10, 25, 50 and 75 kGy

Table 48 T_{max} Values for 10 wt. % Barite Loaded Polycarbonate Samples Irradiated up to 75 kGy

Test Sample	**T_{max} (℃) Values with Respect to Total Doses (kGy)**				
	NON-IRRA	**10 kGy**	**25 kGy**	**50 kGy**	**75 kGy**
PC/10Ba	510.6 ℃	512.7 ℃	513.7 ℃	509.7 ℃	509.2 ℃
PC	537.7 ℃	539.2 ℃	-	512.7 ℃	523.2 ℃

Table 49 T_{50} Values for 10 wt. % Barite Loaded Polycarbonate Samples Irradiated up to 75 kGy

Test Sample	**T_{50} (℃) Values with Respect to Total Doses (kGy)**				
	NON-IRRA	**10 kGy**	**25 kGy**	**50 kGy**	**75 kGy**
PC/10Ba	516.8 ℃	516.7 ℃	518.5 ℃	514.3 ℃	514.5 ℃
PC	539.8 ℃	541.7 ℃	-	511.7 ℃	526.3 ℃

Irradiation of barite-filled composites improved the thermal stability up to 25 kGy. T_{max} was improved by 2.1 and 3.1℃, which were correspond to 10, 25 kGy irradiation, respectively. T_{50} was improved by 1.7℃ at 25 kGy irradiation. Further irradiation up to 75 kGy decreased the decomposition temperatures slightly. T_{max} was diminished by 0.9 and 1.4℃ at 50 and 75 kGy irradiation, respectively. T_{50} was also reduced by 2.5 and 2.3℃ at 50 and 75 kGy irradiation, respectively. The enhancement and reduction in the decomposition temperatures were not significant such that variation in these temperatures were in between ±3℃. Due to the radiation attenuation property, barite attenuated the negative effects of the gamma radiation to some extent (Akkurt, et al., 2010; Oto, et al., 2013). Incorporation of the barite into polycarbonate could retard the degradation of composites. Therefore, deterioration in the thermal stability of the composites (containing 10 wt.% barite) was not observed up to 75 kGy irradiation.

3.2.6.5. Thermogravimetric Analysis (TGA) for 10 wt. % Carbon Fiber Loaded Polycarbonate Exposed to 10, 25, 50 and 75 kGy Irradiation

Thermogravimetric (TG) curves and First Derivative of the Thermogravimetric (DTG) Curves of 10 wt. % carbon fiber loaded polycarbonate samples (irradiated up to 75 kGy) were shown in **Figure 68** and **Figure 69**. T_{max} (temperature, at which highest rate of weight loss occurs, was obtained from first derivative of TG curve) and T_{50} (temperature, at which 50 % weight loss occur, was obtained from DTG curve) values of 10 wt. % carbon fiber loaded polycarbonate samples (irradiated up to 75 kGy) were given in **Table 50** and **Table 51**.

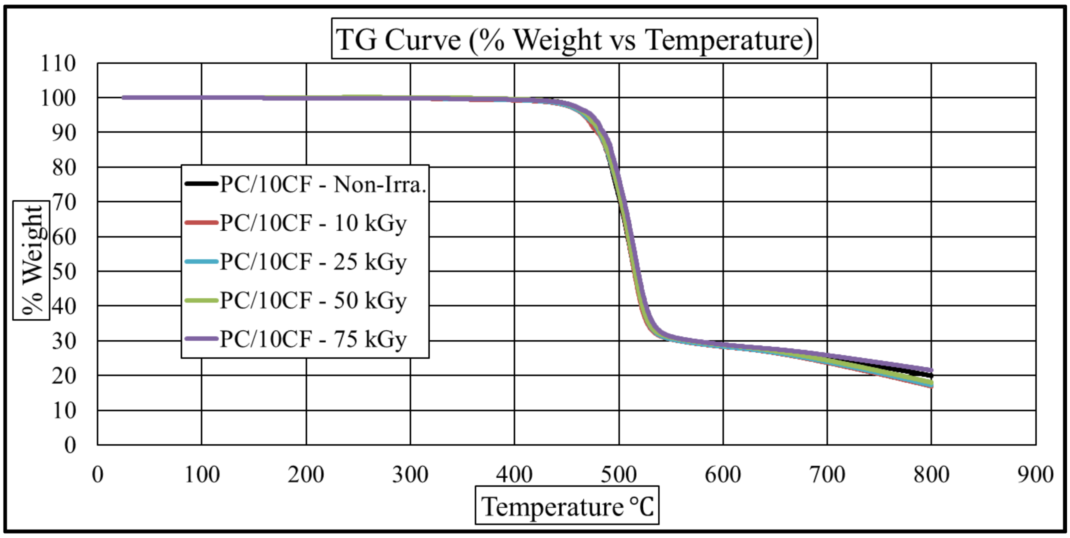

Figure 68 TG Curves of 10 wt. % Carbon Fiber Loaded Polycarbonate Samples Irradiated with 10, 25, 50 and 75 kGy

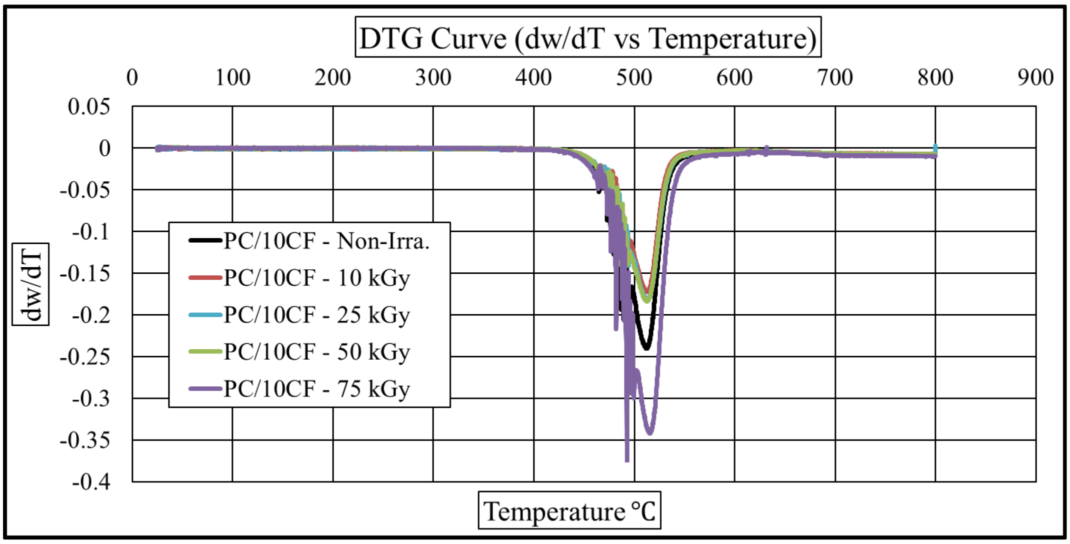

Figure 69 DTG Curves of 10 wt. % Carbon Fiber Loaded Polycarbonate Samples Irradiated with 10, 25, 50 and 75 kGy

Table 50 T_{max} Values for 10 wt. % Carbon Fiber Loaded Polycarbonate Samples Irradiated up to 75 kGy

Test Sample	**T_{max} (°C) Values with Respect to Total Doses (kGy)**				
	NON-IRRA	**10 kGy**	**25 kGy**	**50 kGy**	**75 kGy**
PC/10CF	512.6 °C	513.2 °C	513.2 °C	512.7 °C	515.2 °C
PC	537.7 °C	539.2 °C	-	512.7 °C	523.2 °C

Table 51 T_{50} Values for 10 wt. % Carbon Fiber Loaded Polycarbonate Samples Irradiated up to 75 kGy

Test Sample	**T_{50} (℃) Values with Respect to Total Doses (kGy)**				
	NON-IRRA	**10 kGy**	**25 kGy**	**50 kGy**	**75 kGy**
PC/10CF	514.7 ℃	514.7 ℃	515.3 ℃	515.3 ℃	518.5 ℃
PC	539.8 ℃	541.7 ℃	-	511.7 ℃	526.3 ℃

Decomposition temperatures of the carbon fiber reinforced composites were increased upon irradiation. T_{max} was improved by 0.6, 0.6, 0.1 and 2.6℃, which were correspond to 10, 25, 50 and 75 kGy irradiation, respectively. T_{50} was also improved by 0.6, 0.6 and 3.8℃, which were correspond to 25, 50 and 75 kGy irradiation, respectively. Carbon fiber loading into polycarbonate enhanced the thermal stability of the composites upon irradiation. On the other hand, the enhancement in the decomposition temperatures did not significant such that variation in these temperatures were in between 0.6 to 3.8℃. Due to the radiation attenuation property, carbon fiber attenuated the negative effects of the gamma radiation to some extent (Seppälä & Kulmala, 2011). Incorporation of carbon fiber into polycarbonate could retard the degradation of the composites. Therefore, deterioration in the thermal stability of the composites containing (10 wt.% carbon fiber) was not observed up to 75 kGy irradiation.

3.2.6.6. Thermogravimetric Analysis (TGA) for 10 wt. % Glass Fiber Loaded Polycarbonate Exposed to 10, 25, 50 and 75 kGy Irradiation

Thermogravimetric (TG) curves and First Derivative of the Thermogravimetric (DTG) Curves of 10 wt. % glass fiber loaded polycarbonate samples (irradiated up to 75 kGy) were shown in **Figure 70** and **Figure 71**. T_{max} (temperature, at which highest rate of weight loss occurs, was obtained from first derivative of TG curve) and T_{50} (temperature, at which 50 % weight loss occur, was obtained from TG curve) values of 10 wt. % glass fiber loaded polycarbonate samples (irradiated up to 75 kGy) were given in **Table 52** and **Table 53**.

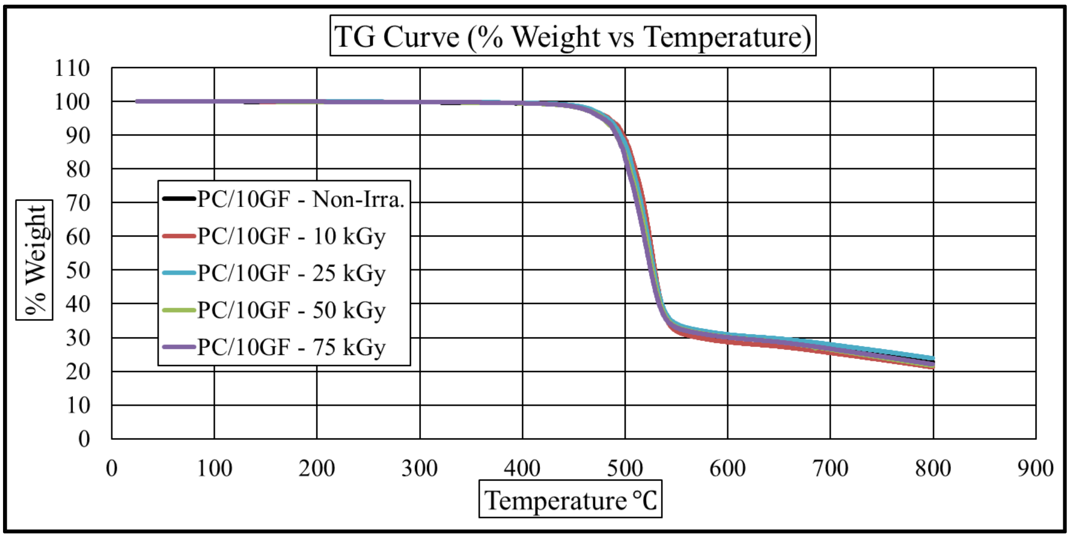

Figure 70 TG Curves of 10 wt. % Glass Fiber Loaded Polycarbonate Samples Irradiated with 10, 25, 50 and 75 kGy

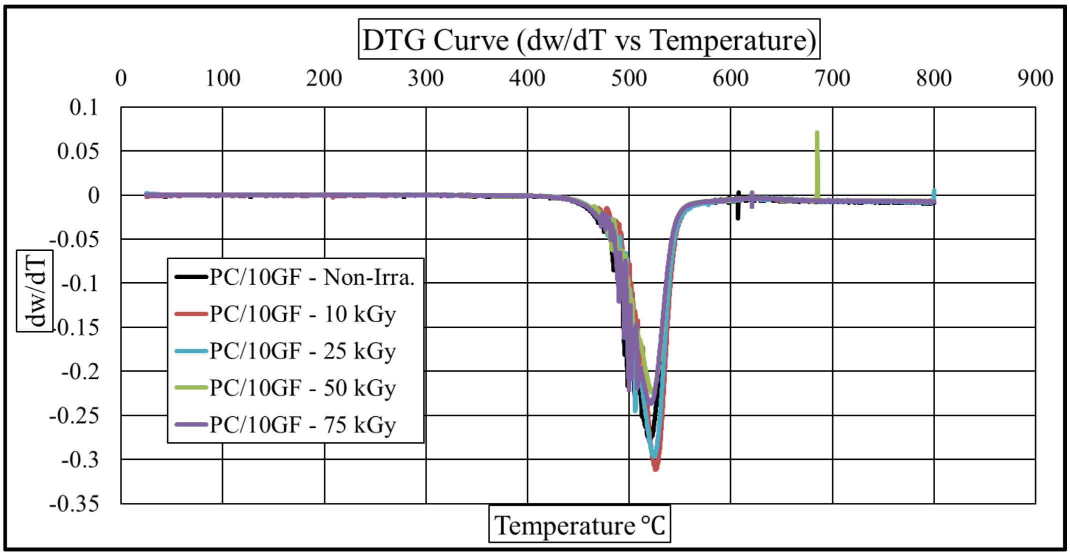

Figure 71 DTG Curves of 10 wt. % Glass Fiber Loaded Polycarbonate Samples Irradiated with 10, 25, 50 and 75 kGy

Table 52 T_{max} Values of 10 wt. % Glass Fiber Loaded Polycarbonate Samples Irradiated up to 75 kGy

Test Sample	**T_{max} (°C) Values with Respect to Total Doses (kGy)**				
	NON-IRRA	**10 kGy**	**25 kGy**	**50 kGy**	**75 kGy**
PC/10GF	519.7 °C	526.2 °C	524.2 °C	523.2 °C	521.2 °C
PC	537.7 °C	539.2 °C	-	512.7 °C	523.2 °C

Table 53 T_{50} Values of 10 wt. % Glass Fiber Loaded Polycarbonate Samples Irradiated up to 75 kGy

Test Sample	**T_{50} (°C) Values with Respect to Total Doses (kGy)**				
	NON-IRRA	**10 kGy**	**25 kGy**	**50 kGy**	**75 kGy**
PC/10GF	525.7 °C	529.0 °C	527.8 °C	526.3 °C	524.8 °C
PC	539.8 °C	541.7 °C	-	511.7 °C	526.3 °C

Decomposition temperatures of the glass fiber reinforced composites were increased upon irradiation. T_{max} was improved by 6.5, 4.5, 3.5 and 1.5℃, which were correspond to 10, 25, 50 and 75 kGy irradiation, respectively. T_{50} was also improved by 3.3, 2.1 and 0.6℃, which were correspond to 10, 25 and 50 kGy irradiation, respectively. The highest improvement in the thermal stability was observed on 10 kGy irradiated specimen. Incorporation of glass fiber into polycarbonate could retard the degradation of the composites. Therefore, deterioration in the thermal stability of the composites containing (10 wt.% glass fiber) was not observed up to 75 kGy irradiation.

3.2.7 Dynamic Mechanical Analysis (DMA)

3.2.7.1. Dynamic Mechanical Analysis (DMA) for Neat Polycarbonate and Composites

Storage Modulus vs Temperature, Loss Modulus vs Temperature and Tan δ vs Temperature Curves of neat, bentonite, barite, carbon fiber and glass fiber loaded polycarbonates were shown in **Figure 72**, **Figure 73** and **Figure 74**. Glass transition temperatures of specimens were shown in **Table 54** and **Table 55**. Storage Modulus values at 25 °C were shown in **Table 56**. The relative modulus values at glass transition temperatures were shown in **Table 57**.

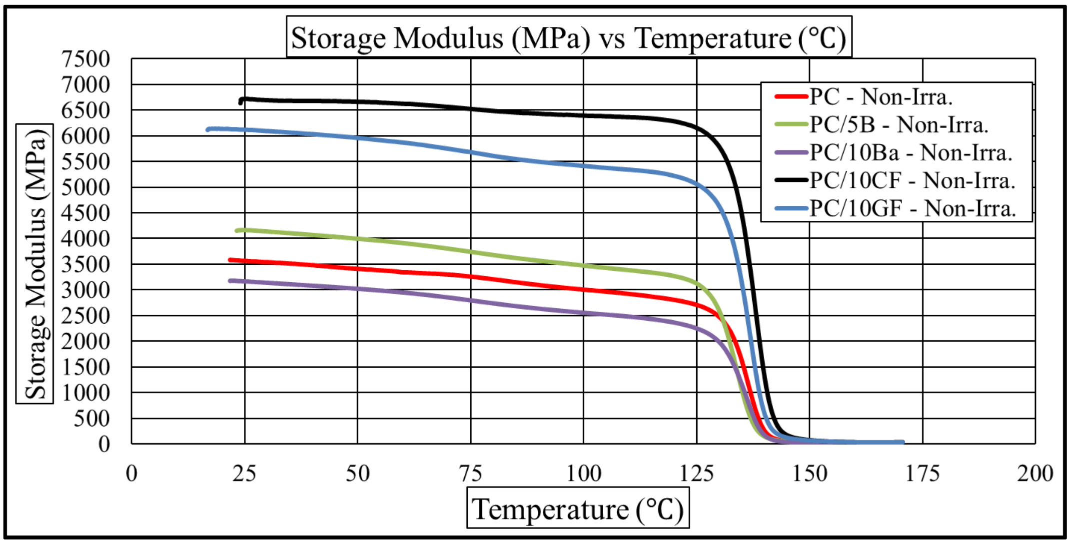

Figure 72 Storage Modulus vs Temperature Curves of Neat, Bentonite, Barite, Glass Fiber and Carbon Fiber Loaded Polycarbonate Samples

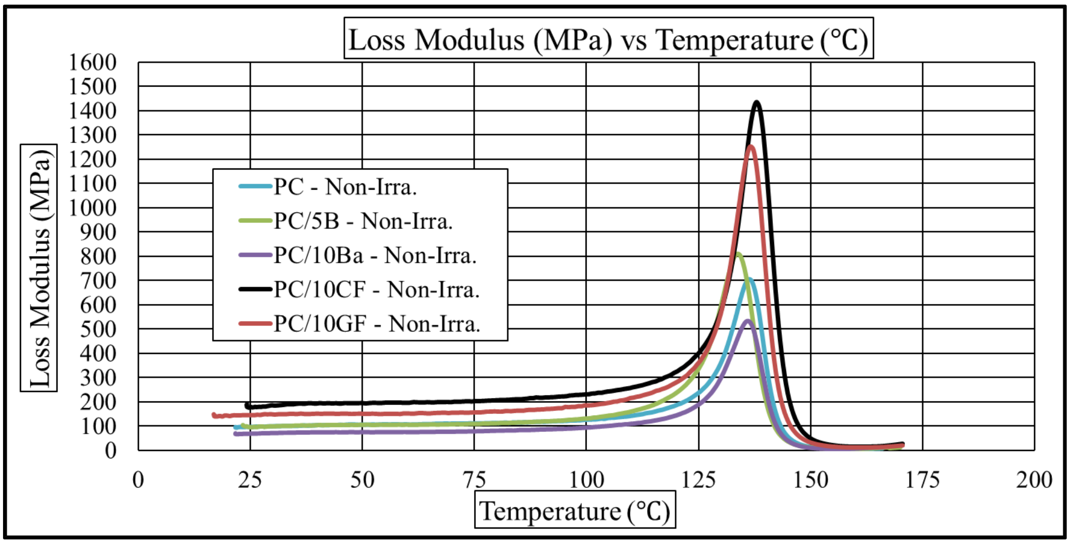

Figure 73 Loss Modulus vs Temperature Curves of Neat, Bentonite, Barite, Glass Fiber and Carbon Fiber Loaded Polycarbonate Samples

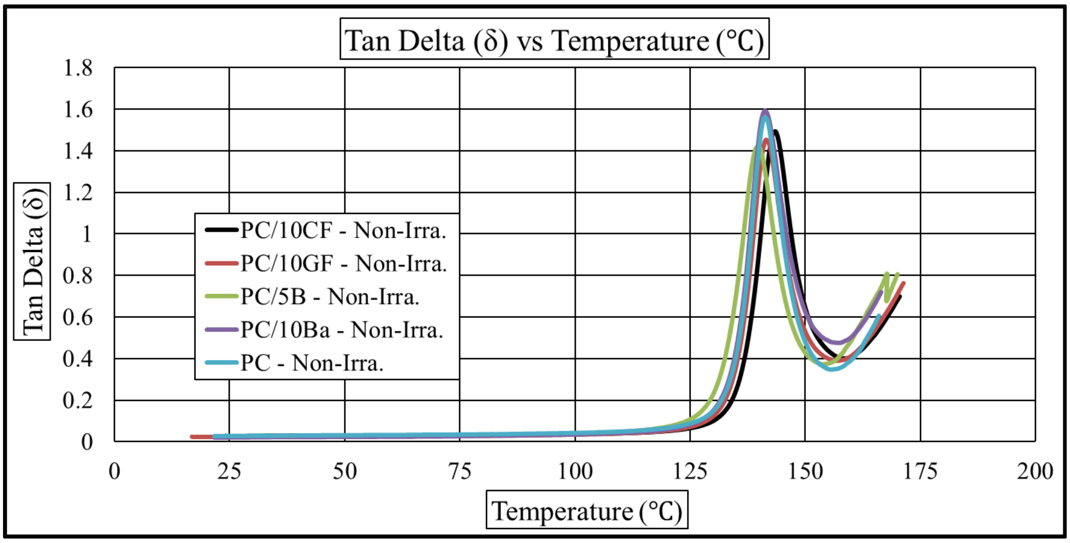

Figure 74 Tan δ vs Temperature Curves of Neat, Bentonite, Barite, Glass Fiber and Carbon Fiber Loaded Polycarbonate Samples

Table 54 Glass Transition Temperatures (T_g) for Neat, Particle and Fiber Filled Polycarbonate Samples According to the Loss Modulus vs Temperature Curve

Test Sample	**T_g (℃) Values**
PC	136.1 ℃
PC/5B	133.5 ℃
PC/10Ba	136.3 ℃
PC/10CF	138.0 ℃
PC/10GF	136.6 ℃

Table 55 Glass Transition Temperatures (T_g) for Neat, Particle and Fiber Filled Polycarbonate Samples According to the Tan δ vs Temperature Curve

Test Sample	**T_g (℃) Values**
PC	141.0 ℃
PC/5B	139.9 ℃
PC/10Ba	141.2 ℃
PC/10CF	143.6 ℃
PC/10GF	141.5 ℃

Table 56 Storage Modulus Values (MPa) for Neat, Particle and Fiber Filled Polycarbonate Samples at 25℃

Test Sample	**Storage Modulus (MPa)**
PC	3559 MPa
PC/5B	4166 MPa
PC/10Ba	3167 MPa
PC/10CF	6717 MPa
PC/10GF	6114 MPa

Table 57 Relative Storage Modulus Values (MPa) for Neat, Particle and Fiber Filled Polycarbonate Samples at Glass Transition Temperatures

Test Sample	**Relative Modulus (%) Values at T_g Obtained From Loss Modulus vs Temp. Graph**	**Relative Modulus (%) Values at T_g Obtained From Tan δ vs Temp. Graph**
PC	35.4 %	4.4 %
PC/5B	38.3 %	3.6 %
PC/10Ba	26.6 %	3.1 %
PC/10CF	40.1 %	4.0 %
PC/10GF	37.2 %	5.0 %

According to the results shown above, storage modulus values of carbon fiber and glass fiber reinforced composites increased significantly. Storage modulus values for bentonite loaded polycarbonates increased as well. The relative improvement (expressed as percentage) on the storage modulus were 88 % for carbon fiber based composite, 72 % for glass fiber based composite and 17% for bentonite based polycarbonate. On the other hand, barite inclusion on polycarbonate decreased the storage modulus. The relative diminishment expressed as percentage) on the storage modulus were 11 % for barite based composite.

It was expected that inclusion of elastic fibers increased the storage modulus values. The 10 wt. % carbon and glass fiber inclusion were resulted with 1.88 and 1.72 times enhancement. The previous studies were also concluded with improvement in the storage modulus values with incorporation of bentonite, carbon and glass fiber into polycarbonate (Sepe, 2000; Sharma, et al., 2016; Feng, et al., 2012; Carrion, et al., 2008) .

Decrease pattern in storage modulus in neat, particle and fiber filled polycarbonate samples was single-step process that modulus was lost all at once which were proven according to the **Table 57** and **Figure 72**. Relative modulus values were almost disappeared (i.e. loss in modulus were higher than 95 %) at glass transition temperatures calculated from “Tan δ & Temperature” graph (Sepe, 2000). On the other hand, the relative modulus values at glass transition temperatures determined from “Loss Modulus & Temperature” graph were comparatively higher. From an engineering standpoint, glass transition temperatures obtained from Tan δ curve were the end point at which polycarbonate specimens softened and were no longer usable in a load-bearing manner (Sepe, 2000). For this reason, the glass transition temperatures obtained from Loss Modulus curve should be taken in to account for usability in load-bearing manner.

Table 57 showed that, relative modulus value at glass transitions (from Loss Modulus curve) was highest in carbon fiber loaded composites. Bentonite and glass fiber filled composites had higher relative modulus values than that of neat polycarbonate as well. On the other hand, relative modulus value was observed lowest in barite loaded polycarbonate.

Figure 73 revealed that maximum peak values were significantly increased in glass and carbon fiber loaded polycarbonate samples. This could be explained by weak interfacial shear strength. Inclusion of 10 wt. % carbon and glass fiber reduced the interfacial shear strength. Reduction in the interfacial shear strength was reflected by increase in the loss modulus’ peak values (Edie, et al., 1993; Yuan, et al., 1996; Sharma, et al., 2016).

Table 54 and **Table 55** showed the glass transition temperature of the specimens. Glass transition temperature for neat polycarbonate were reliable with the results found in previous studies (Sharma, et al., 2016; Carrion, et al., 2008; Feng, et al., 2012; Sharma, et al., 2016). 10 wt. % carbon fiber, 10 wt. % glass fiber, 10 wt. barite inclusion increased the glass transition temperatures by 1.9-2.6 ℃, 0.5 ℃, 0.2 ℃, respectively. Whereas, 5 wt. % bentonite inclusion decreased the glass transition temperature by 1.1-2.6 ℃. Previous studies also consistent with this study with respect to behavior of the glass transition temperature under incorporating carbon fiber and bentonite to the polycarbonate (Sharma, et al., 2016; Carrion, et al., 2008; Feng, et al., 2012).

10 wt % carbon and glass fiber inclusion stiffened the polymer and enhanced the utility of the polycarbonate as a load-bearing material (Sepe, 2000). Glass transition temperature were also improved by fiber loading. Due to the importance of load bearing property in room and elevated temperatures, carbon and glass fiber reinforced polycarbonate had superior properties in terms radioactive waste management.

3.2.7.2. Dynamic Mechanical Analysis (DMA) for Neat Polycarbonate Exposed to 10, 25, 50 and 75 kGy Irradiation

Storage Modulus vs Temperature, Loss Modulus vs Temperature and Tan δ vs Temperature Curves of neat polycarbonate samples (irradiated up to 75 kGy) were shown in **Figure 75**, **Figure 76** and **Figure 77**. Glass transition temperatures of specimens were shown in **Table 58** and **Table 59**. Storage Modulus values at 25 ℃ were shown in **Table 60**. The relative storage modulus values at glass transition temperatures were shown in **Table 61**.

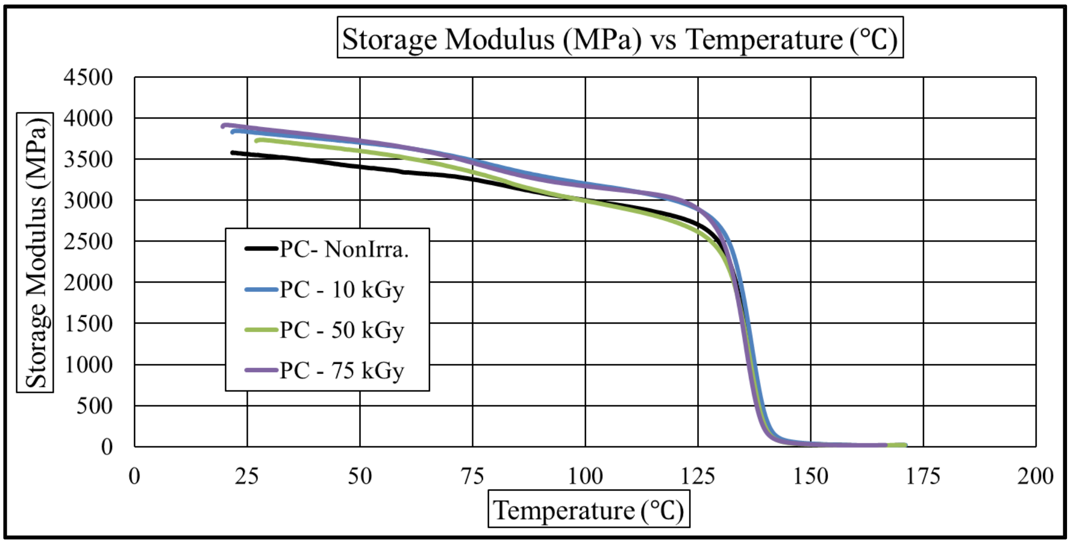

Figure 75 Storage Modulus vs Temperature Curves of Neat Polycarbonate Samples Irradiated up to 75 kGy

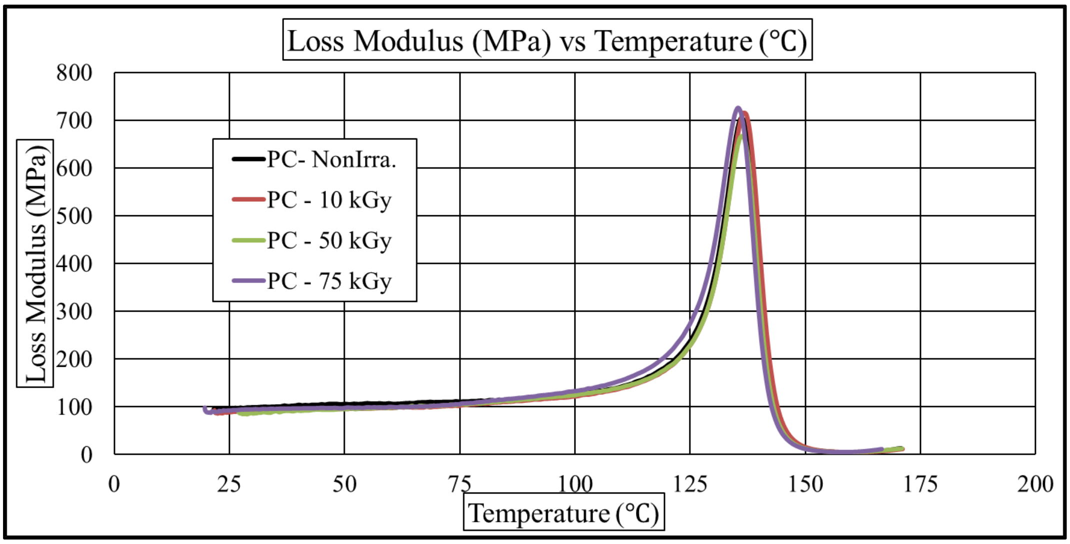

Figure 76 Loss Modulus vs Temperature Curves of Neat Polycarbonate Samples Irradiated up to 75 kGy

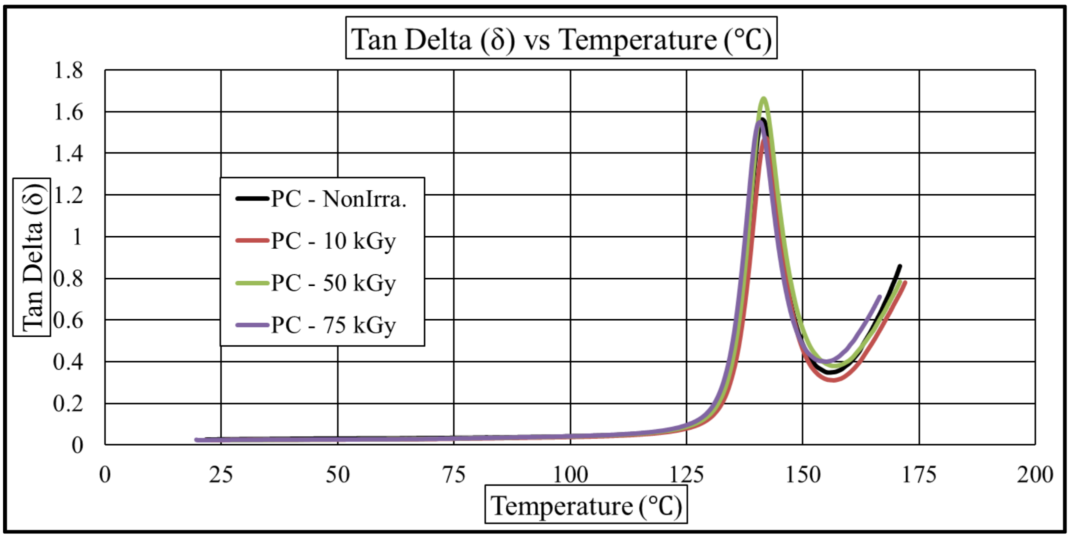

Figure 77 Tan δ vs Temperature Curves of Neat Polycarbonate Samples Irradiated up to 75 kGy

Table 58 Glass Transition Temperatures (T_g) for Neat Polycarbonate Samples (Irradiated up to 75 kGy) According to the Loss Modulus vs Temperature Curve

Test Sample with respect to Total Dose	**T_g (℃) Values**
PC - Non-Irra.	136.1 ℃
PC - 10 kGy	136.5 ℃
PC - 50 kGy	136.5 ℃
PC - 75 kGy	135.4 ℃

Table 59 Glass Transition Temperatures (T_g) for Neat Polycarbonate Samples (Irradiated up to 75 kGy) According to the Tan δ vs Temperature Curve

Test Sample with respect to Total Dose	**T_g (℃) Values**
PC - Non-Irra.	141.0 ℃
PC - 10 kGy	142.2 ℃
PC - 50 kGy	141.6 ℃
PC - 75 kGy	141.0 ℃

Table 60 Storage Modulus Values (MPa) for Neat Polycarbonate Samples (Irradiated up to 75 kGy) at 25℃

Test Sample with respect to Total Dose	**Storage Modulus (MPa)**
PC - Non-Irra.	3559 MPa
PC - 10 kGy	3836 MPa
PC - 50 kGy	3721 MPa
PC - 75 kGy	3885 MPa

Table 61 Relative Storage Modulus Values (MPa) for Neat Polycarbonate Samples (Irradiated up to 75 kGy) at Glass Transition Temperatures

Test Sample with respect to Total Dose	**Relative Modulus (%) Values at T_g Obtained From Loss Modulus vs Temp. Graph**	**Relative Modulus (%) Values at T_g Obtained From Tan δ vs Temp. Graph**
PC - Non-Irra.	35.4 %	4.4 %
PC - 10 kGy	36.2 %	3.6 %
PC - 50 kGy	28.1 %	3.0 %
PC - 75 kGy	33.4 %	3.2 %

In dynamic mechanical analysis, change in glass transition temperature were indicator of radiation induced crosslinking and chain scission. Flory-Fox equation displayed relationship between molecular weight and glass transition temperature. According to the Flory-Fox equation, decrease in the molecular weight were associated with reduction in glass transition temperature. In fact, equation revealed that, glass transition temperature, radiation induced enhancement and molecular weight increase were proportional to each other. Flory-Fox relationship were shown in **Equation 4** (Acierno, et al., 1981)**.** Where $T_{g,\infty}$ is glass transition temperature at an infinite molecular weight, M_n is number average molecular weight and "K" is the constant.

$$T_g = T_{g,\infty} - \frac{K}{M_n}$$

Equation 4 Flory Fox Equation

Storage Modulus values of neat polycarbonate at room temperature were improved via irradiation at all doses when compared the values belonged to non-irradiated specimen. It meant that, irradiation stiffened the polymer acting as hardener, implying enhancement of load-bearing property at room temperature.

Glass transition temperature (from Tan δ) showed maximum at 10 kGy indicating the dominant mechanism as radiation induced crosslinking. Further irradiation up to 50 kGy decreased the glass transition temperature (from Tan δ curve) with respect to cases observed at 10 kGy. Glass transition temperature (from Tan δ curve) of non-irradiated and 75 kGy irradiated specimens were found nearly same. It could be inferred that 75 kGy irradiation compensated the thermal improvement occurred at 10 kGy.

Relative storage modulus at glass transition temperature (from Loss Modulus curve) were increased at 10 kGy, then further irradiation decreased the relative modulus. It revealed that load-bearing property at elevated temperatures were diminished at 50 and 75 kGy.

It could be stated from the test results that crosslinking mechanism were dominant at low doses supported with enhancement both in thermal and load-bearing properties (Acierno, et al., 1981). 75 kGy irradiation reduced enhancement of the load-bearing property at elevated temperature obtained at 10 kGy by increasing the extent of chain scission reactions. After all, result of specimens exposed to 75 kGy irradiation were similar with that of non-irradiated ones. 75 kGy irradiation did not compromise the thermal property of specimens that it could be selected as eventual dose for use of polycarbonate in radioactive waste management.

3.2.7.3. Dynamic Mechanical Analysis (DMA) for 5 wt. % Bentonite Loaded Polycarbonate Exposed to 10, 25, 50 and 75 kGy Irradiation

Storage Modulus vs Temperature, Loss Modulus vs Temperature and Tan δ vs Temperature Curves of 5 wt. % bentonite included polycarbonate samples (irradiated up to 75 kGy) were shown in **Figure 78**, **Figure 79** and **Figure 80**. Glass transition temperatures of specimens were shown in **Table 62** and **Table 63**. Storage Modulus values at 25 ℃ were shown in **Table 64**. The relative storage modulus values at glass transition temperatures were shown in **Table 65**.

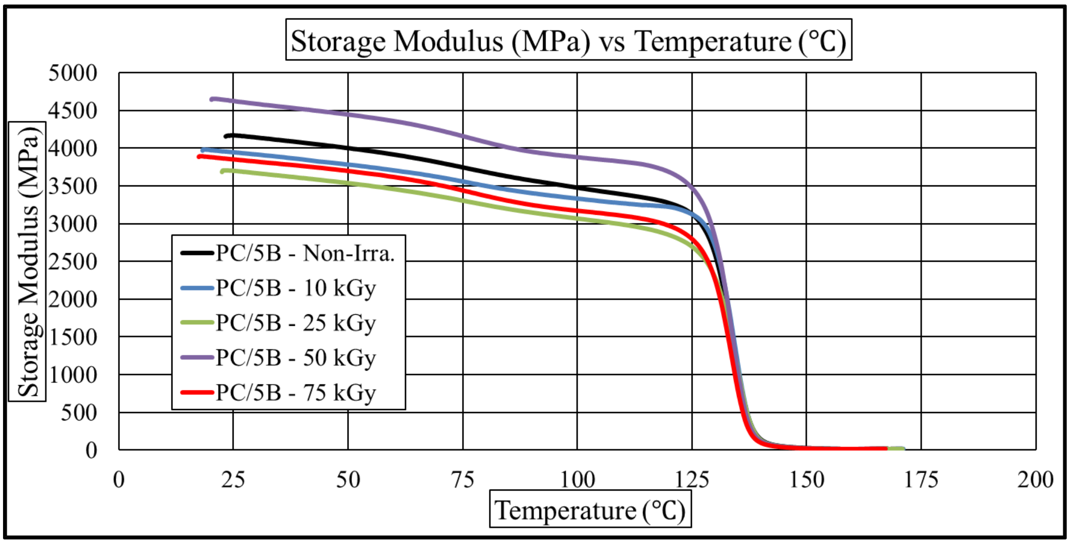

Figure 78 Storage Modulus vs Temperature Curves of 5 wt. % Bentonite Loaded Polycarbonate Samples Irradiated up to 75 kGy

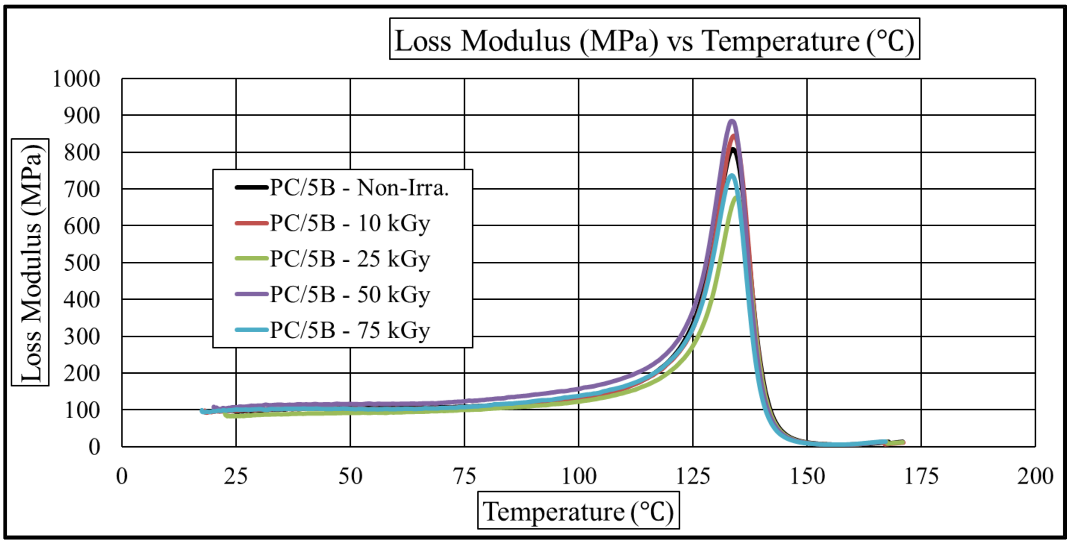

Figure 79 Loss Modulus vs Temperature Curves of 5 wt. % Bentonite Loaded Polycarbonate Samples Irradiated up to 75 kGy

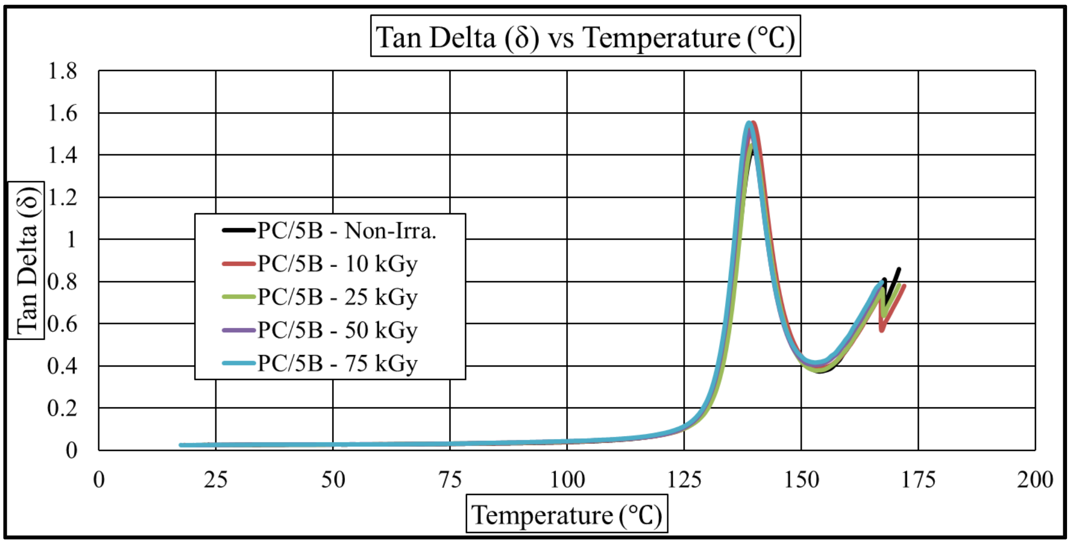

Figure 80 Tan δ vs Temperature Curves of 5 wt. % Bentonite Loaded Polycarbonate Samples Irradiated up to 75 kGy

Table 62 Glass Transition Temperatures (T_g) for 5 wt. % Bentonite Loaded Polycarbonate Samples (Irradiated up to 75 kGy) According to the Loss Modulus vs Temperature Curve

Test Sample with respect to Total Dose	**T_g (℃) Values**
PC/5B - Non-Irra.	133.5 ℃
PC/5B - 10 kGy	134.1 ℃
PC/5B - 25 kGy	134.3 ℃
PC/5B - 50 kGy	133.3 ℃
PC/5B - 75 kGy	133.8 ℃

Table 63 Glass Transition Temperatures (T_g) for 5 wt. % Bentonite Loaded Polycarbonate Samples (Irradiated up to 75 kGy) According to the Tan δ vs Temperature Curve

Test Sample with respect to Total Dose	**T_g (℃) Values**
PC/5B - Non-Irra.	139.9 ℃
PC/5B - 10 kGy	139.7 ℃
PC/5B - 25 kGy	140.0 ℃
PC/5B - 50 kGy	139.0 ℃
PC/5B - 75 kGy	138.7 ℃

Table 64 Storage Modulus Values (MPa) for 5 wt. % Bentonite Loaded Polycarbonate Samples (Irradiated up to 75 kGy) at 25℃

Test Sample with respect to Total Dose	**Storage Modulus (MPa)**
PC/5B - Non-Irra.	4167 MPa
PC/5B - 10 kGy	3940 MPa
PC/5B - 25 kGy	3703 MPa
PC/5B - 50 kGy	4619 MPa
PC/5B - 75 kGy	3848 MPa

Table 65 Relative Storage Modulus Values (MPa) for 5 wt. % Bentonite Loaded Polycarbonate Samples (Irradiated up to 75 kGy) at Glass Transition Temperatures

Test Sample with respect to Total Dose	**Relative Modulus (%) Values at T_g Obtained From Loss Modulus vs Temp. Graph**	**Relative Modulus (%) Values at T_g Obtained From Tan δ vs Temp. Graph**
PC/5B - Non-Irra.	38.3 %	3.6 %
PC/5B - 10 kGy	37.6 %	3.7 %
PC/5B - 25 kGy	34.5 %	3.6 %
PC/5B - 50 kGy	37.0 %	3.6 %
PC/5B - 75 kGy	30.7 %	3.9 %

According to **Figure 78** and **Table 64**, 50 kGy irradiation increased the storage modulus values, whereas 10, 25 and 75 kGy irradiation decreased the modulus. In fact, 50 kGy stiffened the polymer and 10, 25, 75 kGy softened the specimens. This could be associated that 50 kGy irradiation acted as hardener, 10, 25 and 75 kGy acted as plasticizer. It could be also stated that relative modulus values at glass transition temperature (from Loss Modulus curve) were diminished via irradiation. It indicated that load bearing property at elevated temperature were diminished via irradiation.

Figure 79 revealed that maximum peak values were significantly decreased at 75 kGy irradiated composite. This was associated with enhanced interfacial bonding between matrix and filler (Edie, et al., 1993; Yuan, et al., 1996; Sharma, et al., 2016).It could be stated that 75 kGy improved the interfacial bonding between polycarbonate and bentonite by increasing interfacial shear strength. Eventually, 75 kGy might act as surface modifier between matrix and polycarbonate.

Glass transition temperatures, obtained from Tan δ vs Temperature curves, of 5 wt.% bentonite containing polycarbonate did not show any appreciable change upon irradiation (see **Table 63**).

3.2.7.4. Dynamic Mechanical Analysis (DMA) for 10 wt. % Barite Loaded Polycarbonate Exposed to 10, 25, 50 and 75 kGy Irradiation

Storage Modulus vs Temperature, Loss Modulus vs Temperature and Tan δ vs Temperature Curves of 10 wt. % barite included polycarbonate samples (irradiated up to 75 kGy) were shown in **Figure 81**, **Figure 82** and **Figure 83**. Glass transition temperatures of specimens were shown in **Table 66** and **Table 67**. Storage Modulus values at 25 ℃ were shown in **Table 68**. The relative storage modulus values at glass transition temperatures were shown in **Table 69**.

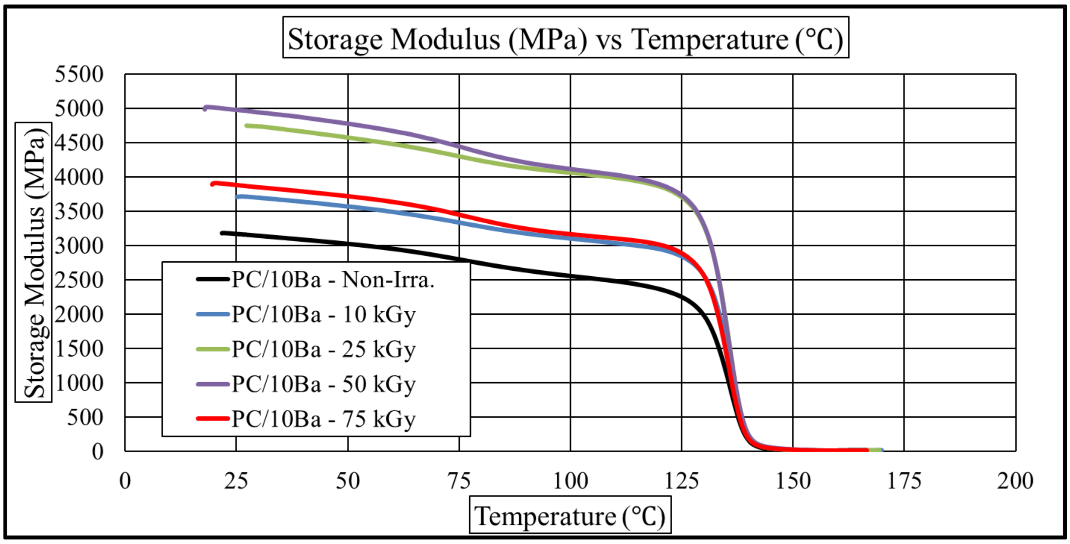

Figure 81 Storage Modulus vs Temperature Curves of 10 wt. % Barite Loaded Polycarbonate Samples Irradiated up to 75 kGy

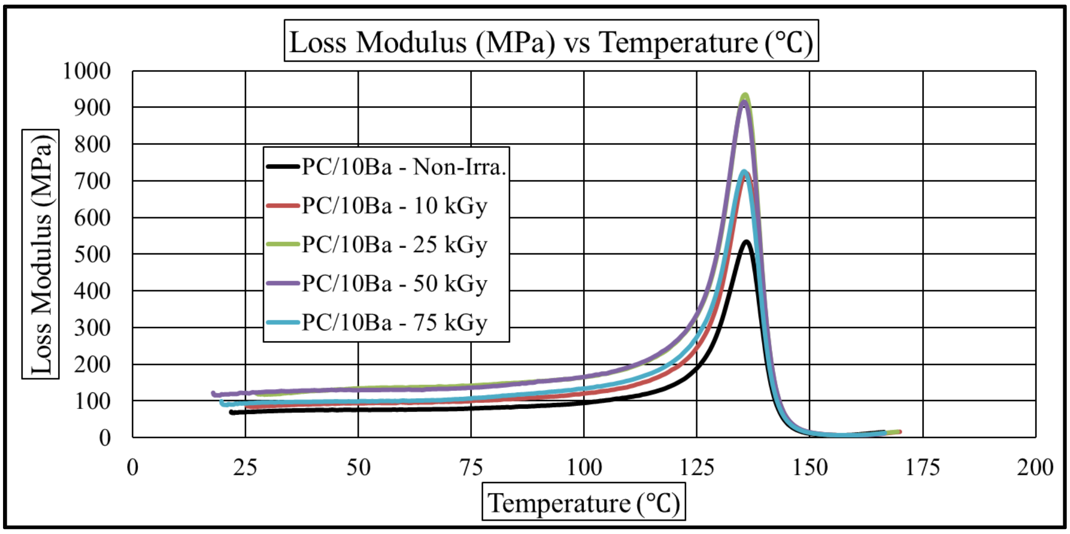

Figure 82 Loss Modulus vs Temperature Curves of 10 wt. % Barite Loaded Polycarbonate Samples Irradiated up to 75 kGy

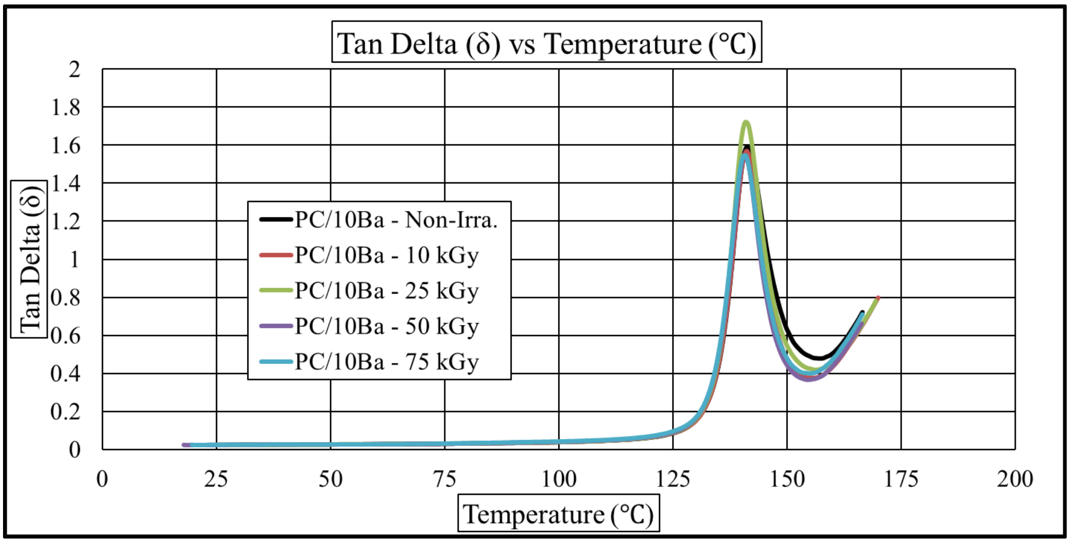

Figure 83 Tanδ Modulus vs Temperature Curves of 10 wt. % Barite Loaded Polycarbonate Samples Irradiated up to 75 kGy

Table 66 Glass Transition Temperatures (T_g) for 10 wt. % Barite Loaded Polycarbonate Samples (Irradiated up to 75 kGy) According to the Loss Modulus vs Temperature Curve

Test Sample with respect to Total Dose	**T_g (℃) Values**
PC/10Ba - Non-Irra.	136.3 ℃
PC/10Ba - 10 kGy	136.2 ℃
PC/10Ba - 25 kGy	135.9 ℃
PC/10Ba - 50 kGy	135.5 ℃
PC/10Ba - 75 kGy	135.4 ℃

Table 67 Glass Transition Temperatures (T_g) for 10 wt. % Barite Loaded Polycarbonate Samples (Irradiated up to 75 kGy) According to the Tan δ vs Temperature Curve

Test Sample with respect to Total Dose	**T_g (℃) Values**
PC/10Ba - Non-Irra.	141.2 ℃
PC/10Ba - 10 kGy	141.2 ℃
PC/10Ba - 25 kGy	140.8 ℃
PC/10Ba - 50 kGy	141.0 ℃
PC/10Ba - 75 kGy	141.0 ℃

Table 68 Storage Modulus Values (MPa) for 10 wt. % Barite Loaded Polycarbonate Samples (Irradiated up to 75 kGy) at 25℃

Test Sample with respect to Total Dose	**Storage Modulus (MPa)**
PC/10Ba - Non-Irra.	3168 MPa
PC/10Ba - 10 kGy	3707 MPa
PC/10Ba - 25 kGy	4740 MPa
PC/10Ba - 50 kGy	4985 MPa
PC/10Ba - 75 kGy	3892 MPa

Table 69 Relative Storage Modulus Values (MPa) for 10 wt. % Barite Loaded Polycarbonate Samples (Irradiated up to 75 kGy) at Glass Transition Temperatures

Test Sample with respect to Total Dose	**Relative Modulus (%) Values at T_g Obtained From Loss Modulus vs Temp. Graph**	**Relative Modulus (%) Values at T_g Obtained From Tan δ vs Temp. Graph**
PC/10Ba - Non-Irra.	26.6 %	3.1 %
PC/10Ba - 10 kGy	31.1 %	3.7 %
PC/10Ba - 25 kGy	31.5 %	3.3 %
PC/10Ba - 50 kGy	32.4 %	3.1 %
PC/10Ba - 75 kGy	33.4 %	3.2 %

According to **Figure 81** and **Table 68**, 10, 25, 50 and 75 kGy irradiation increased the storage modulus values significantly. The highest storage modulus was observed in 50 kGy irradiated specimen. **Table 69** showed that relative storage modulus values at glass transition temperature (from Loss Modulus curve) were increased at all irradiation doses. It was clear that irradiation improved the load-bearing property (at room and elevated temperatures) of 10 wt. % barite based polycarbonate.

Glass transition temperatures (from Tan δ curve) upon irradiation show no considerable change up to 25 kGy indicating that thermal property of 10 wt. % barite included polycarbonate was not affected. The variations in glass transition temperatures (from Tan δ curve) were in between ±0.4 ℃. It could be associated with radiation attenuation of barite. Due to the radiation attenuation property, barite attenuated the both desired and negative effects of gamma radiation to some extent (Akkurt, et al., 2010; Oto, et al., 2013). Glass transition temperatures were almost unchanged at the dose of 75 kGy, thereby not affecting the molecular weight of polymer.

3.2.7.5. Dynamic Mechanical Analysis (DMA) for 10 wt. % Carbon Fiber Loaded Polycarbonate Exposed to 10, 25, 50 and 75 kGy Irradiation

Storage Modulus vs Temperature, Loss Modulus vs Temperature and Tan δ vs Temperature Curves of 10 wt. % carbon fiber loaded polycarbonate samples (irradiated up to 75 kGy) were shown in **Figure 84**, **Figure 85** and **Figure 86**. Glass transition temperatures of specimens were shown in **Table 70** and **Table 71**. Storage Modulus values at 25 ℃ were shown in **Table 72**. The relative storage modulus values at glass transition temperatures were shown in **Table 73**.

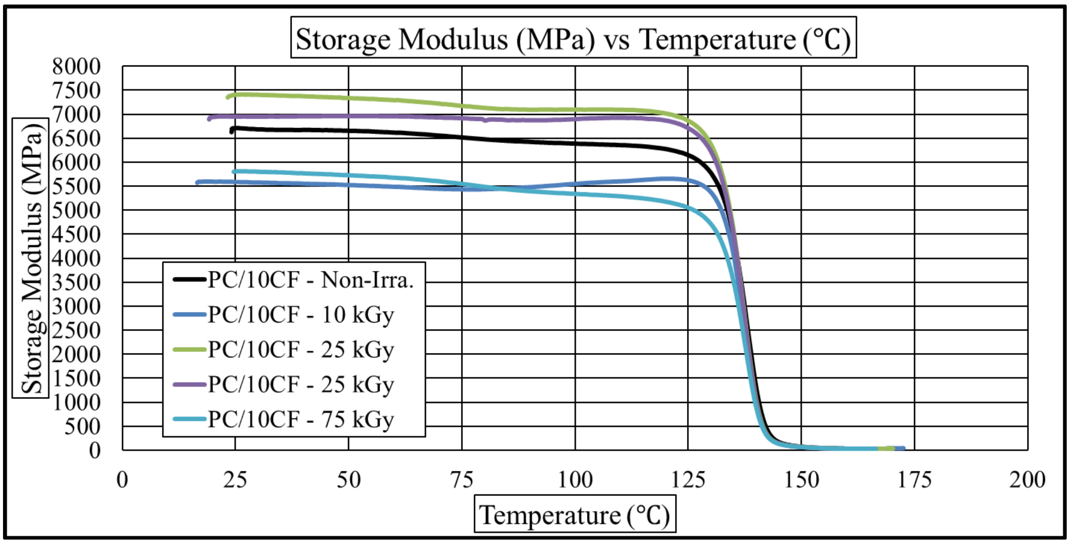

Figure 84 Storage Modulus vs Temperature Curves of 10 wt. % Carbon Fiber Loaded Polycarbonate Samples Irradiated up to 75 kGy

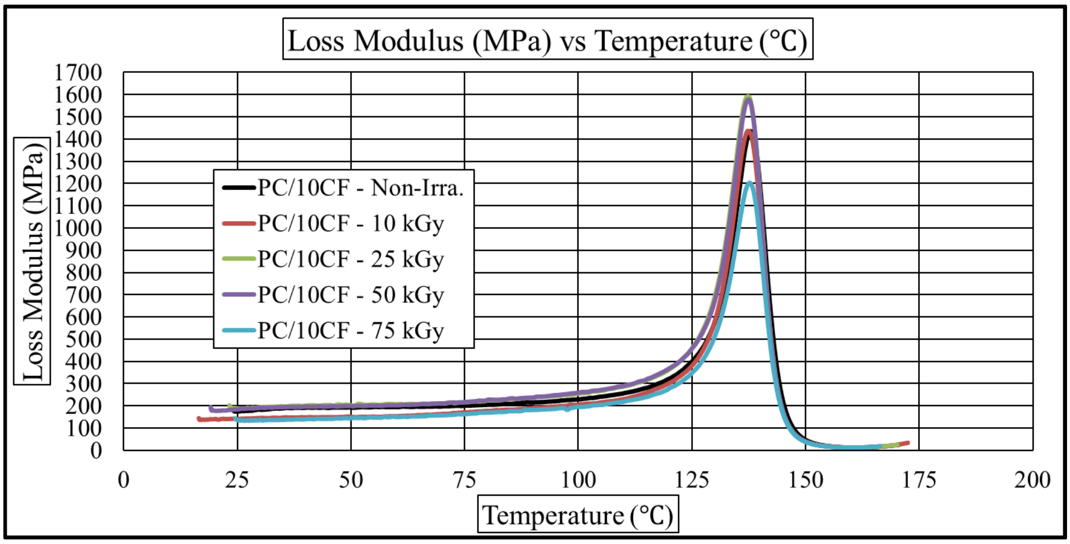

Figure 85 Loss Modulus vs Temperature Curves of 10 wt. % Carbon Fiber Loaded Polycarbonate Samples Irradiated up to 75 kGy

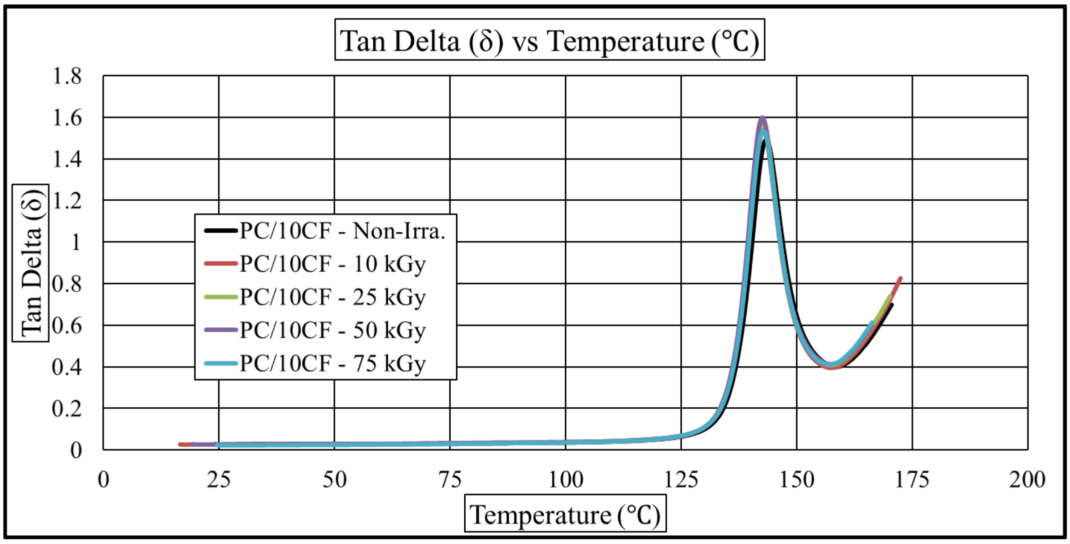

Figure 86 Tan δ vs Temperature Curves of 10 wt. % Carbon Fiber Loaded Polycarbonate Samples Irradiated up to 75 kGy

Table 70 Glass Transition Temperatures (T_g) for 10 wt. % Carbon Fiber Loaded Polycarbonate Samples (Irradiated up to 75 kGy) According to the Loss Modulus vs Temperature Curve

Test Sample with respect to Total Dose	**T_g (℃) Values**
PC/10CF - Non-Irra.	138.0 ℃
PC/10CF - 10 kGy	137.3 ℃
PC/10CF - 25 kGy	136.9 ℃
PC/10CF - 50 kGy	137.6 ℃
PC/10CF - 75 kGy	137.7 ℃

Table 71 Glass Transition Temperatures (T_g) for 10 wt. % Carbon Fiber Loaded Polycarbonate Samples (Irradiated up to 75 kGy) According to the Tan δ vs Temperature Curve

Test Sample with respect to Total Dose	**T_g (℃) Values**
PC/10CF - Non-Irra.	143.6 ℃
PC/10CF - 10 kGy	142.9 ℃
PC/10CF - 25 kGy	142.6 ℃
PC/10CF - 50 kGy	142.6 ℃
PC/10CF - 75 kGy	142.6 ℃

Table 72 Storage Modulus Values (MPa) for 10 wt. % Carbon Fiber Loaded Polycarbonate Samples (Irradiated up to 75 kGy) at 25℃

Test Sample with respect to Total Dose	**Storage Modulus (MPa)**
PC/10CF - Non-Irra.	6712 MPa
PC/10CF - 10 kGy	5591 MPa
PC/10CF - 25 kGy	7407 MPa
PC/10CF - 50 kGy	6952 MPa
PC/10CF - 75 kGy	5804 MPa

Table 73 Relative Storage Modulus Values (MPa) for 10 wt. % Carbon Fiber Loaded Polycarbonate Samples (Irradiated up to 75 kGy) at Glass Transition Temperatures

Test Sample with respect to Total Dose	**Relative Modulus (%) Values at T_g Obtained From Loss Modulus vs Temp. Graph**	**Relative Modulus (%) Values at T_g Obtained From Tan δ vs Temp. Graph**
PC/10CF - Non-Irra.	40.1 %	4.0 %
PC/10CF - 10 kGy	48.3 %	4.6 %
PC/10CF - 25 kGy	43.1 %	4.1 %
PC/10CF - 50 kGy	36.8 %	4.1 %
PC/10CF - 75 kGy	35.9 %	4.6 %

According to **Figure 84** and **Table 72**, 25 and 50 kGy irradiation increased the storage modulus values significantly. On the other hand, 10 and 75 kGy decreased the modulus values. The highest storage modulus was observed in 25 kGy irradiated specimen. The modulus values were higher than that of neat polycarbonates for all irradiation doses. **Table 73** showed that relative storage modulus values at glass transition temperature (from Loss Modulus curve) were increased at 10 and 25 kGy. It was clear that 25 kGy irradiation was the optimum value for improvement of the load-bearing property (at room and elevated temperatures) of 10 wt. % carbon fiber containing composite.

Glass transition temperatures (from Tan δ curve) upon irradiation show no considerable change at 25, 50 and 75 kGy irradiation doses indicating that thermal property of 10 wt. % carbon fiber included polycarbonate was not affected. The variations in glass transition temperatures (from Tan δ curve) were in between ±0.3 ℃ for composites irradiated up to 25, 50 and 75 kGy. It could be associated with radiation attenuation of carbon fiber. Due to the radiation attenuation property, carbon fiber attenuated the negative effects of gamma radiation to some extent (Seppälä & Kulmala, 2011). Glass transition temperatures were almost unchanged at the dose of 75 kGy, thereby not affecting the molecular weight of polymer.

3.2.7.6. Dynamic Mechanical Analysis (DMA) for 10 wt. % Glass Fiber Loaded Polycarbonate Exposed to 10, 25, 50 and 75 kGy Irradiation

Storage Modulus vs Temperature, Loss Modulus vs Temperature and Tan δ vs Temperature Curves of 10 wt. % glass fiber loaded polycarbonate samples (irradiated up to 75 kGy) were shown in **Figure 87**, **Figure 88** and **Figure 89**. Glass transition temperatures of specimens were shown in **Table 74** and **Table 75**. Storage Modulus values at 25 ℃ were shown in **Table 76**. The relative storage modulus values at glass transition temperatures were shown in **Table 77**.

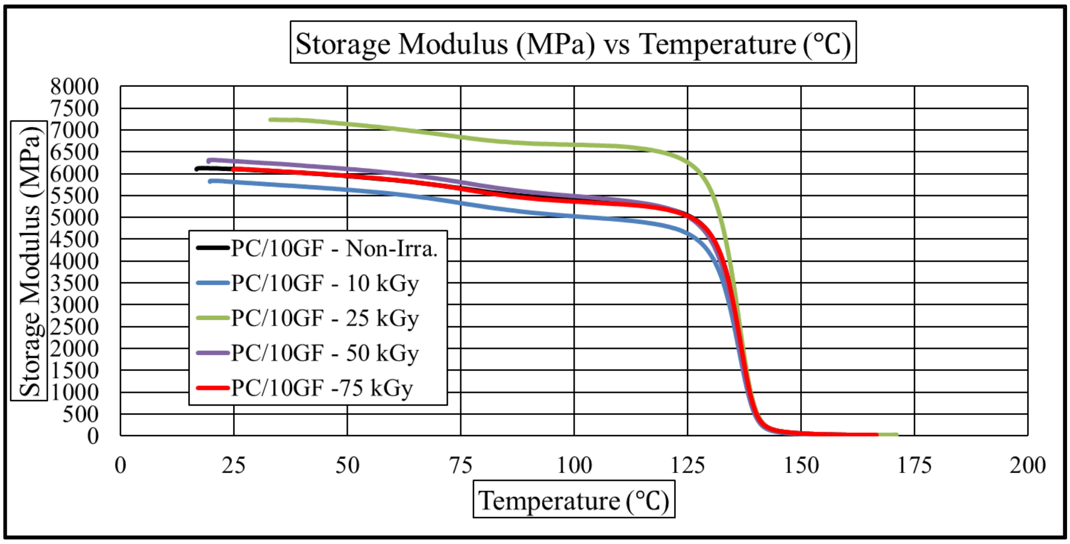

Figure 87 Storage Modulus vs Temperature Curves of 10 wt. % Glass Fiber Loaded Polycarbonate Samples Irradiated up to 75 kGy

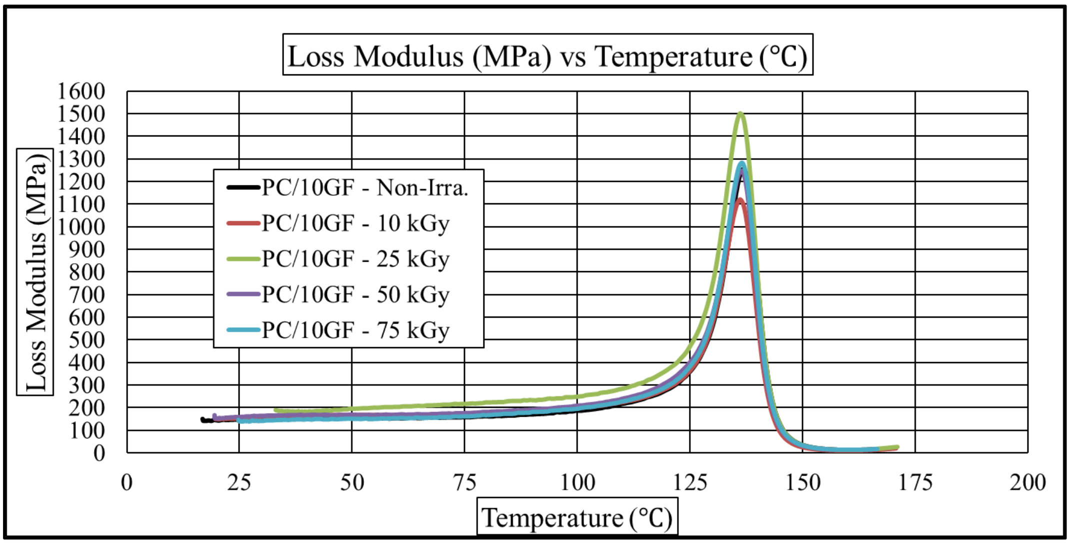

Figure 88 Loss Modulus vs Temperature Curves of 10 wt. % Glass Fiber Loaded Polycarbonate Samples Irradiated up to 75 kGy

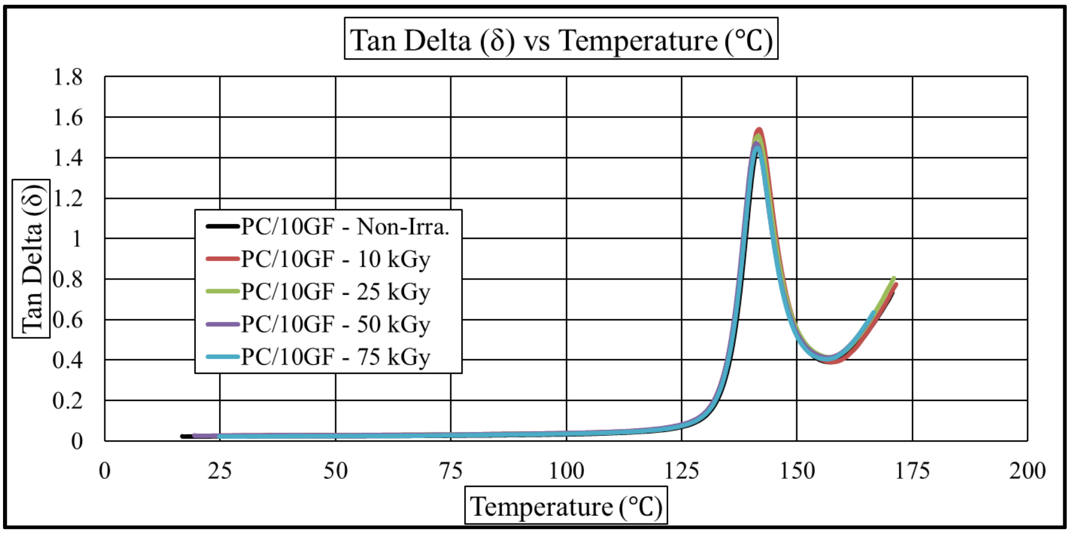

Figure 89 Tan δ vs Temperature Curves of 10 wt. % Glass Fiber Loaded Polycarbonate Samples Irradiated up to 75 kGy

Table 74 Glass Transition Temperatures (T_g) for 10 wt. % Glass Fiber Loaded Polycarbonate Samples (Irradiated up to 75 kGy) According to the Loss Modulus vs Temperature Curve

Test Sample with respect to Total Dose	**T_g (℃) Values**
PC/10GF - Non-Irra.	136.6 ℃
PC/10GF - 10 kGy	136.1 ℃
PC/10GF - 25 kGy	136.1 ℃
PC/10GF - 50kGy	136.2 ℃
PC/10GF - 75kGy	136.6 ℃

Table 75 Glass Transition Temperatures (T_g) for 10 wt. % Glass Fiber Loaded Polycarbonate Samples (Irradiated up to 75 kGy) According to the Tan δ vs Temperature Curve

Test Sample with respect to Total Dose	**T_g (℃) Values**
PC/10GF - Non-Irra.	141.5 ℃
PC/10GF - 10 kGy	142.0 ℃
PC/10GF - 25 kGy	141.7 ℃
PC/10GF - 50kGy	141.1 ℃
PC/10GF - 75kGy	141.5 ℃

Table 76 Storage Modulus Values (MPa) for 10 wt. % Glass Fiber Loaded Polycarbonate Samples (Irradiated up to 75 kGy) at 25℃

Test Sample with respect to Total Dose	**Storage Modulus (MPa)**
PC/10GF - Non-Irra.	6111 MPa
PC/10GF - 10 kGy	5805 MPa
PC/10GF - 25 kGy	7232 MPa
PC/10GF - 50kGy	6276 MPa
PC/10GF - 75kGy	6106 MPa

Table 77 Relative Storage Modulus Values (MPa) for 10 wt. % Glass Fiber Loaded Polycarbonate Samples (Irradiated up to 75 kGy) at Glass Transition Temperatures

Test Sample with respect to Total Dose	**Relative Modulus (%) Values at T_g Obtained From Loss Modulus vs Temp. Graph**	**Relative Modulus (%) Values at T_g Obtained From Tan δ vs Temp. Graph**
PC/10GF - Non-Irra.	37.2 %	5.0 %
PC/10GF - 10 kGy	35.1 %	3.2 %
PC/10GF - 25 kGy	38.4 %	3.8 %
PC/10GF - 50kGy	35.0 %	4.6 %
PC/10GF - 75kGy	34.7 %	4.6 %

According to **Figure 87** and **Table 76**, 25 and 50 kGy irradiation increased the storage modulus values of 10 wt. % glass fiber reinforced composite. On the other hand, 10 and 75 kGy decreased the modulus values. The highest storage modulus was observed in 25 kGy irradiated specimen. The modulus values of 10 wt. % glass fiber based polycarbonate were higher than that of neat polycarbonate samples for all irradiation doses. **Table 77** showed that relative storage modulus values at glass transition temperature (from Loss Modulus curve) were increased at 25 kGy. It was clear that 25 kGy irradiation was the optimum value for improvement of the load-bearing property (at room and elevated temperatures) of 10 wt. % glass fiber based polycarbonate.

Glass transition temperatures (from Tan δ curve) upon irradiation show no considerable change at the total doses of 25, 50 and 75 kGy, indicating that thermal property of 10 wt. % glass fiber included polycarbonate was not affected. The variations in glass transition temperatures (from Tan δ curve) were in between ±0.5 ℃ for composites irradiated up to 10, 25 and 75 kGy. Glass transition temperatures were almost unchanged at the dose of 75 kGy, thereby not affecting the molecular weight of polymer.

3.2.8 Scanning Electron Microscopy Investigation (SEM)

3.2.8.1. SEM Investigation for Neat Polycarbonate and Composites

SEM images taken from fracture surfaces (obtained from tensile test) of bentonite, barite, carbon fiber and glass fiber loaded polycarbonate samples were shown in **Figure 90**, **Figure 91**, **Figure 92** and **Figure 93**, respectively. The fracture surface of neat, particle and fiber filled polycarbonate samples were taken in order to determine the homogenous dispersion of filler with matrix.

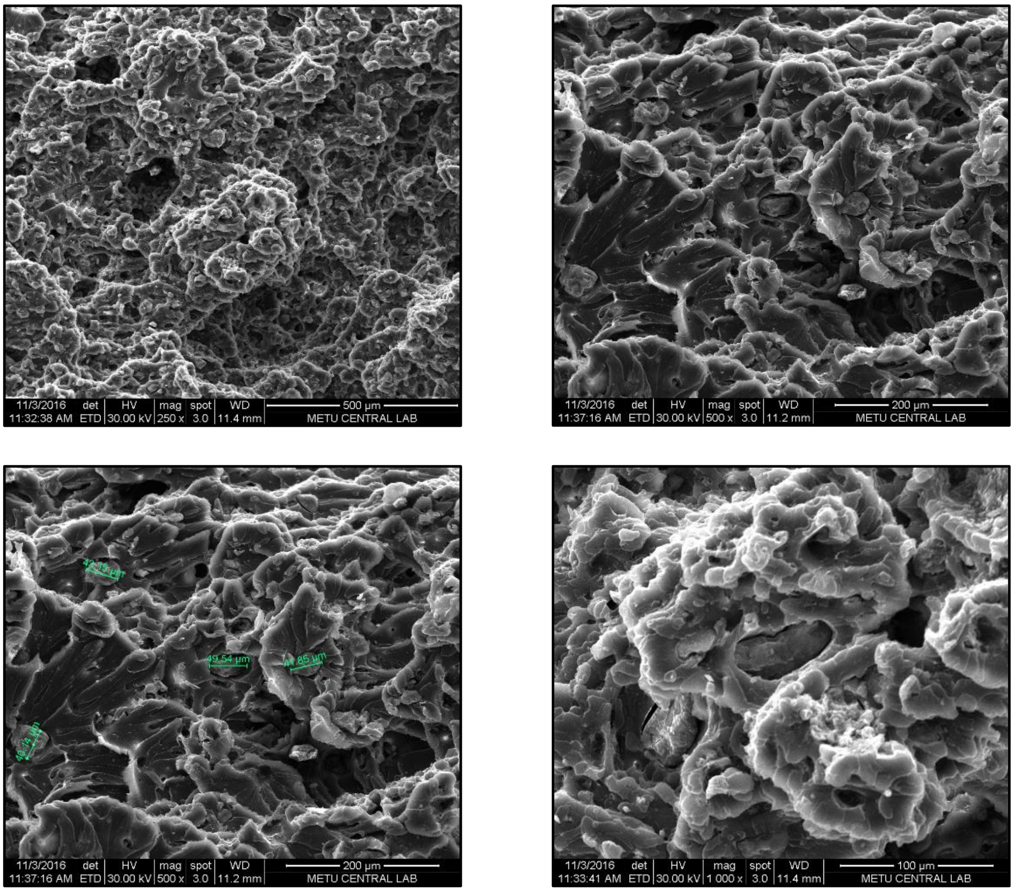

Figure 90 SEM Images 5 wt. % Bentonite Loaded Polycarbonate (Taken from Fracture Surface)

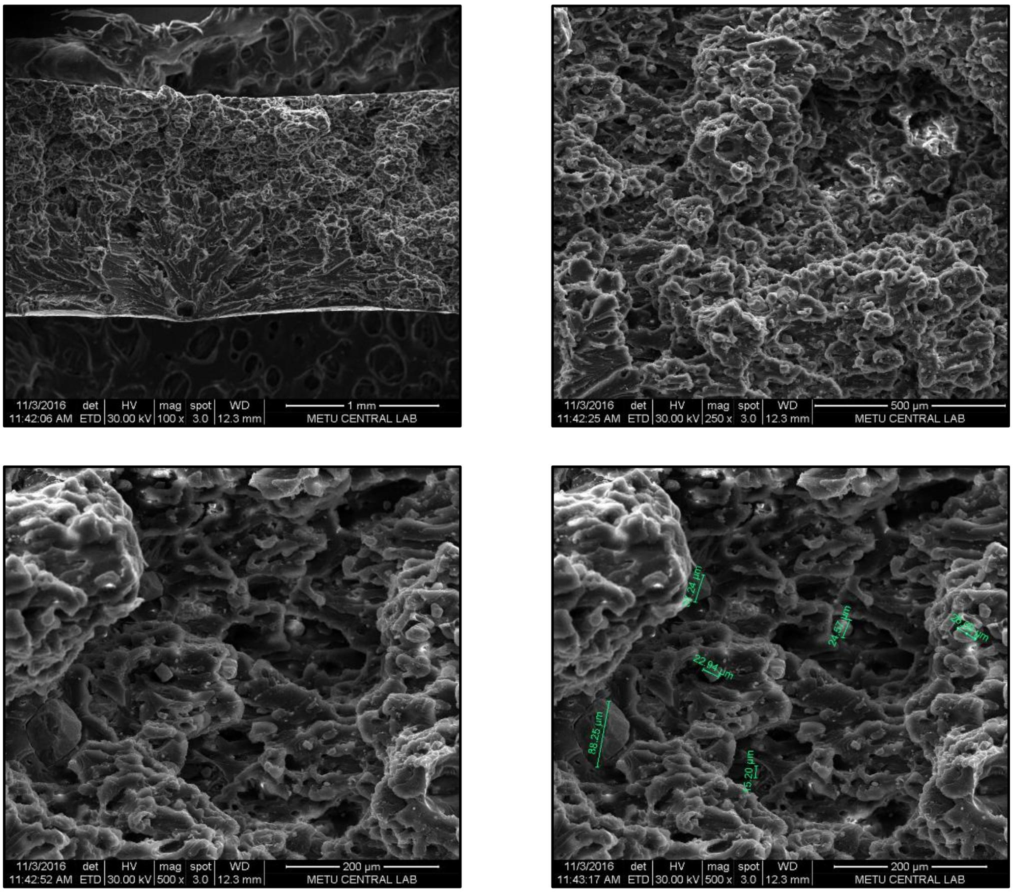

Figure 91 SEM Images 10 wt. % Barite Loaded Polycarbonate (Taken from Fracture Surface)

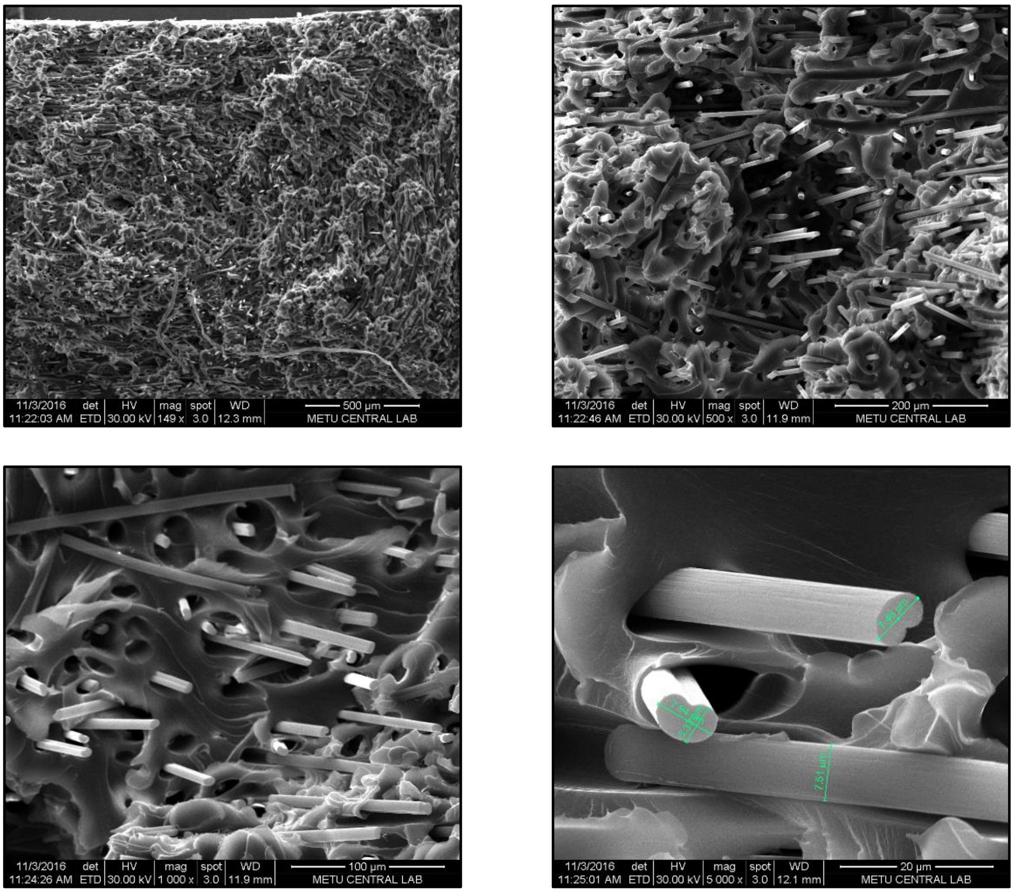

Figure 92 SEM Images 10 wt. % Carbon Fiber Loaded Polycarbonate (Taken from Fracture Surface)

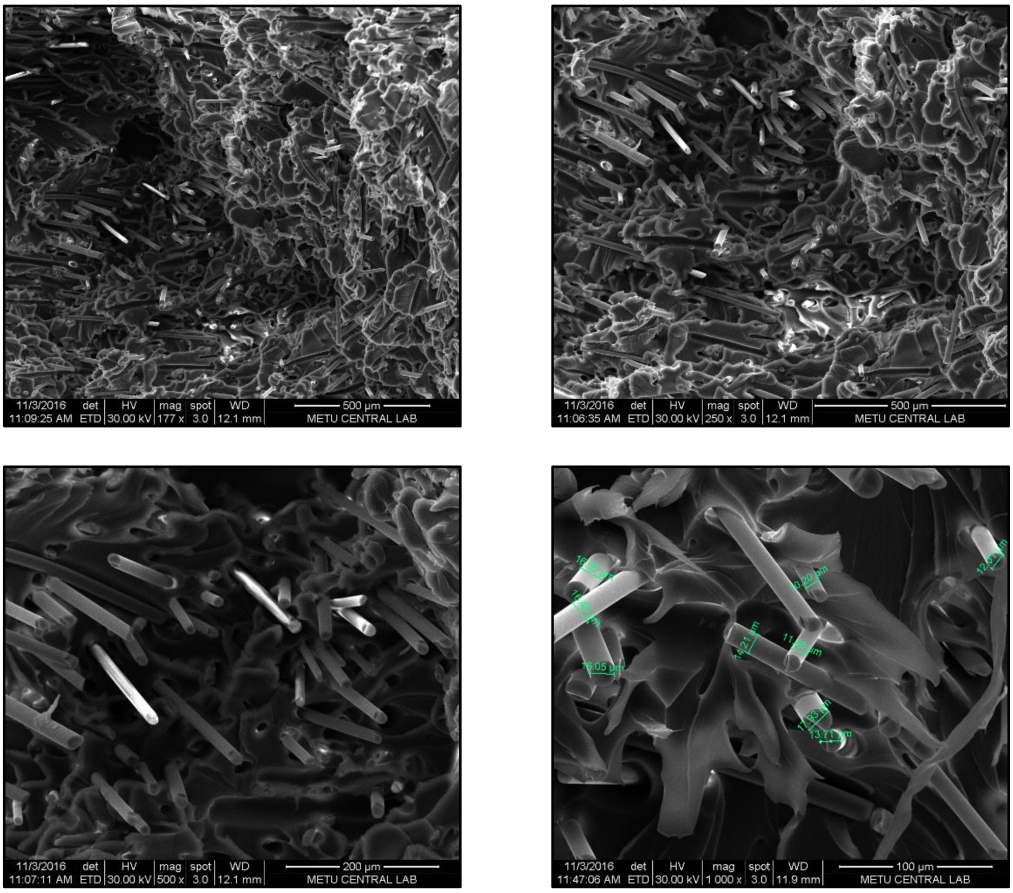

Figure 93 SEM Images 10 wt. % Glass Fiber Loaded Polycarbonate (Taken from Fracture Surface)

According to the SEM images, bentonite, barite, carbon fiber and glass fiber inclusion into polycarbonate were done homogenously. Well dispersion of the fillers into polymer matrix were observed.

Figure 92 and **Figure 93** revealed that carbon and glass fiber were randomly dispersed into polycarbonate matrix. **Figure 92** and **Figure 93** also showed that mean diameter of the carbon fiber and the glass fiber were observed about 7.1 and 14.3 µm, respectively. In the specification of glass fiber, diameter was specified as 13 µm and this value is consistent with that of observed in SEM.

From the SEM pictures shown in **Figure 92** and **Figure 93**, the initial aspect ratios, which was defined as ratio of fiber length to the fiber diameter),for carbon and glass fibers were found as 423 $(\frac{\text{initial length of carbon fiber} = 3\text{ mm}}{\text{diameter of carbon fiber} = 7.1\ \mu\text{m}})$ and 315 $(\frac{\text{initial length of glass fiber} = 4.5\text{ mm}}{\text{diameter of glass fiber} = 14.3\ \mu\text{m}})$, respectively. Higher initial aspect ratio for fiber were resulted with higher mechanical properties (Masoumy, et al., 1983; Carraher, 2014). Therefore, it could be the another reason for higher tensile strength values observed on carbon fiber based polycarbonates than that of glass fiber reinforced one.

According to the **Figure 90** and **Figure 91**, large bentonite and barite particles were observed at the fracture surface. The particle size distribution analysis gave the mean diameters for bentonite and barite minerals as 20.6 and 9.4 µm, respectively. However, in the fracture surfaces, particles with higher diameters were observed. It was clear that the larger particles acted as agglomerate and they were responsible for the early fracture of specimens with reduction in elongations at break.

EDX analysis also proved qualitatively the presence of carbon fiber, glass fiber, bentonite and barite minerals in composites. The diameter measurements were based on fibers and minerals of which EDX qualitatively proved the presence. EDX analyses for bentonite, barite, carbon fiber and glass fiber (carried out in composites surfaces) were shown in Appendix.

3.2.8.1. SEM Investigation for Neat Polycarbonate and Composites Irradiated up to 75 kGy

SEM images taken from surfaces of neat, bentonite, barite, carbon fiber and glass fiber loaded polycarbonates, which were irradiated up to 75 kGy, were shown in **Figure 94**, **Figure 95**, **Figure 96**, **Figure 97** and **Figure 98**.

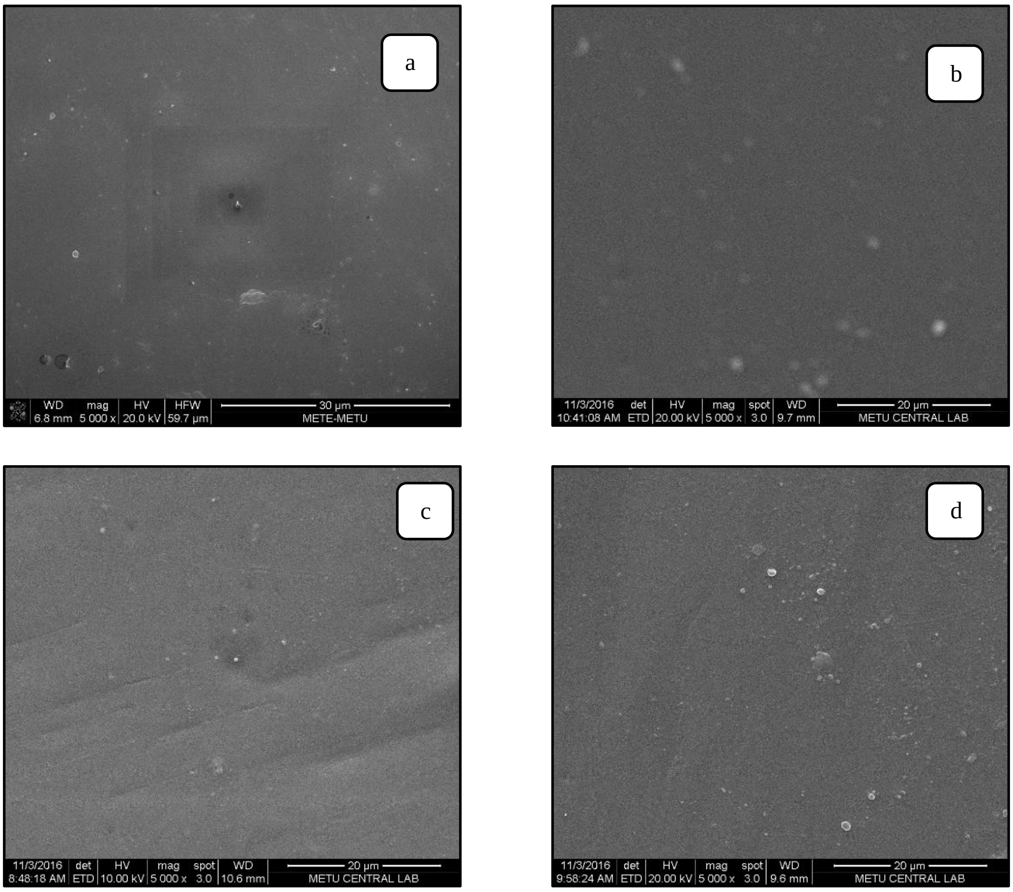

Figure 94 SEM Images of Neat Polycarbonate Specimens Monitored at Magnitude of 5000X a)Non-Irradiated, b) 25 kGy Irradiated, c) 50 kGy Irradiated, d) 75 kGy Irradiated.

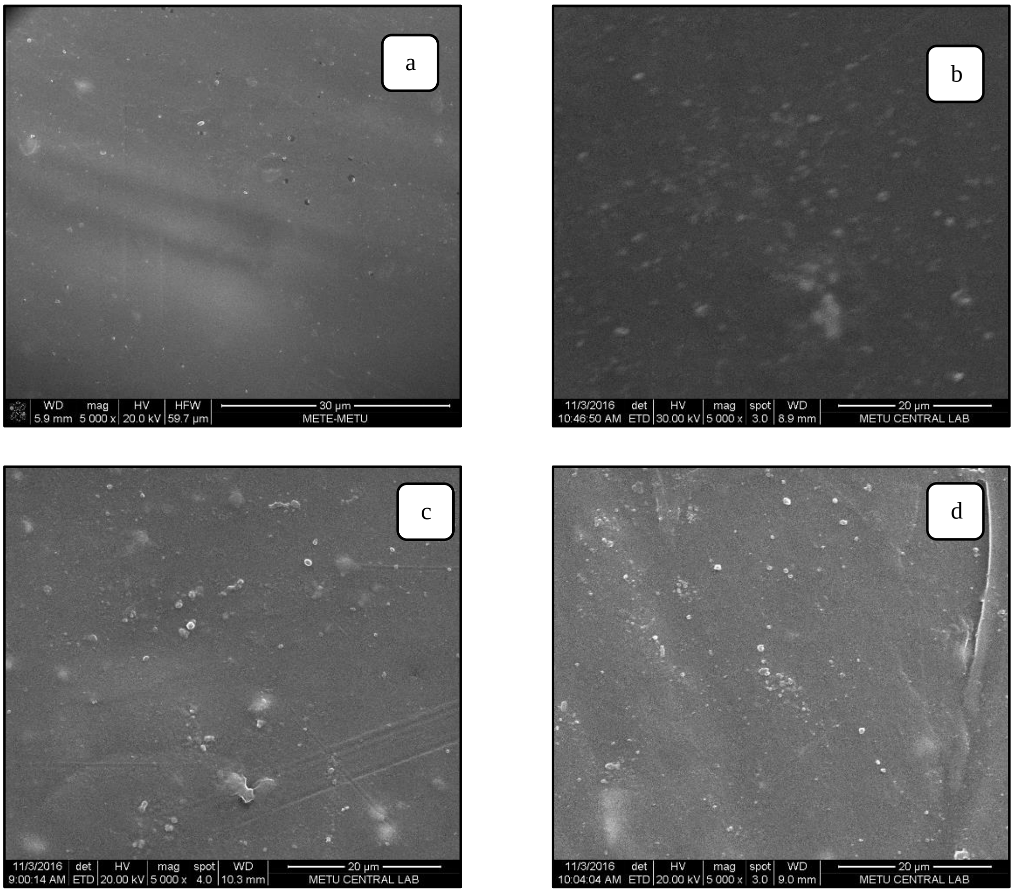

Figure 95 SEM Images of 5 wt. % Bentonite Loaded Polycarbonate Specimens Monitored at Magnitude of 5000X a)Non-Irradiated, b) 25 kGy Irradiated, c) 50 kGy Irradiated, d) 75 kGy Irradiated.

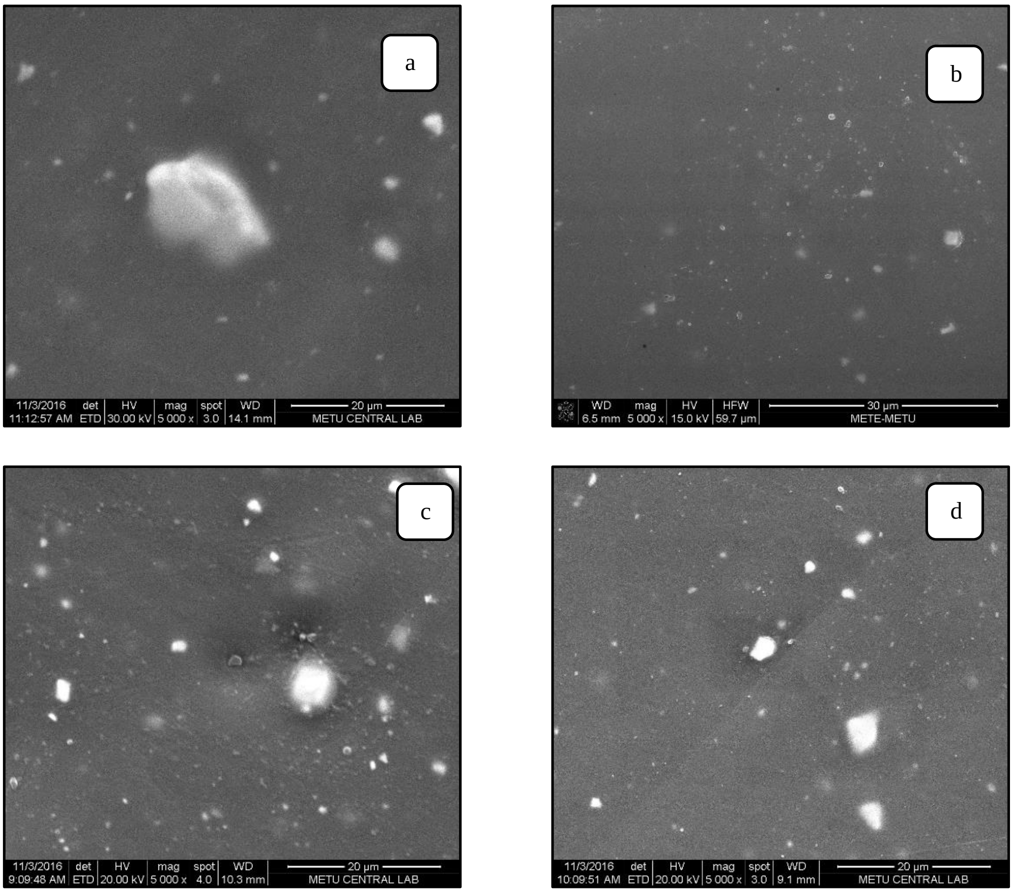

Figure 96 SEM Images of 10 wt. % Barite Loaded Polycarbonate Specimens Monitored at Magnitude of 5000X a)Non-Irradiated, b) 25 kGy Irradiated, c) 50 kGy Irradiated, d) 75 kGy Irradiated.

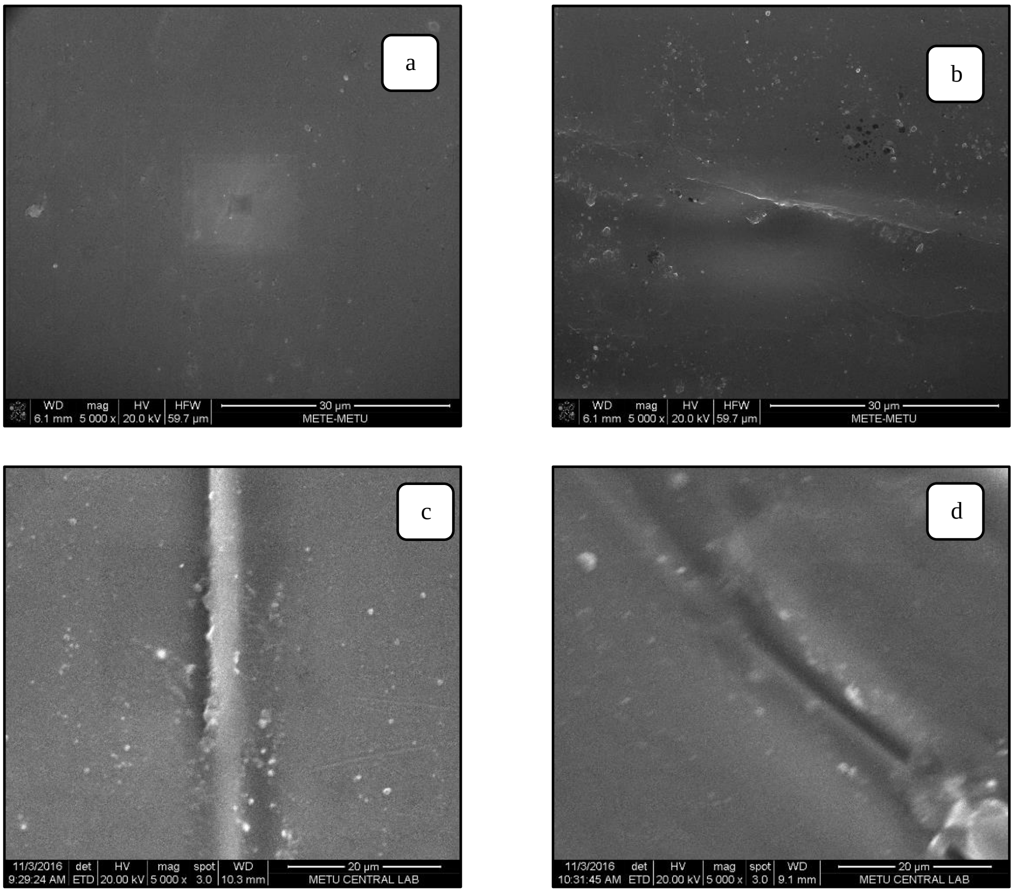

Figure 97 SEM Images of 10 wt. % Carbon Fiber Loaded Polycarbonate Specimens Monitored at Magnitude of 5000X a)Non-Irradiated, b) 25 kGy Irradiated, c) 50 kGy Irradiated, d) 75 kGy Irradiated.

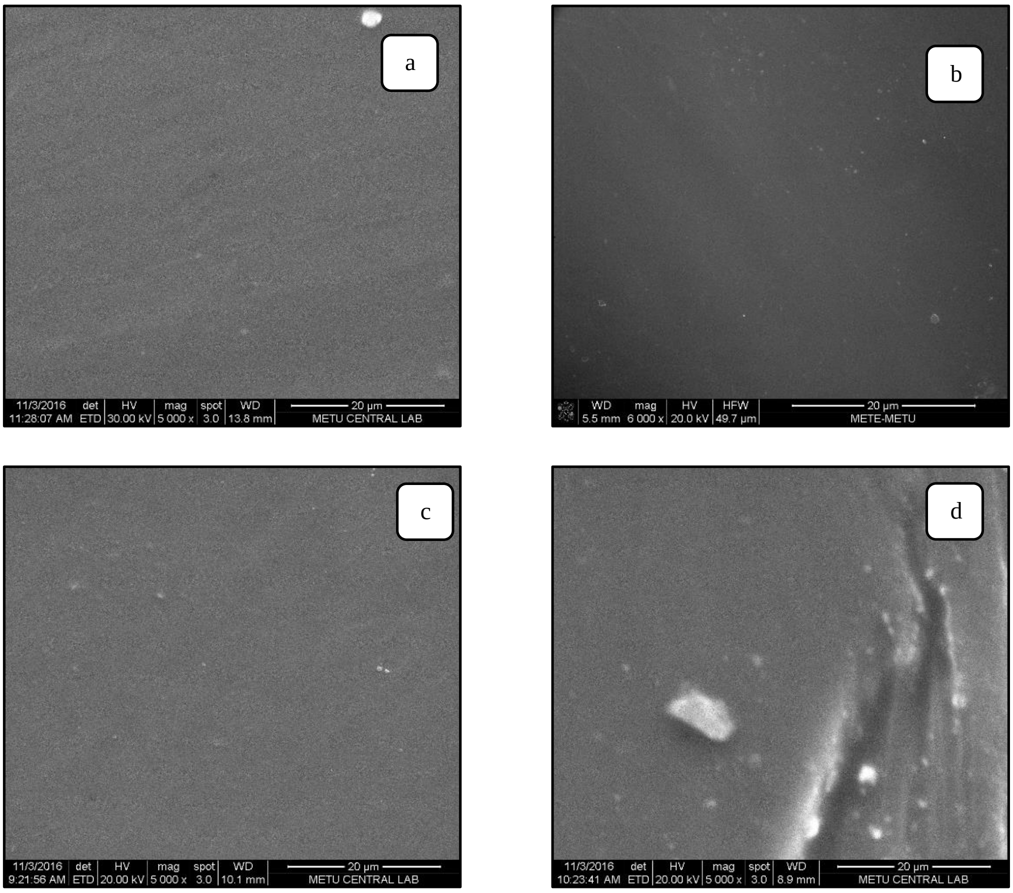

Figure 98 SEM Images of 10 wt. % Glass Fiber Loaded Polycarbonate Specimens Monitored at Magnitude of 5000X a)Non-Irradiated, b) 25 kGy Irradiated, c) 50 kGy Irradiated, d) 75 kGy Irradiated

According to the **Figure 94**,**Figure 95**, **Figure 96 Figure 97** and **Figure 98**, surfaces of the neat, carbon and glass fiber reinforced polycarbonate samples, which were non-irradiated, were smooth. When specimens were irradiated up to 75 kGy, the roughness of surfaces were slightly increased. There were not any distinct fractures upon irradiation. It could be inferred from SEM pictures that 75 kGy irradiation did not compromise the surface of the polymers significantly.

CHAPTER 4

CONCLUSIONS

4.1. Neat Polycarbonate Specimens Irradiated up to 4341 kGy

High dose irradiations up to 4341 kGy changed mechanical properties of polycarbonate dramatically. Elongation at break values showed considerable decrease upon irradiation. Half-value dose, an important parameter for radiation resistance of polymer, were lower than 684 kGy. The half-value dose for neat polycarbonate could not be caught. It was observed that specimens could not resist up to 4341 kGy mechanically. 4341 kGy irradiated samples became brittle and tensile tests could not be carried out. Higher dose irradiations (684, 1291, 3280 kGy) also greatly changed property of polycarbonate. While stress-strain graph of non-irradiated sample resembled the typical thermoplastics' stress-strain graph, the graph of 684, 1291, 3280 kGy irradiated samples resembled stress-strain behavior of typical brittle materials. A ductile to brittle transition was observed with the irradiation. Elastic and storage modulus values at room temperature (obtained from tensile test and DMA analysis, respectively) showed compatible results such that both of them depicted increasing pattern up to 1291 kGy dose. The reason behind the increase in the elastic and storage modulus at room temperature upon irradiation was the fact that the dominant effect was chain scission, increasing the end-groups and intermolecular forces of the chain.

Tensile strength and ultimate elongation values decreased drastically upon irradiation. Decrease in tensile strength and ultimate elongation clearly revealed the fact that radiation induced chain scission predominantly affected the polymer structure at the dose of 684, 1291, 3280 and 4341 kGy (Carlsson & Chmela, 1990; Hill & Whittaker, 2004; International Atomic Energy Agency, 1999; Charlesby, 1960; Tamboli, et al., 2004; Carraher, 2014). Moreover, decrease in the glass transition temperature were observed from the DMA analysis. The tensile strength values and DMA analysis confirmed and supported each other. Storage modulus values at elevated temperature (i.e. at around 140 ℃) were decreased upon irradiation, indicating deterioration in the load-bearing property of polycarbonate at elevated temperature. The lowest stiffness at room and elevated temperature were observed in 3280 kGy irradiated specimen: When TGA results were investigated, thermal stability of polycarbonate significantly reduced upon irradiation such that the difference between the T_5 values of non-irradiated and 4341 kGy irradiated specimens was measured as 62 ℃. SEM images revealed the morphological deformation of the polycarbonate samples. Deformation in the surface of the polycarbonate started with 684 kGy and progressed upon irradiation up to 4341 kGy. ATR-FTIR spectrums revealed that chain scission was occurred at carbonate site.

4.2.Polycarbonate Composites Irradiated up to 10, 25, 50 and 75 kGy

Neat, bentonite, barite, carbon fiber and glass fiber based composites were compounded via using extrusion and injection molding techniques. Incorporation of fillers in to polycarbonate granules were done homogenously which were supported by SEM images taken from fracture surfaces of composites.

Carbon fiber and glass fiber inclusion into polycarbonate improved the mechanical strength significantly. Improved mechanical property in fiber reinforced composites were associated with the fact that carbon and glass fibers had high strength and included surface modifications. Load-bearing property was important for possible use of polymers in radioactive waste management. Therefore, fiber loading enhanced the load-bearing property of polycarbonate.

The strength values of carbon fiber based composites were comparatively higher than that of glass fiber based ones. This was attributed to fact that carbon fiber had higher modulus and initial aspect ratio than that of glass fiber.

Bentonite and barite inclusion into polycarbonate first increased the strength values, then higher amount loading decreased the strength. Reduction in strength of particle filled composites at higher contents were associated with the fact that bentonite and barite had low strength and did not include surface modification.

For all composites, elongation at break values were diminished via loading of particle and fiber types of fillers.

Upon irradiation, mechanical properties of neat, particle and fiber filled polycarbonates were not compromised significantly.

The integration of bentonite with irradiation had an effect analogous to plasticizer such that it decreased the strength values and increased the elongations at break values.

10 wt. % carbon fiber included composites showed best stability among all composites under irradiation in terms of strength. It could be associated with the fact that that radiation shielding property of carbon fiber could retard the radiation induced reactions.

Tensile strength values of 10 wt. % barite loaded samples irradiated with 10, 25, 50 kGy doses were closer to each other revealing that radiation shielding property of barite could retard the radiation induced reactions.

Yellowness index (YI) values increased upon irradiation indicating that higher amounts of chain scissions (formations of phenyl and phenoxy radicals) were present at higher doses. Yellowness index values of 10 wt. % glass fiber reinforced composite were lower than that of neat polycarbonate at 75 kGy. It could be associated with the fact that glass fiber acted as scavenger of phenoxy and phenyl radicals and reduced the chain scission reactions relatively with respect to neat polycarbonate.

The decreases in the intensities of carbonyl and ether bonds were observed in all composites. It could be attributed with the presence of radiation-induced chain-scissions resulting with phenyl and phenoxy radicals formation.

Melt Flow Rate (MFR) results revealed that bentonite and barite loaded composite were higher MFR than neat polycarbonates. Carbon fiber and glass fiber based composite were lower MFR values. The higher MFR values were related with poor interfacial adhesion between filler (bentonite and barite) and matrix. On the other hand, lower MFR values were linked with enhanced interfacial adhesion between fiber (carbon and glass) and matrix.

TGA and DTG curves showed that neat polycarbonate had highest thermal stability among all composites. Upon irradiation, enhancement and reduction in the decomposition temperatures were not significant in 10 wt. % carbon fiber and barite based composites. This was associated with radiation attenuation property of barite and carbon fiber.

Dynamic Mechanical Analysis showed that, storage modulus values were enhanced significantly with inclusion of 10 wt. % carbon and glass fiber in to polycarbonate. Load bearing property of polycarbonates were improved with fiber loading.

Glass transition temperatures of 10 wt. barite, carbon fiber and glass fiber filled composites were almost unchanged at the total dose of 75 kGy, thereby indicating of not affecting the molecular weight of polymer.

SEM images revealed that 75 kGy irradiation did not deteriorate the surface of the composites based on particle and fiber.

End point criterions and radiation index values were not achieved by 75 kGy irradiation. It could easily be stated that neat, bentonite, barite, carbon fiber and glass fiber filled polycarbonates sustained the 75 kGy irradiation without any significant change in mechanical, morphological and thermal properties.

According to the TS EN ISO 11137-2 standard, 25 kGy is the maximum dose for a medical devices intended to be supplied in sterile condition (Turkish Standards Institution, 2015). Results showed that polycarbonate (Lexan LS2™) and its composites used in this study retained mechanical, thermal and morphological properties at 25 kGy. Therefore, radiation sterilization (i.e. 25 kGy) with respect to TS EN ISO 11137-2 could be easily applied on polycarbonate (Lexan LS2™) and its composites. Moreover, multiple radiation sterilization (up to 3 times corresponding to 75 kGy) could be applied on medical devices based on polycarbonate. The only negative consequence of radiation sterilization (i.e. 25 kGy) on polycarbonate (Lexan LS2™) was initiation and progression of yellowness upon irradiation.

The end point criterions could be reached at the dose in between 75 kGy and 684 kGy. Further irradiation could be helpful to determine the exact end-point of neat, particle and fiber loaded polycarbonates.

In order to determine initial dose of the radioactive waste that intended to be embedded into neat, particle and fiber reinforced polycarbonate, 75 kGy was selected to be total dose reached by waste after 300 years. By using **Equation 1**, initial dose rates of selected radionuclides, which were important in Low-Level Radioactive Waste Management, were calculated (Idaho National Engineering Laboratory, 1996; Ojovan & Lee, 2005). **Table 78** showed the initial dose rate of selected radionuclides.

Table 78 Initial Dose Rate of Selected Radionuclide

Nuclide	**Half-Life (in years)**	**Initial Dose Rate (Gy/h)**
^{3}H	12.3	0.48
^{60}Co	5.27	1.12
^{63}Ni	100	0.067
^{90}Sr	29.1	0.20
^{137}Cs	30.17	0.19
^{241}Pu	14.4	0.41
^{242}Cm	0.45	13.18

REFERENCES

Acierno, D., Mantia, F. P. L., Spadaro, G. & Titomanlio, G., 1981. Effect of Radiation Conditions on Some Properties of a Polycarbonate. *Radiation Physics and Chemistry,* Volume 17, pp. 31-34.

Acierno, D., Mantia, F. P. L. & Titomanlio, G., 1980. Gamma Radiation Effects on a Polycarbonate. *Radiation Physics and Chemistry,* Volume 16, pp. 95-99.

Akkurt, I.; Akyildirim, H.; Mavi, B.; Kilincarslan, S.; Basyigit, C., 2010. Gamma-Ray Shielding Properties of Concrete Including Barite at Different Energies. *Progress in Nuclear Energy,* Volume 52, pp. 620-623.

Akkurt, İ.; Emikönel, S.; Akarslan, F.; Günoğlu, F.; Kılınçarslan, Ş.; Üncü, İ. S., 2014. Barite Effect on Radiation Shielding Properties of Cotton–Polyester Fabric. *Acta Physıca Polonıca A,* 128(2-b), pp. 53-54.

Alewelt, W., Margotte;, D., Vernaleken, H. & Kassahn, H.-G., 1979. *Glass Fiber Reinforced Polycarbonates with Improved Mechanical Properties Containing 0.5 to 5.0% of Organopolysiloxane.* United States, Patent No. 4147707.

Alsagayar, Z. S., Rahmat, A. R., Arsad, A. & Mustaph, S. N. H. B., 2015. Tensile and Flexural Properties of Montmorillonite Nanoclay Reinforced Epoxy Resin Composites. *Advanced Materials Research,* Volume 1112, pp. 373-376.

Antonakou, E. V. & Achilias, D. S., 2013. Recent Advances in Polycarbonate Recycling: A Review of Degradation Methods and Their Mechanisms. *Waste Biomass Valor,* Volume 4, pp. 9-21.

Araujo, E. S., Khoury, H. J. & Silveira, S. V., 1998. Effects of gamma-irradiation on some properties of durolon polycarbonate. *Radiation Physics and Chemistry,* Volume 53, pp. 79-84.

Artham, T. & Doble, M., 2008. Biodegradation of Aliphatic and Aromatic Polycarbonates. *Macromolecular Bioscience,* Volume 8, pp. 14-24.

ASTM International, 2009. *ASTM D3935-09: Standard Specification for Polycarbonate (PC) Unfilled and Reinforced Material.* West Conshohocken: ASTM International.

ASTM International, 2009. *ASTM Standard D3935-09: Standard Specification for Polycarbonate (PC) Unfilled and Reinforced Material.* West Conshohocken: ASTM International.

ASTM International, 2010. *ASTM E313: Standard Practice for Calculating Yellowness and Whiteness Indices from Instrumentally Measured Color Coordinates.* West Conshohocken: ASTM International.

ASTM International, 2012. *ASTM D4065-12,Standard Practice for Plastics: Dynamic Mechanical Properties: Determination and Report of Procedures.* West Conshohocken: ASTM International.

ASTM International, 2013. *ASTM D4092-07,Standard Terminology for Plastics: Dynamic Mechanical Properties.* West Conshohocken: ASTM International;.

ASTM International, 2013. *ASTM E308: Standard Practice for Computing the Colors of Objects by Using the CIE System.* West Conshohocken: ASTM International.

ASTM International, 2014. *ASTM E1131: Standard Test Method for Compositional Analysis by Thermogravimetry.* West Conshohocken: ASTM International.

ASTM International, 2015. *ASTM D7028: Standard Test Method for Glass Transition Temperature (DMA Tg) of Polymer Matrix Composites by Dynamic Mechanical Analysis (DMA).* West Conshohocken: ASTM International.

ASTM International, 2015. *ASTM E131: Standard Terminology Relating to Molecular Spectroscopy.* West Conshohocken: ASTM International.

Bonin, H. W.; Bui, V.T. ; Legaut, J. F. ; Davey, A. R.; Douglas, T. D.; Duriez, C. C. S.; MacGregor, G. B., n.d. *High Polymer Composites for Containers for the Long-Term Storage of Spent Nuclear Fuel and High Level Radioactive Waste.* [Online] Available at: http://www.iaea.org/inis/collection/NCLCollectionStore/_Public/30/020/30020407.pdf
[Accessed 02 12 2016].

Booth, A. F., 2001. *Sterilization Validation & Routine Operation Handbook Radiation.* 1 ed. Lancaster: Technomic Publishing Company.

Brownstein, M., 1991. *Radioactive Waste Solidification ASME Short Course: Radioactive Waste Management for Nuclear Power Reactors and Other Facilities,* Tennessee: ASME.

Brunelle, D. J. & Korn, M. R., 2005. Advances in Polycarbonates: An Overwiew. In: D. J. Brunelle, ed. *Advances in Polycarbonates.* Washington: American Chemical Society, pp. 1-7.

Brunelle, D. J. & Korn, M. R., 2005. Composites of Polycarbonate with Multiwalled Carbon Nanotubes Produced by Melt Mixing. In: P. Pötschke, A. R. Bhattacharyya1,3, A. Janke & G. Harald, eds. *Advances in Polycarbonates.* Washington: American Chemical Society, pp. 148-164.

Caldeira, G.; Maia, J. M.; Carneiro, O. S.; Covas, J. A.; Befwardo, C. A., 1998. Production and Characterization of Innovative Carbon Fiber-Polycarbonate Composites. *Polymer Composites,* 19(2), pp. 147-151.

Callister, Jr., W. D., 2007. *Materials Science and Engineering:An Introduction.* 7 ed. New York: John Wiley & Sons, Inc..

Carlsson, D. J. & Chmela, S., 1990. Polymers and High-Energy Irradiation: Degradation and Stabilization. In: G. Scott, ed. *Mechanism of Polymer Degradation and Stabilisation.* London: Elseiver Applied Science, pp. 109-135.

Carraher, C. E., 2014. *Carraher's Polymer Chemistry.* 9 ed. New York: Taylor & Francis Group.

Carrion, F. J., Arribas, A., Bermudez, M.-D. & Guillamon, A., 2008. Physical and Tribological Properties of a New Polycarbonate-Organoclay Nanocomposite. *European Polymer Journal,* Volume 44, pp. 968-977.

Charlesby, A., 1960. *Atomic Radiation and Polymers.* 1 ed. London: Pergamon Press LTD..

Chen, J., Czayka, M. & Uribe, R. M., 2005. Effects of electron beam irradiations on the structure and mechanical properties of polycarbonate. *Radiation Physics and Chemistry,* Volume 74, pp. 31-35.

Ciullo, P. A., 1996. *Industrial Minerals and Their Uses.* New Jersey: Noyes Publications.

Clem, A. G. & Doehler, R. W., 1963. *Industial Apllications of Bentonite.* New York, Macmillan.

Cota, Stela; Oliveira, Tania Valeria S. de; Murillo, Senne Jr; Pacheco, Graziella; Albuquerque, Marcia de, 2009. Immobilization of simulated evaporator concentrate waste. *Progress in Nuclear Energy,* Volume 51, p. 236–239.

Council of Europe, 2005. Barium Sulphate. In: C. o. Europe, ed. *European Pharmacopoeia 6th ed..* Strasbourg: Council of Europe, p. 1053.

Daca Instruments, 1999. *Microinjector Operation Manual, brochure.* Goleta: Daca Instruments.

Dao, Duy Quang; Rogaume, Thomas; Luche, Jocelyn; Richard, Frank; Valencia, Lucas Bustamante; Ruban, Sindonie, 2016. Thermal degradation of epoxy resin/carbon fiber composites: Influence of carbon fiber fraction on the fire reaction properties and on the gaseous species release. *Fire and Materials,* Volume 40, pp. 27-47.

Delage, P., Cui, Y. J. & Tang, M., 2010. Clays in Radioactive Waste disposal. *Journal of Rock Mechanics and Geotechnical Engineering,* Volume 2, pp. 111-123.

Delpech, M. . C., Coutinho, F. M. & Habibe, M. E. S., 2002. Bisphenol A-based polycarbonates: characterization of commercial samples. *Polymer Testing,* Volume 21, pp. 155-161.

Dhibar, S., Kar, P. & Khatua, B. B., 2012. Preparation of Highly Exfoliated and Transparent Polycarbonate/Clay Nanocomposites by Melt Blending of Polycarbonate and Poly(methyl methacrylate)/Clay Nanocomposites. *Journal of Applied Polymer Science,* Volume 125, p. E601–E609.

DowAksa İleri Kompozit Malzemeler Sanayi LTD. ŞTİ., 2014. *AC 1101 Chopped Fiber Technical Data Sheet.* [Online] Available at: http://www.dowaksa.com/wp-content/uploads/2015/02/Chopped-fiber-AC-1101.pdf
[Accessed 20 10 2016].

Dowdy, R. H. & Larson, W. E., 1971. Tensile Strength of Montmorillonite as a Function of Saturating Cation and Water Content. *Soil Science Society of America Proceedings,* Volume 35, pp. 1010-1014.

Duan, Y., Sun, Y., Peng, M. & Guo, Z., 2011. Mechanical and Shielding Properties of an as-cast New Pb-B Shielding Composite Materials. *Advanced Materials Research,* Volume 150-151, pp. 56-63.

Ebewele, R. O., 2000. *Polymer Science and Technology.* New York: CRC Press.

Ebnesajjad, S. & Modjarrad, K., 2014. Plastics Used in Medical Devices. In: W. M. Laurence, ed. *Handbook of Polymer Applications in Medicine and Medical Devices.* New York: Elseiver Inc., pp. 21-53.

Edie, D. D., Kennedy, J. M., Cano, R. J. & Ross, R. A., 1993. Evaluating Surface Treatment Effects on lnterfacial Bond Strength Using Dynamic Mechanical Analysis. In: W. W. Stinchcomb & N. E. Ashbaugh, eds. *Composite Materials: Fatigue and Fracture, Fourth Volume.* Philadelphia: ASTM, pp. 419-430.

Elmaghor, F., Zhang, L., Fan, R. & Li, H., 2004. Recycling of polycarbonate by blending with maleic anhydride grafted ABS. *Polymer,* Volume 45, pp. 6719-6724.

Erdem, M., Baykara, O., Doğru, M. & Kuluöztürk, F., 2010. A Novel Shielding Material Prepared from Solid Waste Containing Lead for Gamma Ray. *Radiation Physics and Chemistry,* Volume 79, pp. 917-922.

European Committee for Standardization, 1998. *European Standard EN ISO 294-1:Plastics - Injection moulding of test specimens of thermoplastic materials - Part 1: General principles, and moulding of multipurpose and bar test specimens.* Brussels: European Committee for Standardization.

European Committee for Standardization, 2006. *European Standard EN ISO 7391-2: Plastics - Polycarbonate (PC) moulding and extrusion materials -Part 2: Preparation* *of test specimens and determination of properties.* Brussels: European Committee for Standardization.

European Committee for Standardization, 2008. *European Standard EN ISO 13500: Petroleum and natural gas industries - Drilling fluid materials - Specifications and tests.* Brussels: European Committee for Standardization.

European Committee For Standardization, 2012. *EN ISO 527-1: Plastics-Determination of tensile properties-Part 1: General.* Brussels: European Committee For Standardization.

European Committee for Standardization, 2012. *European Standard EN ISO 527-2: Plastics-Determination of tensile properties-Part 2: Test conditions for moulding and extrusion.* Brussels: European Committee for Standardization.

European Committee for Standardization, 2014. *European Standard EN ISO 20753:Plastics-Test specimens.* Brussels: European Committee for Standardization.

European Organization for Nuclear Research, 2005. *IS-23: Criteria and Standard Test Methods for the Selection of Electric Cables and Wires with Respect to Fire Safety and Radiation Resistance.* [Online] Available at: http://www.pa.msu.edu/hep/atlas/l1calo/reference/l1calo/CERN/cern_electrical_fire_safety_IS23.pdf
[Accessed 04 12 2016].

Feng, J., Hao, J., Du, J. & Yang, R., 2012. Effects of Organoclay Modifiers on the Flammability, Thermal and Mechanical Properties of Polycarbonate Nanocomposites Filled with a Phosphate and Organoclays. *Polymer Degradation and Stability,* Volume 97, pp. 108-117.

Ferreira, Carlas P. R. C.; Araújo, Elmo S.; Aquino, Kátia A. S.; Araújo, Patricia. L. B.; Silveira, Leopoldo B. B. da, 2011. *Radiolytic Stabilization on Optical Properties of Polycarbonate.* Belo Horizonte, 2011 International Nuclear Atlantic Conference.

Galante, A. M. S. & Campos, L. L., 2012. Mapping radiation fields in containers for industrial gamma-irradiation using polycarbonate dosimeters. *Applied Radiation and Isotopes,* Volume 70, pp. 1264-1266.

George, Jayamol; Janardhan, R.; Anand, J. S.; Bhagawan, S. S.; Thomas, Sabu, 1996. Melt Rheological Behaviour of Short Pineapple Fibre Reinforced Low Density Polyethylene Composites. *Polymer*, 37(24), pp. 5421-5431.

Golden, J. H., Hammant, B. L. & Hazell, E. A., 1964. Degradation of Polycarbonates IV. Effect of Molecular Weight on Flexural Properties. *Journal of Polymer Science: Part A,* Volume 2, pp. 4787-4794.

Goldstein, Joseph I.; Lyman, Charles E.; Newbury, Dale E.; Lifshin, Eric; Echlin, Patrick; Sawyer, Linda ; Joy, David C.; Michael, Joseph R., 2003. *Scanning Electron Microscopy and X-Ray Microanalysis.* 3 ed. New York: Kluwer Academic/Plenum Publishers.

Hacioglu, F., Ozdemir, T., Cavdar, S. & Usanmaz, A., 2013. Possible use of EPDM in radioactive waste disposal:Long term low dose rate and short term high dose rate irradiation in aquatic and atmospheric environment. *Radiation Physics and Chemistry,* Volume 83, pp. 122-130.

Hacıoğlu, F., 2010. *Degradation of EPDM via Gamma Irradiation and Possible Use of EPDM in Radioactive Waste Management.* MSc thesis: Middle East Technical Universtiy.

Hacıoğlu, F., Özdemir, T., Kinalır, K. G. & Usanmaz, A., 2016. Possible Use of Bisphenol-a Polycarbonate in Radioactive Waste Embedding. *Progress in Nuclear Energy,* Volume 90, pp. 98-104.

Hao, Xiao; Yonggen, Lu; Mouhua, Wang; Xianying, Qin; Weizhe, Zhao; Jian, Luan, 2013. Effect of Gamma-Irradiation on the Mechanical Properties of Polyacrylonitrile-Based Carbon Fiber. *Carbon,* Volume 52, pp. 427-439.

Hareesh, K.; Deore, Avinash V.; Dahiwale, S. S.; Sanjeev, Ganesh; Kanjilal, D.; Ojha, Sunil; Dhole, N. A.; Kodam, K. M.; Bhoraskar, V. N.; Dhole, S. D., 2015. Antibacterial properties of Au doped polycarbonate synthesized by gamma radiation assisted diffusion method. *Radiation Physics and Chemistry,* Volume 112, pp. 97-103.

Hareesh, K.; Ranganathaiah, C.; Ramya, P.; Bhargavi, R.; Nair, Geetha G.; Sangappa; Sanjeev, Ganesh, 2013. Variation of Lexan Polycarbonate Properties by Electron Beam. *Journal of Applied Polymer Science,* 127(2), pp. 2010-2018.

Hassan, M. M., Aly, R. O., Hasanen, J. A. & El Sayed, E. S. F., 2014. The Effect of Gamma Irradiation on Mechanical, Thermal and Morphological Properties of Glass Fiber Reinforced Polyethylene Waste/Reclaim Rubber Composites. *Journal of Industrial and Engineering Chemistry,* Volume 20, pp. 947-952.

Hill, D. J. T. & Whittaker, A. K., 2004. Radiation Chemistry of Polymers. In: D. J. Brunelle, ed. *Encyclopedia of Polymer Science and Technology.* New York: John Wiley & Sons, pp. 1-55.

Hoffman, E. N. & Skidmore, T. E., 2009. Radiation effects on epoxy/carbon-fiber composite. *Journal of Nuclear Materials,* Volume 392, p. 371–378.

Holmboe, M., Wold, S., Jonsson, M. & Garcia, S. G., 2009. Effects of Gamma-Irradiation on the Stability of Colloidal Na Montmorillonite Dispersions. *Applied Clay Science*, 43(1), pp. 86-90.

IAEA, 1998. *Technical Reports Series No. 390: Interim Storage of Radioactive Waste Packages.* Vienna: International Atomic Energy Agency.

IAEA, 2004. *Management of Waste Containing Tritium and Carbon-14.* Vienna: International Atomic Energy Agency.

IAEA, 2009. *GSG-1: Classification of Radioactive Waste.* Vienna: INTERNATIONAL ATOMIC ENERGY AGENCY.

IAEA, 2010. *Iaea Safety Standards Series No. SSG-8 : Radiation Safety of Gamma, Electron and X Ray Irradiation Facilities.* Vienna: INTERNATIONAL ATOMIC ENERGY AGENCY.

IAEA, 2010. *SGS-08: Radiation Safety of Gamma, Electron and X Ray Irradiation Facilities.* VIENNA: INTERNATIONAL ATOMIC ENERGY AGENCY.

IAEA, n.d.. *Gamma Irradiators for Radiation Processing.* VIENNA: IAEA.

Idaho National Engineering Laboratory, 1996. *Selected Radionuclides Important to Low-Level Radioactive Waste Management DOE/LLW-238,* s.l.: Idaho National Engineering Laboratory.

Idesaki, Akira; Nakamoto, Tatsushi; Yoshida, Makoto; Shimada, Akihiko; Iio, Masami; Sasaki, Kenichi; Sugano, Michinaka; Makida, Yasuhiro; Ogitsu, Toru, 2016.

Development of High Radiation-Resistant Glass Fiber Reinforced Plastics with Cyanate-Based Resin for Superconducting Magnet Systems. *Fusion Engineering and Design,* Volume Article in Press.

Ilie, S. & Setnescu , R., 2009. *Radiation Induced Aging Effects in Polymeric Cable Insulators at CERN.* Geneva: European Organization for Nuclear Research.

International Atomic Energy Agency, 1999. *Stability and Stabilization of Polymers Under Irradiation.* Vienna: International Atomic Energy Agency.

International Organization for Standardization, 2012. *ISO 6721-11: Plastics-Determination of Dynamic Mechanical Properties. Part 11: Glass transition temperature.* Switzerland: International Organization for Standardization.

International Union of Pure and Applied Chemistry, 2014. *Compendium of Chemical Terminology: Gold Book.* 2.3.3 ed. North Carolina: International Union of Pure and Applied Chemistry.

Jatuwan, M., 2004. *Feasibility Study of an Underground Barite Mining at Pands Barite Mining Co., Ltd., Loei Province.* Nakhon Ratchasima: Suranaree University of Technology.

Jawali, N. D., Siddeshwarappa, B. & Lee, J. H., 2007. Polycarbonate/Short Glass Fiber Reinforced Composites – Physico-mechanical Morphological and FEM Analysis. *Journal of REINFORCED PLASTICS AND COMPOSITES,* Volume 0, pp. 1-7.

Kalogiannakis, G., Hemelrijck, D. V. & Assche, G. V., 2004. Measurements of Thermal Properties of Carbon/Epoxy and Glass/Epoxy using Temperature Differential Scanning Calorimetry. *Journal of Composite Materials*, Volume 38, pp. 163-175.

Kinalir, K. G., 2011. *A Study on the Effects of Gamma Radiation on the Properties of Polycarbonate.* MSc thesis: Middle East Technical University.

Kumar, Rajesh; Virk, H. S.; Verma, K. C.; De, Udayan; Saha, A.; Prasad, Rajendra, 2006. Physico-chemical modifications induced in Makrofol-N polycarbonate by swift heavy ions. *Nuclear Instruments and Methods in Physics Research B,* Volume 251, pp. 163-166.

Kwan, K. S., 1998. *The Role of Penetrant Structure in the Transport and Mechanical Properties of a Thermoset Adhesive.* PhD thesis: Virginia Polytechnic Institute and State University.

Kyriacos, D., 2016. Polycarbonates. In: M. Gilbert, ed. *Brydson's Plastics Materials.* Oxford: Elsevier, pp. 457-485.

Legrand, D. G. & Bendler, J. T., 2000. Introduction and Historical Background. In: E. E. Bostick, ed. *Handbook of Polycarbonate Science and Technology.* New York: Marcel Dekker Inc., pp. 1-7.

Ma, Chen-Chi M.; Gu, Jen-Tau; Shauh, Lih-Haur; Yang, Jen-Chang; Fang, Wen-Chen, 1997. Bisphenol-A Polycarbonate/Polydimethylsiloxane Multiblock Copolymers. I. Synthesis and Characterization. *Journal of Applied Polymer Science,* Volume 66, pp. 57-66.

Mahmoud, N. S. & Geleel, A. M., 2012. Improvement of Radioactive Waste Solidification Process Using Modified Bentonite Materials. *Nature and Science,* Volume 10, pp. 158-164.

Mark, H. F. & Kroschwitz, J. I., 2004. Carbbon Fibers. In: J. A. Newell, ed. *Encyclopedia of Polymer Science and Technology.* New York: John Wiley & Sons, pp. 91-112.

Mark, H. F. & Kroschwitz, J. I., 2004. Polycarbonates. In: D. J. BRUNELLE, ed. *Encyclopedia of Polymer Science and Technology.* New York: John Wiley & Sons, pp. 397-426.

Masoumy, E., Kacir, L. & Kardos, J. L., 1983. Effect of Fiber-Aspect Ratio and Orientation on the Stress-Strain Behavior of Aligned, Short-Fiber-Reinforced, Ductile Epoxy. *Polymer Composites,* 4(1), pp. 64-72.

Massey, L. K., 2004. *The Effects of Sterilization Methods on Plastics and Elastomers.* 2 ed. New York: William Andrew.

Menard, K. P., 2008. *Dynamic Mechanical Analysis - A Practical Introduction.* 2 ed. Boca Raton: CRC Press.

Miranda, L. F., Silviera, L. H., Silva, L. G. A. E. & Munhoz, A. H. J., 2010. Irradiation of a Polypropilene-Glass Fiber Composite. *Advances in Science and Technology,* Volume 71, pp. 138-144.

Nikje, M. M. A. & Askarzadeh, M., 2013. Green and Inexpensive Method to Recover Bisphenol-A from Polycarbonate Wastes. *Polímeros,* 23(1), pp. 29-31.

Ojovan, M. I. & Lee, W. E., 2005. *An Introduction to Nuclear Waste Immobilisation.* San Diego: Elsevier.

Onishi, Yasuhiko; Shiga, Tetsuya; Ohkawa, Yoshinao; Katoh, Haruzou; Nagasawa, Kiyoshi; Okada, Tsuneyoshi; Saimen, Kenji; Itano, Fumihiro; Murano, Yoshihiro; Tsujita, Yoshiharu; Yagi, Toshiaki; Morita, Yousuke; Seguchi, Tadao, 2004. Study on Polymer Materials for Development of the Super 100MGy-Radiation Resistant Motor. *Polymer Journal*, 36(8), pp. 617-622.

Orden, M.U. de la; Pascual, D.; Antelo, A. ; Arranz-Andrés, J.; Lorenzo, V.; Urreaga, J. Martínez, 2013. Polymer Degradation During The Melt Processing of Clay Reinforced Polycarbonate Nanocomposites. *Polymer Degradation and Stability,* Volume 98, pp. 1110-1117.

Oto, Berna; Gür, Aycan; Kaçal, Mustafa Recep; Doğan, Bekir; Arasoğlu, Ali, 2013. Photon Attenuation Properties of Some Concretes Containing Barite and Colemanite In Different Rates. *Annals of Nuclear Energy,* Volume 51, pp. 120-124.

Otterstedt, J.-E. & Brandreth, D. A., 1998. *Small Particles Technology.* 1 ed. New York: Plenum Press.

Ozdemir, T., 2006. *Effect of Ionizing Radiation on Different Polymers and Possible Use of Polymers In Radioactive (Nuclear) Waste Management.* Ankara: Middle East Technical University.

Ozdemir, T., 2014. Monte Carlo simulations of radioactive waste embedded into EPDM and effect of lead filler. *Radiation Physics and Chemistry,* Volume 98, pp. 150-154.

Ozdemir, T. & Usanmaz, A., 2007. Degradation of poly(carbonate urethane) by gamma irradiation. *Radiation Physics and Chemistry,* Volume 76, p. 1069–1074.

Ozdemir, T. & Usanmaz, A., 2008. Degradation of poly(bisphenol-a-epichlorohydrin) by gamma irradiation. *Radiation Physics and Chemistry,* Volume 77, pp. 779-805.

Ozdemir, T. & Usanmaz, A., 2009. Monte Carlo simulations of radioactive waste embedded into polymer. *Radiation Physics and Chemistry,* Volume 78, pp. 800-805.

Ozdemir, T. & Usanmaz, A., 2009. Use of poly(methyl methacrylate) in radioactive waste management:I. Radiation stability and degradation. *Progress in Nuclear Energy,* Volume 51, pp. 240-245.

Ozdemir, T. & Usanmaz, A., 2009. Use of poly(methyl methacrylate) in radioactive waste management:II. Monte Carlo simulations. *Progress in Nuclear Energy,* Volume 51, pp. 845-848.

Pashaei, S., Siddaramaiah, Avval, M. M. & Syed, A. A., 2011. Thermal Degradation Kinetics of Nylon6/GF/Crysnano Nanoclay Nanocomposites by TGA. *CI&CEQ,* 17(2), pp. 141-151.

Perkin Elmer Corporation, 2013. *Dynamic Mechanical Analysis (DMA) A Beginner's Guide.* [Online]
Available at: http://www.perkinelmer.com/CMSResources/Images/44-74546GDE_IntroductionToDMA.pdf
[Accessed 10 31 2016].

Perkin Elmer Corporation, 2015. *A Beginner's Guide Thermogravimetric Analysis (TGA).* [Online]
Available at: https://www.perkinelmer.com/lab-solutions/resources/docs/FAQ_Beginners-Guide-to-Thermogravimetric-Analysis_009380C_01.pdf
[Accessed 07 11 2016].

Phua, Y. J. & Ishak, Z. A. M., 2010. Injection Molded Short Glass and Carbon Fibers Reinforced Polycarbonate Hybrid Composites: Effects of Fiber Loading. *Journal of REINFORCED PLASTICS AND COMPOSITES,* 29(17), pp. 2592-2603.

Rabek, J. F., 1995. *Polymer Photodegradation: Mechanisms and experimental methods.* 1 ed. London: Chapman & Hall.

Rabinovich, F. N. & Lemysh, L. L., 1997. Use of Composition Materials Based on Dispersely Reinforced Concrete in Containers and Storehouses for Radioactive Waste. *Atomic Energy,* 82(2), pp. 89-91.

Reichmanis, E., Frank, C. W., O'Donnell, J. H. & Hill, D. J. T., 1993. Radiation Effects on Polymeric Materials. In: E. Reichmanis, C. W. Frank & J. H. O'Donnell, eds. *Irradiation of Polymeric Materials.* Washington: American Chemical Society, pp. 1-8.

Rosi, L.; Bartoli, M.; Undri, A.; Frediani, M.; Frediani, P., 2015. Synthesis of dianols or BPA through catalytic hydrolyisis/glycolysis of waste polycarbonates using a microwave heating. *Journal of Molecular Catalysis A: Chemical,* Volume 408, pp. 278-286.

Ruland, W., 1990. Carbon Fibers. *Advanced Materials,* Volume 11, pp. 528-536.

SABIC Chemical Manufacturing Company, 2016. *LEXAN ™ Resin LS2 Property.* [Online]
Available at: https://www.sabic-ip.com/gepapp/eng/weather/weatherhtml?sltRegionList=1002002001&sltPrd=1002003051&sltGrd=1002012052&sltUnit=0&sltModule=DATASHEETS&sltVersion=Internet&sltType=Online
[Accessed 18 10 2016].

Sakr, K., Sayed, M. S. & Hafez, M. B., 2003. Immobilization of radioactive waste in mixture of cement, clay and polymer. *Journal of Radioanalytical and Nuclear Chemistry,* 256(2), p. 179–184.

Sato, N., Kurauchi, T., Sato, S. & Kamigaito, O., 1991. Microfailure Behaviour of Randomly Dispersed Short Fibre Reinforced Thermoplastic Composites Obtained by Direct SEM Observation. *Journal of Material Science,* Volume 26, pp. 3891-3898.

Savas, L. A., Tayfun, U. & Dogan, M., 2016. The Use of Polyethylene Copolymers as Compatibilizers in Carbon Fiber Reinforced High Density Polyethylene Composites. *Composites Part B,* Volume 99, pp. 188-195.

Seguchi , T. & Morita, Y., 1999. Radiation Resistance of Plastics and Elastmers. In: J. BRANDRUP, E. H. IMMERGUT & E. A. GRULKE, eds. *Polymer Handbook VI.* New York: John Wiley & Sons, Inc., p. 583–589.

Sellin, P. & Leupin, O. X., 2013. The Use of Clay as an Engıneered Barrier In Radioactıve Waste Management-A Revıew. *Clays and Clay Minerals,* 61(6), pp. 477-498.

Sepe, M. P., 2000. The Usefulness of HDT and a Better Alternative to Describe the Temperature Dependence of Modulus. In: J. S. Peraro, ed. *Limitations of Test Methods for Plastics.* West Conshohocken: ASTM, pp. 44-54.

Seppälä, J. K. & Kulmala, J. A. J., 2011. Increased Beam Attenuation and Surface Dose by Different Couch Inserts of Treatment Tables Used in Megavoltage Radiotherapy. *Journal of Applied Clinical Medical Physics*, 12(4).

Severe, G., Hsieh, A. J. & Koene, B. E., 2000. *Effect of Layered Silicates on Thermal Characteristics of Polycarbonate Nanocomposites.* Orlando, Antec.

Shaaban, I. & Assi, N., 2011. Measurement of the Leaching Rate of Radionuclide Cesium (134) from the Solidified Radioactive Sources In Portland Cement Mixed with Microsilica and Barite Matrixes. *Journal of Nuclear Materials,* Volume 415, pp. 132-137.

Sharma, Raghunandan; Kar, Kamal K.; Das, Malay K.; Gupta, Gaurav K.; Kumar, Sudhir, 2016. Short Carbon Fiber-Reinforced Polycarbonate Composites. In: K. K. Kar, ed. *Composite Materials Processing, Applications, Characterizations.* Berlin: Springer, pp. 199-223.

Sharma, S. D., Sowntharya, L. & Kar, K. K., 2016. Polymer-Based Composite Structures: Processing and Applications. In: K. K. Kar, ed. *Composite Materials Processing, Applications, Characterizations.* Berlin: Springer, pp. 1-37.

Shokrieh, M. M., Kefayati, A. R. & Chitsazzadeh, M., 2012. Fabrication and Mechanical Properties of Clay/epoxy Nanocomposite and Its Polymer Concrete. *Materials and Design,* Volume 40, pp. 443-452.

Silverstein, R. M., Webster, F. X. & Kiemle, D. J., 2005. *Spectrometric Identification of Organic Compounds.* 7 ed. New Jersey: John Wiley & Sons Inc..

Singh, S. & Prasher, S., 2005. The optical, chemical and spectral response of gamma-irradiated Lexan polymeric track recorder. *Radiation Measurements,* Volume 40, pp. 50-54.

Sinha, D.; Sahoo, K. L.; Sinha, U. B.; Swu, T.; Chemseddine, A.; Fink, D., 2004. Gamma-Induced Modifications of Polycarbonate Polymer. *Radiation Effects & Defects in Solids,* Volume 159, pp. 587-595.

Skidmore, T. & Fondeur, F., 2013. *SRNL-STI-2013-00224: The Use of Polymers in Radioactive Waste Processing System,* Aiken: Savannah River Nuclear Solutions.

Suin, S. & Khatua, B. B., 2012. Exfoliated and Optically Transparent Polycarbonate/Clay Nanocomposites Using Phosphonium Modified Organoclay: Preparation and Characterizations. *Industrial & Engineering Chemistry Research,* Volume 51, p. 15096−15108.

Sui, Xianhang; Xu, Zhiwei; Hu, Chuansheng; Chen, Lei; Liu, Liangsen; Kuang, Liyun; Ma, Meijun; Zhao, Lihuan; Li, Jing; Deng, Hui, 2016. Microstructure Evolution in Gamma-Irradiated Carbon Fibers Revealed by a Hierarchical Model and Raman Spectra from Fiber Section. *Composites Science and Technology,* Volume 130, pp. 46-52.

Şişecam Cam Elyaf Sanayii A.Ş., 2016. *Şişecam Chopped Strand Product Specification.* [Online]
Available at: http://www.sisecamkimyasallar.com/sites/catalogs/en/Documents/glass-fiber-product-spec/Chopped%20Strands/CAMELYAF_PH2.pdf
[Accessed 20 10 2016].

TA Instruments Corporation, 2016. *TA Instruments Dynamic Mechanical Analyzer.* [Online]
Available at: http://www.tainstruments.com/pdf/literature/TA284.pdf
[Accessed 31 10 2016].

Tamboli, S. M., Mhaske, S. T. & Kale, D. D., 2004. Crosslinked Polyethylene. *Indian Journal of Chemical Technology,* Volume 11, pp. 853-864.

Tayel, A., Zaki, M. F., El Basaty, A. B. & Hegazy, T. M., 2015. Modifications induced by gamma irradiation to Makrofol polymer nuclear track detector. *Journal of Advanced Research,* Volume 6, pp. 219-224.

Turkish Standards Institution, 1992. *TS 10252: Bentonite - For Use in Drug and Cosmetic Production.* Ankara: Turkish Standards Institution.

Turkish Standards Institution, 1993. *TS 11136 : Bentonite for Use in Ceramics.* Ankara: Turkish Standards Institution.

Turkish Standards Institution, 1994. *TS 11326 : Bentonite for Use in Detergents.* Ankara: Turkish Standards Institution.

Turkish Standards Institution, 1994. *TS 11441: Bentonite for Use in Paper İndustry.* Ankara: Turkish Standards Institution.

Turkish Standards Institution, 1994. *TS 11442 : Bentonite for Use in Rubber Industry.* Ankara: Turkish Standards Institution.

Turkish Standards Institution, 1996. *TS 5360: Fundry Bentonite.* Ankara: Turkish Standards Institution.

Turkish Standards Institution, 2001. *TS EN ISO 3262-2: Extenders for paints - Specifications and method sof test - Part 2: Baryte (natural barium sulfat).* Ankara: Turkish Standards Institution.

Turkish Standards Institution, 2004. *TS EN 60544-4: Electrical Insulating Materials - Determination of the Effects of Ionizing Radiation - Part 4: Classification System for Service in Radiation Environments.* Ankara: Turkish Standards Institution.

Turkish Standards Institution, 2006. *TS EN ISO 868: Plastics and Ebonite - Determination of Indentation Hardness by Means of a Durometer (Shore Hardness).* Ankara: Turkish Standards Institution.

Turkish Standards Institution, 2010. *TS EN 13754 : Products used for treatment of water intended for human consumption - Bentonite.* Ankara: Turkish Standards Institution.

Turkish Standards Institution, 2010. *TS EN ISO 13500 : Petroleum and natural gas industries - Drilling fluid materials - Specifications and tests.* Ankara: Turkish Standards Institution.

Turkish Standards Institution, 2011. *TS EN ISO 6721-1: Plastics-Determination of Dynamic Mechanical Properties-Part 1: General Principles.* Ankara: Turkish Standards Institution.

Turkish Standards Institution, 2012. *TS EN ISO 1133-1: Plastics - Determination of the Melt Mass-Flow Rate (MFR) and Melt Volume-Flow Rate (MVR) of Thermoplastics-Part 1: Standard Method.* Ankara: Turkish Standards Institution.

Turkish Standards Institution, 2013. *TS 5632: Barite - for Glass Making.* Ankara: Turkish Standards Institution.

Turkish Standards Institution, 2013. *TS EN 12912: Products Used for Treatment of Water İntended for Human Consumption - Barite.* Ankara: Turkish Standards Institution.

Turkish Standards Institution, 2013. *TS EN 60544-2: Electrical Insulating Materials - Determination of the Effects of Ionizing Radiation on Insulating Materials - Part 2: Procedures for Irradiation and Test.* Ankara: Turkish Standards Institution.

Turkish Standards Institution, 2013. *TS EN ISO 11963 Plastics-Polycarbonate Sheets-Types, Dimensions and Characteristics.* Ankara: Turkish Standards Institution.

Turkish Standards Institution, 2014. *TS EN ISO 11358-1: Plastics-Thermogravimetry (TG) of Polymers - Part 1: General Principles.* Ankara: Turkish Standards Institution.

Turkish Standards Institution, 2015. *Sterilization of Health Care Products - Radiation - Part 2: Establishing the Sterilization Dose.* Ankara: Turkish Standards Institution.

Uawongsuwan, P. & Ichikawa, H., 2014. *DIRECT FIBER FEEDING INJECTION MOLDING OF CARBON FIBER REINFORCED POLYCARBONATE COMPOSITES.* [Online] Available at: http://www.speautomotive.com/SPEA_CD/SPEA2014/pdf/ET/ET3.pdf [Accessed 05 09 2016].

Wallenberger, F. T. & Bingham, P. A., 2010. Commercial and Experimental Glass Fibers. In: F. T. Wallenberger, ed. *Fiberglass and Glass Technology Energy-Friendly Compositions and Applications.* New York: Springer, pp. 3-84.

Wallenberger, F. T., Watson, J. C. & Li, H., 2001. Glass Fibers. In: D. B. Miracle & S. L. Donaldson, eds. *ASM Handbook Volume 21 Composites.* Ohio: ASM International, pp. 27-34.

Wang, Peng; Tang, Xiaobin; Chai, Hao; Chen, Da; Qiu, Yunlong, 2015. Design, fabrication, and properties of a continuous carbon-fiber reinforced Sm2O3/polyimide gamma ray/neutron shielding material. *Fusion Engineering and Design,* Volume 101, pp. 218-225.

Weber, R. P., Vecchio, K. S. & Suarez, J. C. M., 2010. Dynamic behavior of gamma-irradiated polycarbonate. *Revista Matéria,* Volume 15, pp. 218-224.

Wee, J.-W., Park, S.-Y. & Choi, B.-H., 2015. Observation and Understanding of Scratch Behaviors of Glass Fiber Reinforced Polycarbonate Plates with Various Packing Pressures During the Injection Molding Process. *Tribology International,* Volume 90, pp. 491-501.

Wilski, H., 1987. The Radiation Induced Degradation of Polymers. *Radiation Physics and Chemistry,* 29(1), pp. 1-14.

Xiao, J., Wang, S., Lu, P. & Hu, Y., 2013. Effect of Organically Modified Montmorillonite on Thermal Degradation Mechanism of Polycarbonate Nanocomposites. *Procedia Engineering,* Volume 62, pp. 791-796.

Xie, Wei; Gao, Zongming; Pan, Wei-Ping; Hunter, Doug; Singh, Anant; Vaia, Richard, 2001. Thermal Degradation Chemistry of Alkyl Quaternary Ammonium Montmorillonite. *Chemistry of Materials,* Volume 13, pp. 2979-2990.

Xplore Instruments, n.d.. *Xplore® MC 15 15 ml Micro Compounder, Brochure.* Geleen: Xplore Instruments.

Xu, Zhiwei; Huang, Yudong; Min, Chunying; Chen, Lei; Chen, Li, 2010. Effect of Gamma-Ray Radiation on the Polyacrylonitrile Based Carbon Fibers. *Radiation Physics and Chemistry,* Volume 79, pp. 839-843.

Yoon, P. J., Hunter, D. L. & Paul, D. R., 2003. Polycarbonate Nanocomposites. Part 1. Effect of Organoclay Structure on Morphology and Properties. *Polymer,* Volume 44, p. 5323–5339.

Yoon, P. J., Hunter, D. L. & Paul, D. R., 2003. Polycarbonate Nanocomposites: Part 2. Degradation and Color Formation. *Polymer,* Volume 44, pp. 5341-5354.

Yuan, J. J., Kennedy, J. M. & Edie, D. D., 1996. Modeling the Dynamic Response of the Fiber/Matrix Interphase in Continuous Fiber Composite Materials. In: C. J. Spragg & L. T. Drzal, eds. *Fiber, Matrix, and Interface Properties.* West Conshohocken: ASTM, pp. 67-84.

Zhao, Weizhe; Lu, Yonggen; Wang, Jing; Chen, Qiang; Zhou, Liangxiao; Jiang, Junqi; Chen, Li, 2016. Improving crosslinking of stabilized polyacrylonitrile fibers and mechanical properties of carbon fibers by irradiating with gamma-ray. *Polymer Degradation and Stability,* Volume 133, pp. 16-26.

Zimmerman, K. A., Langford, S. C., Dickinson, J. T. & Dion, R. P., 1993. Electron and Photon Emission Accompanying Deformation and Fracture of Polycarbonate. *Journal of Polymer Science: Part B: Polymer Physics,* Volume 31, pp. 1229-1243.

Zumdahl, S. S. & Zumdahl, S. A., 2010. *Chemistry.* 8 ed. Belmont: Brooks Cole.

APPENDIX A

EXAMPLES OF THE STRESS VS STRAIN CURVES OF THE NEAT AND FILLED POLYCARBONATE SAMPLES

Examples of the stress vs strain curves of the neat and the filled polycarbonate samples were shown below.

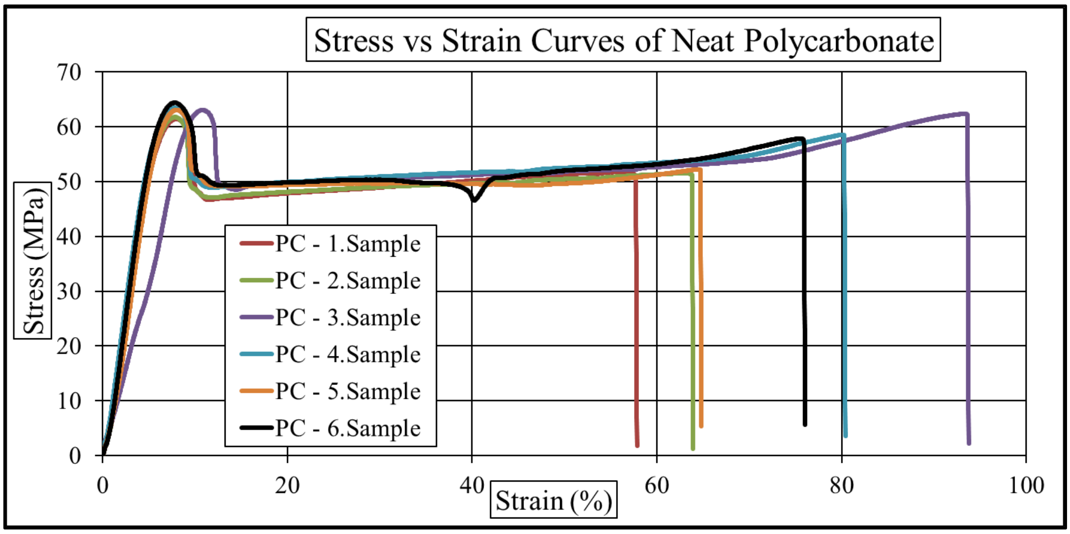

Figure 99 Stress vs Strain Curves of Neat Polycarbonate

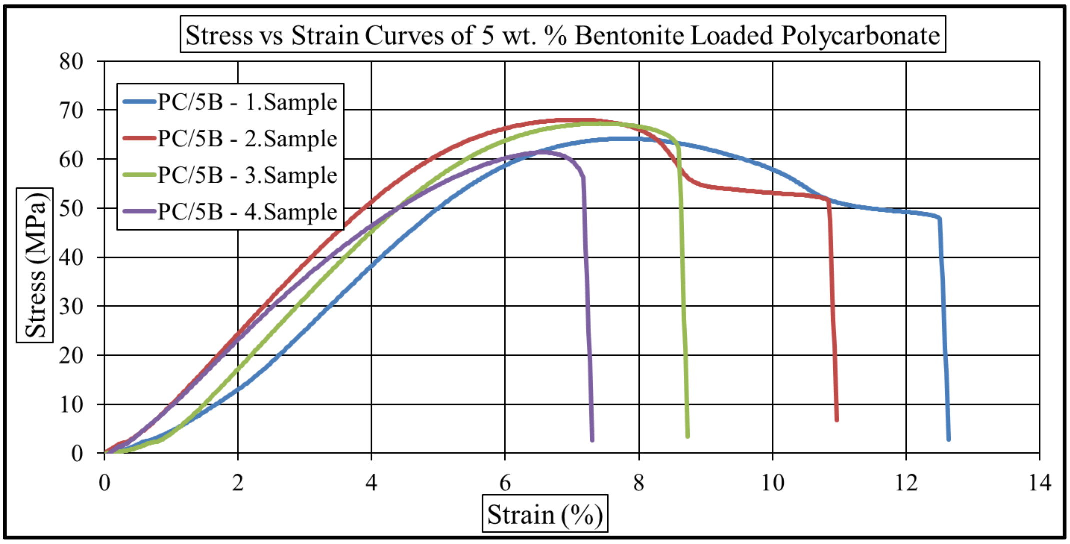

Figure 100 Stress vs Strain Curves of 5 wt. % Bentonite Filled Polycarbonate

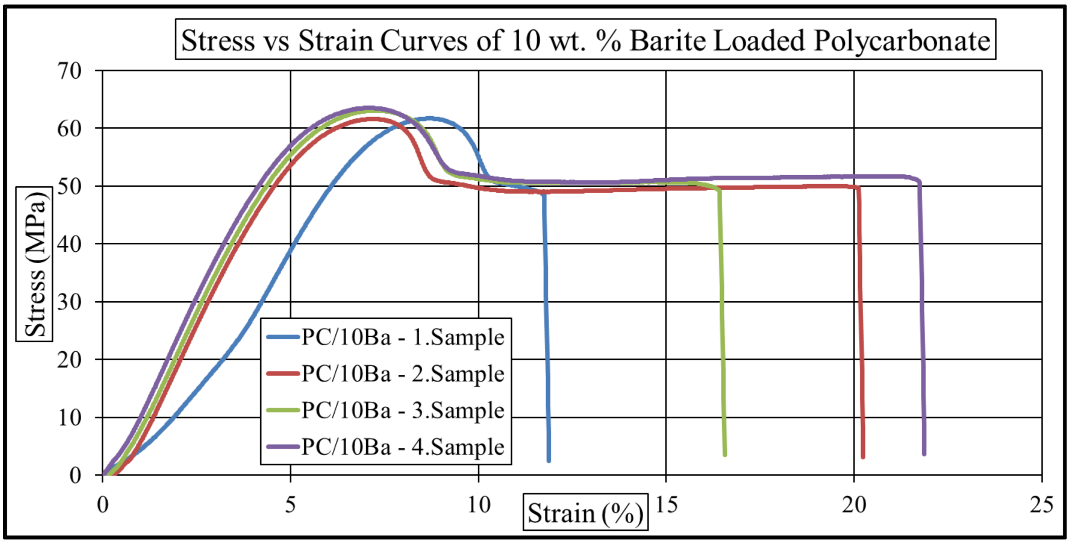

Figure 101 Stress vs Strain Curves of 10 wt. % Barite Filled Polycarbonate

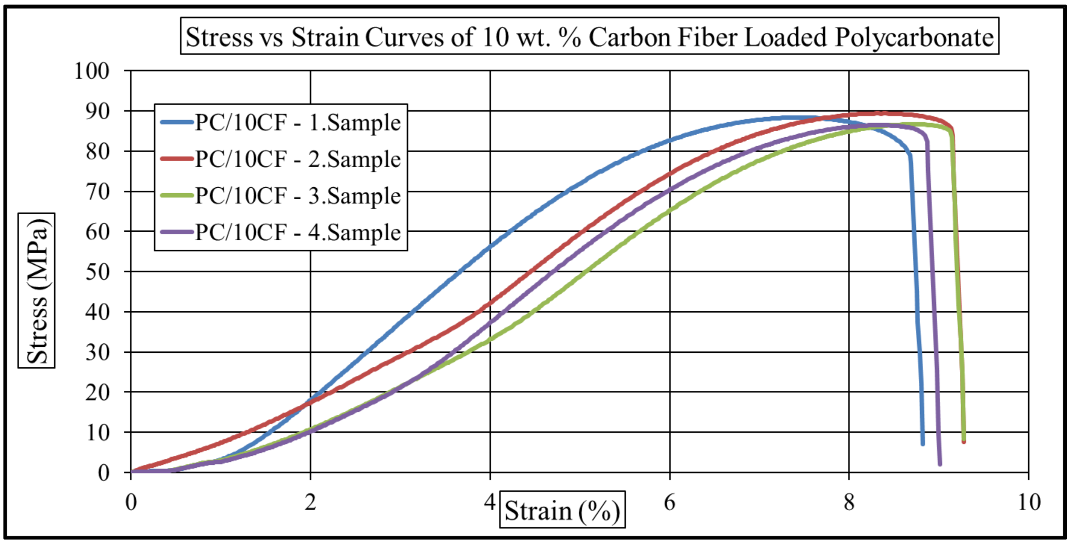

Figure 102 Stress vs Strain Curves of 10 wt. % Carbon Fiber Filled Polycarbonate kGy

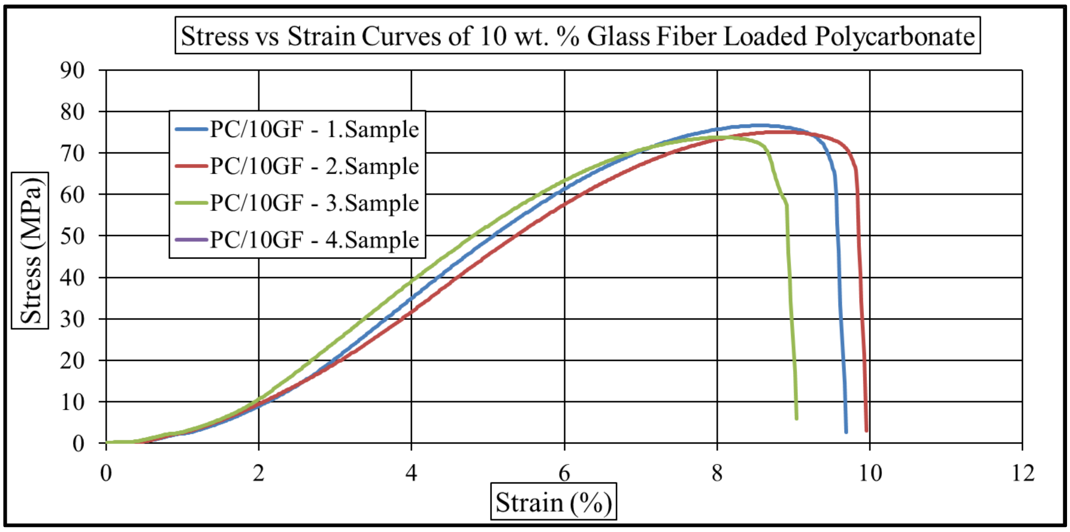

Figure 103 Stress vs Strain Curves of 10 wt. % Glass Fiber Filled Polycarbonate

APPENDIX B

PARTICLE SIZE DISTRIBUTION OF BENTONITE AND BARITE

Output for particle size distribution of bentonite and barite, which were used in this study, were shown below.

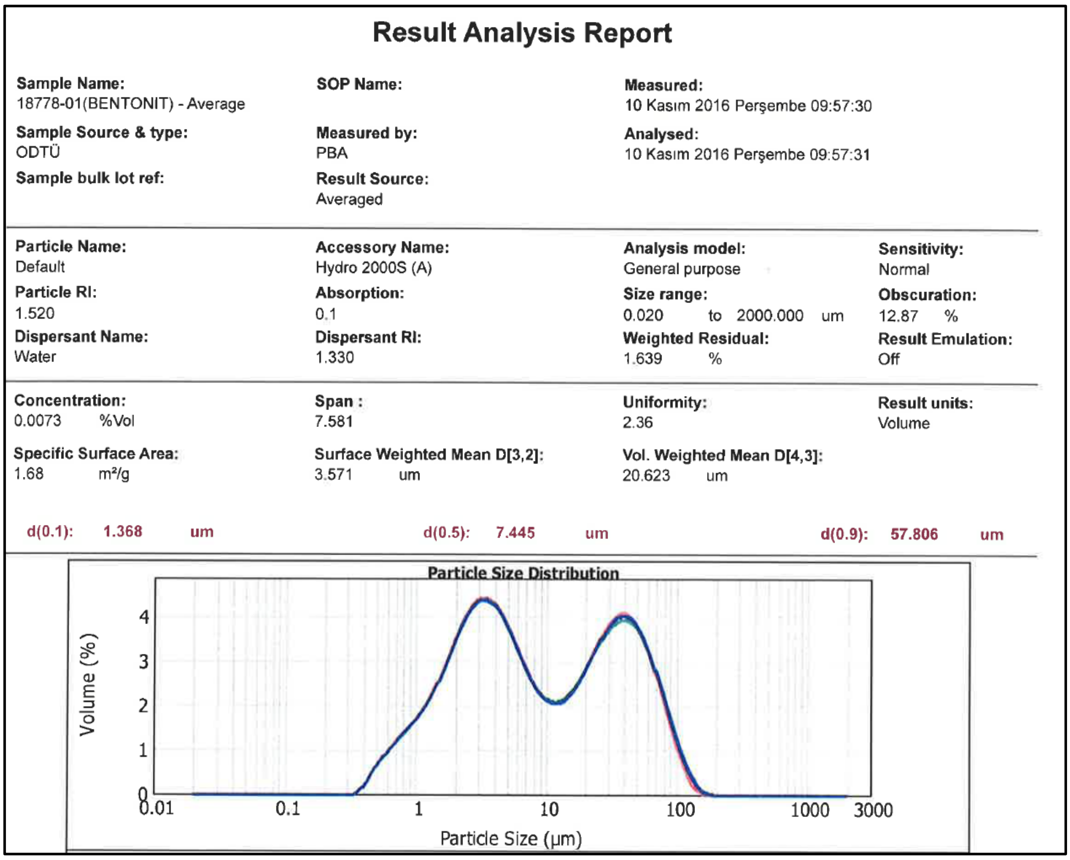

Result Analysis Report

Sample Name:
18778-01(BENTONIT) - Average

Sample Source & type:
ODTÜ

Sample bulk lot ref:

SOP Name:

Measured by:
PBA

Result Source:
Averaged

Measured:
10 Kasım 2016 Perşembe 09:57:30

Analysed:
10 Kasım 2016 Perşembe 09:57:31

Particle Name:
Default

Particle RI:
1.520

Dispersant Name:
Water

Accessory Name:
Hydro 2000S (A)

Absorption:
0.1

Dispersant RI:
1.330

Analysis model:
General purpose

Size range:
0.020 to 2000.000 um

Weighted Residual:
1.639 %

Sensitivity:
Normal

Obscuration:
12.87 %

Result Emulation:
Off

Concentration:
0.0073 %Vol

Specific Surface Area:
1.68 m²/g

Span :
7.581

Surface Weighted Mean D[3,2]:
3.571 um

Uniformity:
2.36

Vol. Weighted Mean D[4,3]:
20.623 um

Result units:
Volume

d(0.1): **1.368** **um**　**d(0.5):** **7.445** **um**　**d(0.9):** **57.806** **um**

Figure 104 Particle Size Distribution of Bentonite

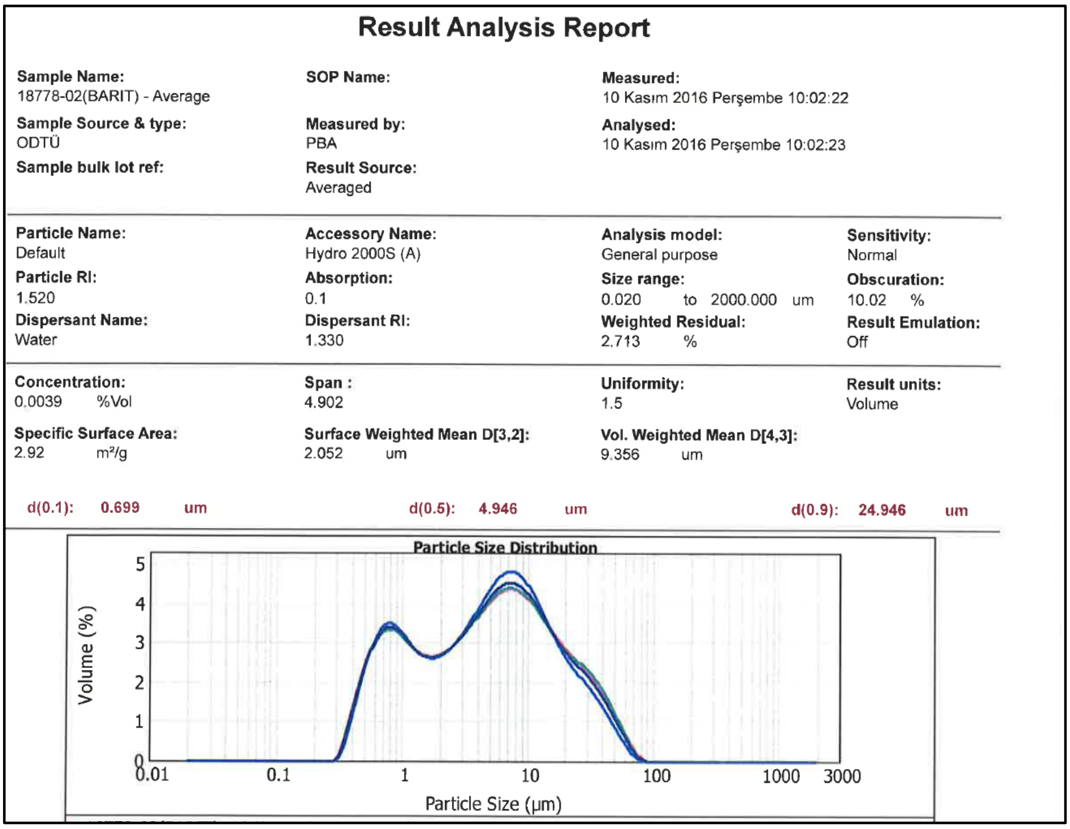

Result Analysis Report

Sample Name: 18778-02(BARIT) - Average	**SOP Name:**	**Measured:** 10 Kasım 2016 Perşembe 10:02:22	
Sample Source & type: ODTÜ	**Measured by:** PBA	**Analysed:** 10 Kasım 2016 Perşembe 10:02:23	
Sample bulk lot ref:	**Result Source:** Averaged		
Particle Name: Default	**Accessory Name:** Hydro 2000S (A)	**Analysis model:** General purpose	**Sensitivity:** Normal
Particle RI: 1.520	**Absorption:** 0.1	**Size range:** 0.020 to 2000.000 um	**Obscuration:** 10.02 %
Dispersant Name: Water	**Dispersant RI:** 1.330	**Weighted Residual:** 2.713 %	**Result Emulation:** Off
Concentration: 0.0039 %Vol	**Span :** 4.902	**Uniformity:** 1.5	**Result units:** Volume
Specific Surface Area: 2.92 m²/g	**Surface Weighted Mean D[3,2]:** 2.052 um	**Vol. Weighted Mean D[4,3]:** 9.356 um	

d(0.1): 0.699 um **d(0.5): 4.946 um** **d(0.9): 24.946 um**

Particle Size Distribution

Figure 105 Particle Size Distribution of Barite

APPENDIX C

EDX ANALYSIS

EDX outputs for qualitative analysis of bentonite, barite, carbon fiber and glass fiber in composites were shown below.

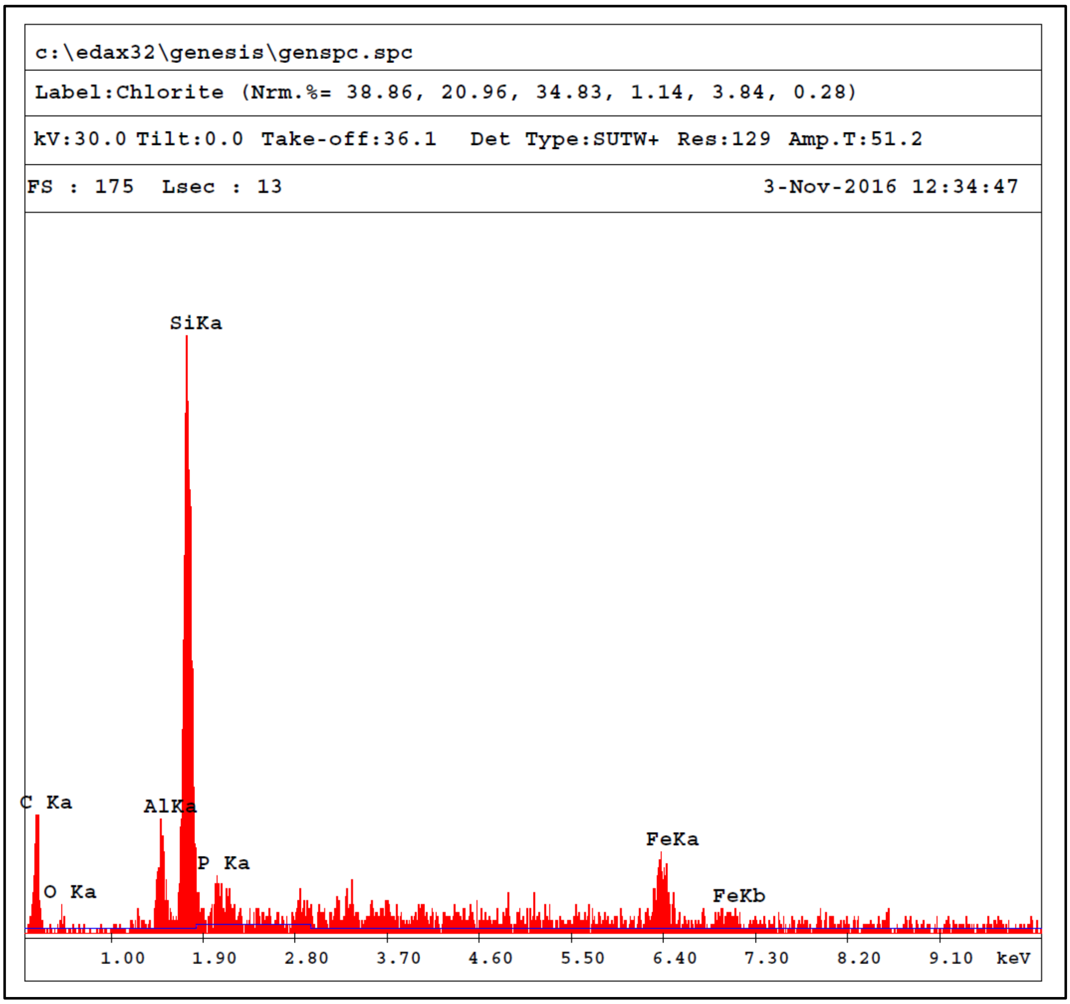

```
c:\edax32\genesis\genspc.spc
Label:Chlorite (Nrm.%= 38.86, 20.96, 34.83, 1.14, 3.84, 0.28)
kV:30.0 Tilt:0.0 Take-off:36.1  Det Type:SUTW+ Res:129 Amp.T:51.2
FS : 175  Lsec : 13                              3-Nov-2016 12:34:47
```

Figure 106 EDX Analysis for 5 wt. % Bentonite Filled Polycarbonate

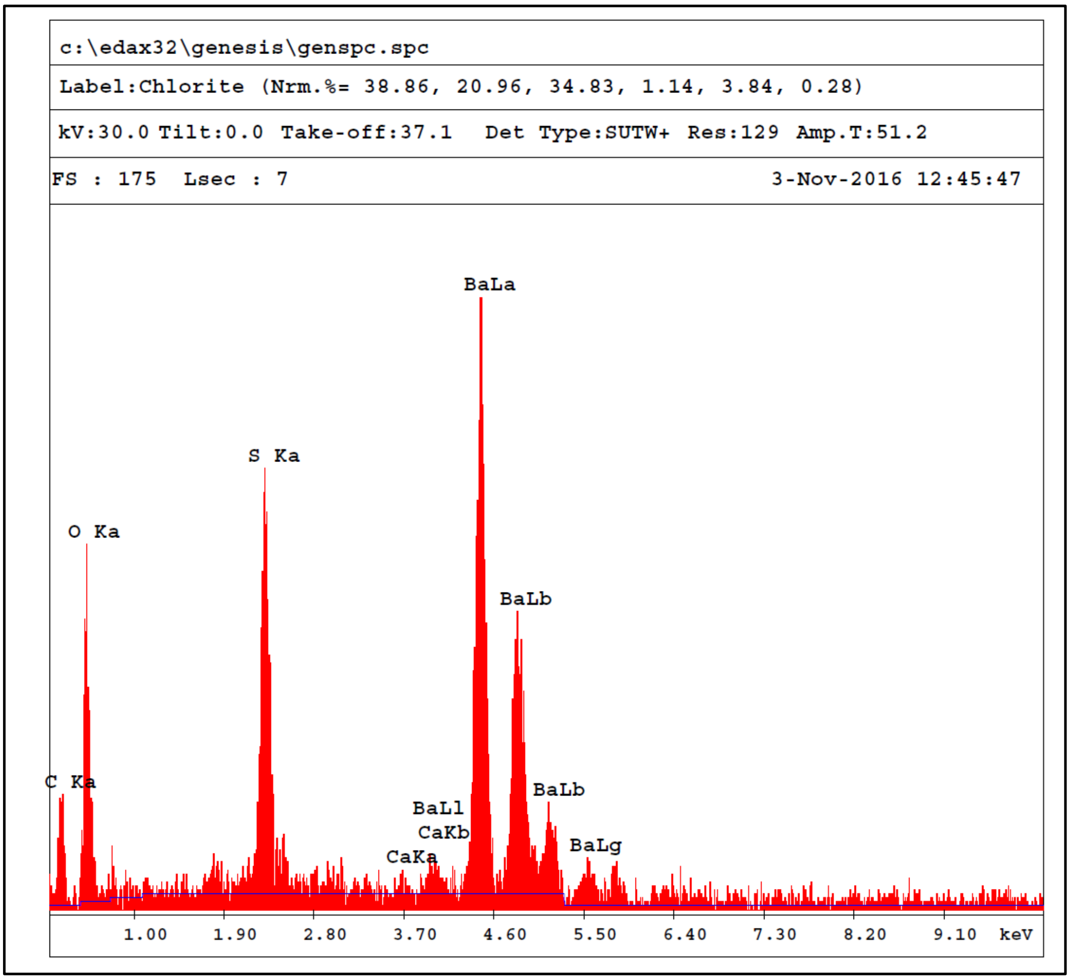

Figure 107 EDX Analysis for 10 wt. % Barite Filled Polycarbonate

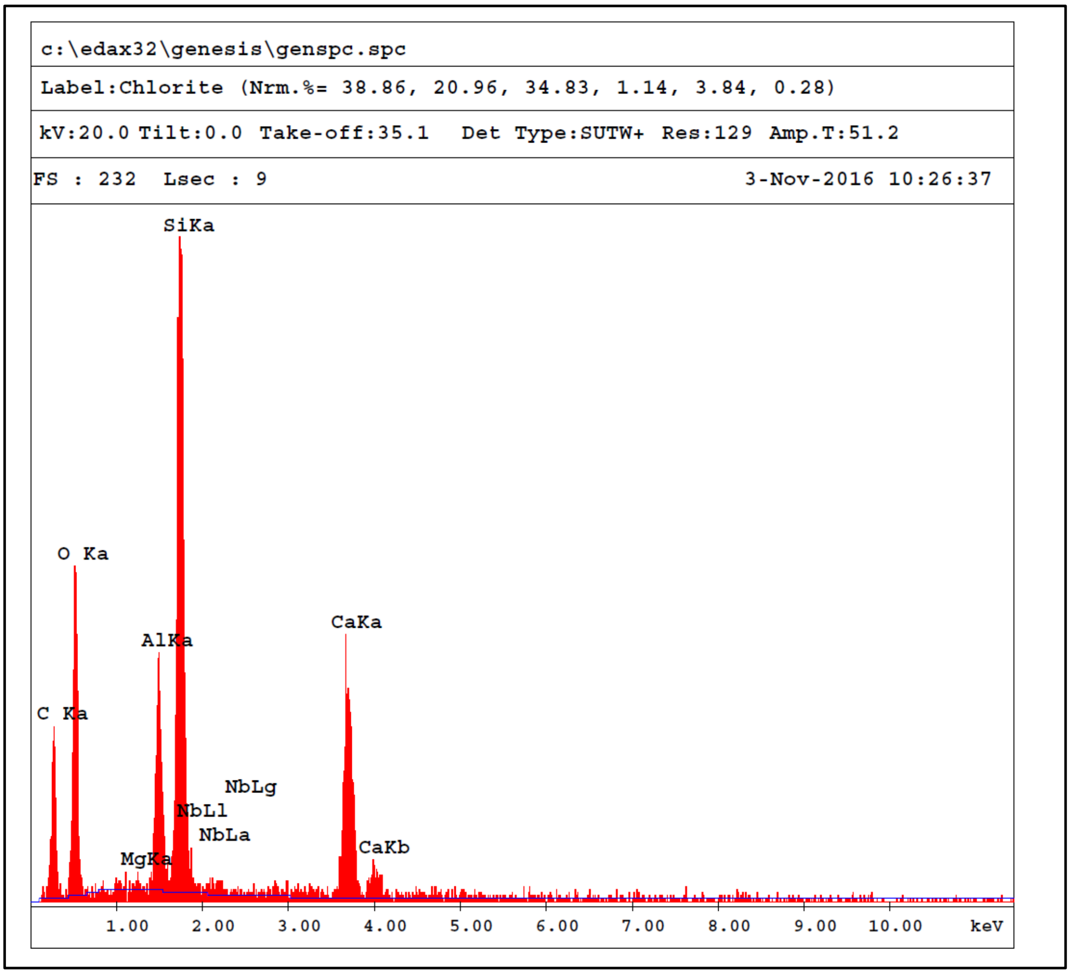

```
c:\edax32\genesis\genspc.spc
Label:Chlorite (Nrm.%= 38.86, 20.96, 34.83, 1.14, 3.84, 0.28)
kV:20.0 Tilt:0.0 Take-off:35.1  Det Type:SUTW+ Res:129 Amp.T:51.2
FS : 232  Lsec : 9                              3-Nov-2016 10:26:37
```

Figure 108 EDX Analysis for 10 wt. % Glass Fiber Filled Polycarbonate

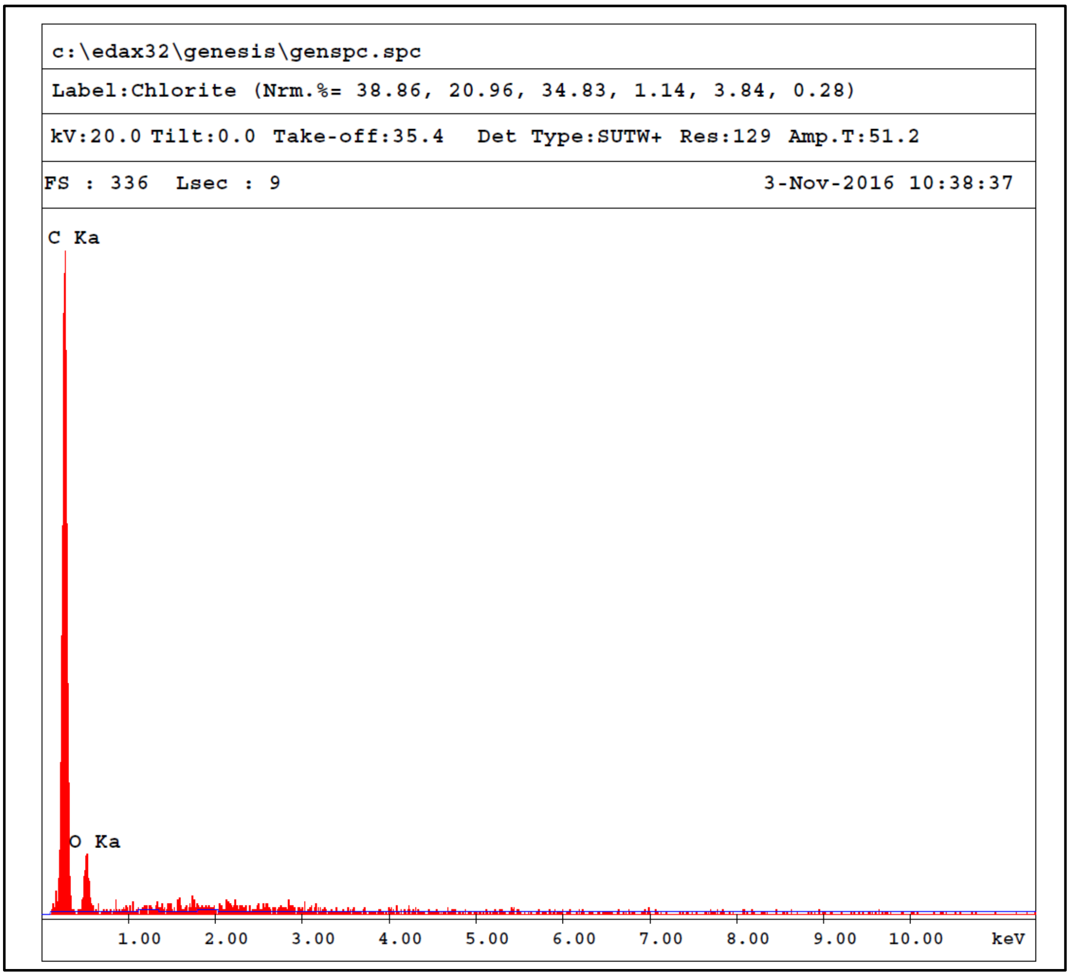

Figure 109 EDX Analysis for 10 wt. % Carbon Fiber Filled Polycarbonate

APPENDIX D

STRUCTURE OF BISPHENOL-A POLYCARBONATE

Structure of bisphenol-a polycarbonate, which were used in this study were shown below.

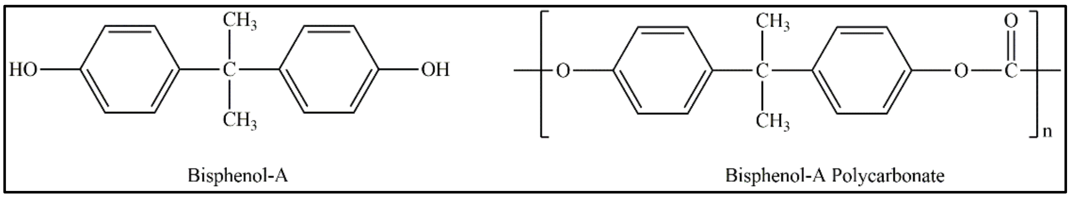

Figure 110 Structures of Bisphenol A and Polycarbonate (Kyriacos, 2016)

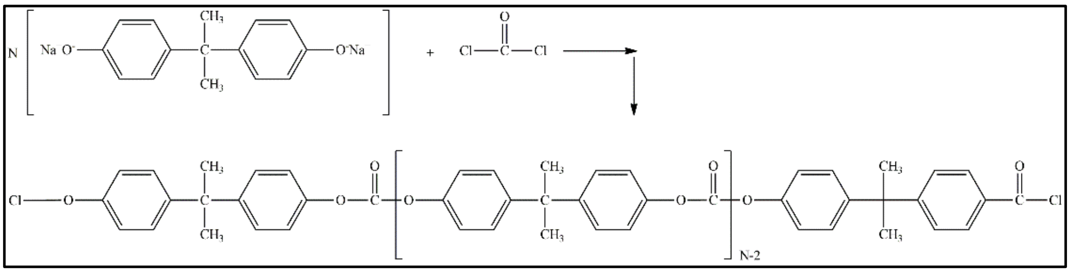

Figure 111 Interfacial Polymerization between Disodium Salt of Bisphenol A and Phosgene (Kyriacos, 2016)

APPENDIX E

PHOTOGRAPHS OF NEAT AND 10 WT. % GLASS FIBER LOADED POLYCARBONATES AFTER IRRADIATION

Photographs of the neat and 10 wt. % glass fiber loaded polycarbonates after irradiation period were shown below.

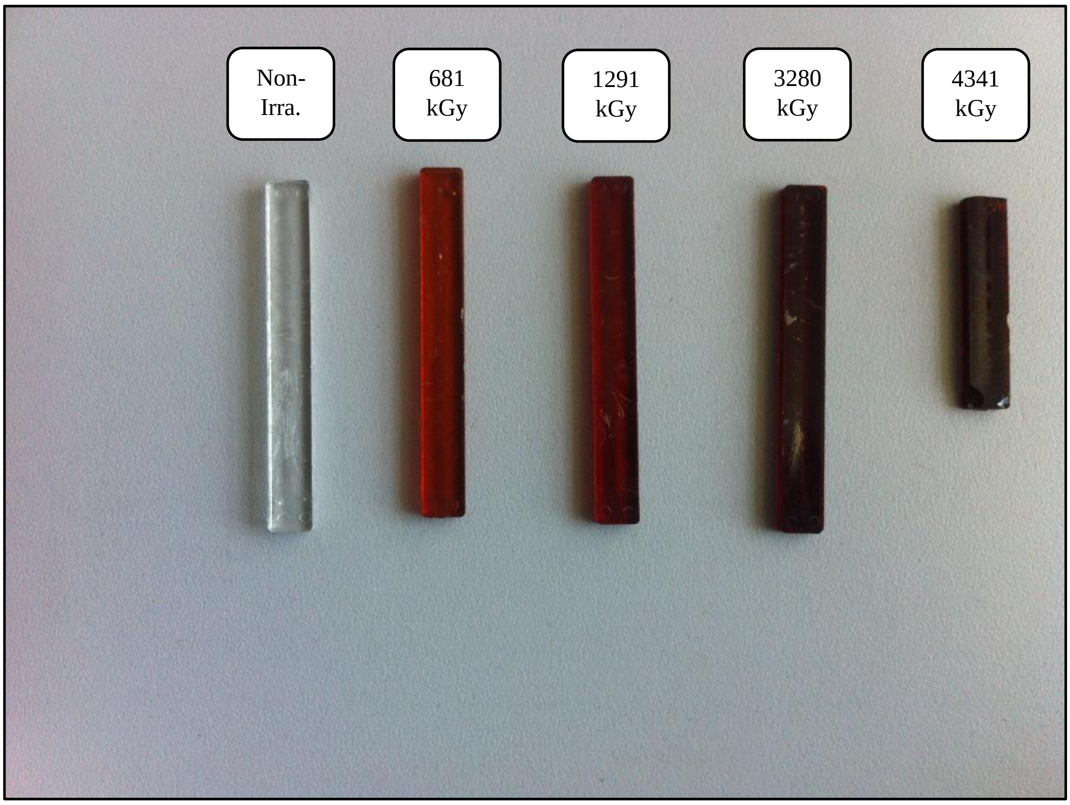

Figure 112 Photograph of the Neat Polycarbonates which were irradiated by 681, 1291, 3280 and 4341 kGy

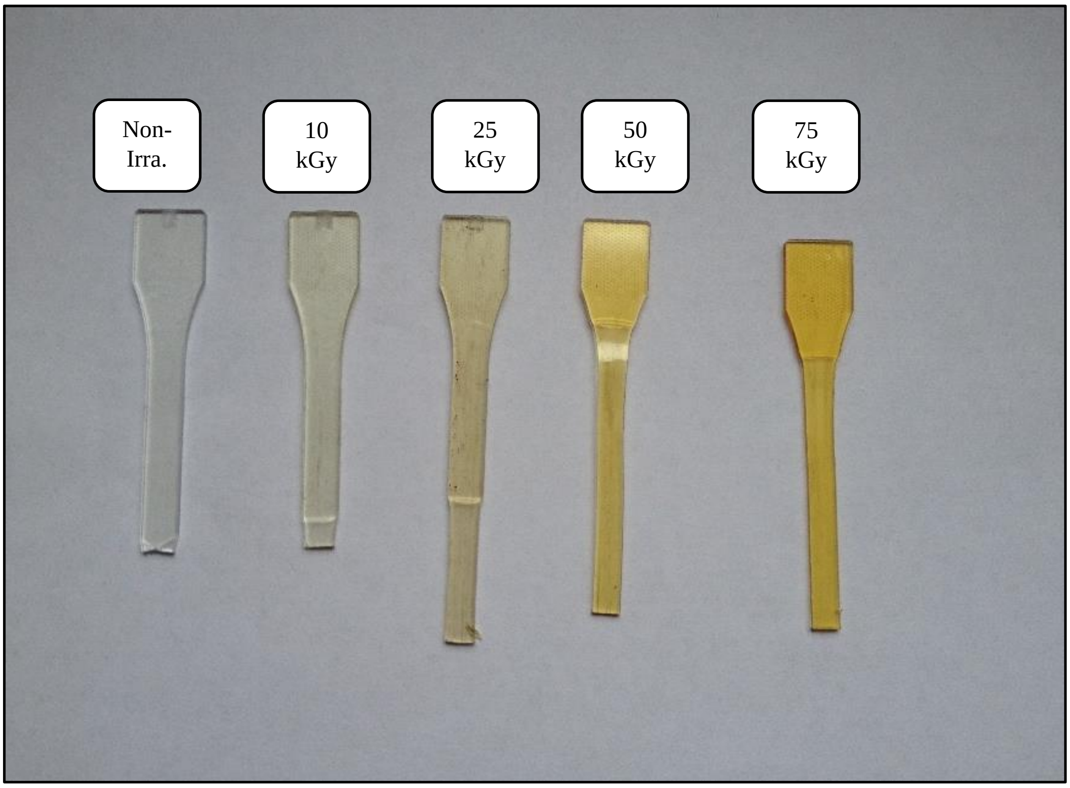

Figure 113 Photograph of the Neat Polycarbonates which were irradiated by 10, 25, 50 and 75 kGy

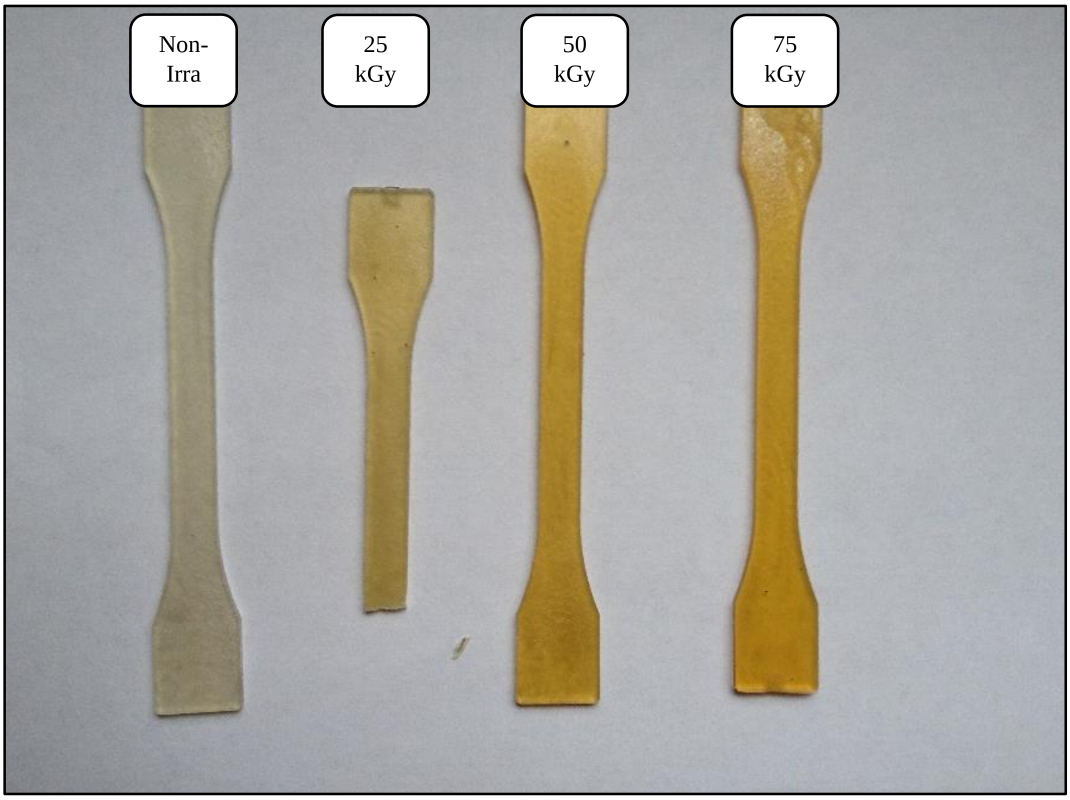

Figure 114 Photograph of the 10 wt. Glass Fiber Included Polycarbonates which were irradiated by 25, 50 and 75 kGy

APPENDIX F

CHEMICAL KINETICS OF RADIOACTIVE WASTES AND GAMMA DECAY OF ^{60}Co

Rate of decay for samples containing radionuclides is considered as first order rate law. Rate law for decay of radionuclides and decay of ^{60}Co were shown below. Where A could be concentration, activity and dose rate. “k” is rate constant and it is equal to $\frac{\ln(2)}{t_{half\ life\ of\ radionuclide}}$. Time is designated as “t”.

$$\mathrm{Rate} = \frac{\Delta\,[\mathrm{A}]}{\Delta \mathrm{t}} = -\,\mathrm{k} \times [\mathrm{A}]^1 \;\rightarrow\; \frac{\Delta\,[\mathrm{A}]}{[\mathrm{A}]^1} = -\,\mathrm{k} \times \Delta \mathrm{t}$$

$$\int_{\mathrm{A}_0}^{\mathrm{A}} \frac{\Delta\,[\mathrm{A}]}{[\mathrm{A}]^1} = \int_0^{\mathrm{t}} -\mathrm{k} \times \Delta \mathrm{t} \;\rightarrow\; \ln\left(\frac{\mathrm{A}}{\mathrm{A}_0}\right) = -\,\mathrm{k} \times \mathrm{t}$$

$$\mathrm{e}^{\ln\left(\frac{\mathrm{A}}{\mathrm{A}_0}\right)} = \mathrm{e}^{-\mathrm{kt}} \;\rightarrow\; \mathrm{A} = \mathrm{A}_0 \times \mathrm{e}^{-\mathrm{kt}}$$

Equation 5 Rate of Decay of Radioactive Waste (Zumdahl & Zumdahl, 2010)

$${}^{60}_{27}\mathrm{Co} \rightarrow {}^{60}_{28}\mathrm{Ni} + {}^{\;0}_{-1}\mathrm{e}\ (0.31\ \mathrm{MeV}) + {}^{0}_{0}\gamma(1.33\ \mathrm{MeV}) + {}^{0}_{0}\gamma(1.17\ \mathrm{MeV})$$

Equation 6 Decay of ^{60}Co

APPENDIX G

POSSIBLE STRUCTURAL CHANGES IN POLYMERS AND POLYCARBONATES UPON IRRADIATION

Possible structural changes in polymers and polycarbonates upon irradiation were shown below.

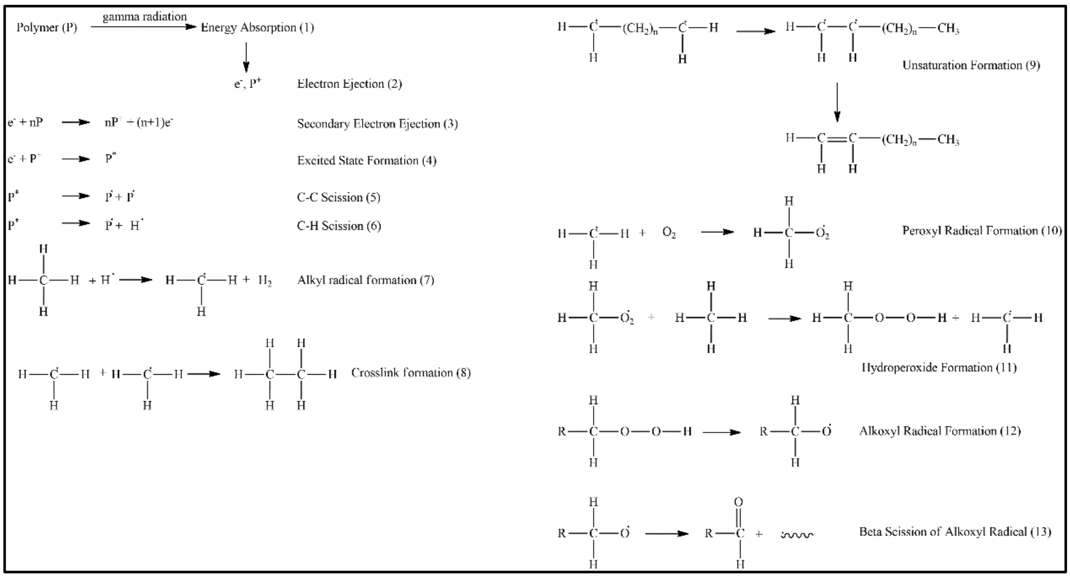

Figure 115 Illustrative Scheme for Possible Structural Changes in Polymers upon Irradiation (Carlsson & Chmela, 1990)

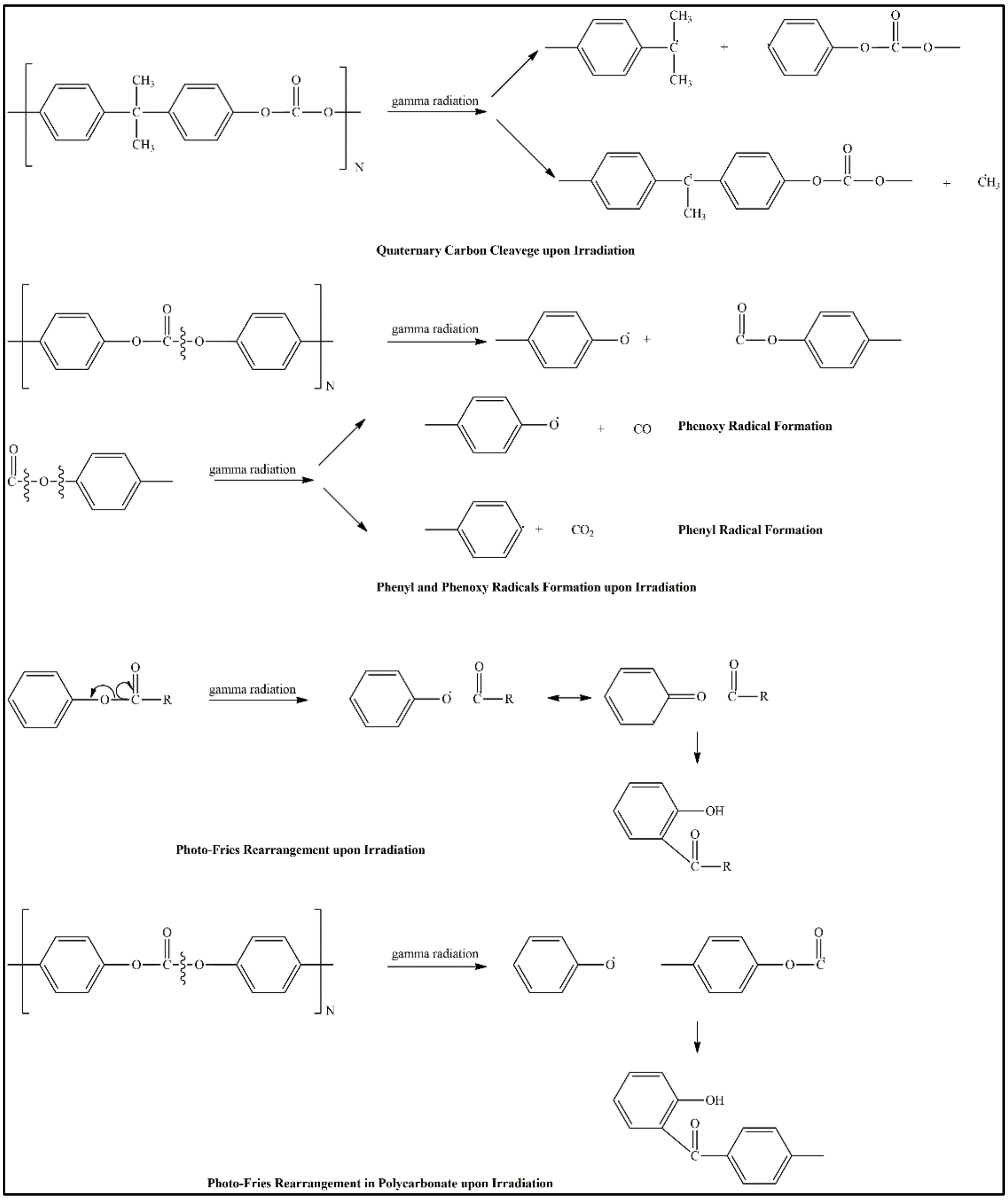

Figure 116 Illustrative Scheme for Possible Structural Changes in Bisphenol-A-Polycarbonate upon Irradiation (Rabek, 1995; International Union of Pure and Applied Chemistry, 2014)

APPENDIX H

TGA AND DTG CURVES OF BENTONITE, BARITE, CARBON FIBER AND GLASS FIBER

TGA and DTG Curves of bentonite, barite, carbon fiber and glass fiber were shown below.

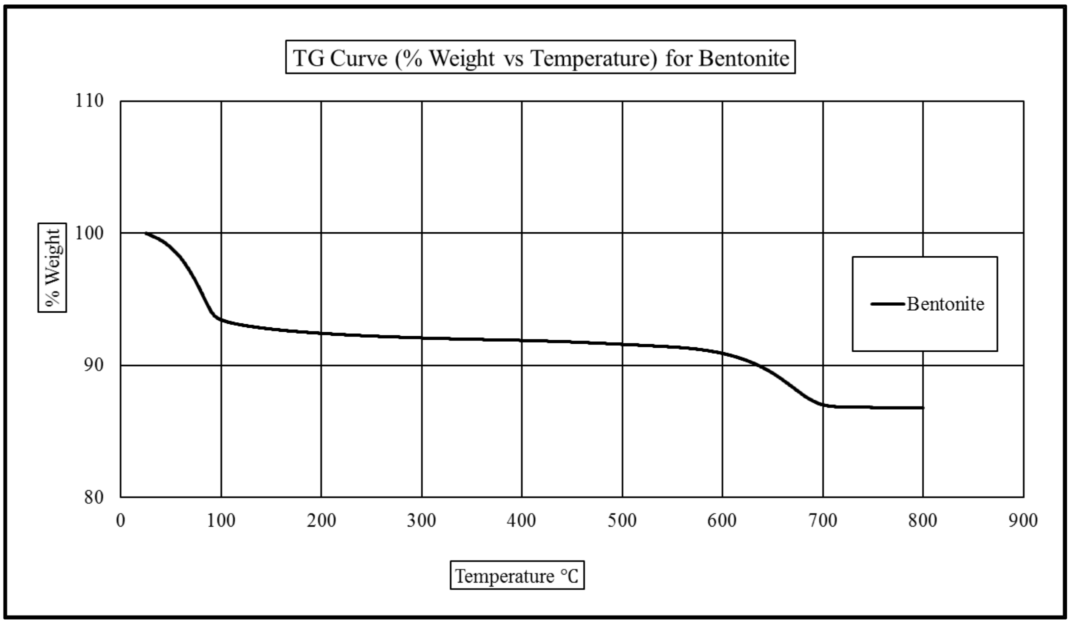

Figure 117 TG Curve of Bentonite

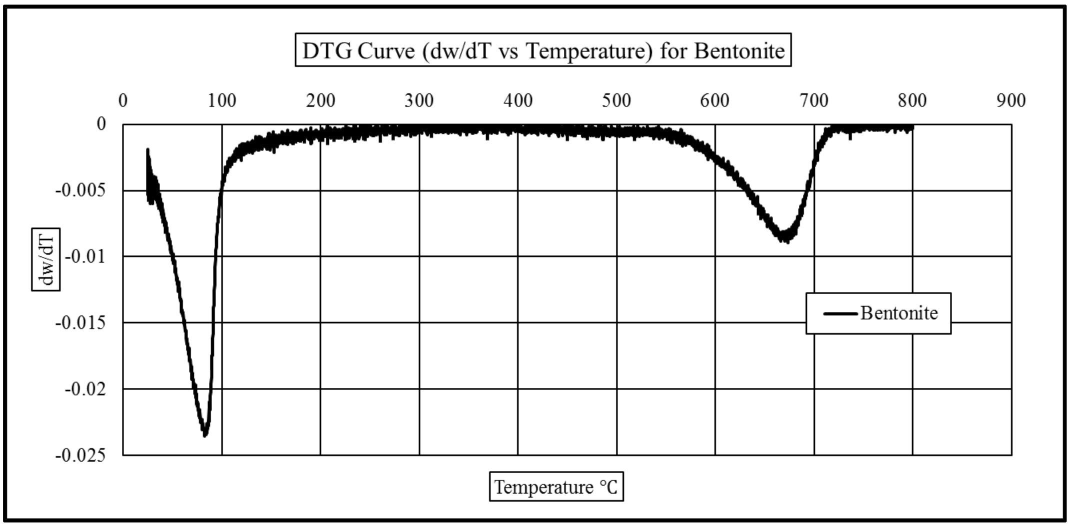

Figure 118 DTG Curve of Bentonite

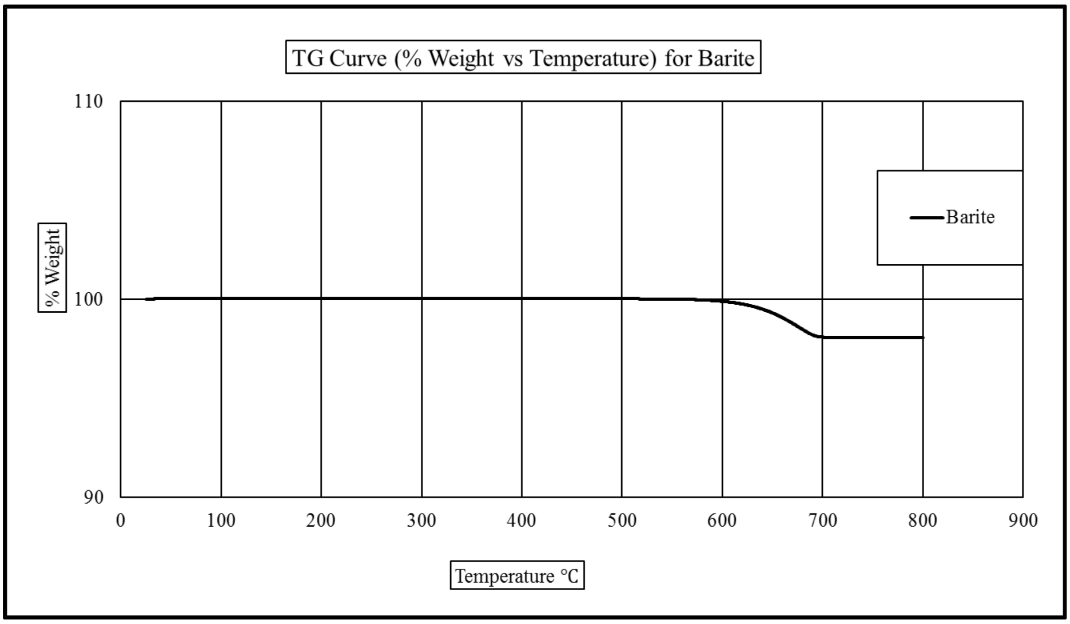

Figure 119 TG Curve of Barite

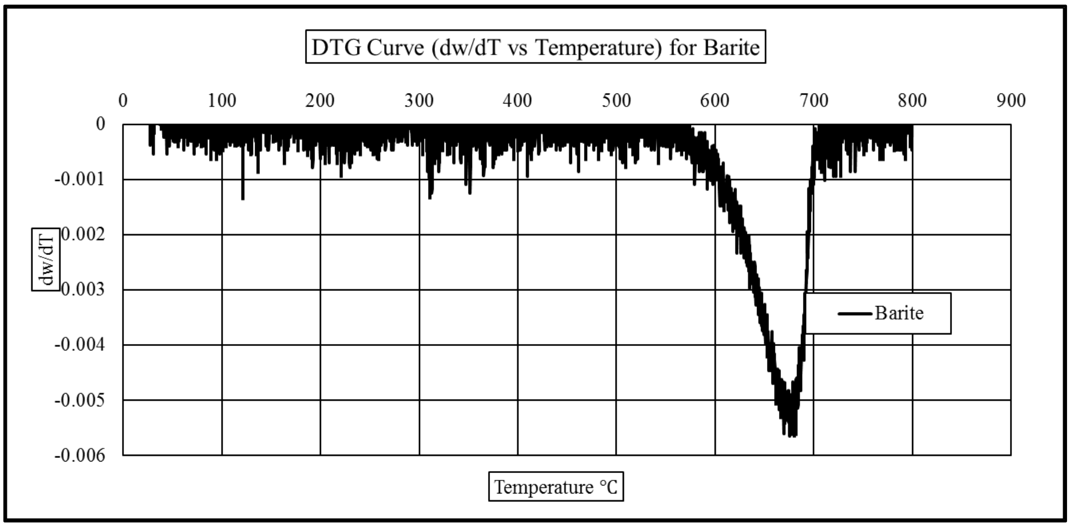

Figure 120 DTG Curve of Barite

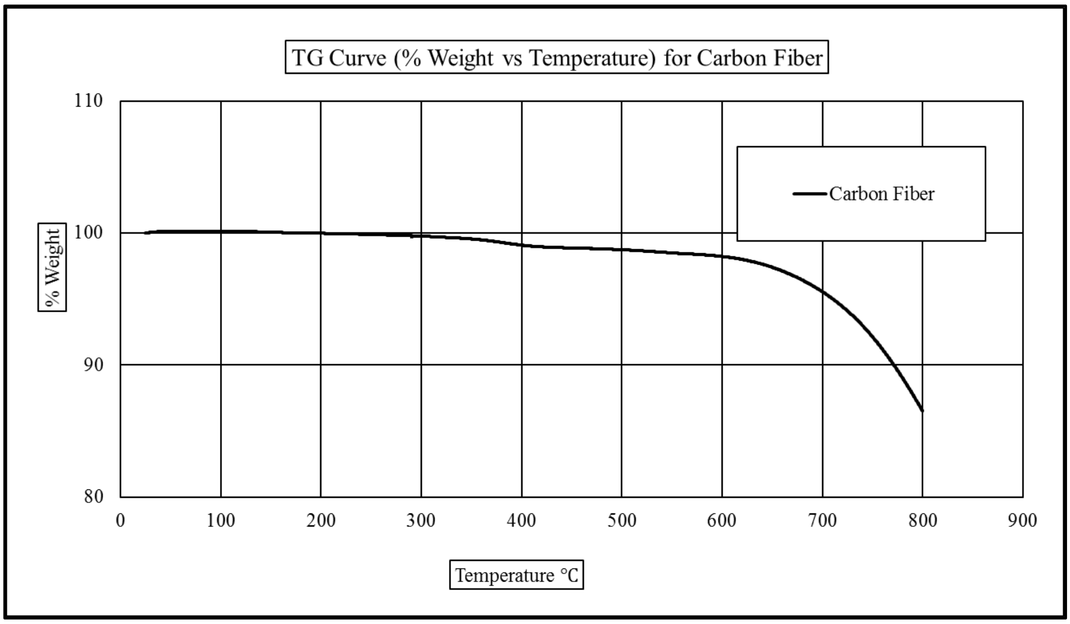

Figure 121 TG Curve of Carbon Fiber

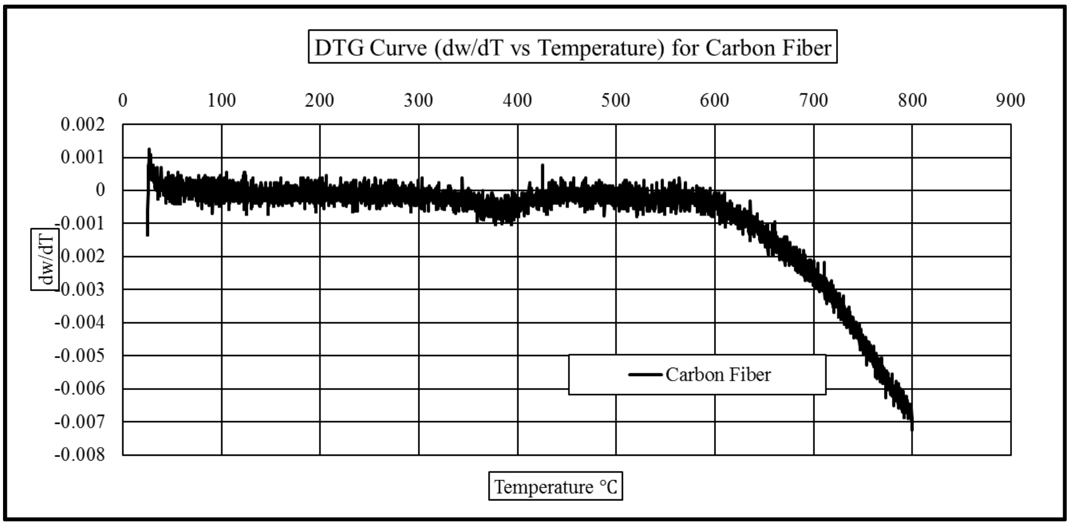

Figure 122 DTG Curve of Carbon Fiber

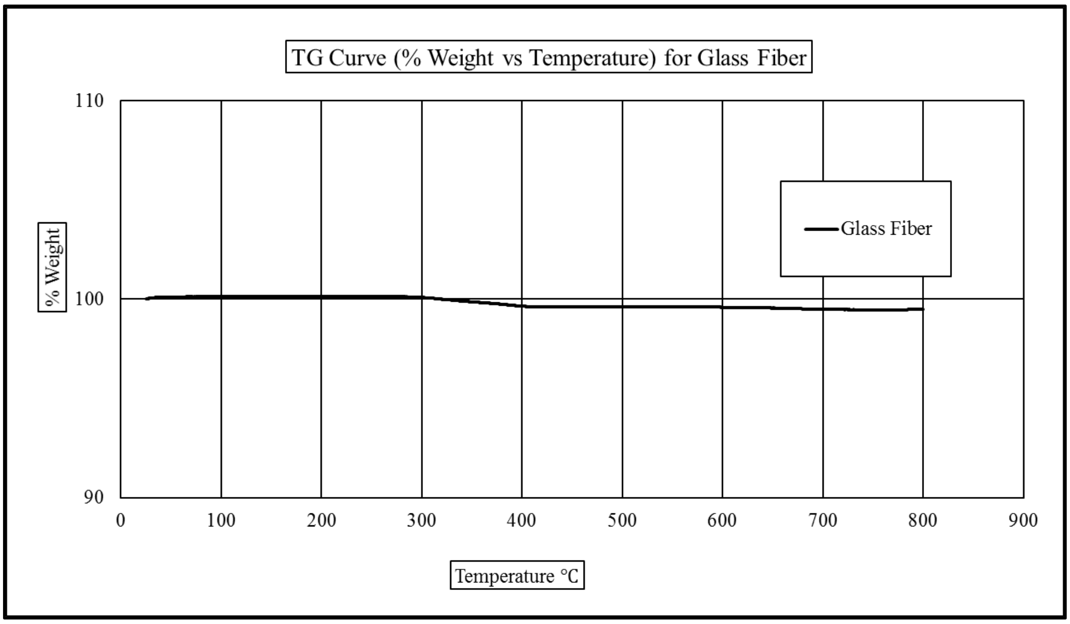

Figure 123 TG Curve of Glass Fiber

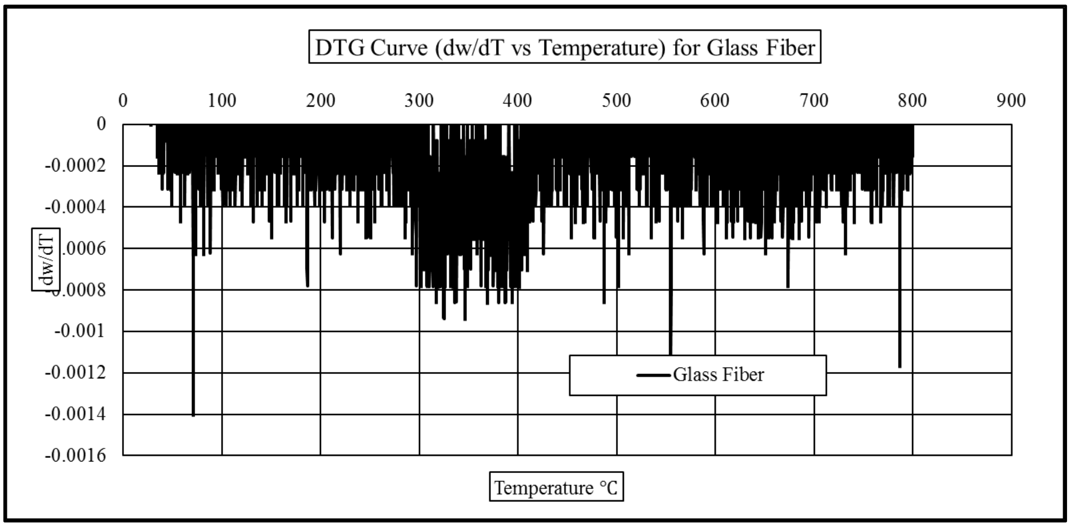

Figure 124 DTG Curve of Glass Fiber

CURRICULUM VITAE

PERSONAL INFORMATION

PERSONAL INFORMATION

Name and Surname:	Fırat Hacıoğlu
Date and Place of Birth:	29.01.1985, Ankara
Sex:	Male
Nationality:	Republic of Turkey
Work Address:	TSE, Necatibey Caddesi No: 112 Bakanlıklar/Ankara
Phone:	+90 505 228 28 11 (Mobile)
E-mail:	firathacioglu@gmail.com

EDUCATIONAL BACKGROUND

Ph. D. :	METU Polymer Science and Technology Department, Ankara (3.14/4.00) Expected Date of Graduation: February, 2017
M.S.:	METU Polymer Science and Technology Department, Ankara (3.00/4.00) Date of Graduation: September, 2010

B.Sc.: METU Department of Chemistry, Ankara (2.88/4.00),
Date of Graduation: July, 2008

B.Sc.: METU Department of Industrial Engineering, Ankara (2.35/4.00),
Expected Date of Graduation: January, 2019

WORK EXPERIENCE

2010-present: Certification Expert

Directorate of Directives, Turkish Standards Institution, Ankara/TURKEY

2009–2010: Research Assistant
Graduate School of Natural and Applied Sciences, Middle East Technical University, 06800 Ankara/TURKEY

PUBLICATIONS

Possible use of EPDM in radioactive waste disposal: Long term low dose rate and short term high dose rate irradiation in aquatic and atmospheric environment, Fırat Hacıoğlu, Tonguç Özdemir, Seda Çavdar, Ali Usanmaz, Radiation Physics and Chemistry (2013) 83, 122-130.

Possible use of bisphenol-a polycarbonate in radioactive waste embedding, Fırat Hacıoğlu, Tonguç Özdemir, Gökhan Kinalır, Ali Usanmaz, Progress in Nuclear Energy (2016) 90, 98-104.

TECHNICAL SKILLS

Dynamic Mechanical Analysis (DMA)
ATR-FTIR
Thermogravimetric Analysis (TGA)
Extruder
Injection Molding
Tensile Testing
Hardness (Shore)
Melf Flow Index